Universidade Estadual de Campinas
Instituto de Física Gleb Wataghin

Adriano Grigolo

Multiconfigurational Trajectory-Guided Quantum Dynamics with Generalized Coherent States

"Dinâmica Quântica Multiconfiguracional Guiada por Trajetórias com Estados Coerentes Generalizados"

campinas
2017

Universidade Estadual de Campinas
Instituto de Física Gleb Wataghin

Adriano Grigolo

Multiconfigurational Trajectory-Guided Quantum Dynamics with Generalized Coherent States

"Dinâmica Quântica Multiconfiguracional Guiada por Trajetórias com Estados Coerentes Generalizados"

Tese apresentada ao Instituto de Física Gleb Wataghin da Universidade Estadual de Campinas como parte dos requisitos exigidos para a obtenção do título de Doutor em Ciências.

Thesis presented to the Institute of Physics of the University of Campinas in partial fulfillment of the requirements for the degree of Doctor of Sciences.

Orientador/Supervisor: Marcus Aloizio Martinez de Aguiar

Este exemplar corresponde à versão final da tese defendida pelo aluno Adriano Grigolo e orientada pelo Prof. Dr. Marcus Aloizio Martinez de Aguiar.

Assinatura do Orientador

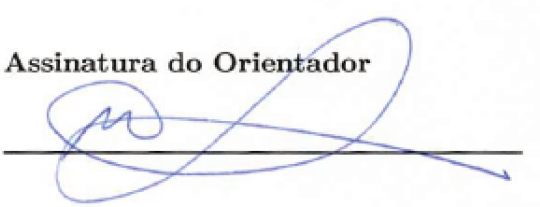

Campinas
2017

Agência(s) de fomento e nº(s) de processo(s): FAPESP, 2011/20065-4; CNPq, 141338/2011-3
ORCID: http://orcid.org/0000-0002-6418-6583

Ficha catalográfica
Universidade Estadual de Campinas
Biblioteca do Instituto de Física Gleb Wataghin
Lucimeire de Oliveira Silva da Rocha - CRB 8/9174

G877m

Grigolo, Adriano, 1986-
Multiconfigurational trajectory-guided quantum dynamics with generalized coherent states / Adriano Grigolo. – Campinas, SP : [s.n.], 2017.

Orientador: Marcus Aloizio Martinez de Aguiar.
Tese (doutorado) – Universidade Estadual de Campinas, Instituto de Física Gleb Wataghin.

1. Teoria quântica. 2. Estados coerentes. 3. Métodos semiclássicos. I. Aguiar, Marcus Aloizio Martinez de,1960-. II. Universidade Estadual de Campinas. Instituto de Física Gleb Wataghin. III. Título.

Informações para Biblioteca Digital

Título em outro idioma: Dinâmica quântica multiconfiguracional guiada por trajetórias com estados coerentes generalizados
Palavras-chave em inglês:
Quantum theory
Coherent states
Semiclassical methods
Área de concentração: Física
Titulação: Doutor em Ciências
Banca examinadora:
Marcus Aloizio Martinez de Aguiar [Orientador]
Alfredo Miguel Ozório de Almeida
Marcel Novaes
Amir Ordacgi Caldeira
Ricardo Luís Doretto
Data de defesa: 08-05-2017
Programa de Pós-Graduação: Física

MEMBROS DA COMISSÃO JULGADORA DA TESE DE DOUTORADO DE

ADRIANO GRIGOLO – RA 030809

APRESENTADA E APROVADA AO INSTITUTO DE FÍSICA GLEB WATAGHIN (IFGW), DA UNIVERSIDADE ESTADUAL DE CAMPINAS (UNICAMP), EM 08/05/2017.

COMISSÃO JULGADORA:

- **Prof. Dr. Marcus Aloizio Martinez de Aguiar (Orientador) – DFMC/IFGW/UNICAMP**
- **Prof. Dr. Alfredo Miguel Ozório de Almeida – CBPF – RJ**
- **Prof. Dr. Marcel Novaes – IF/UFU – MG**
- **Prof. Dr. Amir Ordacgi Caldeira – DFMC/IFGW/UNICAMP**
- **Prof. Dr. Ricardo Luís Doretto – DFMC/IFGW/UNICAMP**

OBS.: Informo que as assinaturas dos respectivos professores membros da banca constam na ata de defesa já juntada no processo de vida acadêmica do aluno.

CAMPINAS
2017

Agradecimentos

Agradeço o professor Marcus Aguiar, que foi meu orientador desde os tempos de iniciação científica. Foi um privilégio ter trabalhado com o senhor.

Agradeço ao professor Dmitry Shalashilin por me receber e orientar durante um ano em Leeds – um abraço a todos do grupo.

Agradeço meus amigos de Curitiba e de Campinas – a amizade de vocês sempre foi indispensável e me deu motivação para seguir em frente.

Agradeço à minha namorada Carol, pelo carinho e compreensão, principalmente durante os últimos estágios deste projeto.

Agradeço, sobretudo, à minha família, por todo o suporte dado ao longo dos anos. Obrigado, pai, mãe, Vini.

Por fim, gostaria de agradecer à Fundação de Amparo à Pesquisa do Estado de São Paulo (FAPESP), o apoio financeiro sob os projetos 2011/20065-4 e 2013/00145-9; ao Conselho Nacional de Pesquisa e Desenvolvimento (CNPq), a verba concedida sob o projeto 141338/2011-3; e ao Fundo de Apoio ao Ensino, à Pesquisa, e Extensão (FAEPEX) da Unicamp, o auxílio disponibilizado através da solicitação 2065/17.

Acknowledgements

This thesis was supported by FAPESP under projects 2011/20065-4 and 2013/00145-9; funding was also received from CNPq under project 141338/2011-3, and FAEPEX through application 2065/17.

Resumo

Uma versão generalizada do método 'coupled coherent states' é desenvolvida para estados coerentes associados a grupos de Lie arbitrários. Em contraste com a abordagem original, restrita a funções de base gaussianas, o método estendido é adequado para propagação de estados quânticos de sistemas exibindo propriedades físicas destituídas de análogo clássico, tais como graus de liberdade de spin ou indistinguibilidade de partículas. A formulação para o caso de sistemas com um número fixo de partículas idênticas interagentes é examinada em detalhe, sendo este um caso relevante descrito em termos de estados coerentes do grupo especial unitário. A técnica é ilustrada com aplicações simples, envolvendo modelos de Hubbard bosônicos e fermiônicos. Diversos aspectos da implementação numérica são discutidos.

Palavras-chave: métodos numéricos, estados coerentes, métodos semiclássicos.

Abstract

A generalized version of the coupled coherent states method for coherent states of arbitrary Lie groups is developed. In contrast to the original approach, which is restricted to frozen-Gaussian basis sets, the extended method is suitable for propagating quantum states of systems featuring non-classical physical properties, such as spin degrees of freedom or particle interchange symmetry. The formulation for the relevant case of number-conserving systems of interacting identical particles, most adequately described in terms of coherent states of the special unitary group, is studied in detail. The technique is illustrated with applications to simple Hubbard-like models for both bosons and fermions. Several aspects of the numerical implementation are discussed.

Keywords: numerical methods, coherent states, semiclassical methods.

Contents

Introduction 11

1 Time-dependent variational principle and generalized coherent states 15
- 1.1 Quantum equations from a minimum principle . . . 15
  - 1.1.1 Unrestricted variations . . . 17
- 1.2 Norm-constrained form of the TDVP . . . 20
  - 1.2.1 Full variational equations with static basis functions . . . 22
  - 1.2.2 Full variational equations with time-dependent basis functions . . . 24
- 1.3 Generalized coherent states – overview . . . 26
  - 1.3.1 Preliminaries . . . 26
  - 1.3.2 Coherent states as trial functions . . . 29
  - 1.3.3 Classical propagation scheme . . . 32
  - 1.3.4 Example: Glauber's coherent states/gaussian wavepackets . . . 33

2 Bosonic coherent states 37
- 2.1 The Bose-Einstein condensate parametrization . . . 37
  - 2.1.1 Preliminaries . . . 37
  - 2.1.2 Coherent states: definition and macroscopic mode . . . 39
  - 2.1.3 * Complementary modes and projectors . . . 42
  - 2.1.4 The geometry of bosonic coherent states . . . 43
- 2.2 Mean-field dynamics of interacting bosons . . . 45
  - 2.2.1 The one-density . . . 45
  - 2.2.2 Energy function and mean-field dynamics . . . 46
  - 2.2.3 * Exact solutions for non-interacting systems . . . 48
- 2.3 * More geometry: transformation of single-particle modes . . . 48

3 Fermionic coherent states 52
- 3.1 Thouless determinants . . . 52
  - 3.1.1 Preliminaries . . . 52
  - 3.1.2 Coherent states: definition and dynamical orbitals . . . 54
  - 3.1.3 * Complementary orbitals and projectors . . . 58
  - 3.1.4 The geometry of Thouless states . . . 59
- 3.2 Mean-field dynamics of interacting fermions . . . 61
  - 3.2.1 The one-density . . . 62
  - 3.2.2 Number density and intrinsic orbitals of the Thouless determinant . . . 64
  - 3.2.3 Spin structure of the Thouless determinant . . . 64
  - 3.2.4 Energy function and mean-field dynamics . . . 66
  - 3.2.5 * Exact solutions for non-interacting systems . . . 67
- 3.3 More geometry: transformation of single-particle orbitals . . . 68
  - 3.3.1 * Alternative expressions for the transformation rule . . . 71

4 Multiconfigurational method **73**
4.1 The continuum version . . . 73
4.2 Discrete unitary version . . . 77
4.2.1 * Accumulated error in the CCS propagation . . . 78
4.2.2 Auxiliary amplitudes . . . 79
4.2.3 Norm conservation . . . 80
4.2.4 * The variational picture . . . 81
4.2.5 A remark on energy conservation . . . 83
4.2.6 * Non-unitary case . . . 84
4.2.7 The standard form of the generalized CCS method: a few remarks . . . 85
4.3 The CCS coupling for specific parametrizations . . . 89
4.3.1 The bosonic case . . . 89
4.3.2 The fermionic case . . . 92
4.4 Sampling protocol . . . 94
4.5 A 'pave-the-way' parallelization scheme . . . 96
4.5.1 * Implementation types – a few examples . . . 98
4.5.2 The three-stage 'pave-the-way' implementation . . . 99
4.6 * Extensions of the multiconfigurational method . . . 102
4.6.1 * Extended overlap . . . 102
4.6.2 * Extended configurations . . . 104
4.6.3 * CCS amplitudes in the extended framework . . . 106
4.6.4 * Matrix elements . . . 107

5 Applications in test-systems **112**
5.1 Mean-field dynamics with Hubbard-like Hamiltonians . . . 112
5.1.1 Bosonic case . . . 113
5.1.2 Fermionic case . . . 114
5.2 On the purpose of the results compiled in this work . . . 115
5.3 Bose-Einstein condensate in a symmetric triple-well . . . 115
5.3.1 Three-mode approximation . . . 115
5.3.2 SU(3) bosonic coherent-state description . . . 116
5.3.3 Exact quantum propagation . . . 117
5.3.4 Monitored quantities . . . 118
5.3.5 Opposite-phase mode and population imbalance . . . 118
5.3.6 Basis set sampling . . . 120
5.3.7 A note on dynamical regimes . . . 120
5.3.8 Runs: general remarks . . . 122
5.3.9 Run: $N = 100$ . . . 123
5.3.10 Run: $N = 80$ . . . 125
5.3.11 Run: $N = 70$ . . . 127
5.3.12 Run: $N = 40$ . . . 129
5.4 Electrons in a Hubbard ring . . . 131
5.4.1 Lattice space . . . 131
5.4.2 Reciprocal space . . . 134
5.4.3 Two-representation strategy for trajectory propagation . . . 136
5.4.4 Two-representation approach to the multiconfigurational propagation . . . 140
5.4.5 Initial state and sampling . . . 142
5.4.6 Exact quantum propagation (Full-CI) . . . 144
5.4.7 Monitored quantities . . . 144
5.4.8 Runs: general remarks . . . 145
5.4.9 Run: $S = 6$ sites, $N = 3$ electrons. . . . 147
5.4.10 Run: $S = 6$ sites, $N = 4$ electrons. . . . 149
5.4.11 Run: $S = 8$ sites, $N = 3$ electrons. . . . 151
5.4.12 Run: $S = 9$ sites, $N = 3$ electrons. (CCS vs. mean-field) . . . 153
5.4.13 Run: $S = 12$ sites, $N = 3$ electrons. . . . 156
5.4.14 Run: $S = 10$ sites, $N = 4$ electrons. . . . 158

6 Semiclassical initial-value representation **160**
6.1 The stability matrix . . . 160
6.1.1 Symplectic properties . . . 162
6.2 Integral expression for the coherent-state propagator . . . 164
6.2.1 * Classical propagator and zeroth-order semiclassical approximation . . . 165
6.3 Semiclassical amplitude . . . 167
6.3.1 Equation of motion for the amplitude . . . 168
6.4 Semiclassical approximation . . . 169
6.4.1 The expansion protocol . . . 170
6.4.2 First order derivatives and tuning of w . . . 173
6.4.3 * Second-order derivatives . . . 176
6.5 The semiclassical time-evolution operator . . . 178
6.5.1 * Alternative expression . . . 182
6.6 The Z matrix . . . 183
6.6.1 * Semiclassical phase correction and modulation . . . 184
6.7 * Invariance under group transformations . . . 185
6.8 Semiclassical IVR: complete scheme . . . 188

Concluding remarks **192**

Bibliography **194**

A Phase-space volume conservation and properties of the complex action **201**
A.1 Invariance of the phase-space measure under classical flow . . . 201
A.2 The complex action . . . 202

B Bosonic coherent states: survey **205**
B.1 Condensate density matrix . . . 205
B.1.1 One-body density . . . 205
B.1.2 Two-body matrix element . . . 206
B.1.3 Gradients of the density matrix . . . 206
B.2 Normalization of the bosonic closure relation . . . 207
B.3 Fock projection of a condensate state . . . 209

C Fermionic coherent states: survey **211**
C.1 Thouless density matrix . . . 211
C.1.1 One-body density . . . 211
C.1.2 Two-body matrix element . . . 212
C.1.3 Gradients of the density matrix . . . 213
C.2 Normalization of the fermionic closure relation . . . 215
C.3 Fock projection of a Thouless state . . . 218

D Hubbard model – standard diagonalization **221**
D.1 Fermi systems . . . 221
D.1.1 Matrix elements . . . 221
D.1.2 Transformation of fermionic Fock states . . . 222
D.2 Bose systems . . . 223
D.2.1 Matrix elements . . . 224
D.2.2 Transformation of bosonic Fock states . . . 225

E Spectral analysis **228**
E.1 Auto-correlation function and spectral density . . . 228

Introduction

A vast number of physical systems exhibit the property that some of their parts behave in a sort of classical way, meaning that quantum effects play only a minor role in the description of those parts. This distinctive classical character of specific degrees of freedom is a much welcomed attribute, for it makes possible the development of tractable computational approaches capable of carrying out the time-evolution of complex quantum systems, being thus the fundamental property upon which *time-dependent trajectory-guided methods* are based.

In this kind of technique quantum states are represented in terms of time-dependent basis functions or 'configurations'. Within a single configuration, those degrees of freedom in which quantum effects are negligible are evolved according to classical equations of motion. This classical dynamics may be prescribed in a number of different ways and different choices correspond to different propagation schemes.

In spite of the fact that individual configurations have some of their parts bound to obey classical laws, a complete quantum solution is in principle attainable by combining many configurations. The key idea behind such 'multiconfigurational' approaches is that trajectory-guided basis functions, if properly optimized, are more likely to remain in the important regions of the Hilbert space, thus being more efficient at representing the quantum state in the sense that a reduced number of basis elements is required in order to achieve an accurate description. And it is precisely through a significant reduction in the number of basis functions needed to propagate the system that one hopes to escape the exponential scaling of basis-set size with dimensionality typical of standard static-basis formulations. This 'mixed quantum-classical' picture is adopted in many methods of quantum chemistry.[1]

A recurrent theme in this field is the development of techniques which, by means of equally simple recipes to guide the basis functions, would be readily applicable to systems presenting authentically non-classical qualities, such as spin degrees of freedom or particle exchange symmetry. Several works have been directed to that purpose, most often aiming at a time-dependent description of the electronic structure of molecules during non-adiabatic processes. One particular example of such a recipe is the classical model for electronic degrees of freedom proposed by Miller and White[2] where a second-quantized fermionic Hamiltonian is properly reduced to a classical function wherein number and

phase variables play the role of generalized coordinates. In contrast, a more 'mechanistic' approach to fermion dynamics is found on the multiconfigurational formula proposed by Kirrander and Shalashilin[3] in which the basis functions consist of antisymmetrized frozen Gaussians[i] guided by fermionic molecular dynamics.[5]

Yet, if one seeks to describe non-classical degrees of freedom by means of classical-like variables, then generalized coherent states – defined in the group-theoretical sense – are undoubtedly among the most appropriate tools to be employed. There are many reasons supporting this assertion.

First of all, coherent states are defined in terms of non-redundant parameters and equations of motion for these parameters can be readily obtained from the time-dependent variational principle.[6] In this way an optimized time evolution can be assigned to specific degrees of freedom in an unambiguous manner. Moreover, they are naturally able to capture the desired symmetries of the system, and these are maintained during propagation. Furthermore, the coherent-state parameters evolve in a classical phase space in the strict sense of the word, hence we automatically have at our disposal the wealth of analytical techniques applicable to Hamiltonian systems. At the same time, through this intimate connection to classical dynamics, coherent states provide a compelling classical interpretation to quantum phenomena, in so far as individual configurations are chosen to represent familiar objects – i.e. in such a way that it is meaningful to discuss the dynamics of the system in terms of their trajectories. To this extent, coherent states – which are also minimum uncertainty states (as long as a proper meaning is assigned to the term 'uncertainty')[7;8] – are valuable tools in enhancing our comprehension with respect to the semiclassical features of the quantum system under investigation. In addition, and from a more mathematical perspective, the group-theoretical formalism secures a well-defined integral form for the coherent-state closure relation[9] – a crucial element to the developments presented in this work. This list of virtues is not exhausted and other advantages of a generalized coherent-state representation will be evidenced throughout the thesis.

Along these lines, Van Voorhis and Reichman[10] have considered a number of alternative representations of electronic structure making use of different coherent-state parametrizations and also examined their adequacy to a variety of systems.[ii] Within the context of non-adiabatic molecular dynamics, a particularly interesting fermionic coherent-state representation, known as 'Thouless determinant' in the field of quantum chemistry,[14;15] is employed in the simplest and most throughly investigated version of the Electron-Nuclear Dynamics theory, developed by Deumens, Öhrn and collaborators.[16;17] The same kind of coherent state has been discussed at length, within the field of nuclear physics, by Suzuki and Kuratsuji.[18–20] (Thouless determinants will be studied in detail in

[i] More recently, Grossmann *et. al.*[4] have investigated, in a semiclassical context, whether propagation with antisymmetrized basis states is essential for the description of electron scattering.

[ii] Their discussion is based on a rough extension of Solari's semiclassical propagators[11;12] – a rigorous derivation of the generalized coherent-state propagator can be found in a recent work.[13]

the present work.)

Turning to bosonic dynamics, a semiclassical trajectory-based formula in the special unitary group coherent-state representation has been recently derived and successfully applied to a model of trapped bosons.[21;22] (The propagation methodology developed in this thesis is also implemented with bosonic coherent states of the same kind.)

The aforementioned methods are representative of the kind of technique one has in mind when a description of intrinsically quantum degrees of freedom in terms of classical-like variables is desired. However, they either constitute approximate single-configuration approaches[16;17] or involve complicated trajectories that live in a duplicated phase space,[21;22] sometimes relying on sophisticated root-search techniques in order to determine them.[10;23;24] It seems that a multiconfigurational, generalized coherent-state approach, based on simple – as opposed to duplicated – phase-space trajectories would be more in the spirit of the familiar time-dependent guided-basis methods of quantum chemistry.[iii] This is precisely the direction we take here.

In this work a quantum initial-value representation method, which employs a generalized coherent-state basis set guided by classical trajectories, is formulated. The resulting propagation scheme is regarded as a natural extension of the coupled coherent states technique of Shalashilin and Child[25–27] in so far as (i) basis-set elements represent localized quantum states; (ii) each element evolves independently in a generalized classical phase space and carries an action phase; and (iii) the quantum amplitudes associated with individual elements obey fully coupled equations of motion which present a number of attractive qualities.

Thesis organization

We begin, at Chapter 1, with a review of two fundamental topics: the time-dependent variational principle (TDVP) and the theory of generalized coherent states. The purpose of this chapter is to demonstrate how the machinery of the TDVP works and, most importantly, how it leads to classical equations of motion in a curved phase space when a coherent state is taken as a trial function. Next, Chapters 2 and 3 are dedicated to bosonic and fermionic coherent states, respectively. Their geometrical properties are reviewed and, more specifically, their dynamics under certain prototype Hamiltonians is characterized. These first three chapters have a preparatory objective where the essential tools required for the subsequent developments are introduced.

It is at Chapter 4 that we set forth to derive the working equations of the generalized coupled coherent states method. This is the central chapter of the thesis, where the main theoretical constructs are presented. In particular, the discrete unitary version of the

[iii] We note that the approximations to the generalized coherent-state path integral considered by Kuratsuji and Suzuki[20] – as well as specific formulations for Slater determinants[18;19] – are very much akin to the techniques develop in this paper.

method – the standard formulation – is throughly analyzed and a parallelization scheme is devised for its numerical implementation. The technique is then put to use in Chapter 5 where model systems for bosons and fermions described by Hubbard-like Hamiltonians are studied. The results obtained are compared against exact quantum data and general trends of the methodology are identified.

At Chapter 6 we take on a more formal discussion. In this independent chapter, a semiclassical approximation for the generalized coherent propagator is constructed.

This thesis was meant to have a general didactic tone and to be self-contained to some degree. Since a lot of material has to be reviewed before the key developments are considered, the end result was a rather lengthy manuscript. To partially alleviate this inconvenience, we have marked with asterisks '*' those sections of the body text that can be skipped at a first reading. Also, the 'thesis map' displayed below is intended to aid the reader. Finally, it also should be mentioned that several parts of this work were adapted from Ref. [28] (including the introduction above).

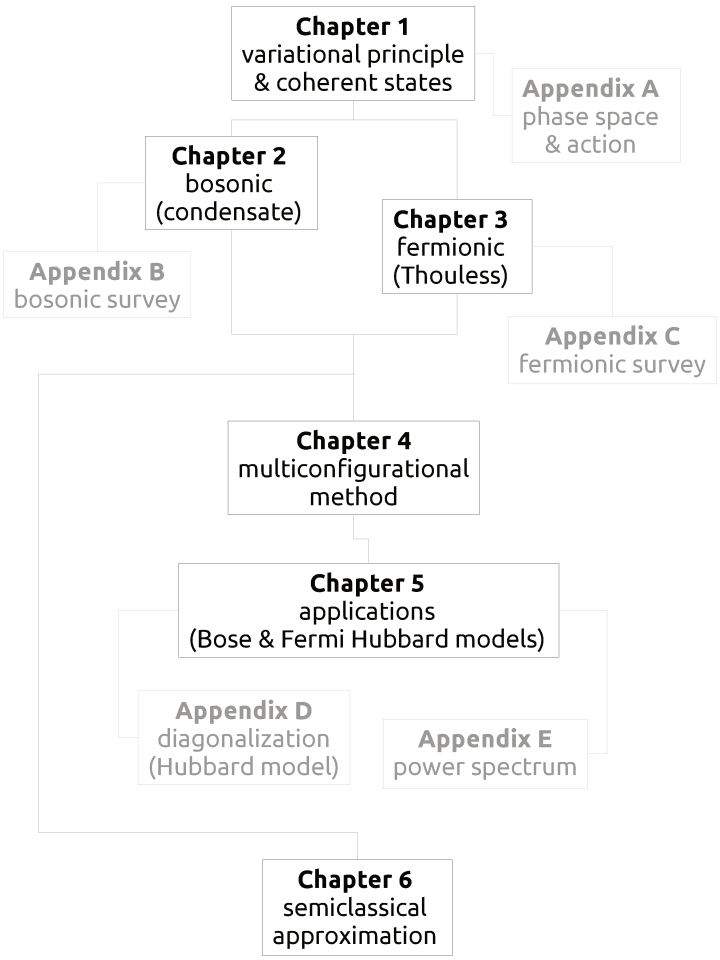

Thesis map.

Chapter 1

Time-dependent variational principle and generalized coherent states

Overview. The time-dependent variational principle is reviewed. The procedure is first illustrated with unrestricted trial states; this establishes some notation and terminology. A modified version of the principle, which includes a normalization constraint, is then formulated and shown to be more convenient when considering multiconfigurational trial functions. Generalized coherent states are introduced and their basic geometrical properties are outlined. Seen as special types of trial states, their dynamics under general Hamiltonians is worked out from the basic Euler-Lagrange equations. The presentation mostly follows the classic text by Kramer and Saraceno;[6] additional details are incorporated from Refs. [13;29].

1.1 Quantum equations from a minimum principle

The fundamental idea behind the time-dependent variational principle (TDVP) is that approximate quantum solutions to a given problem can be obtained by optimizing a *trial state*: a state that depends on a number of adjustable time-dependent parameters. The optimization is effected by requiring that the trial state yields a stationary solution to a certain action functional defined for a predetermined time interval.

Denoting the trial state by $\psi = \psi(t)$, the *total action* functional A is:[i]

$$A_\tau[\psi] = S_\tau[\psi] - \frac{i\hbar}{2}\Big[\log\langle\psi_\tau|\psi_\tau\rangle + \log\langle\psi_0|\psi_0\rangle\Big], \tag{1.1}$$

where the initial time is $t = 0$ and the final time is $t = \tau$ (for brevity, we occasionally indicate specific time arguments with a subscript, e.g. $|\psi(0)\rangle = |\psi_0\rangle$ and $|\psi(\tau)\rangle = |\psi_\tau\rangle$). The reason why this functional incorporates unusual *surface terms* (the logarithmic terms)

[i] In this thesis, '$\log x$' is the natural logarithm of x. For complex z, '$\log z$' refers to the principal branch. Also, the complex conjugate of z will be indicated with an asterisk: z^*.

will be clarified in a moment – notice that the trial state is left unnormalized. The bare action, or simply *action* S is the time integral of a Lagrangian function L,[6]

$$S_\tau[\psi] = \int_0^\tau dt\, L(\psi) \equiv \int_0^\tau dt\, \langle\psi|\psi\rangle^{-1}\langle\psi|\Big[\frac{i\hbar}{2}\Big(\frac{d}{dt} - \frac{d^*}{dt}\Big) - \hat{H}\Big]|\psi\rangle, \tag{1.2}$$

where the conjugate derivative is meant to operate 'backwards', i.e. $\langle\psi|(d^*/dt) = \langle d\psi/dt|$.

We see that the Lagrangian is defined in terms of the mean value of an hermitian version of the linear operator whose action upon a wavefunction[ii] $|\Psi\rangle$ produces the Schrödinger equation,

$$\Big(i\hbar\frac{d}{dt} - \hat{H}\Big)|\Psi\rangle = 0.$$

In this way the TDVP bears some resemblance to its more familiar time-independent version.

Computing the mean value the Lagrangian is found to be:

$$L(\psi) = \frac{i\hbar}{2}\frac{\langle\psi|\dot{\psi}\rangle - \langle\dot{\psi}|\psi\rangle}{\langle\psi|\psi\rangle} - \frac{\langle\psi|\hat{H}|\psi\rangle}{\langle\psi|\psi\rangle}, \tag{1.3}$$

where a dot denotes differentiation with respect to the time variable t – this will be a recurrent notation throughout this work.

In performing the TDVP calculations, the *ket* state $|\psi\rangle$ and *bra* state $\langle\psi|$ shall be regarded as independent quantities – only at the end we shall recognize them as dual vectors, even though we still refer to 'ψ' as *the* trial state. Correspondingly, the Lagrangian function should be understood as $L(\psi, \psi^*, \dot{\psi}, \dot{\psi}^*)$, i.e. a function depending on both variational parameters and their derivatives, as usual. We shall write simply $L(\psi)$, for short.

A stationary point of the total action is associated with a *path* $\psi(t)$, for $0 \leq t \leq \tau$, having the following property: when small displacements are effected at each time instant of such path, $\psi(t) \to \psi(t) + \delta\psi(t)$, the functional A is unchanged to first order. Therefore, such stationary solutions can be found by enforcing the condition $\delta A = 0$, together with fixed end-point boundary conditions, as is common practice in variational calculus.

The problem is thus formulated:

$$\begin{cases} |\psi(t)\rangle \to |\psi(t)\rangle + |\delta\psi(t)\rangle \\ \langle\psi(t)| \to \langle\psi(t)| + \langle\delta\psi(t)| \end{cases} \quad \Leftrightarrow \quad \delta A_\tau = 0 \quad \text{with:} \quad \begin{cases} |\delta\psi(0)\rangle = 0 \\ \langle\delta\psi(\tau)| = 0 \end{cases} . \tag{1.4}$$

Notice that the initial-time boundary condition is enforced on the *ket* $|\psi_0\rangle$, whereas the final-time condition is enforced on the *bra* $\langle\psi_\tau|$. The surface terms in A ensure the consistency of this boundary-value problem,[29] as we will see.

[ii] Throughout this thesis the terms 'state' and 'wavefunction' are used as synonyms.

1.1.1 Unrestricted variations

In practice the trial state is invariably parametrized by a smaller number of variables than that necessary to span the full Hilbert space where the exact quantum solution evolves – otherwise the variational approach would not be justifiable in the first place. It is instructive, nevertheless, to see what happens when one is able to perform *unrestricted variations* on $\psi(t)$, i.e. to effect displacements $\delta\psi(t)$ in the trial state as if it were completely flexible.

Let us begin by writing the first-order change of the total action,

$$\delta A_\tau = \delta S_\tau - \frac{i\hbar}{2}\Big[\frac{\langle\psi_\tau|\delta\psi_\tau\rangle}{\langle\psi_\tau|\psi_\tau\rangle} + \frac{\langle\delta\psi_0|\psi_0\rangle}{\langle\psi_0|\psi_0\rangle}\Big] - \frac{i\hbar}{2}\Big[\frac{\langle\delta\psi_\tau|\psi_\tau\rangle}{\langle\psi_\tau|\psi_\tau\rangle} + \frac{\langle\psi_0|\delta\psi_0\rangle}{\langle\psi_0|\psi_0\rangle}\Big]. \tag{1.5}$$

For unrestricted variations, the change in the bare action S can be expressed as:

$$\delta S_\tau = \int_0^\tau dt\, \left[\frac{\partial L}{\partial|\psi\rangle}|\delta\psi\rangle + \frac{\partial L}{\partial|\dot\psi\rangle}|\delta\dot\psi\rangle + \langle\delta\psi|\frac{\partial L}{\partial\langle\psi|} + \langle\delta\dot\psi|\frac{\partial L}{\partial\langle\dot\psi|}\right]. \tag{1.6}$$

In the above equation all terms are scalars, and derivatives with respect to *bras* and *kets* should be understood as functional derivatives; for instance, using the position representation, with $\psi(x) = \langle x|\psi\rangle$ and $\psi(x)^* = \langle\psi|x\rangle$, for x with the appropriate number of dimensions, we would have:

$$\frac{\partial L}{\partial|\psi\rangle}|\delta\psi\rangle = \int dx\,\Big[\frac{\delta L(\psi)}{\delta\psi(x)}\delta\psi(x)\Big],\quad \langle\delta\dot\psi|\frac{\partial L}{\partial\langle\dot\psi|} = \int dx\,\Big[\delta\dot\psi(x)^*\frac{\delta L(\psi)}{\delta\dot\psi(x)^*}\Big],\quad \text{etc.}$$

Next, we proceed with the usual steps of time-dependent variational problems.[30] Integrating by parts the $|\delta\dot\psi\rangle$ and $\langle\delta\dot\psi|$ terms of (1.6) we obtain:

$$\delta S_\tau = \frac{\partial L}{\partial|\dot\psi\rangle}|\delta\psi\rangle\Big|_0^\tau + \langle\delta\psi|\frac{\partial L}{\partial\langle\dot\psi|}\Big|_0^\tau + \int_0^\tau dt\,\left\{\left[\frac{\partial L}{\partial|\psi\rangle} - \frac{d}{dt}\frac{\partial L}{\partial|\dot\psi\rangle}\right]|\delta\psi\rangle + \langle\delta\psi|\left[\frac{\partial L}{\partial\langle\psi|} - \frac{d}{dt}\frac{\partial L}{\partial\langle\dot\psi|}\right]\right\}.$$

The derivatives with respect to $|\dot\psi\rangle$ and $\langle\dot\psi|$ are:

$$\frac{\partial L}{\partial\langle\dot\psi|} = -\frac{i\hbar}{2}\frac{|\psi\rangle}{\langle\psi|\psi\rangle}, \tag{1.7a}$$

$$\frac{\partial L}{\partial|\dot\psi\rangle} = \frac{i\hbar}{2}\frac{\langle\psi|}{\langle\psi|\psi\rangle}. \tag{1.7b}$$

Thus the factors removed from the time integral give

$$\frac{\partial L}{\partial|\dot\psi\rangle}|\delta\psi\rangle\Big|_0^\tau + \langle\delta\psi|\frac{\partial L}{\partial\langle\dot\psi|}\Big|_0^\tau = \frac{i\hbar}{2}\Big[\frac{\langle\psi_\tau|\delta\psi_\tau\rangle}{\langle\psi_\tau|\psi_\tau\rangle} + \frac{\langle\delta\psi_0|\psi_0\rangle}{\langle\psi_0|\psi_0\rangle}\Big] - \frac{i\hbar}{2}\Big[\frac{\langle\delta\psi_\tau|\psi_\tau\rangle}{\langle\psi_\tau|\psi_\tau\rangle} + \frac{\langle\psi_0|\delta\psi_0\rangle}{\langle\psi_0|\psi_0\rangle}\Big], \tag{1.8}$$

effectively canceling the first of the surface terms in Eq. (1.5). At this stage we have:

$$\delta A_\tau = \int_0^\tau dt \left\{ \Big[\frac{\partial L}{\partial|\psi\rangle} - \frac{d}{dt}\frac{\partial L}{\partial|\dot\psi\rangle}\Big]|\delta\psi\rangle + \langle\delta\psi|\Big[\frac{\partial L}{\partial\langle\psi|} - \frac{d}{dt}\frac{\partial L}{\partial\langle\dot\psi|}\Big] \right\} - i\hbar\Big[\underbrace{\frac{\langle\delta\psi_\tau|\psi_\tau\rangle}{\langle\psi_\tau|\psi_\tau\rangle} + \frac{\langle\psi_0|\delta\psi_0\rangle}{\langle\psi_0|\psi_0\rangle}}_{=0}\Big], \tag{1.9}$$

where we observe that the last factor vanishes by virtue of the boundary conditions, and no quantities are left outside the integral sign. This overall cancellation, which is crucial for reaching the conclusions stated in the next paragraph, would not occur without the surface terms of A [cf. Eq. (1.1)], hence their importance.[29]

Since $|\delta\psi(t)\rangle$ and $\langle\delta\psi(t)|$ are independent at each instant, the condition $\delta A_\tau = 0$ implies that both factors multiplying these displacements inside the integral of Eq. (1.9) must be zero; we thus arrive at the Euler-Lagrange equations:

$$\frac{\partial L}{\partial\langle\psi|} - \frac{d}{dt}\frac{\partial L}{\partial\langle\dot\psi|} = 0, \tag{1.10a}$$

$$\frac{\partial L}{\partial|\psi\rangle} - \frac{d}{dt}\frac{\partial L}{\partial|\dot\psi\rangle} = 0. \tag{1.10b}$$

For clarity, let us compute all terms involved. Derivatives with respect to $\langle\psi|$ and $|\psi\rangle$ are

$$\frac{\partial L}{\partial\langle\psi|} = \frac{i\hbar}{2}\frac{|\dot\psi\rangle}{\langle\psi|\psi\rangle} - \frac{\hat H|\psi\rangle}{\langle\psi|\psi\rangle} - \frac{L|\psi\rangle}{\langle\psi|\psi\rangle}, \tag{1.11a}$$

$$\frac{\partial L}{\partial|\psi\rangle} = -\frac{i\hbar}{2}\frac{\langle\dot\psi|}{\langle\psi|\psi\rangle} - \frac{\langle\psi|\hat H}{\langle\psi|\psi\rangle} - \frac{\langle\psi|L}{\langle\psi|\psi\rangle}. \tag{1.11b}$$

Meanwhile, differentiating Eqs. (1.7) with respect to t gives

$$\frac{d}{dt}\frac{\partial L}{\partial\langle\dot\psi|} = -\frac{i\hbar}{2}\frac{|\dot\psi\rangle}{\langle\psi|\psi\rangle} + \frac{i\hbar}{2}\Big[\frac{\langle\psi|\dot\psi\rangle + \langle\dot\psi|\psi\rangle}{\langle\psi|\psi\rangle}\Big]\frac{|\psi\rangle}{\langle\psi|\psi\rangle}, \tag{1.12a}$$

$$\frac{d}{dt}\frac{\partial L}{\partial|\dot\psi\rangle} = \frac{i\hbar}{2}\frac{\langle\dot\psi|}{\langle\psi|\psi\rangle} - \frac{i\hbar}{2}\Big[\frac{\langle\psi|\dot\psi\rangle + \langle\dot\psi|\psi\rangle}{\langle\psi|\psi\rangle}\Big]\frac{\langle\psi|}{\langle\psi|\psi\rangle}. \tag{1.12b}$$

Finally, collecting terms we find, from (1.10),

$$\Big(i\hbar\frac{d}{dt} - \dot\gamma_1\Big)|\psi\rangle = \hat H|\psi\rangle, \tag{1.13a}$$

$$\langle\psi|\Big(i\hbar\frac{d^*}{dt} + \dot\gamma_2\Big) = -\langle\psi|\hat H, \tag{1.13b}$$

where $\dot\gamma_1$ and $\dot\gamma_2$ are defined as:

$$\dot\gamma_1 = i\hbar\frac{\langle\psi|\dot\psi\rangle}{\langle\psi|\psi\rangle} - \frac{\langle\psi|\hat H|\psi\rangle}{\langle\psi|\psi\rangle}, \quad \dot\gamma_2 = -i\hbar\frac{\langle\dot\psi|\psi\rangle}{\langle\psi|\psi\rangle} - \frac{\langle\psi|\hat H|\psi\rangle}{\langle\psi|\psi\rangle}. \tag{1.14}$$

Up to this point $|\psi\rangle$ and $\langle\psi|$ were regarded as independent quantities and therefore $\dot{\gamma}_1$ and $\dot{\gamma}_2$, the complex functions responsible for a gauge coupling between $|\psi\rangle$ and $\langle\psi|$ in Eqs. (1.13a) and (1.13b), are not supposed to be the conjugate of one another.

If, however, the Hamiltonian is hermitian (as it is in the vast majority of problems) then there exists a subset of solutions where $\langle\psi(t)| = [|\psi(t)\rangle]^\dagger$, for $0 \leq t \leq \tau$.[iii] Recall that the boundary conditions fix $|\psi_0\rangle$ and $\langle\psi_\tau|$, *but not* $|\psi_\tau\rangle$ and $\langle\psi_0|$. The subset of solutions we are concerned with is defined by the extra requirement that the end-point $\langle\psi_\tau|$ is fixed in such a way that when propagated backwards in time it matches $[|\psi_0\rangle]^\dagger$. With an hermitian Hamiltonian, Eq. (1.13b) *is* the dual of Eq. (1.13a), and therefore the requirement implies $|\psi_\tau\rangle = [\langle\psi_\tau|]^\dagger$, and, consequently, $\langle\psi(t)| = [|\psi(t)\rangle]^\dagger$ for all t. This reasoning also applies to restricted trial states.[iv]

Henceforth we shall always work with hermitian Hamiltonians and variational solutions where $|\psi\rangle$ and $\langle\psi|$ are dual vectors for all t. The boundary conditions are thus replaced by simple initial conditions and, since the *bra* and *ket* equations are equivalent, we will mostly work with the latter.

With these considerations in mind we rename the gauge factors, $\dot{\gamma}_1 = \dot{\gamma}$ and $\dot{\gamma}_2 = \dot{\gamma}^*$, and rewrite Eq. (1.13a) as:

$$\Big(i\hbar\frac{d}{dt} - \dot{\gamma}\Big)|\psi\rangle = \hat{H}|\psi\rangle. \tag{1.15}$$

The scalar $\dot{\gamma}$ can be removed by a simple transformation. Let us define the new, transformed wavefunction $|\Psi\rangle$ according to:

$$|\Psi\rangle \equiv |\psi\rangle e^{\frac{i}{\hbar}\gamma}. \tag{1.16}$$

It follows immediately that $|\Psi\rangle$ satisfies the familiar Schrödinger equation,

$$i\hbar|\dot{\Psi}\rangle = \hat{H}|\Psi\rangle. \tag{1.17}$$

Before drawing conclusions let us calculate the real and imaginary parts of $\dot{\gamma}$:

$$\frac{\dot{\gamma}+\dot{\gamma}^*}{2} = \frac{i\hbar}{2}\frac{\langle\psi|\dot{\psi}\rangle - \langle\dot{\psi}|\psi\rangle}{\langle\psi|\psi\rangle} - \frac{\langle\psi|H|\psi\rangle}{\langle\psi|\psi\rangle} = L(\psi),$$
$$\frac{\dot{\gamma}-\dot{\gamma}^*}{2i} = \frac{\hbar}{2}\frac{\langle\psi|\dot{\psi}\rangle + \langle\dot{\psi}|\psi\rangle}{\langle\psi|\psi\rangle} = \frac{\hbar}{2}\frac{d\log\langle\psi|\psi\rangle}{dt}.$$

Hence,

$$\dot{\gamma} = L(\psi) + \frac{i\hbar}{2}\frac{d\log\langle\psi|\psi\rangle}{dt}, \tag{1.19}$$

[iii] The hermitian adjoint of an object A is denoted by $A^\dagger$.

[iv] The preceding discussion may sound confusing, but this sort of analysis is typical in applications of the TDVP. In semiclassical methods, for example, variational solutions where the distinction between *bra* and *ket* variables is maintained prove to be both interesting and useful.[21;22;29;31]

and subsequent integration from 0 to t yields (setting $\gamma(0)$ to zero):

$$\gamma(t) = S(\psi) + i\hbar \log \sqrt{\langle\psi|\psi\rangle}. \tag{1.20}$$

Putting this back in Eq. (1.16) we deduce the insightful result:

$$|\Psi\rangle = \frac{|\psi\rangle}{\sqrt{\langle\psi|\psi\rangle}}\, e^{\frac{i}{\hbar}S(\psi)}. \tag{1.21}$$

Thus, the state $|\Psi\rangle$, which satisfies the usual Schrödinger equation, is just the original unrestricted trial state, but properly normalized and with an action phase. The phase is immaterial if $|\Psi\rangle$ stands for the state of the full system, since it represents only a global phase in that case.

However, the fact the time-dependent variational principle attaches a phase to the 'optimized' state vector, as we shall call it, is not an exclusivity of the unrestricted parametrization considered here – it is a general result, equally valid for other trial states. And, in many situations, the variational phase does become important, as is the case in guided-basis methods, where optimized states with restricted parametrizations (thus incapable of representing the entire system by themselves) are combined together in order to produce a more sophisticated total wavefunction. The technique developed in detail at Chapter 4 is an example of such kind of method.

1.2 Norm-constrained form of the TDVP

Direct application of the TDVP in the form presented earlier, for general unnormalized states, can be quite cumbersome in some cases, particularly when the trial state is represented as a linear superposition of basis functions, that is, when it consists of a *multiconfigurational ansatz*. To remedy this, we consider an alternative formulation, where normalization is secured by enforcing a constraint in the variational problem. The derivation below has been presented in Appendix A of Ref. [32] and is reproduced here with more details.[v]

Let us define the *modified Lagrangian* $\mathcal{L}$ and the squared-norm function $\mathcal{N}$,

$$\mathcal{L} = i\hbar\langle\psi|\dot{\psi}\rangle - \langle\psi|\hat{H}|\psi\rangle, \tag{1.22a}$$

$$\mathcal{N} = \langle\psi|\psi\rangle. \tag{1.22b}$$

[v] Constrained forms of the TDVP are studied in a series of papers by Ohta, beginning with Ref. [33]. However, in these works the issues regarding the consistency of boundary conditions in the variational problem and the need for including surface terms in the action functional are not discussed. More details on this subject are found in Refs. [13;29].

We notice that the original Lagrangian can be written as:

$$L = \frac{\mathcal{L}}{\mathcal{N}} - \frac{i\hbar}{2}\frac{d\log\mathcal{N}}{dt}. \tag{1.23}$$

In order to introduce the normalization constraint in the TDVP, we employ a real-valued Lagrange multiplier λ (because $\mathcal{N}$ is real) and reformulate the action functional (1.1) as follows:

$$A_\tau[\psi,\lambda] = \int_0^\tau dt\,\Big[\frac{\mathcal{L}}{\mathcal{N}} - \lambda(\mathcal{N}-1)\Big] - i\hbar\log\langle\psi_\tau|\psi_\tau\rangle, \tag{1.24}$$

where the total time derivative of Eq. (1.23) has been integrated and combined with the surface terms of A. We shall refer to the functional given in Eq. (1.24) as the *norm-constrained* action functional.

Evidently, imposition of a norm constraint is only feasible if free parameters, suitable for this purpose, are available in the trial state. A state expressed as a linear superposition of more elementary basis functions is the prototype trial state and fulfills this condition – examples are given in subsequent sections. For now, let us work with a generic trial state $|\psi\rangle$ and suppose that it copes with the above requirement. A small amount of definitiveness is convenient, however, and thus we assume $|\psi\rangle$ is parametrized by a finite set of n variables,

$$|\psi\rangle = |\psi(\xi)\rangle = |\psi(\xi_1,\xi_2,\ldots,\xi_n)\rangle, \quad \langle\psi| = \langle\psi(\xi^*)| = \langle\psi(\xi_1^*,\xi_2^*,\ldots,\xi_n^*)|. \tag{1.25}$$

Here, the parameters ξ are not necessarily complex – one may think of the complex conjugate sign as a device for distinguishing among *ket* parameters (ξ) and *bra* parameters (ξ^*). In particular, displacements induced by variations $\delta\xi$ and $\delta\xi^*$ are:

$$|\delta\psi\rangle = \sum_{k=1}^{n}\Big|\frac{\partial\psi}{\partial\xi_k}\Big\rangle\delta\xi_k, \quad \langle\delta\psi| = \sum_{k=1}^{n}\delta\xi_k^*\Big\langle\frac{\partial\psi}{\partial\xi_k^*}\Big|, \tag{1.26}$$

where the *bra* and *ket* derivatives can be calculated from any specific representation of $|\psi(\xi)\rangle$, e.g. in position representation we would have $\psi(x;\xi) = \langle x|\psi\rangle$, and therefore $\langle x|\partial\psi/\partial\xi_k\rangle = \partial\psi(x;\xi)/\partial\xi_k$.

In this way, the modified Lagrangian can be expressed as:

$$\mathcal{L}(\xi) = \sum_{k=1}^{n}\langle\psi|\partial\psi/\partial\xi_k\rangle\dot{\xi}_k - \langle\psi|\hat{H}|\psi\rangle. \tag{1.27}$$

Notice that $\mathcal{L}$ is independent of $\dot{\xi}^*$.

Following these considerations, variation of the norm-constrained action functional

with respect to the set of variables λ, ξ and ξ^*, yields

$$\delta A_\tau = \delta\Gamma + \int_0^\tau dt\Big[(\mathcal{N}-1)\delta\lambda\Big] + \int_0^\tau dt \sum_{k=1}^n \left\{ \Big[\frac{\partial(\mathcal{L}/\mathcal{N})}{\partial\xi_k} - \frac{d}{dt}\frac{\partial(\mathcal{L}/\mathcal{N})}{\partial\dot{\xi}_k} - \lambda\frac{\partial\mathcal{N}}{\partial\xi_k}\Big]\delta\xi_k + \delta\xi_k^*\Big[\frac{\partial(\mathcal{L}/\mathcal{N})}{\partial\xi_k^*} - \lambda\frac{\partial\mathcal{N}}{\partial\xi_k^*}\Big]\right\}, \quad (1.28)$$

where we have already performed the partial integrations and collected surface terms into the quantity $\delta\Gamma$. Once more these terms cancel off by virtue of the boundary conditions:

$$\delta\Gamma = \sum_{k=1}^n \frac{\partial(\mathcal{L}/\mathcal{N})}{\partial\dot{\xi}_k}\delta\xi_k\bigg|_0^\tau - i\hbar\,\delta\Big(\log\langle\psi_\tau|\psi_\tau\rangle\Big) \quad (1.29)$$

$$= i\hbar\sum_{k=1}^n \frac{\langle\psi|(\partial\psi/\partial\xi_k)\rangle\delta\xi_k}{\langle\psi|\psi\rangle}\bigg|_0^\tau - i\hbar\sum_{k=1}^n\Big[\frac{\delta\xi_{\tau k}^*\langle(\partial\psi_\tau/\partial\xi_{\tau k}^*)|\psi_\tau\rangle}{\langle\psi_\tau|\psi_\tau\rangle} + \frac{\langle\psi_\tau|(\partial\psi_\tau/\partial\xi_{\tau k})\rangle\delta\xi_{\tau k}}{\langle\psi_\tau|\psi_\tau\rangle}\Big]$$

$$= i\hbar\Big[\frac{\langle\psi_\tau|\delta\psi_\tau\rangle}{\langle\psi_\tau|\psi_\tau\rangle} - \frac{\langle\psi_0|\delta\psi_0\rangle}{\langle\psi_0|\psi_0\rangle}\Big] - i\hbar\Big[\frac{\langle\delta\psi_\tau|\psi_\tau\rangle}{\langle\psi_\tau|\psi_\tau\rangle} + \frac{\langle\psi_\tau|\delta\psi_\tau\rangle}{\langle\psi_\tau|\psi_\tau\rangle}\Big]$$

$$= -i\hbar\Big[\frac{\langle\delta\psi_\tau|\psi_\tau\rangle}{\langle\psi_\tau|\psi_\tau\rangle} + \frac{\langle\psi_0|\delta\psi_0\rangle}{\langle\psi_0|\psi_0\rangle}\Big] = 0, \quad (1.30)$$

where (1.4) has been invoked in the last line.

Since $\delta\lambda$, $\delta\xi$ and $\delta\xi^*$ are independent, the factors multiplying these variations under the integral sign in (1.28) must vanish identically. We are thus left with the system of equations:

$$\frac{\partial\mathcal{L}}{\partial\xi_k} - \frac{d}{dt}\frac{\partial\mathcal{L}}{\partial\dot{\xi}_k} - (\lambda+\mathcal{L})\frac{\partial\mathcal{N}}{\partial\xi_k} = 0, \quad (1.31a)$$

$$\frac{\partial\mathcal{L}}{\partial\xi_k^*} - (\lambda+\mathcal{L})\frac{\partial\mathcal{N}}{\partial\xi_k^*} = 0, \quad (1.31b)$$

$$\mathcal{N}-1 = 0, \quad (1.31c)$$

for $1 \le k \le n$. By enforcing the additional requirement that $|\psi\rangle$ and $\langle\psi|$ represent dual vectors for all t, Eqs. (1.31a) and (1.31b), despite their apparent difference, become strictly equivalent (this can be easily verified for the examples given in the next two subsections). In practice, Eq. (1.31b) is more convenient to work with, since there is no need for computing total derivatives. Meanwhile, Eq. (1.31c) ensures norm conservation of the trial state (in writing the system we have already put $\mathcal{N} = 1$ in the first two equations).

1.2.1 Full variational equations with static basis functions

Let us exemplify the norm-constrained formulation by considering a widely used variational trial state:

$$|\psi\rangle = \sum_{j=1}^m |\phi_j\rangle c_j, \quad (1.32)$$

with a *static*, non-orthogonal basis set spanned by m states $|\phi\rangle$, whose projector is

$$\hat{P} = \sum_{i=1}^{m}\sum_{j=1}^{m} |\phi_i\rangle (P^{-1})_{ij} \langle\phi_j|, \quad P_{ij} = \langle\phi_i|\phi_j\rangle. \tag{1.33}$$

Notice that the basis set is not assumed to be complete, i.e. in general $\hat{P} \neq \hat{1}$. Variations in the trial state are therefore restricted, with the complex amplitudes c playing the role of variables ξ of the previous section. In what follows summation ranges are omitted.

The modified Lagrangian and squared norm are, respectively,

$$\mathcal{L} = \sum_{ij} \left(i\hbar\, c_i^* \langle\phi_i|\phi_j\rangle \dot{c}_j - c_i^* c_j \langle\phi_i|\hat{H}|\phi_j\rangle \right), \quad \mathcal{N} = \sum_{ij} c_i^* \langle\phi_i|\phi_j\rangle c_j, \tag{1.34}$$

and the Euler-Lagrange equation (1.31b) translates to:

$$\frac{\partial \mathcal{L}}{\partial c_i^*} = (\lambda + \mathcal{L}) \frac{\partial \mathcal{N}}{\partial c_i^*}. \tag{1.35}$$

Computing the required partial derivatives we arrive at:

$$\sum_j \langle\phi_i|\phi_j\rangle (i\hbar\, \dot{c}_j - \mathcal{L}\, c_j) - \sum_j \langle\phi_i|\hat{H}|\phi_j\rangle c_j = \lambda \sum_j \langle\phi_i|\phi_j\rangle c_j. \tag{1.36}$$

The Lagrange multiplier can be easily determined. Multiplying the above equation by c_i^*, summing on i, and identifying $\mathcal{L}$ and $\mathcal{N}$ from (1.34) in the resulting expression, one finds $\lambda = 0$. Moreover, the equation of motion can be further simplified by defining a new set of amplitudes a, related to c by a global phase as follows

$$a_j = c_j e^{\frac{i}{\hbar}\int_0^\tau dt\, \mathcal{L}}. \tag{1.37}$$

Therefore, setting $\lambda = 0$ and employing the new set of amplitudes, Eq. (1.36) reduces to:

$$i\hbar \sum_j \langle\phi_i|\phi_j\rangle \dot{a}_j = \sum_j \langle\phi_i|\hat{H}|\phi_j\rangle a_j, \tag{1.38}$$

which is the well-known form assumed by the Schrödinger equation when a finite, static, and non-orthogonal basis set is used to represent the quantum state $|\psi\rangle$.

The system's wavefunction with the phase-shifted amplitudes is:

$$|\Psi\rangle = \sum_j |\phi_j\rangle a_j = \sum_j |\phi_j\rangle c_j e^{\frac{i}{\hbar}\int_0^\tau dt\, \mathcal{L}} = |\psi\rangle e^{\frac{i}{\hbar}\int_0^\tau dt\, \mathcal{L}}. \tag{1.39}$$

Note that the condition $\mathcal{N} = \langle\psi|\psi\rangle = 1$ implies $\langle\psi|\dot{\psi}\rangle$ purely imaginary (because $d\mathcal{N}/dt = 2\,\mathrm{Re}\,\langle\psi|\dot{\psi}\rangle = 0$); thus $\mathcal{L}$ is real and so is the accumulated phase between $|\Psi\rangle$ and $|\psi\rangle$.

Finally, we note that, in terms of $|\Psi\rangle$, the Euler-Lagrange equations can be summarized

by

$$\frac{\partial}{\partial a_i^*}\sum_{kj}\Big(i\hbar\, a_k^*\langle\phi_k|\phi_j\rangle\dot{a}_j - a_k^* a_j\langle\phi_k|\hat{H}|\phi_j\rangle\Big) = 0, \tag{1.40}$$

or, more generally,

$$\langle\delta\Psi|\Big[i\hbar\frac{d}{dt} - \hat{H}\Big]|\Psi\rangle = 0. \tag{1.41}$$

This is the so-called Dirac-Frenkel version of the variational principle.[34;35]

As we mentioned, Eq. (1.38) could have been worked out directly from the Schrödinger equation, and this makes the whole variational machinery seem unnecessary. The usefulness of the TDVP can only be truly appreciated when it is applied to more sophisticated trial states. Next we look at one such example.

1.2.2 Full variational equations with time-dependent basis functions

Once again we consider the multiconfigurational trial state:

$$|\psi\rangle = \sum_{j=1}^{m}|\phi_j\rangle c_j, \quad \text{with:} \quad \hat{P} = \sum_{i=1}^{m}\sum_{j=1}^{m}|\phi_i\rangle(P^{-1})_{ij}\langle\phi_j|, \quad P_{ij} = \langle\phi_i|\phi_j\rangle. \tag{1.42}$$

This time, however, the basis functions are assumed to be dynamic, i.e. each basis element $|\phi_j\rangle$ depends on a s-dimensional array of parameters $x_j = x_j(t)$, and evolves in time according to:

$$|\phi_j\rangle = |\phi(x_j)\rangle = |\phi(x_{j1}, x_{j2}, \ldots, x_{js})\rangle \quad \Rightarrow \quad \frac{d}{dt}|\phi_j\rangle = \sum_{\nu=1}^{s}|\partial_\nu\phi_j\rangle\dot{x}_{j\nu}, \quad (1 \le j \le m), \tag{1.43}$$

where a short-hand notation for partial derivatives is employed: $\partial_\nu\phi_j = \partial\phi_j/\partial x_{j\nu}$. In this way, a more flexible wavefunction is produced and, in principle, more accurate solutions can be achieved through the TDVP, since both amplitudes c and basis-set variables x are allowed to be adjusted.

The modified Lagrangian is:

$$\mathcal{L} = \sum_{ij}\Big(i\hbar\, c_i^*\dot{c}_j\langle\phi_i|\phi_j\rangle + i\hbar\, c_i^* c_j\sum_{\nu}\langle\phi_i|\partial_\nu\phi_j\rangle\dot{x}_{j\nu} - c_i^* c_j\langle\phi_i|\hat{H}|\phi_j\rangle\Big). \tag{1.44}$$

Similarly to the example developed earlier, one easily concludes that the multiplier associated with the norm constraint is zero, and that the equations are simplified by adding a global phase to the quantum state. In order to avoid repetitive arguments, instead of starting from the Euler-Lagrange equations in the form (1.31), here we shall consider the phase-shifted state,

$$|\Psi\rangle = \sum_j|\phi_j\rangle a_j = |\psi\rangle e^{\frac{i}{\hbar}\int_0^\tau dt\,\mathcal{L}}, \tag{1.45}$$

and work directly from the Dirac-Frenkel variational equation (1.41), which in the present

case reads

$$\frac{\partial}{\partial \xi^*}\sum_{kj}\Big(i\hbar\, a_k^*\langle\phi_k|\phi_j\rangle\dot{a}_j + i\hbar\, a_k^* a_j\sum_\nu\langle\phi_k|\partial_\nu\phi_j\rangle\dot{x}_{j\nu} - a_k^* a_j\langle\phi_k|\hat{H}|\phi_j\rangle\Big) = 0, \tag{1.46}$$

for $\xi^* = (x_{i\mu}, a_i^*)$, with $1 \leq i \leq m$, $1 \leq \mu \leq s$.

The equation for the set of amplitudes a is immediately found from (1.46) – setting $\xi^* = a_i^*$ and performing the partial derivatives we get:

$$i\hbar\sum_j\langle\phi_i|\phi_j\rangle\dot{a}_j = \sum_j\Big[\langle\phi_i|\hat{H}|\phi_j\rangle - i\hbar\sum_\nu\langle\phi_i|\partial_\nu\phi_j\rangle\dot{x}_{j\nu}\Big]a_j. \tag{1.47}$$

On the other hand, setting $\xi^* = x_{i\mu}$, and recalling that $x_{i\mu}$ must be a *bra* variable (we are not supposed to differentiate with respect to x's belonging to the *ket* $|\Psi\rangle$) leads to:

$$i\hbar\sum_j a_i^* a_j\sum_\nu\langle\partial_\mu\phi_i|\partial_\nu\phi_j\rangle\dot{x}_{j\nu} + i\hbar\sum_j a_i^*\langle\partial_\mu\phi_i|\phi_j\rangle\dot{a}_j = \sum_j a_i^* a_j\langle\partial_\mu\phi_i|\hat{H}|\phi_j\rangle. \tag{1.48}$$

The latter equation takes on a much more illuminating form if we use the amplitude equation to replace the terms containing $\dot{a}$. For that purpose, we rewrite (1.47) as:

$$i\hbar\,\dot{a}_j = \sum_{kl}(P^{-1})_{jk}\Big[\langle\phi_k|\hat{H}|\phi_l\rangle - i\hbar\sum_\nu\langle\phi_k|\partial_\nu\phi_l\rangle\dot{x}_{l\nu}\Big]a_l. \tag{1.49}$$

Then we proceed with the following manipulations,

$$\begin{aligned} i\hbar\sum_j a_i^*\langle\partial_\mu\phi_i|\phi_j\rangle\dot{a}_j &= \sum_{jkl} a_i^*\langle\partial_\mu\phi_i|\phi_j\rangle(P^{-1})_{jk}\Big[\langle\phi_k|\hat{H}|\phi_l\rangle - i\hbar\sum_\nu\langle\phi_k|\partial_\nu\phi_l\rangle\dot{x}_{l\nu}\Big]a_l \\ &= \sum_l a_i^*\langle\partial_\mu\phi_i|\Big\{\sum_{jk}|\phi_j\rangle(P^{-1})_{jk}\langle\phi_k|\Big\}\Big[\hat{H}|\phi_l\rangle - i\hbar\sum_\nu|\partial_\nu\phi_l\rangle\dot{x}_{l\nu}\Big]a_l \\ &= \sum_j a_i^* a_j\langle\partial_\mu\phi_i|\hat{P}\hat{H}|\phi_j\rangle - i\hbar\sum_j a_i^* a_j\sum_\nu\langle\partial_\mu\phi_i|\hat{P}|\partial_\nu\phi_j\rangle\dot{x}_{j\nu}, \end{aligned} \tag{1.50}$$

where we have identified the basis projector $\hat{P}$, defined in (1.42), and renamed dummy indexes in the last line. Putting this in (1.48) yields (using $|\phi\rangle = \hat{P}|\phi\rangle$ on the right-hand side):

$$i\hbar\sum_{j\nu}\Big[a_i^*\langle\partial_\mu\phi_i|(\hat{1}-\hat{P})|\partial_\nu\phi_j\rangle a_j\Big]\dot{x}_{j\nu} = \sum_j a_i^*\langle\partial_\mu\phi_i|(\hat{H}\hat{P}-\hat{P}\hat{H})|\phi_j\rangle a_j. \tag{1.51}$$

The above result shows that, if the time evolution drives the system's wavefunction to a region in parameter space where $\langle\partial_\mu\phi_i|\partial_\nu\phi_j\rangle = \langle\partial_\mu\phi_i|\hat{P}|\partial_\nu\phi_j\rangle$ (i.e. a region where the basis-set is effectively complete) the equations for the variables x become undetermined; in other words, the dynamics of individual basis functions is immaterial during the times at which the basis set projector $\hat{P}$ behaves as the identity operator – under such circumstances,

the Hamiltonian will also commute with $\hat{P}$, and both sides of Eq. (1.51) approach zero.

As a final remark, we note that the multiconfigurational trial state (1.42) is actually ambiguous, with many possible values of parameters x and a representing the same physical state. In conventional multiconfigurational techniques[36] other constraints (of a more complicated sort) are imposed (for example, the basis functions are assumed to be orthonormal for all t, and non-holonomic constraints, involving conditions over time-derivatives, are often employed) so that redundancies are lifted and the indeterminate character of solutions is avoided. Nevertheless, this illustrative example provides many insights concerning the TDVP. In this work, we shall not consider full-variational multiconfigurational methods any further, but the observations made here will be useful in clarifying some aspects of the guided-basis technique to be developed at Chapter 4.

1.3 Generalized coherent states – overview

Coherent states are most elegantly discussed within the context of group theory; this is the point of view advocated in this work. We shall not venture into the group-theoretical formalism itself though – on that subject see Refs. [6;9;37–39]. In this thesis, we deliberately adopt a more pragmatic approach according to which a coherent state is given a functional definition from where its fundamental geometrical properties can be straightforwardly derived. The functional form can also be worked down to a Hilbert space expansion over a proper set of orthonormal basis functions, thus providing further insight in what concerns the coherent-state's structure.

For the moment, all such concepts shall be considered in broad terms only, since this chapter is dedicated to a brief overview of the generalized formalism (although Glauber coherent states are used in §1.3.4 to partially illustrate the discussion). The ideas presented here will truly materialize later in Chapters 2 and 3 where specific sets of coherent states with non-trivial geometries are examined in detail. The development closely follows Refs. [13;29].

1.3.1 Preliminaries

Coherent states are Hilbert space vectors labeled by a complex array $z = (z_1, \ldots, z_d)$. They can be understood as the result of a z-parametrized displacement operator acting on a *reference state* $|\Phi_0\rangle$ which should be adequately chosen among the basis vectors of the Hilbert space in question, hereby denoted $\mathcal{H}$ – this is precisely the 'functional definition' mentioned earlier. The general non-normalized form is

$$|z\} = \hat{\mathcal{G}}(z)|\Phi_0\rangle, \quad \hat{\mathcal{G}}(z=0) = \hat{1}, \tag{1.52}$$

where $\hat{1}$ is the identity operator in $\mathcal{H}$. As shown above, the reference state is recovered by setting all entries of z to zero.

A special notation is introduced in Eq. (1.52): a *non-normalized* coherent state will be denoted as $|z\}$. These curly *ket* states are analytical in z, while the *bra* states $\{z|$ are analytical in the complex conjugate variable,

$$\frac{\partial |z\}}{\partial z_\alpha^*} = 0, \quad \frac{\partial \{z|}{\partial z_\alpha} = 0, \quad (1 \leq \alpha \leq d). \tag{1.53}$$

Notice that the normalized state $|z\rangle$ is not analytical in z for it depends on z^* through the normalization factor $\{z|z\}^{-\frac{1}{2}}$; an analogous observation applies to $\langle z|$.

In this work, the following convention is adopted: entries of the coherent-state vector z will be labeled by Greek letters, primarily α, β, γ and secondarily μ, ν, η. Also, the number of elements in the z array will be denoted d. In the next section this size will be identified as the number of degrees of freedom of the classical phase space associated with the coherent-state's dynamics.

Let n be the dimension of $\mathcal{H}$; this space is thus spanned by n orthonormal basis vectors $|\Phi\rangle$ (including the reference state) and the closure relation may be written as:

$$\hat{1} = \sum_{k=0}^{n-1} |\Phi_k\rangle\langle\Phi_k|, \quad \langle\Phi_k|\Phi_l\rangle = \delta_{kl} \quad (0 \leq k, l \leq n-1). \tag{1.54}$$

Since the set $\{|\Phi_0\rangle, |\Phi_1\rangle, \ldots, |\Phi_{n-1}\rangle\}$ is assumed to be complete, it is possible to reduce the functional form of $|z\}$, as given in Eq. (1.52), into a linear combination of the n basis vectors,

$$|z\} = |\Phi_0\rangle + \sum_{k=1}^{n-1} |\Phi_k\rangle \, \mathcal{C}_k(z), \quad (\mathcal{C}_k(0) = 0), \tag{1.55}$$

with the coefficients $\mathcal{C}_k(z)$ usually being highly nonlinear functions of the complex variable z; it is in this sense that one says coherent states constitute *nonlinear parametrizations*. An important observation is that, in general, we have $d \ll n$, i.e. the dimension of z is normally much less than the size of the Hilbert space where $|z\rangle$ lives, as we shall see.

Coherent states belonging to different groups are characterized by their distinct geometrical properties. These, in turn, are described in terms of a function f related to the scalar product between two non-normalized coherent states, defined by

$$f(z^*, z') = \log\{z|z'\}. \tag{1.56}$$

This function is a central object of the formalism; it is called the *Kähler potential*[6] (or more correctly, its analytical continuation, since we have $z' \neq z$).

For instance, in terms of f, the normalized state may be simply expressed as

$$|z\rangle = \frac{|z\}}{\sqrt{\{z|z\}}} = |z\} \exp\Big[-\tfrac{1}{2} f(z^*, z)\Big]. \tag{1.57}$$

Lets introduce further geometrical elements.

The *classical phase-space metric* $g(z^*, z)_{\alpha\beta}$ is an hermitian $d \times d$ matrix defined through the cross derivatives of the real function $f(z^*, z)$ with respect to its complex arguments, treating z and z^* as independent variables:

$$g(z^*, z)_{\alpha\beta} = \frac{\partial^2 f(z^*, z)}{\partial z_\alpha \partial z^*_\beta}. \tag{1.58}$$

The one-to-one relation between coherent states and elements of well-defined quotient spaces of Lie groups ensures that the z parametrization is non-redundant; and this, in turn, ensures that g is a non-degenerate matrix.[6;9]

One of the most important results provided by the group-theoretical framework is the existence of a resolution of the identity operator (1.54) in terms of coherent states. This means that the non-orthogonal coherent states span an over-complete basis of $\mathcal{H}$; the closure relation is expressed in integral form:

$$\hat{1} = \int d\mu(z^*, z) |z\rangle\langle z| = \int d\mu(z^*, z) e^{-f(z^*,z)} |z\}\{z|. \tag{1.59}$$

The integration domain depends on the specific type of coherent state being considered – for semisimple compact Lie Groups or the Heisenberg-Weyl group, for example, the domain extends over the entire d-dimensional complex plane. This includes the parametrizations studied in Chapters 2 and 3. Thus, despite the fact that, usually, $d \ll n$ (as mentioned earlier) it is generally possible to represent an arbitrary state belonging to $\mathcal{H}$ in terms of coherent states using a continuous superposition of $|z\rangle$ vectors (or a judiciously chosen discrete set).

The general form of the *integration measure* $d\mu(z^*, z)$ in (1.59) is also found by group-theory arguments; it is proportional to the metric's determinant,

$$d\mu(z^*, z) = \kappa \det[g(z^*, z)] \frac{d^2 z}{\pi^d}, \tag{1.60}$$

where the area element (written in abbreviated form in the above equation) may be expressed in any of the following equivalent ways:

$$\frac{d^2 z}{\pi^d} \equiv \prod_{\alpha=1}^{d} \frac{d^2 z_\alpha}{\pi} = \prod_{\alpha=1}^{d} \frac{d(\mathrm{Re}\, z_\alpha) d(\mathrm{Im}\, z_\alpha)}{\pi} = \prod_{\alpha=1}^{d} \frac{dz_\alpha dz^*_\alpha}{2\pi i}. \tag{1.61}$$

By definition, the measure is *invariant* under group transformations of the z variables.

These group transformations refer to the particular Lie group associated with the coherent state description. They are induced on the parameters z by means of the action of group operators (or rather, their Hilbert space realizations) upon the state $|z\rangle$. This attribute is important for future developments in this work.

The constant κ figuring in Eq. (1.60) is determined by normalization of the closure relation (1.59) – e.g. by setting the expectation value of (1.59) in the reference state to unity, $\langle\Phi_0|\hat{1}|\Phi_0\rangle = 1$. Therefore, κ depends on the quantum numbers that characterize $\mathcal{H}$ (cf. Appendixes B and C for specific examples). Notice that, as indicated in (1.60), the measure is a real function of both z and z^*; however, in order to shorten the notation, we shall write simply $d\mu(z)$.

Finally, let us consider arbitrary states $|\psi\rangle$ and $\langle\varphi^*|$;[vi] We may write, using (1.59),

$$\psi(w^*) = \int d\mu(z^*, z)\, \{w|z\}\, \psi(z^*)\, e^{-f(z^*,z)}, \tag{1.62a}$$

$$\varphi(w) = \int d\mu(z^*, z)\, \varphi(z)\, \{z|w\}\, e^{-f(z^*,z)}. \tag{1.62b}$$

Notice that $\psi(z^*) = \{z|\psi\rangle$ is an analytical function of z^* and, conversely, $\varphi(z) = \langle\varphi^*|z\}$ is analytical in z.[6] We shall put these identities to use later on, at Chapter 6.

1.3.2 Coherent states as trial functions

Let us now look at the coherent-state variables $(z_1, z_2, \ldots, z_d)$ as a set of time-dependent parameters $z(t)$ and investigate the consequences of taking $|z\}$ as a trial state in the TDVP. The purpose here is to approximately describe the dynamics of a quantum system governed by an Hamiltonian $\hat{H}$ (which is left unspecified). In the present case, it is convenient to work with the standard form of the variational principle (i.e. without normalization constraints).[6]

We begin by writing the general form of the Lagrangian,

$$L(z) = \frac{i\hbar}{2}\Big[\frac{\{z|\dot{z}\} - \{\dot{z}|z\}}{\{z|z\}}\Big] - \frac{\{z|\hat{H}|z\}}{\{z|z\}}, \tag{1.63}$$

and by introducing some useful terminology. The first term of (1.63), the one containing the time-derivatives $|\dot{z}\}$ and $\{\dot{z}|$, will be referred to as the *geometrical* part of $L(z)$. Meanwhile, the second term, which is simply the coherent-state expectation value of the Hamiltonian, will be referred to as the *dynamical part*; this part defines the *energy function*,

$$E(z^*, z) = \frac{\{z|\hat{H}|z\}}{\{z|z\}} = \langle z|\hat{H}|z\rangle, \tag{1.64}$$

which is a real function, since $\hat{H}$ is hermitian.

[vi] The asterisk on $\langle\varphi^*|$ is simply meant to compensate for the complex conjugation of *bra* representations, for example: $\langle\varphi^*|x\rangle = \varphi(x)$.

By virtue of the coherent-state's analytical property (1.53) the geometrical part of the Lagrangian can be straightforwardly expressed in terms of derivatives of the Kähler potential $f(z^*, z)$ [cf. Eq. (1.56)], which we denominate *Kähler gradients*; for example:

$$\frac{\{z|\dot{z}\}}{\{z|z\}} = \sum_{\alpha=1}^{d} \frac{\partial \log\{z|z\}}{\partial z_\alpha} \dot{z}_\alpha = \sum_{\alpha=1}^{d} \frac{\partial f(z^*, z)}{\partial z_\alpha} \dot{z}_\alpha. \tag{1.65}$$

Hence we find a workable formula for $L(z)$,

$$L(z) = \frac{i\hbar}{2} \sum_{\alpha=1}^{d} \left[\frac{\partial f(z^*, z)}{\partial z_\alpha} \dot{z}_\alpha - \frac{\partial f(z^*, z)}{\partial z_\alpha^*} \dot{z}_\alpha^* \right] - E(z^*, z). \tag{1.66}$$

The action functional (1.1), for paths $z(t)$ with $0 \leq t \leq \tau$, in the present case reads:

$$A_\tau(z) = \int_0^\tau dt\, L(z) - \frac{i\hbar}{2} \Big[f(z_\tau^*, z_\tau) + f(z_0^*, z_0) \Big]. \tag{1.67}$$

The variational problem consists of finding paths that obey the stationary condition $\delta A_\tau(z) = 0$, together with boundary conditions (1.4), which here translate to $|\delta z_0\} = 0$ and $\{\delta z_\tau| = 0$, thereby fixing the values of initial and final points, $z_0 = z(0)$ and $z_\tau^* = z^*(\tau)$, respectively.

The usual manipulations yield the Euler-Lagrange equations,

$$\frac{\partial L}{\partial z_\alpha^*} - \frac{d}{dt} \frac{\partial L}{\partial \dot{z}_\alpha^*} = 0, \tag{1.68a}$$

$$\frac{\partial L}{\partial z_\alpha} - \frac{d}{dt} \frac{\partial L}{\partial \dot{z}_\alpha} = 0. \tag{1.68b}$$

We recall that, in carrying out the calculations leading to Eqs. (1.68), one pretends that $|z\}$ and $\{z|$ are independent. However, following the prescription delineated earlier in §1.1.1, once the Euler-Lagrange equations are found, attention shall be restricted to solutions where the *bra* and *ket* states represent dual vectors, i.e. solutions where $z(t)$ and $z^*(t)$ are in fact related by complex conjugation. Then, Eqs. (1.68a) and (1.68b) are equivalent – we choose to work with the former.

The equations of motion for the coherent-state vector z are immediately obtained from (1.68a) – computing the required derivatives and expressing these in terms of already known geometrical ingredients, one arrives at:

$$\sum_{\beta=1}^{d} \dot{z}_\beta g(z^*, z)_{\beta\alpha} = -\frac{i}{\hbar} \frac{\partial E(z^*, z)}{\partial z_\alpha^*}, \quad (1 \leq \alpha \leq d). \tag{1.69}$$

Let us now make a few comments regarding this dynamical equation.

The group-theoretical formalism assures us that Eq. (1.69) describes a *classical* Hamiltonian system in a strict sense: the space spanned by z constitutes a *phase space* with d

degrees of freedom which exhibits a symplectic structure, i.e. the equation of motion can be written in terms of non-degenerate Poisson brackets.[9;29]

Moreover, the measure (1.60) that equips the coherent-state closure relation, is not only invariant under group transformations but also invariant under the 'classical flow' produced by Eq. (1.69); that is, if $z(t)$ obeys the latter equation, then

$$d\mu(z(t_2)) = d\mu(z(t_1)), \tag{1.70}$$

for any two instants t_1 and t_2 – a property that we recognize as a generalized form of the Liouville theorem. The above relation is proved in Appendix A. Remarkably, it remains valid even when the system's Hamiltonian has explicit time dependence.[29]

An additional connection between the present framework and the classical Hamiltonian formalism is found by considering the action functional (1.67). It is shown in Appendix A that, when $A_\tau(z)$ is evaluated over a trajectory $z(t)$ satisfying (1.69), it becomes a complex-valued function whose 'natural' arguments are (z^*_τ, z_0, τ), in the sense that derivatives with respect to these variables are well defined and given by:

$$\frac{i}{\hbar}\frac{\partial A_\tau(z^*_\tau, z_0)}{\partial z^*_{\tau\gamma}} = \frac{\partial f(z^*_\tau, z_\tau)}{\partial z^*_{\tau\gamma}}, \quad \frac{i}{\hbar}\frac{\partial A_\tau(z^*_\tau, z_0)}{\partial z_{0\gamma}} = \frac{\partial f(z^*_0, z_0)}{\partial z_{0\gamma}}, \quad \frac{\partial A_\tau(z^*_\tau, z_0)}{\partial \tau} = -E(z^*_\tau, z_\tau), \tag{1.71}$$

while derivatives with respect to z^*_0 and z_τ vanish. The above relations are the signature of a properly defined classical action integral,[13] and the function $A_\tau(z^*_\tau, z_0, \tau)$ is thus called the *complex action*. The relations listed in (1.71) are put to use in Chapter 6, where further classical aspects of the coherent-state formalism (related to the system's stability matrix) are uncovered.

Going back to Eq. (1.69), another interesting point to be noticed is the fact that the coherent-state geometry introduces a curvature in phase space by means of the metric $g(z^*, z)$. One now can distinguish between two kinds of coupling between the components of the vector z: a *dynamical coupling* via the energy function $E(z^*, z)$, and a *geometrical coupling* induced by $g(z^*, z)$.

As previously mentioned, the metric is non-degenerate, meaning that it can always be inverted. Thus we may rewrite (1.69) as below,[vii]

$$\dot{z}_\alpha = -\frac{i}{\hbar}\sum_{\beta=1}^{d} g^{-T}_{\alpha\beta}\frac{\partial E}{\partial z^*_\beta}, \quad (1 \leq \alpha \leq d), \tag{1.72}$$

where the arguments of E and g have been omitted for compactness. For the same reason, we write $g^{-T}_{\alpha\beta}$ instead of $(g^{-T})_{\alpha\beta}$ – we shall recurrently employ this kind of notation, relying on the context to prevent confusions. It is often found that considerable simplification is achieved by effecting the multiplication that brings (1.69) to (1.72).

[vii] The transpose of a matrix A is denoted A^T. The inverse transpose is abbreviated as A^{-T}.

Finally, we note that the traditional time-independent variational principle is recovered by considering critical points of (1.72). Indeed, putting $\dot{z} = 0$ in that equation we get:

$$\frac{\partial E(z^*, z)}{\partial z_\alpha} = 0, \quad (1 \leq \alpha \leq d), \tag{1.73}$$

where the fact that g is non-degenerated has been invoked in order to eliminate it from the above system.[viii] Since the energy function is usually nonlinear in the coherent-state's parameters z, roots to Eq. (1.73) have to be found by iterative self-consistent techniques.

1.3.3 Classical propagation scheme

As previously discussed in §1.1, the TDVP not only provides equations of motion for the trial state's parameters but it additionally attaches a phase to the corresponding state vector, which is simply the time integral of the Lagrangian function computed over the stationary path. In the present case, the phase is the *classical action*,[ix] or simply *action*, computed along the trajectory $z(t)$ governed by Eq. (1.72) – explicitly:

$$S(z;\tau) = \int_0^\tau dt\, L(z) = \int_0^\tau dt\, \Big\{ \mathrm{Im}\Big[-\hbar \sum_{\alpha=1}^{d} \frac{\partial f(z^*, z)}{\partial z_\alpha} \dot{z}_\alpha \Big] - E(z^*, z) \Big\}, \tag{1.74}$$

where τ denotes the final time, and Eq. (1.66) has been substituted with a minor abbreviation. Thus the properly normalized and 'optimized' coherent-state is

$$|z_t\rangle e^{\frac{i}{\hbar} S(z_t)}, \quad \text{with} \quad z_t = z(z_0, t), \tag{1.75}$$

where time arguments have been written as subscripts.

Let us now consider the following situation. Suppose we are investigating a system whose initial state $|\psi_0\rangle$ can be prepared in such a way that it may be adequately represented by a coherent-state, i.e. $|\psi_0\rangle = |z_i\rangle$. Then we could attempt a crude dynamical description by approximating $|\psi_t\rangle$, for $t > 0$ by a coherent state $|z_t\rangle$; or, in other words, by taking $|z_t\rangle$ as a trial state subjected to the boundary condition $|z_0\rangle = |z_i\rangle$ in the TDVP. The approximate solution would be

$$|\psi_t\rangle = e^{-\frac{i}{\hbar}\hat{H}t} |z_i\rangle \approx |z_t\rangle e^{\frac{i}{\hbar} S(z_t)}, \quad \text{with} \quad z_t = z(z_i, t). \tag{1.76}$$

The above equation, together with (1.72) and (1.74), defines a primitive propagation method, the *classical propagation scheme*, according to the terminology of Ref. [29] (see 'Appendix B' of that work for a complementary discussion). The denomination stems from

[viii] It may be mathematically convenient, however, to keep g in (1.73) since it usually simplifies the algebraic equation.

[ix] We shall always refer to the integral $S(z;t)$ of Eq. (1.74) simply as the *action*; meanwhile the quantity $A(z_t^*, z_0)$ of Eq. (1.67) will always be referred to as the *complex action*.

the fact that only classical ingredients (in the generalized sense) are present in Eq. (1.76).

Most often, the classical propagation scheme provides reasonable wavefunctions only for very short propagation times – although, occasionally, mean-values computed with said wavefunction may be surprisingly accurate. At any rate, the prescription summarized in Eq. (1.76) serves as a reference method against which more sophisticated approaches (such as that developed in Chapter 4) may be confronted, being thus useful, to that extent, for identifying 'non-classical' behavior. Note that the meaning of 'classical', as the term is understood here, depends on the particular coherent-state parametrization chosen for the analysis of a given problem; e.g. for the bosonic and fermionic coherent states discussed in Chapters 2 and 3, the classical scheme leads to mean-field solutions, equivalent to those obtained through time-dependent Gross-Pitaevskii/Hartree-Fock equations when treating bosonic/fermionic systems.

Finally, it should be pointed out that, if the Hamiltonian is an element of the Lie algebra associated with the set of coherent states under consideration – i.e. when $\hat{H}$ is *linear* in the group's generators – then the time-evolution operator '$\exp(-\frac{i}{\hbar}\hat{H}t)$' merely represents a group transformation – it simply maps one coherent state onto another. In such a situation, the classical propagation scheme actually gives the exact wavefunction for $t > 0$.

1.3.4 Example: Glauber's coherent states/gaussian wavepackets

Lastly, we illustrate some of the concepts developed in this section using canonical coherent states, or *Glauber coherent states*,[40;41] as they are known in the field of Quantum Optics – from where we borrow the physical background for the subsequent presentation.

Let us consider a system wherein photons can be excited at d optical frequencies, or *modes*. In the language of second quantization, bosonic creation and annihilation operators, $a_\alpha^\dagger$ and a_α respectively, are assigned to each mode, with $1 \leq \alpha \leq d$. The Hilbert space basis consists of occupation number eigenstates,

$$|m_1, m_2, \ldots, m_d\rangle = \frac{(a_1^\dagger)^{m_1}(a_2^\dagger)^{m_2}\ldots(a_d^\dagger)^{m_d}}{\sqrt{m_1!\, m_2!\, \ldots\, m_d!}}|0\rangle, \tag{1.77}$$

where $|0\rangle$ denotes the vacuum state. Since the number of photons is unrestricted ($0 \leq m_\alpha < \infty$) the Hilbert space (in this case a bosonic Fock space) is infinite-dimensional.

The reference state is chosen to be the vacuum state, $|\Phi_0\rangle = |0\rangle$. Then the functional definition of the non-normalized Glauber coherent state, parametrized by the vector $z = (z_1, \ldots, z_d)$ (whose length equals the number of optical modes), is:

$$|z\} = \exp\Big[\sum_{\alpha=1}^{d} z_\alpha a_\alpha^\dagger\Big]|0\rangle. \tag{1.78}$$

The decomposition of $|z\}$ in terms of basis elements $|m_1, m_2, \ldots, m_d\rangle$ is easily found by expanding the above exponential and using the commutativity of the creation operators,

$$|z\} = \sum_{m_1=0}^{\infty} \cdots \sum_{m_d=0}^{\infty} \left[\frac{z_1^{m_1} z_2^{m_2} \cdots z_d^{m_d}}{\sqrt{m_1!\, m_2!\, \cdots\, m_d!}} \right] |m_1, m_2, \ldots, m_d\rangle. \tag{1.79}$$

These last two equations exemplify the general formulas (1.52) and (1.55).

Since the modes are assumed to be orthonormal, the overlap $\{z|z\}$ is found without difficulty from (1.79), the result being

$$\{z|z\} = \exp\Big(\sum_{\alpha=1}^{d} z_\alpha^* z_\alpha \Big). \tag{1.80}$$

Thus we identify the Kähler potential [cf. Eq. (1.56)] as:

$$f(z^*, z) = \sum_{\alpha=1}^{d} z_\alpha^* z_\alpha. \tag{1.81}$$

Whence we find that the metric [cf. Eq. (1.58)] for Glauber states is simply the identity matrix,

$$g(z^*, z)_{\alpha\beta} = \delta_{\alpha\beta}. \tag{1.82}$$

The phase space is therefore flat, which means that the d degrees of freedom are not 'geometrically coupled', in the sense described earlier. From (1.82) it follows that the measure [cf. Eq. (1.60)] is trivial:

$$d\mu(z) = \prod_{\alpha=1}^{d} \frac{d^2 z_\alpha}{\pi}. \tag{1.83}$$

The physical interpretation of Glauber coherent states is based on the fact that each entry z_α is associated with the mean occupation of the corresponding mode,

$$\langle z| a_\alpha^\dagger a_\alpha |z\rangle = |z_\alpha|^2, \tag{1.84}$$

where the normalized state is $|z\rangle = |z\} \exp(-\frac{1}{2} \sum_{\alpha=1}^{d} |z_\alpha|^2)$. The relation (1.84) is easily obtained from the formulas given above. It also follows from the well-known fact that $|z\rangle$ is an eigenket of the annihilation operator, $a_\alpha |z\rangle = z_\alpha |z\rangle$.[42]

Gaussian wavepackets. The bosonic occupations can also be pictured as excitations in a quantum harmonic oscillator with d degrees of freedom, whose ground-state wavefunction (the position representation of the vacuum state) is a d-dimensional Gaussian,

$$\langle x|\Phi_0\rangle = (\pi\gamma^2)^{-d/4} \exp\Big[-\sum_{\alpha=1}^{d} (x_\alpha/\gamma)^2 \Big], \tag{1.85}$$

where $x = (x_1, x_2, \ldots, x_d)$ and γ is a length parameter (for a mechanical oscillator, γ depends on its mass and natural frequency). From this point of view, the states in (1.77) are proportional to the well-known eigenfunctions of the harmonic oscillator, whose position representation is given in terms of Hermite polynomials.[42]

We are interested in the position representation of the coherent state $|z\rangle$. In order to find it, a well-known relation among the bosonic operators $a_\alpha^\dagger$ and a_α and the elementary position and momentum operators, $\hat{Q}_\alpha$ and $\hat{P}_\alpha$, is employed:

$$\hat{Q}_\alpha = \frac{\gamma}{\sqrt{2}}(a_\alpha^\dagger + a_\alpha), \quad \hat{P}_\alpha = \frac{i\hbar}{\gamma\sqrt{2}}(a_\alpha^\dagger - a_\alpha) \quad \Rightarrow \quad [\hat{Q}_\alpha, \hat{P}_\beta] = i\hbar\,\delta_{\alpha\beta}. \tag{1.86}$$

Using the above formulas, together with the basic property $a_\alpha|z\rangle = z_\alpha|z\rangle$, it is possible to determine the function $\langle x|z\rangle$.[43] The calculation is straightforward, but we shall not go into its details. As it turns out, the result is more conveniently expressed in terms of the mean-values:

$$Q_\alpha = \langle z|\hat{Q}_\alpha|z\rangle = \frac{\gamma}{\sqrt{2}}(z_\alpha^* + z_\alpha), \quad P_\alpha = \langle z|\hat{P}_\alpha|z\rangle = \frac{i\hbar}{\gamma\sqrt{2}}(z_\alpha^* - z_\alpha); \tag{1.87}$$

and, since Q and P are essentially the real and imaginary parts of z, we may re-label the coherent state as $|z\rangle = |g(Q,P)\rangle$. With this notation, the sought function is then expressed as:

$$\langle x|g(Q,P)\rangle = (\pi\gamma^2)^{-d/4} \prod_{\alpha=1}^{d} \exp\left[-\frac{(x_\alpha - Q_\alpha)^2}{2\gamma^2} + \frac{i}{\hbar}P_\alpha(x_\alpha - Q_\alpha) + \frac{i}{2\hbar}P_\alpha Q_\alpha\right]. \tag{1.88}$$

Thus, Glauber coherent states can also be understood as *gaussian wavepackets*. A notable property of these states is that they satisfy, by construction, a minimum uncertainty relation:

$$\Delta Q_\alpha = \sqrt{\langle g|\hat{Q}_\alpha^2|g\rangle - Q_\alpha^2} = \frac{\gamma}{\sqrt{2}}, \quad \Delta P_\alpha = \sqrt{\langle g|\hat{P}_\alpha^2|g\rangle - P_\alpha^2} = \frac{\hbar}{\gamma\sqrt{2}} \quad \Rightarrow \quad \Delta Q_\alpha \Delta P_\alpha = \frac{\hbar}{2}. \tag{1.89}$$

The equations of motion [cf. (1.72)] can be written in terms of the real parameters Q and P and they reduce to the familiar Hamilton equations of classical mechanics:

$$\dot{Q}_\alpha = \frac{\partial E}{\partial P_\alpha}, \quad \dot{P}_\alpha = -\frac{\partial E}{\partial Q_\alpha}, \quad (1 \le \alpha \le d). \tag{1.90}$$

If the Hamiltonian has the usual form,

$$\hat{H} = \sum_{\alpha=1}^{d} \frac{\hat{P}_\alpha^2}{2M} + V(\hat{Q}_1, \hat{Q}_2, \ldots, \hat{Q}_d), \tag{1.91}$$

(for simplicity, we assume all particles have the same mass) the energy function in

Eq. (1.90) is then given by:

$$E(Q,P) = E_0 + \sum_{\alpha=1}^{d} \frac{P_\alpha^2}{2M} + \tilde{V}(Q), \tag{1.92}$$

where E_0 is a constant. The effective potential $\tilde{V}(Q)$ is the mean value $\tilde{V}(Q) = \langle g|V(\hat{Q})|g\rangle$, which can be computed from the (diagonal) position representation $V(x) = \langle x|V(\hat{Q})|x\rangle$ by insertion of the closure relation, $\hat{1} = \int dx\, |x\rangle\langle x|$; that is:

$$\tilde{V}(Q_1,\ldots,Q_d) = (\pi\gamma^2)^{-d/2} \int (dx_1 \ldots dx_d)\, V(x_1,\ldots,x_d) e^{-\sum_{\alpha=1}^{d}(x_\alpha - Q_\alpha)^2/\gamma^2}. \tag{1.93}$$

Due to the finite width γ of the Gaussians, the potential $\tilde{V}(Q)$ results to be a smoothed-out version of $V(x)$; this feature is sometimes interpreted as if 'quantum corrections' were included in the otherwise purely classical system.[27]

Gaussian wavepackets are ubiquitous in Quantum Chemistry, particularly in semi-classical methods, where they are most often combined into an integral expression, or 'initial-value representation' (IVR) formula.[44] Individually, each wavepacket is suitable for representing an ensemble of heavy, localized, and distinguishable particles (e.g. the nuclei in a molecule) for its parameters Q and P behave in a classical fashion while the Gaussian width is kept constant – in this so-called 'frozen-Gaussian representation'[45] the identity of each particle is preserved and the 'interpretativeness' of the problem in such terms is ensured. Collectively, as in any IVR formula, the independently evolved wavepackets are allowed to interfere with one another and are thus capable of producing approximate quantum solutions.

Chapter 2

Bosonic coherent states

Overview. Bosonic coherent states of the special unitary group are reviewed. They are interpreted as Bose-Einstein condensate states, where all particles occupy a single macroscopic mode. Their dynamics is first discussed in general terms; later, equations of motion for a specific class of Hamiltonians are obtained and the connection with bosonic mean-field theories is established. The effect that group transformations have on the coherent-state parameters is also studied.[i]

2.1 The Bose-Einstein condensate parametrization

2.1.1 Preliminaries

Let us consider a single-particle space spanned by a finite set of orthonormal states, which we shall refer to as 'modes' in the bosonic formalism. The projector onto this space is:

$$\hat{P} = \sum_{p=0}^{d} |\phi_p\rangle\langle\phi_p|, \quad \phi_p(\mathbf{x}) = \langle \mathbf{x}|\phi_p\rangle, \quad d \equiv K - 1. \tag{2.1}$$

The K modes $|\phi\rangle$ have been numbered from 0 to $K-1 \equiv d$. This notation is chosen in view of the coherent-state framework – we shall find that d is the number of degrees of freedom in the coherent-state description. As the number of modes is increased the limit of a complete basis is approached,

$$P(\mathbf{x}, \mathbf{x}') = \langle \mathbf{x}|\hat{P}|\mathbf{x}'\rangle \overset{K\to\infty}{=} \delta(\mathbf{x} - \mathbf{x}'). \tag{2.2}$$

However, one almost invariably works with a truncated basis set under the assumption that it suffices for an appropriate treatment of the physical situation.

[i] In this work, bosonic coherent states are introduced before their fermionic counterparts; this choice was made because the latter are somewhat more intricate. The organization of this chapter, however, is entirely inspired by that of Chapter 3 which, in turn, closely follows the exposition given in the review article by Deumens *et. al.*.[17]

Creation and annihilation operators are associated with each single-particle mode. These operators obey the usual commutation rules:

$$\begin{cases} |\phi_p\rangle = b_p^\dagger|0\rangle \\ \langle\phi_q| = \langle 0|b_q \end{cases} \text{with:} \quad \begin{cases} [b_p, b_q^\dagger] = \delta_{pq} \\ [b_p, b_q] = [b_p^\dagger, b_q^\dagger] = 0 \end{cases} , \quad 0 \leq p, q \leq d. \tag{2.3}$$

where $[\hat{A}, \hat{B}] = \hat{A}\hat{B} - \hat{B}\hat{A}$. The bosonic field operators, defined over the truncated space, are:

$$\begin{cases} \hat{\psi}(\mathbf{x}) = \sum_{p=0}^d \phi_p(\mathbf{x}) b_p \\ \hat{\psi}^\dagger(\mathbf{x}) = \sum_{p=0}^d \phi_p^*(\mathbf{x}) b_p^\dagger \end{cases} \Leftrightarrow \begin{cases} b_p = \int d\mathbf{x}\, \phi_p^*(\mathbf{x})\hat{\psi}(\mathbf{x}) \\ b_p^\dagger = \int d\mathbf{x}\, \phi_p(\mathbf{x})\hat{\psi}^\dagger(\mathbf{x}) \end{cases} , \quad 0 \leq p \leq d. \tag{2.4}$$

They satisfy:

$$[\hat{\psi}(\mathbf{x}), \hat{\psi}^\dagger(\mathbf{x}')] = P(\mathbf{x}, \mathbf{x}'), \quad [\hat{\psi}(\mathbf{x}), \hat{\psi}(\mathbf{x}')] = [\hat{\psi}^\dagger(\mathbf{x}), \hat{\psi}^\dagger(\mathbf{x}')] = 0. \tag{2.5}$$

Let us now consider the bosonic many-body description. A complete set of basis vectors is provided by the eigenstates of the number operator,[46]

$$\hat{n}_p = b_p^\dagger b_p, \quad \hat{n}_p|m_0, \ldots, m_d\rangle = m_p|m_0, \ldots, m_d\rangle, \quad 0 \leq p \leq d. \tag{2.6}$$

These states, labeled by an array of occupation numbers $m = (m_0, m_1, \ldots, m_d)$, are defined in terms of the basic creation operators according to

$$|m_0, m_1, m_2, \ldots, m_d\rangle = \frac{(b_0^\dagger)^{m_0}(b_1^\dagger)^{m_1}(b_2^\dagger)^{m_2}\ldots(b_d^\dagger)^{m_d}}{\sqrt{m_0!\, m_1!\, m_2!\, \ldots\, m_d!}}|0\rangle, \tag{2.7}$$

where $|0\rangle$ denotes the vacuum state.

We shall restrict our analysis to number-conserving systems. In this case the set of occupation numbers corresponding to each bosonic state must comply with the condition:

$$m_0 + m_1 + m_2 + \cdots + m_d = N, \tag{2.8}$$

where N is the total number of bosons present in the system; this constraint will sometimes be abbreviated as $|m| = N$.

The dimension of the Fock space $\mathcal{B}(K, N)$, for a system of N bosons which are allowed to occupy K single-particle modes, equals the number of possible sets m such that $|m| = N$; combinatorics gives:[21]

$$\dim \mathcal{B}(K, N) = \frac{(N + K - 1)!}{(K - 1)!N!}. \tag{2.9}$$

The number-conserving restriction implies that the total particle number operator $\hat{N}$

is a constant of the motion,

$$\hat{N} = \sum_p \hat{n}_p, \quad [\hat{H}, \hat{N}] = 0. \tag{2.10}$$

Hamiltonians belonging to such a class can be expressed in terms of the bilinear forms $b_p^\dagger b_q$, which satisfy the following commutation relations:

$$[b_p^\dagger b_q, b_r^\dagger b_s] = b_p^\dagger b_s \, \delta_{qr} - b_r^\dagger b_q \, \delta_{sp}, \quad 0 \leq p, q, r, s \leq d. \tag{2.11}$$

A basis for the algebra su(K) of the special unitary group SU(K) may be written in terms of these operators. This is the dynamical group we associate with the number-conserving time evolution of a bosonic system.[29]

2.1.2 Coherent states: definition and macroscopic mode

The bosonic coherent states we shall work with aim at describing Bose-Einstein condensates. The appropriate physical context is that in which one of the single-particle modes, taken to be $|\phi_0\rangle = b_0^\dagger|0\rangle$, is macroscopically occupied most of the time[ii] and only a relatively small occupation of the remaining modes is expected. In this scenario, the reference state in terms of which the coherent state is defined is

$$|\Phi_0\rangle = \frac{(b_0^\dagger)^N}{\sqrt{N!}}|0\rangle; \tag{2.12}$$

i.e. the state in which all bosons are found in the 'reference mode', $|\phi_0\rangle = b_0^\dagger|0\rangle$. This mode is therefore special and we shall adapt our notation accordingly: distinct sets of subscripts will be employed when referring to different index ranges, the convention being as follows:

$$0 \leq (p, q, r, s) \leq d, \quad 1 \leq (\mu, \nu) \leq d. \tag{2.13}$$

With that understanding we shall henceforth omit the limits in summations and products. As an example, the basic commutation rules can be re-stated as:

$$[b_0, b_0^\dagger] = 1, \quad [b_\mu, b_\nu^\dagger] = \delta_{\mu\nu}, \quad [b_0, b_\nu^\dagger] = [b_\mu, b_0^\dagger] = 0, \quad [b_0, b_0] = [b_\mu, b_\nu] = 0. \tag{2.14}$$

The unnormalized bosonic coherent state is defined in terms of a displacement operator acting on the reference state according to:

$$|z\} = \exp\Big(\sum_\mu z_\mu b_\mu^\dagger b_0\Big)|\Phi_0\rangle. \tag{2.15}$$

[ii] The term 'macroscopic' is loosely employed here; we simply mean that most of the particles occupy the reference mode – we do not necessarily have $N \sim 10^{23}$ (e.g. the numerical examples in Chapter 5 use $N \sim 40 - -100$).

These states are labeled by the complex array $z = (z_1, z_2, \ldots, z_d)$ which we take to be a column vector in the formalism to be developed below. Correspondingly, the complex-conjugate array, z^*, is to be understood as a row vector.[iii] We see that each entry z_μ is related to the process of removing a boson from the reference mode and placing it at the mode $|\phi_\mu\rangle$.

Let us now work down the coherent state definition to a more comprehensible form. We begin by noting that all terms in the exponent commute, i.e. $[b_\mu^\dagger b_0, b_\nu^\dagger b_0] = 0$, and therefore the exponential can be factored into a product, $\prod_\mu e^{z_\mu b_\mu^\dagger b_0}$. Now, suppose $\xi^\dagger$ is a function of all creation operators, except $b_0^\dagger$. This means that $[b_0, \xi^\dagger] = 0$ and $[b_p^\dagger, \xi^\dagger] = 0$. Let us then evaluate the following commutator:

$$\begin{aligned}
[\, e^{z_\mu b_\mu^\dagger b_0} \,,\, (b_0^\dagger + \xi^\dagger)\,] &= \sum_{k=0}^{\infty} \frac{z_\mu^k}{k!} \,[\, (b_\mu^\dagger b_0)^k,\, (b_0^\dagger + \xi^\dagger)\,] \\
&= \sum_{k=0}^{\infty} \frac{(z_\mu b_\mu^\dagger)^k}{k!}\, [b_0^k, b_0^\dagger] \\
&= z_\mu b_\mu^\dagger \cdot \sum_{k=1}^{\infty} \frac{(z_\mu b_\mu^\dagger b_0)^{k-1}}{(k-1)!} \;= (z_\mu b_\mu^\dagger)\, e^{z_\mu b_\mu^\dagger b_0},
\end{aligned} \tag{2.16}$$

where in going from the second to the third line we have used the relation $[b_0^k, b_0^\dagger] = k\, b_0^{k-1}$. The latter result implies the identity:

$$e^{z_\mu b_\mu^\dagger b_0}(b_0^\dagger + \xi^\dagger) = (b_0^\dagger + \xi^\dagger + z_\mu b_\mu^\dagger) e^{z_\mu b_\mu^\dagger b_0},$$

which can be iterated n times, by multiplying both sides from the right with $(b_0^\dagger + \xi^\dagger)$, leading to:

$$e^{z_\mu b_\mu^\dagger b_0}(b_0^\dagger + \xi^\dagger)^n = (b_0^\dagger + \xi^\dagger + z_\mu b_\mu^\dagger)^n e^{z_\mu b_\mu^\dagger b_0}. \tag{2.17}$$

With the help of this formula we are able to rewrite (2.15) as:

$$\begin{aligned}
\sqrt{N!}|z\} &= e^{z_d b_d^\dagger b_0}\, e^{z_{d-1} b_{d-1}^\dagger b_0} \cdots e^{z_2 b_2^\dagger b_0}\, e^{z_1 b_1^\dagger b_0}\, (b_0^\dagger)^N |0\rangle \\
&= e^{z_d b_d^\dagger b_0}\, e^{z_{d-1} b_{d-1}^\dagger b_0} \cdots e^{z_2 b_2^\dagger b_0}\, (b_0^\dagger + z_1 b_1^\dagger)^N\, e^{z_1 b_1^\dagger b_0} |0\rangle \\
&= e^{z_d b_d^\dagger b_0}\, e^{z_{d-1} b_{d-1}^\dagger b_0} \cdots (b_0^\dagger + z_1 b_1^\dagger + z_2 b_2^\dagger)^N\, e^{z_2 b_2^\dagger b_0}\, e^{z_1 b_1^\dagger b_0} |0\rangle \\
&\;\;\vdots \\
&= (b_0^\dagger + z_1 b_1^\dagger + z_2 b_2^\dagger + \ldots + z_d b_d^\dagger)^N (e^{z_d b_d^\dagger b_0} \cdots e^{z_1 b_1^\dagger b_0}) |0\rangle \\
&= (b_0^\dagger + z_1 b_1^\dagger + z_2 b_2^\dagger + \ldots + z_d b_d^\dagger)^N |0\rangle.
\end{aligned} \tag{2.18}$$

[iii] We reserve the symbol '†' for denoting either adjoint operators or the complex-transpose of matrices.

We thus arrive at the following expression for the unnormalized coherent state:

$$|z\} = \frac{(\zeta_0^\dagger)^N}{\sqrt{N!}}|0\rangle, \quad \text{where:} \quad \zeta_0^\dagger(z) = b_0^\dagger + \sum_\mu z_\mu b_\mu^\dagger. \tag{2.19}$$

The newly defined operator $\zeta_0^\dagger(z)$ is itself a bosonic creation operator. This can be immediately verified by considering the adjoint $\zeta_0(z^*) = b_0 + \sum_\nu b_\nu z_\nu^*$ and evaluating, with the help of (2.14), the commutators (here computed for possibly different coherent-state labels):

$$[\zeta_0(z^*), \zeta_0^\dagger(z')] = 1 + z^* z', \tag{2.20a}$$

$$[\zeta_0(z^*), \zeta_0(z')] = [\zeta_0^\dagger(z^*), \zeta_0^\dagger(z')] = 0. \tag{2.20b}$$

The conclusion is that $|z\}$ represents a Bose-Einstein condensate in which all N particles of the system occupy an effective single-particle mode which is parametrized by z. This macroscopic mode, denoted by $|\zeta_0(z)\} = \zeta_0^\dagger(z)|0\rangle$, corresponds to a simple (unnormalized) superposition of the basic modes:

$$|\zeta_0(z)\} = |\phi_0\rangle + \sum_\mu z_\mu |\phi_\mu\rangle. \tag{2.21}$$

For future reference, we list some useful commutation rules:

$$[b_0, \zeta_0^\dagger] = 1, \quad [b_0^\dagger, \zeta_0^\dagger] = 0, \quad [b_\mu, \zeta_0^\dagger] = z_\mu, \quad [b_\mu^\dagger, \zeta_0^\dagger] = 0. \tag{2.22}$$

Let us next compute the overlap $\{z|z'\}$, which is the basic quantity required for constructing the coherent-state formalism. We note that from commutation rules (2.20) we get, by simple induction,

$$[\zeta_0^k(z^*), \zeta_0^\dagger(z')] = k(1 + z^* z')\zeta_0^{k-1}(z^*). \tag{2.23}$$

Then, with some slightly abbreviations, we proceed as follows:

$$\begin{aligned}
N!\,\{z|z'\} &= \langle 0|\zeta_0^N\,(\zeta'^\dagger_0)^N|0\rangle = \langle 0|(\zeta_0^N \zeta'^\dagger_0)\cdot(\zeta'^\dagger_0)^{N-1}|0\rangle \\
&= \langle 0|\Big\{[\zeta_0^N, \zeta'^\dagger_0] - \zeta'^\dagger_0 \zeta_0^N\Big\}\cdot(\zeta'^\dagger_0)^{N-1}|0\rangle \qquad \Big(\text{obs: } \langle 0|\zeta'^\dagger_0 = 0\Big) \\
&= N(1 + z^* z')\langle 0|\zeta_0^{N-1}(\zeta'^\dagger_0)^{N-1}|0\rangle = N(1 + z^* z')\langle 0|(\zeta_0^{N-1}\zeta'^\dagger_0)\cdot(\zeta'^\dagger_0)^{N-2}|0\rangle \\
&= N(N-1)(1 + z^* z')^2\langle 0|\zeta_0^{N-2}(\zeta'^\dagger_0)^{N-2}|0\rangle \\
&\;\;\vdots \\
&= N!(1 + z^* z')^N,
\end{aligned} \tag{2.24}$$

i.e. the exponent of the operators ζ_0 and $\zeta'^\dagger_0$ is decreased at each step, eventually leading

to $\langle 0|0\rangle = 1$. Therefore, the unnormalized overlap is:

$$\{z|z'\} = (1 + z^* z')^N. \tag{2.25}$$

Finally, we remark that, by making use of the commutation rules listed in (2.22), one is also able to find the Fock decomposition of $|z\}$:

$$|z\} = \sum_{|m|=N} \binom{N}{m_0\, m_1\, \cdots\, m_d}^{\frac{1}{2}} \left[z_1^{m_1} z_2^{m_2} \cdots z_d^{m_d}\right] |m_0, m_1, \ldots, m_d\rangle. \tag{2.26}$$

A detailed derivation of this result is found in Appendix B.

2.1.3 * Complementary modes and projectors

The vector z can also be used to define a set of d complementary modes,

$$|\bar{\zeta}_\mu(z^*)\} = |\phi_\mu\rangle - z_\mu^*|\phi_0\rangle, \tag{2.27}$$

whose creation operators are:

$$\bar{\zeta}_\mu^\dagger(z^*) = b_\mu^\dagger - z_\mu^* b_0^\dagger, \quad 1 \leq \mu \leq d. \tag{2.28}$$

These operators, together with their respective adjoints, satisfy the commutation relations:

$$[\bar{\zeta}_\mu(z), \bar{\zeta}_\nu^\dagger(z^{*\prime})] = \delta_{\mu\nu} - z_\mu z_\nu^{*\prime}, \tag{2.29a}$$

$$[\bar{\zeta}_\mu(z), \bar{\zeta}_\nu(z')] = [\bar{\zeta}_\mu^\dagger(z^*), \bar{\zeta}_\nu^\dagger(z^{*\prime})] = 0. \tag{2.29b}$$

By construction, all complementary modes, though not orthogonal amongst themselves, are orthogonal to the coherent-state's macroscopic mode, provided both sets correspond to the same coherent-state label, as can be seen from the overlap

$$\{\bar{\zeta}_\mu(z)|\zeta_0(z')\} = z_\mu - z'_\mu, \tag{2.30}$$

which vanishes for $z' = z$.

The macroscopic and complementary modes taken together constitute again a complete single-particle basis. In fact, starting from Eqs. (2.21) and (2.27), we may write the basis transformation rule in matrix form as follows:

$$\begin{bmatrix}\zeta_0^\dagger & (\bar{\zeta}_1^\dagger, \ldots, \bar{\zeta}_d^\dagger)\end{bmatrix} = \begin{bmatrix}b_0^\dagger & (b_1^\dagger, \ldots, b_d^\dagger)\end{bmatrix} \begin{bmatrix}1 & -z^* \\ z & I_d\end{bmatrix}, \tag{2.31}$$

from which the reverse transformation is obtained with the help of the matrix identity:

$$\begin{bmatrix} 1 & 0 \\ 0 & I_d \end{bmatrix} = \begin{bmatrix} 1 & z^* \\ -z & I_d \end{bmatrix} \begin{bmatrix} (1+z^*z)^{-1} & 0 \\ 0 & (I_d + zz^*)^{-1} \end{bmatrix} \begin{bmatrix} 1 & -z^* \\ z & I_d \end{bmatrix}, \tag{2.32}$$

leading to:

$$b_0^\dagger = (\zeta_0^\dagger - \sum_\nu \bar{\zeta}_\nu^\dagger z_\nu)(1+z^*z)^{-1}, \tag{2.33a}$$

$$b_\mu^\dagger = \sum_\nu (\zeta_0^\dagger z_\nu^* + \bar{\zeta}_\nu^\dagger)(I_d + zz^*)^{-1}_{\nu\mu}. \tag{2.33b}$$

Using the above relations one proves that both basis indeed span the same single-particle space:

$$\begin{aligned} \hat{P} &= |\phi_0\rangle\langle\phi_0| + \sum_\mu |\phi_\mu\rangle\langle\phi_\mu| \\ &= |\zeta_0\}(1+z^*z)^{-1}\{\zeta_0| + \sum_{\mu\nu} |\bar{\zeta}_\mu\}(I_d + zz^*)^{-1}_{\mu\nu}\{\bar{\zeta}_\nu|, \end{aligned} \tag{2.34}$$

with the projector splitting into two orthogonal and disjoint parts: the first referring to the macroscopic mode and the second to the remaining complementary modes.

2.1.4 The geometry of bosonic coherent states

From Eq. (2.25) and definition (1.56) it follows that the Kähler potential for the bosonic coherent state parametrization is:

$$f(z^*, z') = N \log(1 + z^*z') = N \log\Big[1 + \sum_\mu z_\mu^* z'_\mu\Big]. \tag{2.35}$$

We will be requiring the first gradients of $f(z^*, z')$ later on – for future reference, they are:

$$\frac{\partial f(z^*, z')}{\partial z'_\mu} = \frac{N z_\mu^*}{1 + z^*z'}, \tag{2.36a}$$

$$\frac{\partial f(z^*, z')}{\partial z_\mu^*} = \frac{N z'_\mu}{1 + z^*z'}. \tag{2.36b}$$

The metric matrix elements are obtained by straightforward computation of the mixed partial derivatives:

$$g(z^*, z)_{\mu\nu} = \frac{\partial^2 f(z^*, z)}{\partial z_\mu \partial z_\nu^*} = N \frac{(1+z^*z)\delta_{\mu\nu} - z_\mu^* z_\nu}{(1+z^*z)^2}. \tag{2.37}$$

The metric's determinant can be found without difficulty by first writing g^T in matrix form,[iv]

$$g^T = \frac{N}{1+z^*z}(I_{K-1} - z(1+z^*z)^{-1}z^*),$$

and invoking Sylvester's theorem, which states that for any pair of matrices A and B, of sizes $n \times m$ and $m \times n$ respectively, the following equality holds: $\det(I_m + BA) = \det(I_n + AB)$. In the present case this means:

$$\begin{aligned}\det g^T &= \frac{N^{K-1}}{(1+z^*z)^{K-1}} \cdot \det(I_{K-1} - z(1+z^*z)^{-1}z^*) \\ &= \frac{N^{K-1}}{(1+z^*z)^{K-1}} \cdot (1 - z^*(1+z^*z)^{-1}z) = \frac{N^{K-1}}{(1+z^*z)^K}.\end{aligned} \tag{2.38}$$

Hence, from definition (1.60), we get the integration measure that equips the bosonic closure relation:

$$d\mu(z) = \frac{\kappa\, N^{K-1}}{(1+z^*z)^K}\,\frac{d^2z}{\pi^d} = \frac{(N+K-1)!}{N!(1+z^*z)^K}\,\frac{d^2z}{\pi^d}, \tag{2.39}$$

where we have substituted the value of the normalization constant κ, computed in Appendix B.

The inverse of g can be easily found with the help of the identities:

$$I_{K-1} - z(1+z^*z)^{-1}z^* = (I_{K-1} + zz^*)^{-1}, \tag{2.40a}$$

$$1 - z^*(I_{K-1} + zz^*)^{-1}z = (1+z^*z)^{-1}. \tag{2.40b}$$

In particular, using the first of these expressions, the matrix g^T can be written as:

$$g^T = \frac{N}{1+z^*z}(I_{K-1} + zz^*)^{-1} \quad \Rightarrow \quad g^{-T} = \frac{1+z^*z}{N}(I_{K-1} + zz^*). \tag{2.41}$$

Therefore the inverse matrix elements are:

$$g^{-1}(z^*, z)_{\mu\nu} = \frac{1+z^*z}{N}(\delta_{\mu\nu} + z^*_\mu z_\nu). \tag{2.42}$$

This result allows us to write the variational equation of motion for bosonic coherent states – from the general form given in (1.72) we get:

$$\dot{z}_\mu = -\frac{i}{\hbar}\frac{(1+z^*z)}{N}\sum_\nu(\delta_{\mu\nu} + z_\mu z^*_\nu)\frac{\partial E(z^*, z)}{\partial z^*_\nu}. \tag{2.43}$$

Next we shall restrict attention to a specific type of Hamiltonian and further development of this equation will become possible.

[iv] The product z^*z denotes a scalar product, i.e. $z^*z = \sum_\eta z^*_\eta z_\eta$. Meanwhile, the juxtaposition zz^* stands for an exterior product, i.e. $(zz^*)_{\mu\nu} = z_\mu z^*_\nu$.

2.2 Mean-field dynamics of interacting bosons

Let us consider a system of N interacting bosons whose dynamics is described by a first-quantized Hamiltonian containing one- and two-body terms; in position representation it reads:

$$\hat{H}(\mathbf{x}) = \sum_{i=1}^{N} \hat{h}(\mathbf{x}_i) + \tfrac{1}{2} \sum_{i=1}^{N} \sum_{j=1}^{N} \hat{U}(\mathbf{x}_i, \mathbf{x}_j). \tag{2.44}$$

where $\hat{h}(\mathbf{x})$ includes both the kinetic energy term, $-(\hbar^2/2m)\nabla^2$, and external potentials. Since we are dealing with identical bosons the interacting potential $\hat{U}(\mathbf{x}, \mathbf{x}')$ must be symmetric with respect to particle interchange.

The second-quantized form of the above Hamiltonian is found with the aid of the field operators defined in (2.4). More conveniently, we shall confine the analysis to the truncated-basis scheme, and work with $\hat{H}$ expressed in terms of the creators and annihilators of the K single-particle modes $|\phi\rangle$, in which case it takes the form:[v]

$$\hat{H} = \sum_{pq} h_{pq} b_p^\dagger b_q + \tfrac{1}{2} \sum_{pqrs} U_{pr\cdot qs} b_p^\dagger b_r^\dagger b_s b_q, \tag{2.45}$$

where the one and two-body integrals are:

$$\begin{cases} h_{pq} = \langle \phi_p | \hat{h} | \phi_q \rangle \\ U_{pr\cdot qs} = \langle \phi_p, \phi_r | \hat{U} | \phi_q, \phi_s \rangle \end{cases} \quad \text{with:} \quad \begin{cases} h_{pq} = h_{qp}^* \\ U_{pr\cdot qs} = U_{rp\cdot sq} = U_{qs\cdot pr}^* = U_{sq\cdot rp}^* \end{cases}, \tag{2.46}$$

having the usual properties listed above.

2.2.1 The one-density

We are interested in the coherent-state expectation value of the many-body Hamiltonian. We take $|z\}$ as given by Eq. (2.19), with $|\Phi_0\rangle$ being the state where all N particles occupy the reference mode $|\phi_0\rangle$. A central object of the present formalism is the matrix $\Gamma(z^*, z)$, the bosonic 'one-density', whose elements are defined according to

$$\Gamma_{qp}(z^*, z) \equiv N^{-1} \langle z | b_p^\dagger b_q | z \rangle = N^{-1} \frac{\{z | b_p^\dagger b_q | z\}}{\{z | z\}}, \quad 0 \leq p, q \leq d. \tag{2.47}$$

[v] Notice that $b_p^\dagger b_r^\dagger b_s b_q = b_p^\dagger b_q b_r^\dagger b_s - b_p^\dagger b_s \delta_{qr}$, and $\hat{H}$ is a function of the basic bilinears, as it should be.

In Appendix B these elements are computed using second-quantization techniques. The result can be expressed in matrix form as below:

$$\Gamma(z^*,z)=\frac{1}{1+z^*z}\begin{bmatrix}1 & z^*\\ z & zz^*\end{bmatrix}=\frac{1}{1+z_1^*z_1+\cdots+z_d^*z_d}\begin{bmatrix}1 & z_1^* & z_2^* & \cdots & z_d^*\\ z_1 & z_1z_1^* & z_1z_2^* & \cdots & z_1z_d^*\\ z_2 & z_2z_1^* & z_2z_2^* & \cdots & z_2z_d^*\\ \vdots & \vdots & \vdots & \ddots & \vdots\\ z_d & z_dz_1^* & z_dz_2^* & \cdots & z_dz_d^*\end{bmatrix}. \tag{2.48}$$

The one-density is an hermitian matrix with the following properties:

$$\mathrm{tr}[\Gamma(z^*,z)]=1 \quad \text{and} \quad \Gamma(z^*,z)\Gamma(z^*,z)=\Gamma(z^*,z), \tag{2.49}$$

which hold for all values of z. Moreover, each of the K diagonal elements is directly related to the population of the corresponding mode:

$$n_p(z)=\langle z|b_p^\dagger b_p|z\rangle = N\,\Gamma_{pp}(z^*,z), \quad \textstyle\sum_p n_p(z)=N. \tag{2.50}$$

where the normalized trace assures that the populations correctly add to the total number of particles.

The idempotency of Γ – the second of the properties listed in (2.49) – is characteristic of projectors. Indeed, the one-density associated with a bosonic coherent state is nothing but the matrix representation of the macroscopic mode projector (normalized to unity):

$$\hat{\Gamma}(z^*,z)=|\zeta_0(z)\}(1+z^*z)^{-1}\{\zeta_0(z)| = \sum_{pq}|\phi_p\rangle\Gamma_{pq}(z^*,z)\langle\phi_q|. \tag{2.51}$$

Check. Multiplying the first form on the left and right sides with $\langle\phi_p|$ and $|\phi_q\rangle$ one gets $\Gamma_{pq}(z^*,z)=(1+z^*z)^{-1}\langle\phi_p|\zeta_0(z)\}\{\zeta_0(z)|\phi_q\rangle$; then, substituting the scalar products $\langle\phi_p|\zeta_0(z)\}$ and $\{\zeta_0(z)|\phi_q\rangle$ (straightforwardly computed from previous relations) one easily recovers formula (2.48).

2.2.2 Energy function and mean-field dynamics

The one-density immediately gives the coherent-state matrix element of the one-body part of $\hat{H}$. In order to proceed we further require the expectation value of the two-body interaction term. This quantity is also computed in Appendix B, and it turns out that it can be directly expressed in terms of the one-density (for brevity, we omit the z arguments from now on):

$$\langle z|b_p^\dagger b_r^\dagger b_s b_q|z\rangle = N(N-1)\,\Gamma_{qp}\Gamma_{sr} = N(N-1)\,\Gamma_{sp}\Gamma_{qr} \tag{2.52}$$

(both ways of writing it are equivalent, but we shall employ mostly the first, which proves to be more convenient).

Combining the results (2.47), (2.48), and (2.52), we find that the energy function, given by the relation $E(z^*, z) = \langle z|\hat{H}|z\rangle$, assumes the form:

$$\begin{aligned} E &= N\sum_{pq} h_{pq}\Gamma_{qp} + \tfrac{1}{2}N(N-1)\sum_{pqrs} U_{pr\cdot qs}\Gamma_{sr}\Gamma_{qp} \\ &= N\sum_{pq}\Big[h_{pq} + \tfrac{1}{2}(N-1)\sum_{rs} U_{pr\cdot qs}\Gamma_{sr}\Big]\Gamma_{qp} \\ &= N\sum_{pq}(h_{pq} + \tfrac{1}{2}v_{pq})\Gamma_{qp} = N\,\mathrm{tr}\Big[(h+\tfrac{1}{2}v)\Gamma\Big]. \end{aligned} \tag{2.53}$$

In the last line we have defined a new and very important quantity, the bosonic *mean-field* matrix v, whose elements are:

$$v_{pq} = (N-1)\sum_{rs} U_{pr\cdot qs}\,\Gamma_{sr}, \quad v_{pq} = v^*_{qp}. \tag{2.54}$$

The term 'mean-field' has the usual meaning: the matrix v, which depends on Γ, represents an effective one-body potential constructed out of pairwise interactions by adding up all second-particle contributions – this is mathematically accomplished by tracing the two-body integrals over all secondary modes (indexes s and r) with the one-density playing the role of a weight factor.

Our next task is to express the coherent-state equation of motion for the particular Hamiltonian in question. For that purpose we require the derivative of the energy function with respect to z^*. Noticing that all dependence of E on both z and z^* comes from $\Gamma(z^*, z)$ we can make use of the chain rule to obtain:

$$\frac{\partial E}{\partial z^*_\mu} = \sum_{pq} G_{pq}\frac{\partial \Gamma_{qp}}{\partial z^*_\mu}, \tag{2.55}$$

where the density-dependent matrix G, a key quantity that we shall denominate the 'Gross-Pitaevskii matrix', is simply:

$$G_{pq}(\Gamma) = h_{pq} + v_{pq}(\Gamma) = h_{pq} + (N-1)\sum_{rs} U_{pr\cdot qs}\Gamma_{sr}. \tag{2.56}$$

The gradients of Γ are computed in Appendix B. Substituting the appropriate formulas in Eq. (2.55) and plugging the resulting expression into Eq. (2.43) one gets, after some straightforward algebra,

$$i\hbar\,\dot{z}_\mu = G_{\mu 0} + \sum_\nu G_{\mu\nu}z_\nu - z_\mu G_{00} - z_\mu\sum_\nu G_{0\nu}z_\nu. \tag{2.57}$$

Notice that this equation of motion is highly non-linear.

Finally, let us consider the Lagrangian, which is obtained from (1.66) upon substitution of E and $\dot{z}$, as given by Eqs. (2.53) and (2.57), as well as the Kähler gradients listed in (2.36). By means of these relations (and other connections involving the one-density elements) the general expression can be worked down in terms of more basic ingredients and it can be organized in many possible ways. We have found that a useful form for practical purposes is:

$$L = -NG_{00} - \tfrac{1}{2}N\sum_{\mu}(G_{0\mu}z_{\mu} + z^{*}_{\mu}G_{\mu 0}) + \tfrac{1}{2}N\sum_{pq} v_{pq}\Gamma_{qp}. \tag{2.58}$$

2.2.3 * Exact solutions for non-interacting systems

In order to gain some insight let us briefly discuss explicit solutions to the equation of motion. As always, these are only available for non-interacting systems. In this special case we conveniently assume that we are working with the specific set of single-particle modes that diagonalizes the one-body integral. There is no loss of generality in doing so for this can be accomplished through a simple unitary transformation of the basic set $|\phi\rangle$. We thus have $v = 0$ and h in the diagonal form:

$$h = \mathrm{diag}(\varepsilon_0, \lambda_1, \lambda_2, \ldots, \lambda_d) \tag{2.59}$$

(it is not important to our purposes whether degenerate eigenvalues occur or not). In terms of this particular set of modes, and since we have $G = h$, Eq. (2.57) is dramatically simplified and its solution can be written at once:

$$i\hbar\,\dot{z}_{\mu} = (\lambda_{\mu} - \varepsilon_0)z_{\mu} \quad \Rightarrow \quad z_{\mu}(t) = z_{\mu}(0)e^{-\frac{i}{\hbar}(\lambda_{\mu}-\varepsilon_0)t}. \tag{2.60}$$

Meanwhile, the Lagrangian is just $L = -N\varepsilon_0$, and therefore the action evaluates to $S = -N\varepsilon_0 t$. Then, according to Eq. (1.75), the time-evolved state reads:

$$|z_t\rangle e^{\frac{i}{\hbar}S_t(z)} = |z(z_0,t)\rangle\; e^{-\frac{i}{\hbar}N\varepsilon_0 t}, \quad \text{where:} \;\; z_{\mu}(z_0,t) = z_{0\mu}\; e^{-\frac{i}{\hbar}(\lambda_{\mu}-\varepsilon_0)t}. \tag{2.61}$$

This exercise shows that, in the absence of interactions, the state remains coherent throughout the dynamics, the only effect being a rotation of the argument of each element of the z vector and the accumulation of a global phase.

2.3 * More geometry: transformation of single-particle modes

In this last section we shall investigate the effect that a unitary transformation of the underlying single-particle modes has on the coherent state. In other words, we seek to understand the connection between coherent states defined over different sets of basis

functions spanning the same space. This is useful since sometimes matrix elements of certain operators are more easily computed if their second-quantized expressions are written in terms of a specific set, and that set may be different from the one which is more appropriate to carry out the dynamics.

Let us then consider two sets of single-particle modes, $|\phi\rangle$ and $|\chi\rangle$, with corresponding creation operators $b^\dagger$ and $a^\dagger$:

$$|\phi_p\rangle = b_p^\dagger|0\rangle \quad \text{and} \quad |\chi_p\rangle = a_p^\dagger|0\rangle, \quad 0 \leq p \leq d. \tag{2.62}$$

Both sets are constituted by orthonormal functions and both span the same single-particle space:

$$\hat{P} = \sum_p |\phi_p\rangle\langle\phi_p| = \sum_p |\chi_p\rangle\langle\chi_p|. \tag{2.63}$$

Denoting by X the transformation matrix of $|\phi\rangle \leftarrow |\chi\rangle$ ($b^\dagger \leftarrow a^\dagger$) and by Y its inverse (which is equal to its adjoint) we establish the transformation rules:

$$\begin{cases} |\phi_p\rangle = \sum_q |\chi_q\rangle\langle\chi_q|\phi_p\rangle = \sum_q |\chi_q\rangle X_{qp} \\ |\chi_p\rangle = \sum_q |\phi_q\rangle\langle\phi_q|\chi_p\rangle = \sum_q |\phi_q\rangle Y_{qp} \end{cases} \Rightarrow \begin{cases} b_p^\dagger = \sum_q a_q^\dagger X_{qp} \\ a_p^\dagger = \sum_q b_q^\dagger Y_{qp} \end{cases} \quad \text{with: } Y = X^\dagger = X^{-1}. \tag{2.64}$$

In particular, the connection involving creation and annihilation operators can be written as:

$$b_0^\dagger = a_0^\dagger X_{00} + \sum_\nu a_\nu^\dagger X_{\nu 0} \tag{2.65a}$$

$$b_\mu^\dagger = a_0^\dagger X_{0\mu} + \sum_\nu a_\nu^\dagger X_{\nu\mu} \tag{2.65b}$$

Let us now substitute these relations in the coherent state definition, Eq. (2.19), to see what happens once the original basic operators b and $b^\dagger$, associated with the modes $|\phi\rangle$ that underly the state $|z\}_\phi$ (as explicitly indicated here), are replaced by a different set; working down the expression we find:

$$\begin{aligned} \sqrt{N!}|z\}_\phi &= \left(b_0^\dagger + \textstyle\sum_\mu z_\mu b_\mu^\dagger\right)^N |0\rangle \\ &= \left[(a_0^\dagger X_{00} + \textstyle\sum_\nu a_\nu^\dagger X_{\nu 0}) + \sum_\mu z_\mu (a_0^\dagger X_{0\mu} + \sum_\nu a_\nu^\dagger X_{\nu\mu})\right]^N |0\rangle \\ &= \left[a_0^\dagger (X_{00} + \textstyle\sum_\mu X_{0\mu} z_\mu) + \sum_\nu a_\nu^\dagger (X_{\nu 0} + \sum_\mu X_{\nu\mu} z_\mu)\right]^N |0\rangle \\ &= (X_{00} + \textstyle\sum_\mu X_{0\mu} z_\mu)^N \left[a_0^\dagger + \sum_\nu a_\nu^\dagger (X_{\nu 0} + \sum_\mu X_{\nu\mu} z_\mu)(X_{00} + \sum_\mu X_{0\mu} z_\mu)^{-1}\right]^N |0\rangle \\ &= (X_{00} + \textstyle\sum_\mu X_{0\mu} z_\mu)^N \left(a_0^\dagger + \sum_\nu a_\nu^\dagger w_\nu\right)^N |0\rangle, \end{aligned} \tag{2.66}$$

where in the last line we have defined:

$$w_\nu = \Big(X_{\nu 0} + \sum_\mu X_{\nu\mu} z_\mu\Big)\Big(X_{00} + \sum_\mu X_{0\mu} z_\mu\Big)^{-1}. \tag{2.67}$$

Now, again from Eq. (2.19), we know that a coherent-state $|w\}_\chi$, defined over the set $|\chi\rangle$ (as indicated), has the form:

$$|w\}_\chi = \frac{1}{\sqrt{N!}}\Big(a_0^\dagger + \sum_\nu a_\nu^\dagger w_\nu\Big)^N |0\rangle. \tag{2.68}$$

Comparing this with Eq. (2.66) we conclude that:

$$|w\}_\chi = |z\}_\phi (X_{00} + \textstyle\sum_\mu X_{0\mu} z_\mu)^{-N}, \tag{2.69}$$

with w given by (2.67). This is the connecting formula that we were seeking.

Similarly, had we considered the transformation in the opposite direction, it would give:

$$|z\}_\phi = |w\}_\chi (Y_{00} + \textstyle\sum_\mu Y_{0\mu} w_\mu)^{-N}, \tag{2.70}$$

with z given in terms of w as:

$$z_\mu = \Big(Y_{\mu 0} + \sum_\nu Y_{\mu\nu} w_\nu\Big)\Big(Y_{00} + \sum_\nu Y_{0\nu} w_\nu\Big)^{-1}. \tag{2.71}$$

Note that Eqs. (2.69) and (2.70) imply the equality:

$$(X_{00} + \textstyle\sum_\mu X_{0\mu} z_\mu) = (Y_{00} + \sum_\mu Y_{0\mu} w_\mu)^{-1}, \tag{2.72}$$

which is easily verifiable.

Let us now study the connecting formulas in terms of normalized states. The relation between $|z\rangle_\phi$ and $|w\rangle_\chi$ is found by adding the respective normalization factors:

$$|z\rangle_\phi = |w\rangle_\chi (Y_{00} + \textstyle\sum_\mu Y_{0\mu} w_\mu)^{-N} (1 + w^* w)^{N/2} (1 + z^* z)^{-N/2}. \tag{2.73}$$

On the right side we opt to eliminate z in favor of w, which will lead us to a transformation in the direction $|z\rangle_\phi \leftarrow |w\rangle_\chi$. Using the complex conjugate of (2.70), and the fact the $X = Y^\dagger$, we write:

$$z_\mu^* = \frac{Y_{\mu 0}^* + \sum_\nu Y_{\mu\nu}^* w_\nu^*}{Y_{00}^* + \sum_\nu Y_{0\nu}^* w_\nu^*} = \frac{X_{0\mu} + \sum_\nu w_\nu^* X_{\nu\mu}}{X_{00} + \sum_\nu w_\nu^* X_{\nu 0}}, \tag{2.74}$$

and use this to evaluate the normalization factor involving z:

$$\begin{aligned}
1+z^*z &= 1+\sum_\mu \frac{(X_{0\mu}+\sum_\nu w_\nu^* X_{\nu\mu})(Y_{\mu 0}+\sum_{\nu'} Y_{\mu\nu'}w_{\nu'})}{(X_{00}+\sum_\nu w_\nu^* X_{\nu 0})(Y_{00}+\sum_{\nu'} Y_{0\nu'}w_{\nu'})} \\
&= (X_{00}+\textstyle\sum_\nu w_\nu^* X_{\nu 0})^{-1}(Y_{00}+\sum_{\nu'} Y_{0\nu'}w_{\nu'})^{-1} \\
&\quad \times \Big[(X_{00}Y_{00}+\textstyle\sum_\mu X_{0\mu}Y_{\mu 0})+\sum_\nu (X_{00}Y_{0\nu}+\sum_\mu X_{0\mu}Y_{\mu\nu})w_\nu \\
&\qquad +\textstyle\sum_\nu w_\nu^*(X_{\nu 0}Y_{00}+\sum_\mu X_{\nu\mu}Y_{\mu 0})+\sum_\nu w_\nu^*(X_{\nu 0}Y_{0\nu}+\sum_\mu X_{\nu\mu}Y_{\mu\nu})w_\nu\Big] \\
&= (X_{00}+\textstyle\sum_\nu w_\nu^* X_{\nu 0})^{-1}(Y_{00}+\sum_{\nu'} Y_{0\nu'}w_{\nu'})^{-1}(1+w^*w). \qquad (2.75)
\end{aligned}$$

Putting this result into Eq. (2.73) we find:

$$|z\rangle_\phi = |w\rangle_\chi \left[\frac{X_{00}+\sum_\nu w_\nu^* X_{\nu 0}}{Y_{00}+\sum_\nu Y_{0\nu}w_\nu}\right]^{N/2} = |w\rangle_\chi \left[\frac{Y_{00}+\sum_\nu Y_{0\nu}w_\nu}{Y_{00}^*+\sum_\nu Y_{0\nu}^* w_\nu^*}\right]^{-N/2}. \qquad (2.76)$$

The complex quotient inside the brackets has unity modulus. Denoting its phase by φ we conclude:

$$\begin{cases} |z\rangle_\phi = |w\rangle_\chi e^{-iN\varphi} \\ |w\rangle_\chi = |z\rangle_\phi e^{iN\varphi} \end{cases} \quad \text{with:} \quad \varphi = \begin{cases} \arg[(Y_{00}+\sum_\nu Y_{0\nu}w_\nu)] \\ -\arg[(X_{00}+\sum_\nu X_{0\nu}z_\nu)] \end{cases}. \qquad (2.77)$$

Notice that the equality (2.72) allows us to write the phase φ at our convenience, in terms of either z or w.

The above formulas are the desired connections between coherent-state labels defined over distinct sets of single-particle modes. They reveal that the unitary transformation induces an holomorphic map on the coherent-state variable, and that a consequence of such a map is the appearance of a phase factor on the transformed vector.

Chapter 3

Fermionic coherent states

Overview. Fermionic coherent states of the special unitary group, also known as *Thouless determinants*, are reviewed. They are understood in terms of an underlying set of dynamical orbitals. Their dynamics is worked out for general systems using the time-dependent variational principle. The important class of Hamiltonians containing one- and two-body terms is then considered. Equations of motion for this particular case are derived and the connection to mean-field theories is established. Spin structure is explicitly examined. Additional properties, concerning the effects of group transformations, are investigated. The exposition closely follows that of Ref. [17].

3.1 Thouless determinants

3.1.1 Preliminaries

Once more we begin by introducing the single-particle space that underlies the many-body problem. A finite set of K orthonormal states constitutes a basis for such space – the projector is:

$$\hat{P} = \sum_{p=1}^{K} |\phi_p\rangle\langle\phi_p|, \quad \phi_p(\mathbf{x}) = \langle\mathbf{x}|\phi_p\rangle. \tag{3.1}$$

In the fermionic framework the states $|\phi\rangle$ are called 'orbitals'. The formalism makes no distinction between molecular and atomic orbitals – any set will do provided the orthonormality requirement is observed. The limit of completeness is approached by enlarging the basis set:

$$P(\mathbf{x},\mathbf{x}') = \langle\mathbf{x}|\hat{P}|\mathbf{x}'\rangle \overset{K\to\infty}{=} \delta(\mathbf{x}-\mathbf{x}'), \tag{3.2}$$

although, in practice, a truncated basis is almost always employed, the accuracy of such a description relying on physical considerations regarding the nature of the system and the type of phenomena under investigation.

It should be observed that, here, $\mathbf{x}$ denotes a conventional three-dimensional position vector. Spin structure is of great relevance to any fermion system and more will be said about it in a moment. For now it suffices to point out that, in the present scheme, each function $\phi_p(\mathbf{x})$ is to be understood as a distinct spin component of an associated 'spin-orbital' (a more general and often employed kind of basis function).

Creation and annihilation operators are assigned to each orbital. They satisfy the anti-commutation relations (anti-commutators are denoted by curly brackets, $\{\hat{A}, \hat{B}\} = \hat{A}\hat{B} + \hat{B}\hat{A}$):

$$\begin{cases} |\phi_p\rangle = c_p^\dagger|0\rangle \\ \langle\phi_q| = \langle 0|c_q \end{cases} \quad \text{with:} \quad \begin{cases} \{c_p, c_q^\dagger\} = \delta_{pq} \\ \{c_p, c_q\} = \{c_p^\dagger, c_q^\dagger\} = 0 \end{cases} \quad , \quad 1 \leq p, q \leq K. \tag{3.3}$$

The fermionic field operators, defined over the finite single-particle space, are:

$$\begin{cases} \hat{\psi}(\mathbf{x}) = \sum_{p=1}^K \phi_p(\mathbf{x}) c_p \\ \hat{\psi}^\dagger(\mathbf{x}) = \sum_{p=1}^K \phi_p^*(\mathbf{x}) c_p^\dagger \end{cases} \Leftrightarrow \begin{cases} c_p = \int d\mathbf{x}\, \phi_p^*(\mathbf{x}) \hat{\psi}(\mathbf{x}) \\ c_p^\dagger = \int d\mathbf{x}\, \phi_p(\mathbf{x}) \hat{\psi}^\dagger(\mathbf{x}) \end{cases} \quad , \quad 1 \leq p \leq K. \tag{3.4}$$

They obey:

$$\{\hat{\psi}(\mathbf{x}), \hat{\psi}^\dagger(\mathbf{x}')\} = P(\mathbf{x}, \mathbf{x}'), \quad \{\hat{\psi}(\mathbf{x}), \hat{\psi}(\mathbf{x}')\} = \{\hat{\psi}^\dagger(\mathbf{x}), \hat{\psi}^\dagger(\mathbf{x}')\} = 0. \tag{3.5}$$

Notice that spin components of the field operators have not yet been distinguished – spin-specific formulas will be given later.

Let us now turn to the many-body problem. A complete set of basis vectors is supplied by the eigenstates of the number operator,[46]

$$\hat{n}_p|n_1, n_2, \ldots, n_K\rangle = n_p|n_1, n_2, \ldots, n_K\rangle, \quad \hat{n}_p = c_p^\dagger c_p, \quad 1 \leq p \leq K. \tag{3.6}$$

These states are given in terms of the basic creation operators,

$$|n_1, n_2, \ldots, n_K\rangle = (c_1^\dagger)^{n_1}(c_2^\dagger)^{n_2} \ldots (c_K^\dagger)^{n_K}|0\rangle, \quad n_p \in \{0, 1\},\ 1 \leq p \leq K, \tag{3.7}$$

with $|0\rangle$ being the vacuum state. As indicated, the label n denotes a binary array of occupation numbers, $n = (n_1, n_2, \ldots, n_K)$, with each n_p being zero or unity in agreement with the exclusion principle.

Once more we shall restrict attention to number-conserving Hamiltonians, so that the possible sets of occupation numbers satisfy the constraint:

$$n_1 + n_2 + \cdots + n_K = N, \tag{3.8}$$

or, in abbreviated form, $|n| = N$. Notice that the exclusion principle demands $K \geq N$.

Since each orbital contains at most a single fermion the dimension of the Fock space $\mathcal{F}(K,N)$ is easily calculated; it is simply the number of possible ways of distributing N indistinguishable objects into K boxes:

$$\dim \mathcal{F}(K,N) = \frac{K!}{N!(K-N)!}. \tag{3.9}$$

Under the enunciated conditions, the total particle number operator $\hat{N}$ must be a constant of motion:

$$\hat{N} = \sum_p \hat{n}_p, \quad [\hat{H}, \hat{N}] = 0, \tag{3.10}$$

and Hamiltonians subjected to this restriction can always be expressed in terms of the bilinear forms $c_p^\dagger c_q$. These forms obey the following *commutation* rules:

$$[c_p^\dagger c_q, c_r^\dagger c_s] = c_p^\dagger c_s\, \delta_{qr} - c_r^\dagger c_q\, \delta_{sp}, \quad 1 \leq p,q,r,s \leq K. \tag{3.11}$$

A basis for the su(K) algebra of the special unitary group SU(K) can be written in terms of these fermionic bilinears. This establishes the dynamical group associated with the system's Hamiltonian.

3.1.2 Coherent states: definition and dynamical orbitals

Following the general theory delineated in Chapter 1, we shall define the fermionic coherent state in terms of a displacement operator acting on a reference state $|\Phi_0\rangle$. This state will be selected from the set of many-body configurations that span the Fock space. The choice is ultimately arbitrary, but a meaningful reference state is crucial for stability in numerical calculations. We thus suppose there exists a certain hierarchy among the K single-particle basis functions $|\phi\rangle$ which determines their indexation order. In treating weakly interacting systems, for example, it is useful to think that orbitals are classified according to their energy expectation values, as computed from the non-interacting part of the Hamiltonian, in ascending energy order (some auxiliary criteria may be needed for handling degeneracies). In this case, an appropriate reference state would be that in which the first N orbitals, those with lowest energy, are filled, while the remaining $K-N$ are empty, i.e. the non-interacting ground state:

$$|\Phi_0\rangle = c_1^\dagger c_2^\dagger \cdots c_N^\dagger |0\rangle = |\underbrace{1,1,\ldots,1}_{N},\underbrace{0,0,\ldots,0}_{M}\rangle, \quad M \equiv K-N. \tag{3.12}$$

The above reference state is a Slater determinant in the orbitals $\{|\phi_1\rangle, |\phi_2\rangle, \ldots, |\phi_N\rangle\}$ and, following common practice in quantum chemistry, each Fock configuration can be visualized as an excitation of this determinant.[47]

As indicated in (3.12), the reference state divides the single-particle space into two

sub-spaces: the first N orbitals are said to belong to the 'occupied space'; the remaining M orbitals are said to belong to the 'virtual space' – these are sometimes called the 'hole' and 'particle' spaces, respectively.[15] This structure is ubiquitous in the fermionic coherent-state formalism and we thus adopt a special notation: creation and annihilation operators belonging to each sub-space are denoted by different letters, as detailed below:

$$\begin{cases} a^\dagger = (a_1^\dagger, a_2^\dagger, \ldots, a_N^\dagger) = (c_1^\dagger, c_2^\dagger, \ldots, c_N^\dagger) \\ b^\dagger = (b_1^\dagger, b_2^\dagger, \ldots, b_M^\dagger) = (c_{N+1}^\dagger, c_{N+2}^\dagger, \ldots, c_K^\dagger). \end{cases} \tag{3.13}$$

Likewise, occupied and virtual orbitals are distinguished according to the following scheme:

$$\begin{cases} (\phi_1^\bullet, \phi_2^\bullet, \ldots, \phi_N^\bullet) = (\phi_1, \phi_2, \ldots, \phi_N) \\ (\phi_1^\circ, \phi_2^\circ, \ldots, \phi_M^\circ) = (\phi_{N+1}, \phi_{N+2}, \ldots, \phi_K) \end{cases} \tag{3.14}$$

– the use of symbols '$\bullet$' and '$\circ$' to label these orbitals is reminiscent of the notation employed by Deumens and collaborators in several works.[15;17]

The above classification is further supported by a subscript convention: different sets of Greek letters will be employed when referring to occupied and virtual index ranges,

$$\begin{cases} 1 \leq (\alpha, \beta, \gamma) \leq N \\ 1 \leq (\mu, \nu, \eta) \leq M \end{cases} \quad \text{and} \quad 1 \leq (p, q, r, s) \leq K; \tag{3.15}$$

the indicated Latin letters refer to the full range of single-particle states, as in the bosonic case. Bearing in mind these conventions we shall henceforth omit the limits in sums and products. To exemplify the new notation, we recast the basic anti-commutation rules:

$$\{a_\alpha, a_\beta^\dagger\} = \delta_{\alpha\beta}, \;\; \{b_\mu, b_\nu^\dagger\} = \delta_{\mu\nu}, \;\; \{a_\alpha, b_\nu^\dagger\} = \{b_\mu, a_\beta^\dagger\} = 0, \;\; \{a_\alpha, a_\beta\} = \{b_\mu, b_\nu\} = 0. \tag{3.16}$$

Let us now introduce the fermionic coherent state; its unnormalized form is:

$$|z\} = \exp\Big(\sum_\mu \sum_\alpha z_{\mu\alpha} b_\mu^\dagger a_\alpha\Big)|\Phi_0\rangle. \tag{3.17}$$

Notice that the coherent-state label z is best understood as a matrix of size $M \times N$,

$$z = \begin{bmatrix} z_{11} & z_{12} & \cdots & z_{1N} \\ z_{21} & z_{22} & \cdots & z_{2N} \\ \vdots & \vdots & \ddots & \vdots \\ z_{M1} & z_{M2} & \cdots & z_{MN} \end{bmatrix}, \quad z^\dagger = \begin{bmatrix} z_{11}^* & z_{21}^* & \cdots & z_{M1}^* \\ z_{12}^* & z_{22}^* & \cdots & z_{M2}^* \\ \vdots & \vdots & \ddots & \vdots \\ z_{1N}^* & z_{2N}^* & \cdots & z_{MN}^* \end{bmatrix}, \tag{3.18}$$

and, therefore, the number of degrees of freedom in the fermionic phase space is $d = MN$. In Eq. (3.18) we also display the adjoint $N \times M$ matrix $z^\dagger$. In most problems we have

$M > N$ and these matrices are rectangular. From (3.17) we see that each matrix entry $z_{\mu\alpha}$ is related to an excitation process, in which a fermion is transferred from the occupied to the virtual space.

Following the same steps of the previous chapter we shall next work down the coherent state definition to a more tractable form. For that purpose we first note that the bilinears in the exponent *commute* among themselves, $[b_\mu^\dagger a_\alpha, b_\nu^\dagger a_\beta] = 0$. Moreover, it can be easily demonstrated that $[b_\mu^\dagger a_\alpha, a_\beta^\dagger] = b_\mu^\dagger \delta_{\alpha\beta}$. These observations permit us to expand (3.17) as

$$\begin{aligned}
|z\} &= (1 + \textstyle\sum_\mu z_{\mu 1} b_\mu^\dagger a_1)(1 + \sum_\mu z_{\mu 2} b_\mu^\dagger a_2) \cdots (1 + \sum_\mu z_{\mu N} b_\mu^\dagger a_N) \;\cdot\; (a_1^\dagger a_2^\dagger \cdots a_N^\dagger)|0\rangle \\
&= (a_1^\dagger + \textstyle\sum_\mu z_{\mu 1} b_\mu^\dagger a_1 a_1^\dagger)(a_2^\dagger + \sum_\mu z_{\mu 2} b_\mu^\dagger a_2 a_2^\dagger) \cdots (a_N^\dagger + \sum_\mu z_{\mu N} b_\mu^\dagger a_N a_N^\dagger)|0\rangle \\
&= (a_1^\dagger + \textstyle\sum_\mu z_{\mu 1} b_\mu^\dagger (1 - \hat{n}_1))(a_2^\dagger + \sum_\mu z_{\mu 2} b_\mu^\dagger (1 - \hat{n}_2)) \cdots (a_N^\dagger + \sum_\mu z_{\mu N} b_\mu^\dagger (1 - \hat{n}_N))|0\rangle \\
&= (a_1^\dagger + \textstyle\sum_\mu z_{\mu 1} b_\mu^\dagger)(a_2^\dagger + \sum_\mu z_{\mu 2} b_\mu^\dagger) \cdots (a_N^\dagger + \sum_\mu z_{\mu N} b_\mu^\dagger)|0\rangle \\
&= \textstyle\prod_\alpha (a_\alpha^\dagger + \sum_\mu b_\mu^\dagger z_{\mu\alpha})|0\rangle
\end{aligned} \tag{3.19}$$

(the trick in going from the third to fourth line is to realize that, evaluating the expression from right to left one term at a time, the number operator $\hat{n}_\alpha$ always acts on a state in which the α-th orbital is vacant). Equation (3.19) reveals that the unnormalized coherent state can be transparently written in terms of a new set of fermionic creation operators:

$$|z\} = \zeta_1^\dagger \zeta_2^\dagger \cdots \zeta_N^\dagger |0\rangle, \quad \zeta_\alpha^\dagger(z) = a_\alpha^\dagger + \sum_\mu b_\mu^\dagger z_{\mu\alpha}, \quad 1 \le \alpha \le N. \tag{3.20}$$

These new operators and their adjoints obey anti-commutation rules of the general form:

$$\{\zeta_\alpha(z^*), \zeta_\beta^\dagger(z')\} = \delta_{\alpha\beta} + \sum_\nu z_{\nu\alpha}^* z'_{\nu\beta}, \tag{3.21a}$$

$$\{\zeta_\alpha(z^*), \zeta_\beta(z^{*\prime})\} = \{\zeta_\alpha^\dagger(z), \zeta_\beta^\dagger(z')\} = 0. \tag{3.21b}$$

here displayed for possibly different coherent-state labels.

The above formulas show that $|z\}$ is a general type of Slater determinant, defined in terms of a non-orthogonal set of single-particle orbitals $|\zeta(z)\}$, called *dynamical orbitals*,[17] parametrized by z in terms of the unnormalized superposition:

$$|\zeta_\alpha(z)\} = |\phi_\alpha^\bullet\rangle + \sum_\mu |\phi_\mu^\circ\rangle z_{\mu\alpha}, \tag{3.22}$$

or, more explicitly,

$$|z\} = \hat{A}_N \prod_\alpha |\zeta_\alpha(z)\} = \hat{A}_N \prod_\alpha \Big[|\phi_\alpha^\bullet\rangle + \sum_\mu |\phi_\mu^\circ\rangle z_{\mu\alpha}\Big], \tag{3.23}$$

where the symbol $\hat{A}_N$ instructs anti-symmetrization of the product of N single-particle states. This type of parametrization for Slater determinants was first proposed by Thouless as a tool for studying the stability of Hartree-Fock equations, particularly in what concerns collective modes of nuclear matter.[14] It has since been known as a *Thouless determinant*.

Before proceeding with the development of the coherent-state formalism, let us list, for future reference, the useful anti-commutation rules:

$$\{a_\alpha, \zeta_\beta^\dagger\} = \delta_{\alpha\beta}, \quad \{a_\alpha^\dagger, \zeta_\beta^\dagger\} = 0, \quad \{b_\mu, \zeta_\beta^\dagger\} = z_{\mu\beta}, \quad \{b_\mu^\dagger, \zeta_\beta^\dagger\} = 0, \tag{3.24}$$

which can be obtained without difficulty from the basic anti-commutators and the definition of $\zeta^\dagger$.

Let us evaluate the overlap $\{z|z'\}$ between two Thouless determinants – this result is easily found once we note that

$$\{\zeta_\alpha(z^*)|\zeta_\beta(z')\} = (I_N + z^\dagger z')_{\alpha\beta}, \tag{3.25}$$

for we may now invoke the fact that the overlap between two general Slater determinants is just the determinant of the matrix defined by the overlaps of its occupied orbitals (this holds even for non-orthogonal orbitals).[48] Abbreviating somewhat the notation, we get immediately:

$$\{z|z'\} = \langle 0|(\zeta_N \dots \zeta_1)(\zeta'^\dagger_1 \dots \zeta'^\dagger_N)|0\rangle = \det_{1\le\alpha,\beta\le N}\{\zeta_\alpha(z^*)|\zeta_\beta(z')\} = \det(I_N + z^\dagger z'). \tag{3.26}$$

Lastly, the Fock decomposition of $|z\}$ can be computed with the help of the anti-commutation rules stated in (3.24). The detailed calculation is found in Appendix C. The final result, here translated to more conventional quantum chemistry language, is:[i]

$$|z\} = \sum_{l=0}^{N} \sum_{\alpha\in C_l^N} \sum_{\mu\in C_l^M} |\Phi_{0\,(\alpha_1\alpha_2\cdots\alpha_l)}^{(\mu_1\mu_2\cdots\mu_l)}\rangle \det[z_{(\mu_1\mu_2\cdots\mu_l)(\alpha_1\alpha_2\cdots\alpha_l)}], \tag{3.27}$$

where $|\Phi_{0\,(\alpha_1\alpha_2\cdots\alpha_l)}^{(\mu_1\mu_2\cdots\mu_l)}\rangle$ is an l-th order excited configuration, built from $|\Phi_0\rangle$ by transferring l fermions from occupied orbitals $(\phi^\bullet_{\alpha_1}, \phi^\bullet_{\alpha_2}, \cdots, \phi^\bullet_{\alpha_l})$ to virtual orbitals $(\phi^\circ_{\mu_1}, \phi^\circ_{\mu_2}, \cdots, \phi^\circ_{\mu_l})$ by successive action of particle-hole creators (which commute):

$$|\Phi_{0\,(\alpha_1\alpha_2\cdots\alpha_l)}^{(\mu_1\mu_2\cdots\mu_l)}\rangle = (b_{\mu_1}^\dagger a_{\alpha_1})(b_{\mu_2}^\dagger a_{\alpha_2})\cdots(b_{\mu_l}^\dagger a_{\alpha_l})|\Phi_0\rangle. \tag{3.28}$$

[i] In Appendix C the decomposition is given in terms of standard Fock states. The states $|\Phi_{0\,(\alpha_1\alpha_2\cdots\alpha_l)}^{(\mu_1\mu_2\cdots\mu_l)}\rangle$, in terms of which the result expressed in Eq. (3.27) is written, are defined according to a non-standard operator ordering – see Eq. (3.28) below. The relative sign between both orderings precisely cancels the signature factor $(-)^\pi$ of Eq. (C.32); this is why there is no such factor in Eq. (3.27).

The sum in Eq. (3.28) is over all possible ways of selecting l out of N objects, i.e. over all elements of the set of combinations C_l^N, times all possible ways of placing them into M boxes, i.e. elements of the set of combinations C_l^M, with l ranging from 0 to N. An important detail here is that combinations are *ordered*: if $\alpha \in C_l^N$, then $\alpha_1 < \alpha_2 < \cdots < \alpha_l$, and similarly for $\mu \in C_l^M$. In this way, all Fock states have a nonzero overlap with $|z\}$, which is controlled by the quantity $\det[z_{(\mu_1\mu_2\cdots\mu_l)(\alpha_1\alpha_2\cdots\alpha_l)}]$, i.e. the sub-determinant of z computed with the indicated rows and columns.

3.1.3 * Complementary orbitals and projectors

A complementary set of M orbitals can also be defined using the z matrix.[17] Their creation operators are:

$$\bar{\zeta}_\mu^\dagger(z^*) = b_\mu^\dagger - \sum_\beta z_{\mu\beta}^* a_\beta^\dagger, \quad 1 \le \mu \le M, \tag{3.29}$$

with corresponding single-particle states:

$$|\bar{\zeta}_\mu(z^*)\} = |\phi_\mu^\circ\rangle - \sum_\beta |\phi_\beta^\bullet\rangle z_{\mu\beta}^*. \tag{3.30}$$

By construction, these states are orthogonal to the set $|\zeta_\alpha(z)\}$, since the overlap

$$\{\bar{\zeta}_\mu(z)|\zeta_\alpha^\dagger(z')\} = z_{\mu\alpha} - z'_{\mu\alpha}, \tag{3.31}$$

vanishes for $z' = z$. Additionally, the complementary creation and annihilation operators satisfy:

$$\{\bar{\zeta}_\mu(z'), \bar{\zeta}_\nu^\dagger(z^*)\} = \delta_{\mu\nu} - \sum_\beta z'_{\mu\beta} z_{\nu\beta}^*, \quad \{\bar{\zeta}_\mu(z'), \bar{\zeta}_\nu(z)\} = 0, \tag{3.32}$$

showing that these complementary states are not orthogonal among themselves.

The sets $\{\zeta(z), \bar{\zeta}(z)\}$ and $\{\phi^\bullet, \phi^\circ\}$ span the same single-particle space. This can be verified as follows: with the aid of Eqs. (3.20) and (3.29) we write the basis transformation in matrix form using creation operators,

$$\begin{bmatrix} \zeta^\dagger & \bar{\zeta}^\dagger \end{bmatrix} = \begin{bmatrix} a^\dagger & b^\dagger \end{bmatrix} \begin{bmatrix} I_N & -z^\dagger \\ z & I_M \end{bmatrix}. \tag{3.33}$$

Next, we employ the matrix identity,

$$\begin{bmatrix} I_N & 0 \\ 0 & I_M \end{bmatrix} = \begin{bmatrix} I_N & z^\dagger \\ -z & I_M \end{bmatrix} \begin{bmatrix} (I_N + z^\dagger z)^{-1} & 0 \\ 0 & (I_M + zz^\dagger)^{-1} \end{bmatrix} \begin{bmatrix} I_N & -z^\dagger \\ z & I_M \end{bmatrix}, \tag{3.34}$$

to get the inverse:

$$a^\dagger_\alpha = \sum_\beta (\zeta^\dagger_\beta - \sum_\nu \bar{\zeta}^\dagger_\nu z_{\nu\beta})(I_N + z^\dagger z)^{-1}_{\beta\alpha}, \tag{3.35a}$$

$$b^\dagger_\mu = \sum_\nu (\bar{\zeta}^\dagger_\nu + \sum_\beta \zeta^\dagger_\beta z^\dagger_{\beta\nu})(I_M + zz^\dagger)^{-1}_{\nu\mu}. \tag{3.35b}$$

Expressing the above formulas in terms of orbitals, and making use of the auxiliary relations

$$z(I_M + zz^\dagger)^{-1} = (I_N + z^\dagger z)^{-1} z, \quad z^\dagger (I_M + zz^\dagger)^{-1} = (I_N + z^\dagger z)^{-1} z^\dagger, \tag{3.36}$$

one is able to write the single-particle projector as follows:

$$\begin{aligned} \hat{P} &= \sum_\alpha |\phi^\bullet_\alpha\rangle\langle\phi^\bullet_\alpha| + \sum_\mu |\phi^\circ_\mu\rangle\langle\phi^\circ_\mu| \\ &= \sum_{\alpha\beta} |\zeta_\alpha\}(I_N + z^\dagger z)^{-1}_{\alpha\beta}\{\zeta_\beta| + \sum_{\mu\nu} |\bar{\zeta}_\mu\}(I_M + zz^\dagger)^{-1}_{\mu\nu}\{\bar{\zeta}_\nu|, \end{aligned} \tag{3.37}$$

i.e. the projector splits into two orthogonal parts: the first consisting of dynamical orbitals $|\zeta(z)\}$, and the second consisting of complementary orbitals $|\bar{\zeta}(z)\}$.

3.1.4 The geometry of Thouless states

Given the analytic expression for the overlap $\{z|z'\}$, Eq. (3.26), we get from definition (1.56) the Kähler potential

$$f(z^*, z') = \log[\det(I_N + z^\dagger z')], \tag{3.38}$$

and proceed to evaluate several quantities involved in the dynamics of Thouless determinants.

Recalling the prescriptions for computing derivatives of both determinants and inverse matrices,

$$\begin{aligned} \frac{\partial(\det A)}{\partial x} &= (\det A) \sum_{ij} (A^{-1})_{ji} \frac{\partial A_{ij}}{\partial x}, \\ \frac{\partial (A^{-1})_{ji}}{\partial x} &= -\sum_{kl} (A^{-1})_{jk} \frac{\partial A_{kl}}{\partial x} (A^{-1})_{li}, \end{aligned}$$

and also the so-called 'Woodbury matrix identities',

$$I_M - z(I_N + z^\dagger z)^{-1} z^\dagger = (I_M + zz^\dagger)^{-1}, \tag{3.40a}$$

$$I_N - z^\dagger (I_M + zz^\dagger)^{-1} z = (I_N + z^\dagger z)^{-1}, \tag{3.40b}$$

we obtain, through straightforward differentiation, the first-order gradients of $f(z^*, z')$,

$$\frac{\partial f(z^*, z')}{\partial z'_{\mu\alpha}} = [z^\dagger (I_M + z' z^\dagger)^{-1}]_{\alpha\mu} = [(I_N + z^\dagger z')^{-1} z^\dagger]_{\alpha\mu}, \tag{3.41a}$$

$$\frac{\partial f(z^*, z')}{\partial z^*_{\nu\beta}} = [z' (I_N + z^\dagger z')^{-1}]_{\nu\beta} = [(I_M + z' z^\dagger)^{-1} z']_{\nu\beta}, \tag{3.41b}$$

as well as the metric matrix, following the definition given in Eq. (1.58),

$$g(z^*, z)_{\mu\alpha,\nu\beta} = \frac{\partial^2 f(z^*, z)}{\partial z_{\mu\alpha} \partial z^*_{\nu\beta}} = [(I_M + z z^\dagger)^{-T}]_{\mu\nu} [(I_N + z^\dagger z)^{-1}]_{\alpha\beta}. \tag{3.42}$$

It is helpful to express the latter in the form of a Kronecker product:

$$g = (I_M + z z^\dagger)^{-T} \otimes (I_N + z^\dagger z)^{-1}, \tag{3.43}$$

in which case g is regarded as a $d \times d$ (i.e. $MN \times MN$) matrix whose entries are indexed as follows:

$$g(z^*, z)_{\mu\alpha,\nu\beta} = [(I_M + z z^\dagger)^{-T} \otimes (I_N + z^\dagger z)^{-1}]_{N(\mu-1)+\alpha, N(\nu-1)+\beta}. \tag{3.44}$$

Writing g as in Eq. (3.43) facilitates the computation of its determinant, since the following identity is available for arbitrary matrices A and B of respective sizes $n \times n$ and $m \times m$,

$$\det(A \otimes B) = (\det A)^m (\det B)^n. \tag{3.45}$$

Thus we conclude that:

$$\det g = [\det(I_M + z z^\dagger)]^{-N} [\det(I_N + z^\dagger z)]^{-M} = [\det(I_N + z^\dagger z)]^{-K}, \tag{3.46}$$

where Sylvester's theorem – enunciated in the previous chapter, when deriving Eq. (2.38) – has been invoked once more.

Then, from Eq. (1.60), we obtain in closed form the integration measure that enters in the expression for the coherent-state closure relation:

$$d\mu(z^*, z) \equiv \kappa (\det g) \prod_\mu \prod_\alpha (d^2 z_{\mu\alpha}/\pi) = \kappa \, [\det(I_N + z^\dagger z)]^{-K} \prod_\mu \prod_\alpha (d^2 z_{\mu\alpha}/\pi). \tag{3.47}$$

The detailed calculation of the normalization constant κ is performed in Appendix C; the result can be written as:

$$\kappa = \prod_{n=1}^{N} \frac{(K - n + 1)!}{(N - n + 1)!}. \tag{3.48}$$

The inverse of the metric matrix, in turn, is obtained without difficulty by means of

the Kronecker product property

$$(A \otimes B)^{-1} = A^{-1} \otimes B^{-1}, \tag{3.49}$$

whence it follows immediately that

$$g^{-1} = (I_M + zz^\dagger)^T \otimes (I_N + z^\dagger z),$$

or explicitly in terms of matrix elements:

$$g^{-1}_{\mu\alpha,\nu\beta} = (I_M + zz^\dagger)^T_{\mu\nu}(I_N + z^\dagger z)_{\alpha\beta}. \tag{3.50}$$

Check. It is instructive to check the consistency of the subscripts used in these formulas by evaluating the product below:

$$\sum_\eta \sum_\gamma g^{-1}_{\mu\alpha,\eta\gamma}\, g_{\eta\gamma,\nu\beta} = \sum_\eta \sum_\gamma (I_M + zz^\dagger)^T_{\mu\eta}(I_N + z^\dagger z)_{\alpha\gamma}(I_M + zz^\dagger)^{-T}_{\eta\nu}(I_N + z^\dagger z)^{-1}_{\gamma\beta} = \delta_{\mu\nu}\delta_{\alpha\beta}.$$

The variational equation of motion is given in general form by Eq. (1.72); in the present case, however, a slight modification is needed in order to account for the matrix-like character of the coherent-state label. The adapted equation reads (note how the indexes of g^T are handled):

$$\dot{z}_{\mu\alpha} = -\frac{i}{\hbar} \sum_\beta \sum_\nu g^{-T}_{\mu\alpha,\nu\beta} \frac{\partial E(z^*, z)}{\partial z^*_{\nu\beta}} = -\frac{i}{\hbar} \sum_\beta \sum_\nu g^{-1}_{\nu\beta,\mu\alpha} \frac{\partial E(z^*, z)}{\partial z^*_{\nu\beta}}, \tag{3.51}$$

Substituting Eq. (3.50) into the latter expression leads to:

$$\dot{z}_{\mu\alpha} = -\frac{i}{\hbar} \sum_\nu \sum_\beta (I_M + zz^\dagger)_{\mu\nu} \frac{\partial E(z^*, z)}{\partial z^*_{\nu\beta}} (I_N + z^\dagger z)_{\beta\alpha}. \tag{3.52}$$

In what follows we pursue further specification of this formula by restricting attention to a particular family of many-body Hamiltonians.

3.2 Mean-field dynamics of interacting fermions

Let us consider the prototype first-quantized Hamiltonian,

$$\hat{H}(\mathbf{x}) = \sum_{i=1}^N \hat{h}(\mathbf{x}_i) + \tfrac{1}{2} \sum_{i=1}^N \sum_{j=1}^N \hat{V}(\mathbf{x}_i, \mathbf{x}_j), \tag{3.53}$$

for a system of N fermions. The one-body term $\hat{h}(\mathbf{x})$ includes the kinetic energy, $-(\hbar^2/2m)\nabla^2$, as well as external potentials. Since particles are identical the interacting potential

$\hat{V}(\mathbf{x},\mathbf{x}')$ must be symmetric with respect to particle interchange. Spin must be accounted for in a Fermi system, thus both $\hat{h}$ and $\hat{V}$ should be seen as operators in spin space (diagonal in most cases).

The second-quantized form of the above Hamiltonian is obtained by means of fermionic field operators which, under the truncated-basis description adopted here, are defined in terms of a finite set of K single-particle orbitals $|\phi\rangle$, as depicted in Eq. (3.4). In this case, the standard procedure leads to:[46]

$$\hat{H} = \sum_{pq} h_{pq} c_p^\dagger c_q + \tfrac{1}{2} \sum_{pqrs} V_{pr\cdot qs} c_p^\dagger c_r^\dagger c_s c_q. \tag{3.54}$$

The one- and two-body integrals are:

$$\begin{cases} h_{pq} = \langle \phi_p | \hat{h} | \phi_q \rangle \\ V_{pr\cdot qs} = \langle \phi_p, \phi_r | \hat{V} | \phi_q, \phi_s \rangle \end{cases} \Rightarrow \begin{cases} h_{pq} = h_{qp}^* \\ V_{pr\cdot qs} = V_{rp\cdot sq} = V_{qs\cdot pr}^* = V_{sq\cdot rp}^* \end{cases}, \tag{3.55}$$

having the usual properties.[ii]

3.2.1 The one-density

We now turn to the coherent-state description of the system governed by Hamiltonian (3.54). We assume that a reference state $|\Phi_0\rangle$ is given as in Eq. (3.12) and orbitals are thus classified into occupied and virtual spaces, $|\phi\rangle = (|\phi^\bullet\rangle, |\phi^\circ\rangle)$, with corresponding creation operators $c^\dagger = (a^\dagger, b^\dagger)$; furthermore, all notational conventions of §3.1 are adopted. A key quantity, the reduced fermionic one-density matrix, is defined as the following expectation value:[17;48]

$$\Gamma_{qp}(z^*, z) \equiv \frac{\{z|c_p^\dagger c_q|z\}}{\{z|z\}} = \langle z|c_p^\dagger c_q|z\rangle, \quad 1 \le p, q \le K. \tag{3.56}$$

In Appendix C the above matrix elements are computed using second-quantization techniques. The result can be written in matrix form in several distinct and useful ways:

$$\begin{aligned} \Gamma &= \begin{bmatrix} (I_N + z^\dagger z)^{-1} & (I_N + z^\dagger z)^{-1} z^\dagger \\ z(I_N + z^\dagger z)^{-1} & z(I_N + z^\dagger z)^{-1} z^\dagger \end{bmatrix} \\ &= \begin{bmatrix} I_N \\ z \end{bmatrix} (I_N + z^\dagger z)^{-1} \begin{bmatrix} I_N & z^\dagger \end{bmatrix} \\ &= \begin{bmatrix} (I_N + z^\dagger z)^{-1} & 0 \\ 0 & (I_M + z z^\dagger)^{-1} \end{bmatrix} \begin{bmatrix} I_N & z^\dagger \\ z & z z^\dagger \end{bmatrix}. \end{aligned} \tag{3.57}$$

The form used in the first line is the one straightforwardly obtained and most useful for numerical purposes; the second form is convenient for analytic manipulations; the

[ii] Notice that $c_p^\dagger c_r^\dagger c_s c_q = c_p^\dagger c_q \delta_{rs} - c_p^\dagger c_s c_r^\dagger c_q$; i.e. the Hamiltonian in Eq. (3.54) is a function of the basic bilinears, as expected.

factored form in the last line is reminiscent of the bosonic case and helps clarifying the interpretation of $\Gamma(z^*, z)$.

The fermionic one-density is an hermitian and idempotent matrix whose trace is normalized to the total number of particles:

$$\mathrm{tr}[\Gamma(z^*, z)] = N \quad \text{and} \quad \Gamma(z^*, z)\Gamma(z^*, z) = \Gamma(z^*, z). \tag{3.58}$$

Indeed, its diagonal elements are nothing but the average populations of each orbital $|\phi\rangle$:

$$n_p(z) = \langle z|c_p^\dagger c_p|z\rangle, \quad \textstyle\sum_p n_p(z) = N. \tag{3.59}$$

The idempotency property listed in (3.58) allows for an appealing interpretation of $\Gamma(z^*, z)$: it is simply the matrix representation of the normalized projector onto the set of occupied dynamical orbitals:[17]

$$\hat{\Gamma}(z^*, z) = \sum_{\alpha\beta} |\zeta_\alpha(z)\}(I_N + z^\dagger z)^{-1}\{\zeta_\beta(z)| = \sum_{pq} |\phi_p\rangle \Gamma_{pq}(z^*, z)\langle\phi_q|. \tag{3.60}$$

Check. 'Sandwiching' this expression with $\langle\phi_p|$ and $|\phi_q\rangle$ one finds $\Gamma_{pq} = \langle\phi_p|\hat{\Gamma}|\phi_q\rangle = \sum_{\alpha\beta}\langle\phi_p|\zeta_\alpha(z)\}(I_N + z^\dagger z)^{-1}_{\alpha\beta}\{\zeta_\beta(z)|\phi_q\rangle$; then, substituting $\langle\phi_p|\zeta_\alpha(z)\}$ and $\{\zeta_\beta(z)|\phi_q\rangle$ from previous equations, one easily recovers (3.57).

The fermionic one-density is naturally partitioned into occupied and virtual blocks. Since we will often manipulate these individual blocks directly it is convenient to establish the following notation:

$$\Gamma = \begin{bmatrix} \Gamma_{11} & \Gamma_{12} \\ \Gamma_{21} & \Gamma_{22} \end{bmatrix} = \begin{bmatrix} (I_N + z^\dagger z)^{-1} & (I_N + z^\dagger z)^{-1} z^\dagger \\ z(I_N + z^\dagger z)^{-1} & z(I_N + z^\dagger z)^{-1} z^\dagger \end{bmatrix}, \tag{3.61}$$

where subscript '1' refers to the occupied space, and subscript '2' to the virtual space. For transparency we give each block's definition in more detail:

$$(\Gamma_{11})_{\alpha\beta} = \langle z|a_\beta^\dagger a_\alpha|z\rangle, \quad (\Gamma_{12})_{\alpha\nu} = \langle z|b_\nu^\dagger a_\alpha|z\rangle, \quad (\Gamma_{21})_{\mu\beta} = \langle z|a_\beta^\dagger b_\mu|z\rangle, \quad (\Gamma_{22})_{\mu\nu} = \langle z|b_\nu^\dagger b_\mu|z\rangle. \tag{3.62}$$

This partitioning is everywhere found in the present formalism, as it will be enforced in several other matrices.

Before proceeding with the evaluation of the coherent-state expectation value of the many-body Hamiltonian and subsequent particularization of the dynamical equations, we shall take a brief detour in order to discuss important aspects of the Thouless parametrization which are pertinent to the fermionic problem; namely, the concept of intrinsic orbitals and spin structure.

3.2.2 Number density and intrinsic orbitals of the Thouless determinant

At this point it is convenient to discuss some features of the one-density and related concepts. The *number density* of fermions in a Thouless determinant is $n(\mathbf{x};z) = \langle \mathbf{x}|\hat{\Gamma}(z^*,z)|\mathbf{x}\rangle$, where $\mathbf{x}$ is a position vector. In terms of the underlying basis functions we have

$$n(\mathbf{x};z) = \sum_{pq} \phi_p(\mathbf{x})\Gamma_{pq}(z^*,z)\phi_q^*(\mathbf{x}). \tag{3.63}$$

The one-density matrix is hermitian and therefore it can be diagonalized by a z-dependent unitary matrix U,

$$\Gamma = U\ \mathrm{diag}(\gamma_1,\gamma_2,\ldots,\gamma_K)\ U^\dagger, \tag{3.64}$$

where the eigenvalues of $\Gamma(z^*,z)$ have been denoted $(\gamma_1,\gamma_2,\ldots,\gamma_K)$. By transforming the original orbitals with the matrix U a new set of basis functions is generated in such a way that the number density reduces to the indicated form:

$$\varphi_q(\mathbf{x};z) = \sum_s \phi_p(\mathbf{x})\ U_{pq}(z) \quad \Rightarrow \quad n(\mathbf{x};z) = \sum_q \gamma_q(z)|\varphi_q(\mathbf{x};z)|^2. \tag{3.65}$$

This simplified formula for $n(\mathbf{x};z)$ reminds us of the analogous expression for a system of independent particles. The orbitals φ thus acquire a special meaning – we may say they are the *intrinsic orbitals* of the Thouless determinant, with the eigenvalues γ being the corresponding *intrinsic occupation numbers*. The fundamental character of these concepts stems from the fact that they are independent of the specific single-particle basis underlying the coherent-state description.[iii]

3.2.3 Spin structure of the Thouless determinant

The spin structure of the fermion problem deserves explicit consideration. Let us concentrate on the spin-1/2 case. As mentioned earlier, in our formalism spin information is encoded within the label of each orbital, i.e. each orbital is associated with a specific spin component. Although not strictly necessary, we may imagine, for simplicity, that orbitals come in pairs which share the same spacial function, but each element of the pair refers to one of the spin projections, $\uparrow$ or $\downarrow$. If S pairs are considered, a possible way of re-labeling the basic orbitals is as follows:

$$K = 2S, \quad (\phi_1,\phi_2,\ldots,\phi_K) \to (\phi_{\uparrow 1},\phi_{\uparrow 2},\ldots,\phi_{\uparrow S},\ \phi_{\downarrow 1},\phi_{\downarrow 2},\ldots,\phi_{\downarrow S}). \tag{3.66}$$

[iii] The terminology employed here, i.e. the use of the word 'intrinsic' when referring to orbitals φ and occupations γ, is meant as an allusion to Löwdin's profound concepts of 'natural orbitals' and 'natural occupation numbers',[48] quantities which are analogous to φ and γ but calculated from a wavefunction that represents an exact solution to the many-body problem.

Then the one-density matrix can be divided into four spin blocks,

$$\Gamma = \begin{bmatrix} \Gamma_{\uparrow\uparrow} & \Gamma_{\uparrow\downarrow} \\ \Gamma_{\downarrow\uparrow} & \Gamma_{\downarrow\downarrow} \end{bmatrix}, \tag{3.67}$$

with each block being of size $S \times S$.

If we make spin projections $\uparrow, \downarrow$ explicit in the orbital labels in the manner of (3.66), and, at the same time, use indexes i, j, k, l, running from 1 to S, in order to indicate the distinct spacial functions, then the spin components of the field operators (3.4) can be written as:

$$\hat{\psi}_\sigma(\mathbf{x}) = \sum_i \phi_{\sigma i}(\mathbf{x}) c_{\sigma i}, \quad \hat{\psi}_\sigma(\mathbf{x}) = \sum_i \phi^*_{\sigma i}(\mathbf{x}) c^\dagger_{\sigma i}, \quad (\sigma = \uparrow, \downarrow), \tag{3.68}$$

and their anti-commutation rules (3.5) become:

$$\{\hat{\psi}_\sigma(\mathbf{x}), \hat{\psi}^\dagger_{\sigma'}(\mathbf{x}')\} = \delta_{\sigma\sigma'} P(\mathbf{x}, \mathbf{x}'), \quad \{\hat{\psi}_\sigma(\mathbf{x}), \hat{\psi}_{\sigma'}(\mathbf{x}')\} = \{\hat{\psi}^\dagger_\sigma(\mathbf{x}), \hat{\psi}^\dagger_{\sigma'}(\mathbf{x}')\} = 0. \tag{3.69}$$

Likewise, the spin-up and spin-down number densities are:

$$\begin{cases} n_\uparrow(\mathbf{x}; z) = \sum_{ij} \phi_{\uparrow i}(\mathbf{x}) [\Gamma_{\uparrow\uparrow}(z^*, z)]_{ij} \phi^*_{\uparrow j}(\mathbf{x}) \\ n_\downarrow(\mathbf{x}; z) = \sum_{ij} \phi_{\downarrow i}(\mathbf{x}) [\Gamma_{\downarrow\downarrow}(z^*, z)]_{ij} \phi^*_{\downarrow j}(\mathbf{x}) \end{cases}. \tag{3.70}$$

Notice that, although $n(\mathbf{x}; z) \neq n_\uparrow(\mathbf{x}; z) + n_\downarrow(\mathbf{x}; z)$, the integral of the sum of these densities correctly gives the total number of particles:

$$\int d\mathbf{x} \left[n_\uparrow(\mathbf{x}; z) + n_\downarrow(\mathbf{x}; z) \right] = \mathrm{tr}\left[\Gamma_{\uparrow\uparrow}(z^*, z) \right] + \mathrm{tr}\left[\Gamma_{\downarrow\downarrow}(z^*, z) \right] = N_\uparrow + N_\downarrow = N. \tag{3.71}$$

Furthermore, notice that, in general, the intrinsic orbitals of the Thouless determinant have no definite spin projection:

$$\begin{cases} \varphi_j(\mathbf{x}; z) = \sum_i \phi_{\uparrow i}(\mathbf{x}) \, [U_{\uparrow\uparrow}(z)]_{ij} + \sum_i \phi_{\downarrow i}(\mathbf{x}) \, [U_{\downarrow\uparrow}(z)]_{ij} \\ \varphi_{S+j}(\mathbf{x}; z) = \sum_i \phi_{\downarrow i}(\mathbf{x}) \, [U_{\downarrow\uparrow}(z)]_{ij} + \sum_i \phi_{\uparrow i}(\mathbf{x}) \, [U_{\downarrow\downarrow}(z)]_{ij} \end{cases}. \tag{3.72}$$

To be sure, if no mixing of spin species occurs, i.e. $\Gamma_{\uparrow\downarrow} = \Gamma_{\downarrow\uparrow} = 0$, then consequently $U_{\uparrow\downarrow} = U_{\downarrow\uparrow} = 0$, and the intrinsic orbitals decouple into two sets corresponding to spin $\uparrow$ and $\downarrow$.

An important observation to be made is that the spin structure of the one-density (and several other quantities pertaining to the coherent state formalism) is completely independent of the occupied/virtual structure of the reference state. These partitions will only coincide in problems with half-filling, i.e. when $N = S = K/2$, and with a reference state which involves only one spin species, e.g. $|\Phi_0\rangle = a^\dagger_{\uparrow 1} a^\dagger_{\uparrow 2} \cdots a^\dagger_{\uparrow N} |0\rangle$. In all other cases

they are completely disjoint.

$$\begin{bmatrix} \Gamma_{\uparrow\uparrow} & \Gamma_{\uparrow\downarrow} \\ \Gamma_{\downarrow\uparrow} & \Gamma_{\downarrow\downarrow} \end{bmatrix} \xleftarrow{\text{- -}} \text{ disjoint structures } \xrightarrow{\text{- -}} \begin{bmatrix} \Gamma_{11} & \Gamma_{12} \\ \Gamma_{21} & \Gamma_{22} \end{bmatrix}. \tag{3.73}$$

Finally, it should be mentioned that in problems with no spin-dependent interactions one can profit from combining the basic single-particle states into orbitals with a well-defined total spin. Conservation laws will ensure that the dynamics takes place on a restricted subspace and the size of the basis set may be decreased significantly. The number of degrees of freedom in the coherent-state description will also be smaller, facilitating numerical calculations. We will not, however, find the opportunity to work out these developments – in the fermionic system studied in Chapter 5 different spin components are coupled through two-body interaction terms.

3.2.4 Energy function and mean-field dynamics

Let us now return to the topic of dynamics. As in the bosonic case, in order to write the energy function we require, besides the one-density, an explicit expression for the coherent-state expectation value of the two-body interaction term. In Appendix C we demonstrate that such expression is given in terms of Γ as follows (for brevity, we omit the z arguments from now on):

$$\langle z|c_p^\dagger c_r^\dagger c_s c_q|z\rangle = \Gamma_{qp}\Gamma_{sr} - \Gamma_{sp}\Gamma_{qr}. \tag{3.74}$$

With Eqs. (3.56) and (3.74) the energy function, $E = \langle z|\hat{H}|z\rangle$, can be computed:

$$\begin{aligned} E &= \sum_{pq} h_{pq}\Gamma_{qp} + \tfrac{1}{2}\sum_{pqrs} V_{pr\cdot qs}(\Gamma_{qp}\Gamma_{sr} - \Gamma_{sp}\Gamma_{qr}) \\ &= \sum_{pq} h_{pq}\Gamma_{qp} + \tfrac{1}{2}\sum_{pqrs}(V_{pr\cdot qs} - V_{pr\cdot sq})\Gamma_{sr}\Gamma_{qp} \\ &= \sum_{pq}(h_{pq} + \tfrac{1}{2}v_{pq})\Gamma_{qp} = \mathrm{tr}\left[(h + \tfrac{1}{2}v)\Gamma\right], \end{aligned} \tag{3.75}$$

where the fermionic *mean-field* matrix has been defined:

$$v_{pq} = \sum_{rs}(V_{pr\cdot qs} - V_{pr\cdot sq})\Gamma_{sr}, \quad v_{pq} = v_{qp}^*. \tag{3.76}$$

Similar to the bosonic case, the Γ-dependent mean-field v stands for an effective one-body potential experienced by each individual fermion due to an average field originated by the remaining particles of the system by means of two-body interactions. If the formulation takes place within the context of electronic structure, then v is precisely the usual mean-field from Hartree-Fock theory, the notable difference in relation to the traditional

approach being the fact that here the one-density features a coherent-state parametrization. Indeed, in the electronic case, the dynamical equations for z are equivalent, in physical content, to those of time-dependent Hartree-Fock theory.

The equation of motion for z is found by substitution of $E(z^*, z)$, as given by Eq. (3.75), in the general prescription (3.52); the required gradient with respect to z^* is found using the chain rule:

$$\frac{\partial E}{\partial z^*_{\mu\alpha}} = \sum_{pq}(h_{pq} + v_{pq})\frac{\partial \Gamma_{qp}}{\partial z^*_{\mu\alpha}} = \sum_{pq} F_{pq}\frac{\partial \Gamma_{qp}}{\partial z^*_{\mu\alpha}}. \tag{3.77}$$

The density-dependent matrix F is a new key quantity – following the terminology of standard Hartree-Fock theory, this matrix is called the 'Fock matrix'; its elements are:

$$F_{pq}(\Gamma) = h_{pq} + v_{pq}(\Gamma) = h_{pq} + \sum_{rs}(V_{pr\cdot qs} - V_{pr\cdot sq})\Gamma_{sr}. \tag{3.78}$$

Meanwhile, the gradients of Γ are computed in Appendix C. Putting those formulas in (3.77) and taking the result back to (3.52) we get, after some algebra:

$$i\hbar\,\dot{z}_{\mu\alpha} = (F_{21})_{\mu\alpha} + \sum_{\nu}(F_{22})_{\mu\nu}z_{\nu\alpha} - \sum_{\beta} z_{\mu\beta}(F_{11})_{\beta\alpha} - \sum_{\beta}\sum_{\nu} z_{\mu\beta}(F_{12})_{\beta\nu}z_{\nu\alpha}, \tag{3.79}$$

where the partitioning of F is the same as that of Γ, depicted in (3.61). The above equation can be more succinctly expressed in matrix form:[17]

$$i\hbar\,\dot{z} = F_{21} + F_{22}z - zF_{11} - zF_{12}z = \begin{bmatrix} -z & I_M \end{bmatrix} F \begin{bmatrix} I_N \\ z \end{bmatrix}, \quad F = h + v. \tag{3.80}$$

Once more we have at our hands a highly non-linear equation.

For completeness we also give an explicit expression for the Lagrangian, which is obtained by the same procedure as that employed in the bosonic case, i.e. by plugging the appropriate formulas into the general expression, Eq. (1.66). Among the many possible ways of writing L a particularly useful form is:

$$L(z) = -\mathrm{tr}(F_{11}) - \tfrac{1}{2}\mathrm{tr}(F_{12}z + z^\dagger F_{21}) + \tfrac{1}{2}\mathrm{tr}(v\Gamma). \tag{3.81}$$

3.2.5 * Exact solutions for non-interacting systems

It is always instructive to examine exact solutions of dynamical equations when they are available. In the absence of interactions, Eq. (3.80) can be greatly simplified. In such circumstances one may always elect a set of single-particle basis functions in terms of which the one-body matrix h takes a diagonal form, $h = \mathrm{diag}(\varepsilon_1, \ldots, \varepsilon_N, \lambda_1, \ldots, \lambda_M)$.

Since in this case $F = h$, the Fock matrix is diagonal and independent of z:

$$\hat{H} = \sum_{pq}(h_{pp}\,\delta_{pq})c_p^\dagger c_q = \sum_\alpha \varepsilon_\alpha \hat{n}_\alpha + \sum_\mu \lambda_\mu \hat{n}_\mu \quad \Rightarrow \quad F = h = \begin{bmatrix} \varepsilon & 0 \\ 0 & \lambda \end{bmatrix}. \tag{3.82}$$

The equation of motion is then trivially solved:

$$i\hbar\,\dot{z}_{\mu\alpha} = (\lambda_\mu - \varepsilon_\alpha)z_{\mu\alpha} \quad \Rightarrow \quad z_{\mu\alpha}(t) = z_{\mu\alpha}(0)e^{-\frac{i}{\hbar}(\lambda_\mu - \varepsilon_\alpha)t}. \tag{3.83}$$

Meanwhile, the Lagrangian (3.81) reduces to $L = -\mathrm{tr}(F_{11}) = -\mathrm{tr}(\varepsilon)$, and hence the action is just $S = -\big(\sum_\alpha \varepsilon_\alpha\big)t$. Then, according to Eq. (1.75), the propagated state reads:

$$|z_t\rangle e^{\frac{i}{\hbar}S_t(z)} = |z(z_0,t)\rangle\; e^{-\frac{i}{\hbar}(\mathrm{tr}\,\varepsilon)t} \quad \text{where:} \quad z(z_0,t)_{\mu\alpha} = z_{0\mu\alpha}\; e^{-\frac{i}{\hbar}(\lambda_\mu - \varepsilon_\alpha)t}. \tag{3.84}$$

Thus the state remains a Thouless determinant throughout its time evolution, with the argument of each element of the initial z vector being rotated at a rate which depends on the eigenvalues of F. Additionally, a global phase is accumulated.

3.3 More geometry: transformation of single-particle orbitals

Let us now consider unitary transformations of the underlying single-particle orbitals and their effect on a coherent state. In particular, we are interested in establishing a connection between coherent states defined over different sets of orbitals.

When this topic was addressed in a bosonic context in §2.3, we remarked on its usefulness in facilitating the evaluation of matrix elements, since second-quantized operators sometimes have a simpler form when expressed in a specific basis which may differ from the one that is adequate for propagation. This is also true in the present case of Thouless determinants, but here there is further reason to investigate the subject of such unitary transformations and their effects.

In a Thouless determinant, Fock configurations corresponding to low-lying excitations of the chosen reference state – those which are 'close' to $|\Phi_0\rangle$ – are more efficiently approximated than those which involve higher-order excitations, particularly those displaying a significant occupation of virtual orbitals. Even if one properly chooses $|\Phi_0\rangle$ as close as possible to the initial state $|z_0\rangle$ to be propagated, i.e. in such a manner that the parameters z_0 are smallest, the mean-field dynamics may drive the state away from the reference configuration. This is problematic from a numerical point of view, since an appreciable occupation of the virtual space requires large values of z, potentially leading to inaccuracies (due to numerical errors) in the time-evolved state $|z_t\rangle$. In this case the recommended prescription is to perform a unitary transformation on the basic single-particle orbitals, thereby changing the old reference configuration into a new one, more appropriate for

representing the physical state at time t, and therefore regularizing the Thouless parameters, which are mapped into a new and more adequate set.[17] Thus there is a strong practical motivation for developing the ideas of this section, which will later be adapted to a multiconfigurational context at the end of Chapter 4.

Let us then introduce two sets of single-particle orbitals, $|\phi\rangle$ and $|\chi\rangle$, with corresponding creation operators $c^\dagger$ and $\tilde{c}^\dagger$:

$$|\phi_p\rangle = c_p^\dagger|0\rangle \quad \text{and} \quad |\chi_p\rangle = \tilde{c}_p^\dagger|0\rangle, \quad 0 \leq p \leq d. \tag{3.85}$$

Both sets are orthonormal and span the same space:

$$\hat{P} = \sum_p |\phi_p\rangle\langle\phi_p| = \sum_p |\chi_p\rangle\langle\chi_p|. \tag{3.86}$$

The unitary matrix of the transformation $|\phi\rangle \leftarrow |\chi\rangle$ ($c^\dagger \leftarrow \tilde{c}^\dagger$) is denoted by X, while its inverse is denoted by Y; we have:

$$\begin{cases} |\phi_p\rangle = \sum_q |\chi_q\rangle\langle\chi_q|\phi_p\rangle = \sum_q |\chi_q\rangle X_{qp} \\ |\chi_p\rangle = \sum_q |\phi_q\rangle\langle\phi_q|\chi_p\rangle = \sum_q |\phi_q\rangle Y_{qp} \end{cases} \Rightarrow \begin{cases} c_p^\dagger = \sum_q \tilde{c}_q^\dagger X_{qp} \\ \tilde{c}_p^\dagger = \sum_q c_q^\dagger Y_{qp} \end{cases} \quad \text{with:} \;\; Y = X^\dagger = X^{-1}. \tag{3.87}$$

Both sets are subdivided into occupied and virtual spaces according to:

$$c = (c_1, \ldots, c_K) = (a_1, \ldots, a_N, b_1, \ldots, b_M), \tag{3.88a}$$

$$\tilde{c} = (\tilde{c}_1, \ldots, \tilde{c}_K) = (\tilde{a}_1, \ldots, \tilde{a}_N, \tilde{b}_1, \ldots, \tilde{b}_M), \tag{3.88b}$$

and a corresponding blockwise partition of matrices X and Y is also enforced. Using creation operators, the transformation $|\phi\rangle \leftarrow |\chi\rangle$, can be written as:

$$a_\alpha^\dagger = \sum_\beta \tilde{a}_\beta^\dagger (X_{11})_{\beta\alpha} + \sum_\nu \tilde{b}_\nu^\dagger (X_{21})_{\nu\alpha}, \tag{3.89a}$$

$$b_\mu^\dagger = \sum_\beta \tilde{a}_\beta^\dagger (X_{12})_{\beta\mu} + \sum_\nu \tilde{b}_\nu^\dagger (X_{22})_{\nu\mu}. \tag{3.89b}$$

The Thouless determinant is defined in terms of N dynamical orbitals $|\zeta_\alpha(z)\}$, which are linear superpositions of the basic single-particle functions, as shown by Eq. (3.20).

Let us see how the replacements of Eq. (3.89) affect their creation operators $\zeta^\dagger_\alpha(z)$:

$$\begin{aligned}\zeta^\dagger_\alpha(z) &= (a^\dagger_\alpha + \textstyle\sum_\mu b^\dagger_\mu z_{\mu\alpha}) \\ &= \textstyle\sum_\beta \tilde{a}^\dagger_\beta (X_{11} + X_{12}z)_{\beta\alpha} + \sum_\nu \tilde{b}^\dagger_\nu (X_{21} + X_{22}z)_{\nu\alpha} \\ &= \textstyle\sum_\beta \Big[\tilde{a}^\dagger_\beta + \sum_\nu \tilde{b}^\dagger_\nu [(X_{21} + X_{22}z)(X_{11} + X_{12}z)^{-1}]_{\nu\beta}\Big](X_{11} + X_{12}z)_{\beta\alpha} \\ &= \textstyle\sum_\beta (\tilde{a}^\dagger_\beta + \sum_\nu \tilde{b}^\dagger_\nu w_{\nu\beta})(X_{11} + X_{12}z)_{\beta\alpha} \\ &= \textstyle\sum_\beta \tilde{\zeta}^\dagger_\beta(w)(X_{11} + X_{12}z)_{\beta\alpha},\end{aligned} \tag{3.90}$$

where we have identified $\tilde{\zeta}^\dagger_\beta(w) = (\tilde{a}^\dagger_\beta + \sum_\nu \tilde{b}^\dagger_\nu w_{\nu\beta})$ with the new label w defined in terms of z through the connection:

$$w = (X_{21} + X_{22}z)(X_{11} + X_{12}z)^{-1}. \tag{3.91}$$

The above calculation shows that the coherent-state $|z\}_\phi$, whose underlying single-particle states are $|\phi\rangle$, can be written as:

$$|z\}_\phi = \prod_\alpha \zeta^\dagger_\alpha(z)|0\rangle = \prod_\alpha \Big[\textstyle\sum_\beta \tilde{\zeta}^\dagger_\beta(w)(X_{11} + X_{12}z)_{\beta\alpha}\Big]|0\rangle = \Big[\prod_\alpha \tilde{\zeta}^\dagger_\alpha(w)|0\rangle\Big] \det(X_{11} + X_{12}z), \tag{3.92}$$

where the operator version of the basic determinant property, $\det(AB) = \det(A)\det(B)$, has been invoked in the last passage. Finally, identifying the new parametrization, $|w\}_\chi = \prod_\beta \tilde{\zeta}^\dagger_\beta(w)|0\rangle$ and re-organizing the expression, we arrive at the desired result:

$$|w\}_\chi = |z\}_\phi [\det(X_{11} + X_{12}z)]^{-1}. \tag{3.93}$$

The reverse formula is immediately found by interchanging $z \leftrightarrow w$ and $X \leftrightarrow Y$:

$$|z\}_\phi = |w\}_\chi [\det(Y_{11} + Y_{12}w)]^{-1}, \tag{3.94}$$

with z given in terms of w by:

$$z = (Y_{21} + Y_{22}w)(Y_{11} + Y_{12}w)^{-1}. \tag{3.95}$$

Note that Eqs. (3.93) and (3.94) suggest the identity:

$$(X_{11} + X_{12}z) = (Y_{11} + Y_{12}w)^{-1}, \tag{3.96}$$

which is found to hold by substituting either z or w and noting that $XY = I_K$.

The next step is to recast these connecting formulas in terms of normalized states.

Inclusion of normalization factors into Eq. (3.94) leads to:

$$|z\rangle_\phi = |w\rangle_\chi \det[(Y_{11}+Y_{12}w)^{-1}] \det[(I_N+z^\dagger z)^{-1}(I_N+w^\dagger w)]^{1/2}. \tag{3.97}$$

Our goal is to eliminate z from the above relation. As it turns out, the product of normalization factors gives

$$(I_N+z^\dagger z)^{-1}(I_N+w^\dagger w) = (Y_{11}+Y_{12}w)^\dagger (I_N+w^\dagger w)^{-1}(Y_{11}+Y_{12}w)(I_N+w^\dagger w), \tag{3.98}$$

and hence:

$$\det[(I_N+z^\dagger z)^{-1}(I_N+w^\dagger w)]^{1/2} = |\det(Y_{11}+Y_{12}w)|. \tag{3.99}$$

Taking this result back to (3.97), we deduce:

$$\begin{cases} |z\rangle_\phi = |w\rangle_\chi e^{-i\varphi} \\ |w\rangle_\chi = |z\rangle_\phi e^{i\varphi} \end{cases} \quad \text{with:} \quad \varphi = \begin{cases} \arg[\det(Y_{11}+Y_{12}w)] \\ -\arg[\det(X_{11}+X_{12}z)] \end{cases}, \tag{3.100}$$

where the identity (3.96) allows the phase φ to be written in terms of either z or w, depending on the direction we perform the transformation.

The above formulas therefore show that a unitary transformation of the basic orbitals induce a holomorphic map on the coherent-state label; at the same time, a geometrical phase is acquired by the transformed vector.

In what concerns the regularization of the coherent-state dynamics, we see that an adjustment of the reference state can be achieved with a simple prescription, summarized by Eqs. (3.91), (3.95), and (3.100). Notice that, when changing single-particle orbitals at some point of the time evolution, one must also be sure to carry out the appropriate transformation of the Hamiltonian – we leave this matter to be addressed later at §4.6. Finally, we note that, in practice, these rules should also be equipped with a protocol for deciding whether regularization is needed at any given instant, together with an algorithm that produces the most adequate transformation – these topics were left out of the discussion, since such amendments may vary from problem to problem.

3.3.1 * Alternative expressions for the transformation rule

For completeness, we list below alternative versions of the formulas connecting the coherent-state labels z and w, whose respective sets of underlying single-particle orbitals are related as explained above.

Consider the following identity, valid for any $M \times N$ matrix τ and matrices A, B, such

that $AB = BA = I_K$:

$$\tau I_N = I_M \tau \quad \Rightarrow \quad \begin{bmatrix} -\tau & I_M \end{bmatrix} \begin{bmatrix} I_N \\ \tau \end{bmatrix} = 0 \quad \text{or:} \quad \begin{bmatrix} -\tau & I_M \end{bmatrix} (AB) \begin{bmatrix} I_N \\ \tau \end{bmatrix} = 0, \quad \text{for} \quad AB = I_K. \tag{3.101}$$

Expanding the matrix product we get

$$\begin{aligned} &(A_{22}B_{21} + A_{21}B_{11}) + (A_{22}B_{22} + A_{21}B_{12})\tau \\ &\quad - \tau(A_{12}B_{21} + A_{11}B_{11}) - \tau(A_{12}B_{22} + A_{11}B_{12})\tau = 0, \end{aligned}$$

which can be reorganized as follows:

$$(A_{22} - \tau A_{12})(B_{21} + B_{22}\tau) = -(A_{21} - \tau A_{11})(B_{11} + B_{12}\tau). \tag{3.102}$$

In terms of coherent-state labels and transformation matrices, the above is valid for either of the two cases: (i) $\tau = w$, $A = X$, $B = Y$; or (ii) $\tau = z$, $A = Y$, $B = X$; thus we establish:

$$(Y_{21} + Y_{22}w)(Y_{11} + Y_{12}w)^{-1} = -(X_{22} - wX_{12})^{-1}(X_{21} - wX_{11}), \tag{3.103a}$$
$$(X_{21} + X_{22}z)(X_{11} + X_{12}z)^{-1} = -(Y_{22} - zY_{12})^{-1}(Y_{21} - zY_{11}). \tag{3.103b}$$

This allows us to write the connecting formulas, (3.91) and (3.95), as:

$$z = (Y_{21} + Y_{22}w)(Y_{11} + Y_{12}w)^{-1} = -(X_{22} - wX_{12})^{-1}(X_{21} - wX_{11}), \tag{3.104a}$$
$$w = (X_{21} + X_{22}z)(X_{11} + X_{12}z)^{-1} = -(Y_{22} - zY_{12})^{-1}(Y_{21} - zY_{11}). \tag{3.104b}$$

Using the relation $X^\dagger = Y$ we find, additionally,

$$z^\dagger = (X_{11} + w^\dagger X_{21})^{-1}(X_{12} + w^\dagger X_{22}) = -(Y_{12} - Y_{11}w^\dagger)(Y_{22} - Y_{21}w^\dagger)^{-1}, \tag{3.105a}$$
$$w^\dagger = (Y_{11} + z^\dagger Y_{21})^{-1}(Y_{12} + z^\dagger Y_{22}) = -(X_{12} - X_{11}z^\dagger)(X_{22} - X_{21}z^\dagger)^{-1}. \tag{3.105b}$$

Chapter 4

Multiconfigurational method

Overview. The trajectory-guided multiconfigurational method based on generalized coherent states is formulated and thoroughly discussed. The approach is seen as an extension of the Gaussian-based coupled coherent states (CCS) technique of Shalashilin and Child,[25–27] and derivation of the basic equations proceeds along the same lines of the original formulation. The method is first derived in continuum form, so that the newly incorporated geometrical features can be better studied. Next, the discrete unitary version is considered – this is the standard form of the method. Several aspects relating to its numerical implementation are examined in detail, and a parallelization strategy, suitable for certain classes of problems, is proposed. Finally, an 'extended' scheme, specifically designed for fermionic coherent states, is advanced. The developments of this chapter constitute the 'theoretical core' of the present thesis.

4.1 The continuum version

We begin by considering the coherent-state decomposition of an arbitrary quantum state,

$$|\psi\rangle = \int d\mu(z)|z\rangle\langle z|\psi\rangle = \int d\mu(z_0)|z\rangle\langle z|\psi\rangle, \tag{4.1}$$

which follows from the closure relation (1.59). It is assumed that $z = z(t)$ is bound to obey the classical equations of motion (1.72). By virtue of phase-space volume conservation, c.f. Appendix A, we are allowed to transfer the integration measure to the initial instant and conveniently integrate over initial conditions $z_0 = z(0)$, as indicated in the second equality in (4.1). The derivation of the CCS equations amounts to finding a solution of the Schrödinger equation

$$i\hbar|\dot{\psi}\rangle = \hat{H}|\psi\rangle, \tag{4.2}$$

for $|\psi\rangle$ in the form given by (4.1) with the *ansatz*:

$$\langle z|\psi\rangle = C(z)e^{\frac{i}{\hbar}S(z)}, \tag{4.3}$$

where $S(z)$ is the action defined in (1.74). In other words, we seek an equation of motion for the time-dependent amplitude $C(z)$ that solves (4.2). Let us make a few observations regarding this particular choice of solution.

First, all quantities that specify $|\psi\rangle$ – i.e. $|z\rangle$, $C(z)$ and $S(z)$ – are to be regarded as functions of the initial conditions z_0. Methods belonging to such a class, where the wavefunction is expressed in terms of an integral over initial conditions of classical trajectories (here, in a generalized sense), are known as *initial-value representations*. They are familiar from the field of quantum chemistry and usually constitute semiclassical approximations designed for the study of time-dependent phenomena, e.g. non-adiabatic transitions in molecules. The present method is thus conceived as a *quantum* initial value representation from the onset – in spite of its semiclassical character.

Second, it follows from (4.3) that $C(z)$ depends on the initial state $|\psi_0\rangle = |\psi(0)\rangle$ through the relation $C(z_0) = \langle z_0|\psi_0\rangle$. In numerical applications, the phase-space integral in (4.1) has to be approximated somehow. The typical procedure is to sample initial conditions z_0 in phase space with the overlap modulus $|\langle z_0|\psi_0\rangle|$ playing the role of a weight function, though a variety of alternative sampling strategies are possible[49;50]. Despite the inherent ambiguity of overcomplete basis sets in what concerns wavefunction representations, once the z_0's have been properly selected in an approximated integral the values of the corresponding $C(z_0)$'s are uniquely defined.

Third, the motivation behind the factorization of $\langle z|\psi\rangle$ into a complex amplitude times an action exponential comes from a general result of semiclassical theory, according to which the classical action provides a first-order approximation to the phase of a quantum state[29;43;51] (see also the discussion in §6.2, in the next chapter). Since this phase accounts for most of the wavefunction's oscillatory behavior, $C(z)$ is expected to present a rather smooth time dependence, thus facilitating numerical treatment.

Having made the above remarks, we now proceed to look for a differential equation for $C(z)$. Taking the total time derivative of (4.3) and making use of the Schrödinger equation, we find (after rearranging terms):

$$i\hbar\,\dot{C}(z) = \left[i\hbar\langle\dot{z}|\psi\rangle + \langle z|\hat{H}|\psi\rangle + L(z)\langle z|\psi\rangle\right] e^{-\frac{i}{\hbar}S(z)}. \tag{4.4}$$

Next, we factor out $|\psi\rangle$ by separating the scalar products on the right-hand side of the equation with the help of the closure relation $\hat{1} = \int d\mu(z')|z'\rangle\langle z'|$, with $z' = z'(t)$, which leads to:

$$i\hbar\,\dot{C}(z) = \int d\mu(z_0')\langle z|z'\rangle\Delta(z^*, z')C(z')e^{\frac{i}{\hbar}(S(z')-S(z))}. \tag{4.5}$$

Here we have already shifted the integration measure of primed variables to the initial instant [$z'_0 = z'(0)$] and replaced the $\langle z'|\psi\rangle$ that appeared under the integral sign for $C(z')e^{\frac{i}{\hbar}S(z')}$.

A key quantity of the present method has been defined in Eq. (4.5): the *CCS coupling* $\Delta(z^*, z')$, whose explicit expression is given by

$$\Delta(z^*, z') = i\hbar\frac{\langle \dot{z}|z'\rangle}{\langle z|z'\rangle} + E(z^*, z') + L(z), \tag{4.6}$$

where the non-diagonal matrix element

$$E(z^*, z') = \frac{\{z|\hat{H}|z'\}}{\{z|z'\}} = \frac{\langle z|\hat{H}|z'\rangle}{\langle z|z'\rangle}, \tag{4.7}$$

is an analytical function of z^* and z' that can be directly obtained by analytical continuation of the energy function (1.64) (i.e. by simply making the change $(z^*, z) \to (z^*, z')$ in the function).

The object $\Delta(z^*, z')$ earns its name, 'CCS coupling', from the fact that it is the quantity responsible for correlating the time evolution of amplitudes $C(z)$ and $C(z')$. In must be kept in mind, though, that the actual *coupling strength* between these amplitudes is further modulated by the overlap $\langle z|z'\rangle$, as evidenced in Eq. (4.5).

Let us now work on the raw formula (4.6) with the purpose of expressing it in terms of readily computable quantities. Since $\langle z| = e^{-\frac{1}{2}f(z^*,z)}\{z|$ we observe that the first term can be rewritten as

$$\frac{\langle \dot{z}|z'\rangle}{\langle z|z'\rangle} = \frac{\{\dot{z}|z'\}}{\{z|z'\}} - \frac{1}{2}\frac{d}{dt}f(z^*, z).$$

In turn, the total time derivative of $f(z^*, z)$ is simply

$$\frac{d}{dt}f(z^*, z) = \sum_{\alpha=1}^{d}\left[\frac{\partial f(z^*, z)}{\partial z^*_\alpha}\dot{z}^*_\alpha + \frac{\partial f(z^*, z)}{\partial z_\alpha}\dot{z}_\alpha\right],$$

while the remaining term involving $\{\dot{z}|$ can be recast as

$$\frac{\{\dot{z}|z'\}}{\{z|z'\}} = \sum_{\alpha=1}^{d}\frac{\partial f(z^*, z')}{\partial z^*_\alpha}\dot{z}^*_\alpha,$$

owing to the analyticity of $\{z|$ on z^*. Hence, collecting together the above results and making the necessary replacements in (4.6), we find that the coupling takes the form:

$$\Delta(z^*, z') = E(z^*, z') - E(z^*, z) + i\hbar\sum_{\alpha=1}^{d}\dot{z}^*_\alpha\left[\frac{\partial f(z^*, z')}{\partial z^*_\alpha} - \frac{\partial f(z^*, z)}{\partial z^*_\alpha}\right], \tag{4.8}$$

which, we note, is an analytic function on z'. Further substitution of $\dot{z}^*_\alpha$ by means of the

dynamical equation (1.72) [or rather (1.69)] produces:

$$\Delta(z^*, z') = E(z^*, z') - E(z^*, z) - \sum_{\alpha,\beta=1}^{d} \left[\frac{\partial f(z^*, z')}{\partial z^*_\alpha} - \frac{\partial f(z^*, z)}{\partial z^*_\alpha} \right] g(z^*, z)_{\alpha\beta} \frac{\partial E(z^*, z)}{\partial z_\beta}, \quad (4.9)$$

which makes all dependence on z^* and z explicit.

We remark that, if one performs a series expansion of $\Delta(z^*, z')$ for small $|z' - z|$, one finds that it begins with a second-order term. In the generalized coherent state case, this expansion[i] is complicated by the non-flat geometry of the phase space and it does not coincide with the second- and higher-order terms in the Taylor series of $E(z^*, z')$ (as is does for canonical coherent states). Nevertheless, the second-order character of $\Delta(z^*, z')$, as understood in energy terms, becomes quite apparent when specific Bose and Fermi Hamiltonians, e.g. those considered in Chapters 2 and 3, are substituted into Eq. (4.9) – this will be the subject of §4.3.

By integrating equation (4.5), the amplitudes at time $t > 0$ can be determined from their initial values. Once the amplitudes are known, we can reconstruct the quantum state with the prescription of Eqs. (4.3) and (4.1), that is,

$$|\psi\rangle = \int d\mu(z_0) |z\rangle C(z) e^{\frac{i}{\hbar} S(z)}. \quad (4.10)$$

The integro-differential equation (4.5) – with $\Delta(z^*, z')$ given by (4.8) – relates directly to the gaussian-wavepacket version of the CCS method[27] and shares some of its attractive characteristics, namely: (i) in the semiclassical regime, according to reasons mentioned earlier, the amplitude $C(z)$ is expected to have a smooth time dependence; (ii) because of the coherent-state overlap $\langle z|z'\rangle$, the z' integral is mostly localized around z;[ii] and (iii) the integrand is identically zero when $z' = z$ (precisely because of the included action phase).

Thus, the kernel which correlates amplitudes of different basis elements decreases fast as the distance $|z' - z|$ grows, on account of the overlap $\langle z|z'\rangle$. In other words, the coupling strength between amplitudes $C(z)$ and $C(z')$, associated with $|z\rangle$ and $|z'\rangle$, is appreciable only if z' lies on the neighborhood of z, though the size of such neighborhood may vary depending on some of the aspects of the problem at hand. Nevertheless, one may anticipate that the method achieves its maximum efficiency if the system evolves under a semiclassical regime, where coherent-state overlaps are intensely localized and the amplitude corresponding to a given coherent state would only change as a result of correlations developed among the latter and other basis elements located in its immediate neighborhood.

[i] A similar expansion is carried out in full detail at Chapter 6

[ii] For coherent states other than canonical, $|\langle z|z'\rangle|$ is no longer a gaussian distribution, but is still localized in phase space.

4.2 Discrete unitary version

Let us now derive the CCS equations using a finite discrete basis. This section deals with the unitary version of the resulting propagation scheme; a less sophisticated non-unitary formula (which can be obtained as a special case) is discussed later.

The first thing one must recognize is that, generally speaking, a basis set constructed with a finite number of coherent states will only provide an approximate description of the full Hilbert space wherein the system's wavefunction evolves. This means that the CCS method, in its discrete version, will not solve the Schrödinger equation exactly, unless the number of basis elements is properly increased to the point where the phase space is completely covered, and the Hilbert space closure relation can be emulated by the basis set projector. Despite this limitation, one finds that, in many cases, the quantum evolution takes place in a restricted region of Hilbert space (at least for sufficiently short propagation time), allowing almost exact results to be obtained with a reasonably small basis set – this signalizes a 'breach' in quantum dynamics, and the CCS method is precisely designed to take advantage of it.

Having made these clarifications, we shall go through essentially the same steps delineated in §4.1, only this time considering a basis set of size m, whose projector is

$$\hat{\Omega} = \sum_{i=1}^{m} \sum_{j=1}^{m} |z_i\rangle \Omega_{ij}^{-1} \langle z_j|. \tag{4.11}$$

Here, a new notational convention is introduced: Latin letters i, j, k, l will be used for labeling basis-set elements and, for convenience, we henceforth abbreviate basis-set summations by omitting their range (which is always from 1 to m). Notice that, since each $|z_i\rangle = |z_i(t)\rangle$ evolves independently according to classical equations (1.72), the space spanned in (4.11) changes with t, i.e. the projector itself is time-dependent, $\hat{\Omega} = \hat{\Omega}(t)$.

The projector's matrix elements define the $m \times m$ *overlap matrix*:

$$\Omega_{ij} = \langle z_i|\hat{\Omega}|z_j\rangle = \langle z_i|z_j\rangle. \tag{4.12}$$

For the moment, we shall not concern ourselves with the particular way the basis elements are chosen (this will be the subject of §4.4) but we observe that the overlap matrix is assumed to be sufficiently well-conditioned during the time interval upon which the propagation takes place, to the extent that operations involving its inverse produce sensible results – otherwise Eq. (4.11) would be ill-defined.

The finite-basis restriction amounts to the following approximation for the quantum state $|\psi\rangle$:

$$|\psi\rangle \approx \hat{\Omega}|\psi\rangle = \sum_{ij} |z_i\rangle \Omega_{ij}^{-1} \langle z_j|\psi\rangle. \tag{4.13}$$

Following the recipe of the previous section, an amplitude and action phase are assigned to each orbit: $C_i = C(z_i)$ and $S_i = S(z_i)$, respectively, with $1 \leq i \leq m$. The coherent-state representation of $|\psi\rangle$ is then written according to the *ansatz*:

$$\langle z_i|\psi\rangle = C_i e^{\frac{i}{\hbar}S_i}. \tag{4.14}$$

Next, using the above relation, we differentiate C_i with respect to time, leading to:

$$i\hbar\,\dot{C}_i = \left[i\hbar\langle\dot{z}_i|\psi\rangle + i\hbar\langle z_i|\dot{\psi}\rangle + L_i\langle z_i|\psi\rangle\right] e^{-\frac{i}{\hbar}S_i}, \tag{4.15}$$

where $L_i = L(z_i)$ is the Lagrangian calculated over the i-th orbit. As before, an equation of motion for C_i is obtained by decomposing the terms on the right-hand side of (4.15) in the coherent-state basis. But, while the last term can be exactly replaced as $\langle z_i|\psi\rangle = \langle z_i|\hat{\Omega}|\psi\rangle$, the same is not true of the other two. Unlike the continuous case, we must rely again on (4.13) in order to approximate the terms involving time-derivatives:

$$|\psi\rangle \approx \hat{\Omega}|\psi\rangle \quad \Rightarrow \quad \langle\dot{z}_i|\psi\rangle \approx \langle\dot{z}_i|\,[\hat{\Omega}|\psi\rangle], \quad i\hbar\langle z_i|\dot{\psi}\rangle = \langle z_i|\hat{H}|\psi\rangle \approx \langle z_i|\hat{H}\,[\hat{\Omega}|\psi\rangle] \tag{4.16}$$

(obs: notice that $|\dot{z}_j\rangle \neq \hat{\Omega}|\dot{z}_j\rangle$ – the derivative of a state is generally not restricted to the same sub-space as the state). As a result we get:

$$\begin{aligned} i\hbar\,\dot{C}_i &\approx \sum_{jk}\left[i\hbar\langle\dot{z}_i|z_j\rangle\Omega^{-1}_{jk}\langle z_k|\psi\rangle + \langle z_i|\hat{H}|z_j\rangle\Omega^{-1}_{jk}\langle z_k|\psi\rangle + L_i\langle z_i|z_j\rangle\Omega^{-1}_{jk}\langle z_k|\psi\rangle\right] e^{-\frac{i}{\hbar}S_i} \\ &= \sum_{jk}\langle z_i|z_j\rangle\left[i\hbar\frac{\langle\dot{z}_i|z_j\rangle}{\langle z_i|z_j\rangle} + E(z_i^*, z_j) + L_i\right]\Omega^{-1}_{jk}\langle z_k|\psi\rangle e^{-\frac{i}{\hbar}S_i} \\ &= \sum_{jk}(\Omega_{ij}\,\Delta_{ij})\,\Omega^{-1}_{jk}\,C_k\,e^{\frac{i}{\hbar}(S_k - S_i)}, \end{aligned} \tag{4.17}$$

where we made the replacements: $\langle z_i|z_j\rangle = \Omega_{ij}$ and $\langle z_k|\psi\rangle = C_k e^{\frac{i}{\hbar}S_k}$. Also, the expression for the CCS coupling, $\Delta_{ij} = \Delta(z_i^*, z_j)$, has been identified within the square brackets at the second line, c.f. Eq. (4.6). For later reference, the reduced form of the coupling is repeated below, this time with discrete basis labels i, j:

$$\Delta_{ij} = E(z_i^*, z_j) - E(z_i^*, z_i) + i\hbar\sum_{\alpha=1}^{d}\left[\frac{\partial f(z_i^*, z_j)}{\partial z_{i\alpha}^*} - \frac{\partial f(z_i^*, z_i)}{\partial z_{i\alpha}^*}\right]\dot{z}_{i\alpha}^*. \tag{4.18}$$

4.2.1 * Accumulated error in the CCS propagation

Because the approximations displayed at (4.16) were required in deriving the equation of motion for C_i, Eq. (4.17), the amplitude accumulates an error. Before proceeding with the present development, it is instructive to take a brief look on this matter.

The error just mentioned, which we may denote as $\dot{\epsilon}$, can be formally expressed if we

introduce the complementary projector $\hat{\Xi}$, defined by the relations:

$$\hat{1} = \hat{\Omega} + \hat{\Xi}, \quad \text{with:} \quad \hat{\Xi}\hat{\Omega} = 0, \tag{4.19}$$

i.e. $\hat{\Xi}$ projects on a space orthogonal to the one spanned by the CCS basis. Then, starting again from Eq. (4.15), with $i\hbar|\dot{\psi}\rangle = \hat{H}|\psi\rangle$, we see that the exact value of $\dot{C}_i$ can be written as follows:

$$\begin{aligned} i\hbar\,\dot{C}_i &= \Big[i\hbar\langle\dot{z}_i|\psi\rangle + \langle z_i|\hat{H}|\psi\rangle + L_i\langle z_i|\psi\rangle\Big]\, e^{-\frac{i}{\hbar}S_i} \\ &= \Big[i\hbar\langle\dot{z}_i|(\hat{\Omega}+\hat{\Xi})|\psi\rangle + \langle z_i|\hat{H}(\hat{\Omega}+\hat{\Xi})|\psi\rangle + L_i\langle z_i|\hat{\Omega}|\psi\rangle\Big]\, e^{-\frac{i}{\hbar}S_i}, \end{aligned} \tag{4.20}$$

or:

$$i\hbar\,\dot{C}_i = \dot{\epsilon}_i + \sum_{jk}(\Omega_{ij}\,\Delta_{ij})\,\Omega^{-1}_{jk}\,C_k\,e^{\frac{i}{\hbar}(S_k - S_i)}, \tag{4.21}$$

where:

$$\dot{\epsilon}_i = i\hbar\langle\dot{z}_i|\hat{\Xi}|\psi\rangle + \langle z_i|\hat{H}\hat{\Xi}|\psi\rangle = \Big[\hat{H}|z_i\rangle - i\hbar|\dot{z}_i\rangle\Big]^{\dagger}\Big[\,\hat{\Xi}|\psi\rangle\,\Big]. \tag{4.22}$$

This little exercise shows that the error implicit in Eq. (4.17) has two interdependent sources: a non-zero component of $|\psi\rangle$ lying outside the space spanned by the basis set, and the violation of Schrödinger's equation by individual basis elements. Moreover, Eq. (4.22) confirms that the method can be made exact regardless of the dynamics prescribed for each $|z\rangle$, as long as the full Hilbert space is contemplated by the basis set, in which case $\hat{\Xi} = 0$ and hence $\dot{\epsilon}_i = 0$.

Bearing in mind these fundamental limitations of the discrete formulation, we henceforth denote the CCS wavefunction by $|\psi\rangle$; when necessary, the exact wavefunction will be indicated by $|\psi_{\text{exact}}\rangle$.

4.2.2 Auxiliary amplitudes

Turning back to the method's derivation, we now address the issue of the inverse overlap matrix figuring in several formulas. In practice, Ω^{-1} is never explicitly computed; rather, one introduces a set of auxiliary amplitudes D_j, defined according to:

$$\sum_j \Omega_{ij} D_j e^{\frac{i}{\hbar}(S_j - S_i)} = C_i. \tag{4.23}$$

Then, the equation of motion for C_i, Eq. (4.17), can be recast as:

$$i\hbar\,\dot{C}_i = \sum_j \Big[\Omega_{ij}\,\Delta_{ij}\,e^{\frac{i}{\hbar}(S_j - S_i)}\Big]\,D_j. \tag{4.24}$$

Thus, at every time step (or, better said, at every evaluation of $\dot{C}$) the auxiliary amplitudes D are obtained from C by means of the intermediate equation (4.23) – an operation that

requires solving a linear system of size m. In most applications this procedure constitutes the main computational bottleneck of the technique. Investigations carried out with the Gaussian-based method showed that there are ways of evading this obstacle by introducing low-level parallelization schemes.[52] An alternative, high-level parallel approach, suitable for basis-set sizes on the order of a few hundred, is proposed and explained at §4.5.

4.2.3 Norm conservation

Let us next demonstrate the unitary property of the present method. This may not be obvious at first sight in view of the approximations made and the fact that the matrix that governs the amplitude's time evolution – whose i,k entry, according to Eq. (4.17), is $\sum_j(\Omega_{ij}\Delta_{ij})\Omega^{-1}_{jk}e^{\frac{i}{\hbar}(S_k-S_i)}$ – is not hermitian (the latter feature, though, is just a consequence of using non-orthogonal basis functions).

For developing the subsequent formulas, it is convenient to introduce the 'phased overlap' (and its inverse):

$$\omega_{ij} \equiv e^{-\frac{i}{\hbar}S_i}\Omega_{ij}e^{\frac{i}{\hbar}S_j}, \quad (\omega^{-1})_{ij} = e^{-\frac{i}{\hbar}S_i}(\Omega^{-1})_{ij}e^{\frac{i}{\hbar}S_j}, \tag{4.25}$$

in terms of which the CCS equations, (4.23) and (4.24), can be more compactly expressed:

$$i\hbar\,\dot{C}_i = \sum_j(\omega_{ij}\,\Delta_{ij})D_j, \quad \sum_j \omega_{ij}D_j = C_i. \tag{4.26}$$

Similarly, from Eqs. (4.13) and (4.14), the CCS wavefunction is:

$$|\psi\rangle = \sum_{ij}|z_i\rangle\Omega^{-1}_{ij}C_j e^{\frac{i}{\hbar}S_j} = \sum_{ij}|z_i\rangle(\omega^{-1}_{ij}C_j)e^{\frac{i}{\hbar}S_i} = \sum_i |z_i\rangle D_i e^{\frac{i}{\hbar}S_i}. \tag{4.27}$$

Let us then calculate the rate of change of the squared norm,

$$\langle\psi|\psi\rangle = \sum_{ij} D^*_i\omega_{ij}D_j = \sum_{ij} C^*_i\omega^{-1}_{ij}C_j = \sum_i C^*_i D_i \tag{4.28}$$

– taking the time derivative one finds, with the aid of (4.26),

$$\begin{aligned}\frac{d}{dt}\langle\psi|\psi\rangle &= \sum_{ij}\Big(\dot{C}^*_i\omega^{-1}_{ij}C_j + C^*_i\omega^{-1}_{ij}\dot{C}_j - C^*_i(\omega^{-1}\dot{\omega}\omega^{-1})_{ij}C_j\Big)\\ &= \sum_i \dot{C}^*_i D_i + \sum_j D^*_j\dot{C}_j - \sum_{ij} D^*_i\dot{\omega}_{ij}D_j = -\sum_{ij} D^*_i\Big(\dot{\omega}_{ij} + \tfrac{i}{\hbar}(\Delta_{ij}-\Delta^*_{ji})\omega_{ij}\Big)D_j.\end{aligned} \tag{4.29}$$

Meanwhile, by differentiating the phased overlap (4.25) with respect to t we get

$$\dot{\omega}_{ij} = -\frac{i}{\hbar}\Big[L(z_i) + i\hbar\frac{\langle\dot{z}_i|z_j\rangle}{\langle z_i|z_j\rangle} + i\hbar\frac{\langle z_i|\dot{z}_j\rangle}{\langle z_i|z_j\rangle} - L(z_j)\Big]\omega_{ij} = -\frac{i}{\hbar}(\Delta_{ij}-\Delta^*_{ji})\omega_{ij}, \tag{4.30}$$

where we have added and subtracted the hermitian term $E(z_i^*, z_j)$ inside the square brackets, so that the result could be expressed in terms of the coupling Δ_{ij} and its complex transpose Δ_{ji}^*. Putting (4.30) into (4.29) we conclude:

$$\frac{d}{dt}\langle\psi|\psi\rangle = 0, \tag{4.31}$$

proving that norm is indeed conserved.

Notice that this result is always valid, regardless of the basis set restrictions, just as long as the overlap matrix remains well-conditioned (we have relied on the definiteness of its inverse several times). Therefore, if norm fluctuation happens to be observed during applications, it should be interpreted as a residue of numerical errors; these, in turn, are either caused by ill-conditioning of the overlap matrix, leading to inaccurate solutions of the linear system (4.23), or by an inadequacy of the stepper routine used for obtaining $C(t+h)$ from $C(t)$, most likely due to a too large time increment h (this includes possible errors during the evolution of individual basis elements).

4.2.4 * The variational picture

We have used Schrödinger's equation to get the CCS formulas in a discrete unitary framework. That route was deliberately chosen so that some subtleties of the method could be brought to discussion. Alternatively we could have advanced the problem from a variational perspective, starting from a trial wavefunction:

$$|\psi\rangle = \sum_j |z_j\rangle a_j. \tag{4.32}$$

This type of trial state was discussed in Chapter 1. The situation here is different, though, since we are not looking for a 'full variational' approach, but rather a more simplistic guided-basis propagation scheme. From a TDVP standpoint, this means that, in Eq. (4.32), the only variables that should be regarded as variational parameters are the amplitudes a_j. The basis elements $|z_j\rangle$, in contrast, are to be understood as mere time-dependent functions – they are not free to vary since their dynamics has been assigned beforehand.

Nevertheless, the equation of motion for a is the same in both cases. Thus, the 'norm-constrained form' of the TDVP, discussed in §1.2, yields:

$$i\hbar \sum_i \langle z_i|z_j\rangle \dot{a}_j = \sum_j [\langle z_i|\hat{H}|z_j\rangle - i\hbar\langle z_i|\dot{z}_j\rangle] a_j, \tag{4.33}$$

which is just Eq. (1.47) translated to the present context. By performing the change of variables, $a_j = D_j e^{\frac{i}{\hbar}S_j}$ (the action phase S_j is, again, just a time-dependent factor), we

get:

$$i\hbar \sum_j \omega_{ij} \dot{D}_j = \sum_j \omega_{ij} \Delta'_{ij} D_j, \tag{4.34}$$

where we have multiplied both sides by $e^{-\frac{i}{\hbar}S_i}$. Observe that, here, a linear system has to be solved in order to get the time derivatives $\dot{D}$ – the bottleneck operation persists. Also, notice that the coupling Δ'_{ij} appearing in Eq. (4.34) is nothing but the complex transpose of the standard CCS coupling (4.18), i.e.

$$\begin{aligned} \Delta'_{ij} &= E(z_i^*, z_j) - i\hbar \frac{\langle z_i | \dot{z}_j \rangle}{\langle z_i | z_j \rangle} + L(z_j) \\ &= E(z_i^*, z_j) - E(z_j^*, z_j) - i\hbar \sum_{\alpha=1}^{d} \left[\frac{\partial f(z_i^*, z_j)}{\partial z_{j\alpha}} - \frac{\partial f(z_j^*, z_j)}{\partial z_{j\alpha}} \right] \dot{z}_{j\alpha} = \Delta^*_{ji}. \end{aligned} \tag{4.35}$$

The equation of motion (4.34), which involves the D amplitudes only, is precisely equivalent to the CCS formulas (4.26) deduced earlier. In order to establish this equivalence, we note that one immediately implies the other – for instance:

$$\begin{aligned} \dot{C}_i = \frac{d}{dt}\Big(\sum_j \omega_{ij} D_j \Big) &= \sum_j \omega_{ij} \dot{D}_j + \sum_j \dot{\omega}_{ij} D_j \\ &= -\frac{i}{\hbar} \sum_j \omega_{ij} \Delta'_{ij} D_j - \frac{i}{\hbar} \sum_j \omega_{ij} (\Delta_{ij} - \Delta^*_{ji}) D_j = -\frac{i}{\hbar} \sum_j \omega_{ij} \Delta_{ij} D_j, \end{aligned} \tag{4.36}$$

where (4.30) was used.

The connection with the TDVP exposed above provides additional insight into the CCS method. It reveals that the approximations (4.16), that we were forced to make earlier in order to get the equation of motion for C, are automatically built into the variational problem, where the wavefunction is understood as an approximate trial state from the beginning. Furthermore, the equivalence of both derivations, together with the fact that Eq. (4.34) was obtained with the TDVP version of §1.2, where normalization is imposed as a constraint, contributes yet another way of understanding how, despite the restrictions of the finite basis set, the unitarity of the quantum time evolution is preserved.

Finally, we note that the 'D-amplitude' version of the method, based on Eq. (4.34), is the one most often employed in the recent CCS-related literature. Certainly, when evaluating matrix elements of typical operators, D is far more useful than C. And, since D can be propagated on its own, that would seem to render a more efficient implementation.

However, it is our experience that D is a poor dynamical variable, whereas C is a good one. There are mainly two reasons.[iii]

[iii] A third but less important reason is that, given a basis set $|z_i\rangle$, initialization is easier with C: for a initial state $|\psi_0\rangle$ the amplitudes at $t = 0$ are just $C(z_i) = \langle z_i | \psi_0 \rangle$; however, if D is used one has to solve $\sum_i \langle z_i | z_j \rangle D_j = \langle z_j | \psi_0 \rangle$.

First, the modulus of D_i is not bounded, while, by definition, that of C_i is, for Eq. (4.14) shows that $0 \leq |C_i| \leq 1$. Second, the considerations of §4.1, regarding inclusion of an action phase and the resulting 'smoothness' of the CCS amplitude associated with each basis element, apply to C only. The method formulated in terms of C is therefore expected to be more stable than the D-based version. (Indeed, we observe in our simulations that D sometimes displays quite an erratic time behavior; C, on the other hand, is always a smooth function of time).

It is thus why we insist in using the C-based version of the method,[iv] though, we must admit that if serious ill-conditioning of the basis set occurs – the major source of instabilities – both formulations break down.

4.2.5 A remark on energy conservation

The variational approach shows that the standard CCS method, by construction, conserves the norm of the propagated quantum state. However, approximating the identity operator by a finite basis set consisting of randomly distributed coherent states affects another important property of the quantum evolution: the total energy of an initial state $E_0 = \langle\psi_0|\hat{H}|\psi_0\rangle$ is not generally maintained during CCS applications.

Let us then evaluate the rate of change of total energy. For this brief calculation, $\hat{H}$ is assumed to be time-independent and the simplified notation of Eq. (4.32) is employed. Differentiating $E(\psi) = \langle\psi|\hat{H}|\psi\rangle$ with respect to time we get:

$$\begin{aligned}\frac{dE}{dt} &= \langle\psi|\hat{H}|\dot{\psi}\rangle + \langle\dot{\psi}|\hat{H}|\psi\rangle \\ &= \sum_{ij}\Big[a_i^*\langle z_i|\hat{H}|z_j\rangle\dot{a}_j + \dot{a}_i^*\langle z_i|\hat{H}|z_j\rangle a_j + a_i^*\langle z_i|\hat{H}|\dot{z}_j\rangle a_j + a_i^*\langle\dot{z}_i|\hat{H}|z_j\rangle a_j\Big]. \end{aligned} \tag{4.37}$$

Substituting the amplitude derivatives, obtained from Eq. (4.33) and its complex conjugate,

$$\dot{a}_j = -\frac{i}{\hbar}\sum_{kl}(\Omega^{-1})_{jk}[\langle z_k|\hat{H}|z_l\rangle - i\hbar\langle z_k|\dot{z}_l\rangle]a_l, \tag{4.38a}$$

$$\dot{a}_i^* = \frac{i}{\hbar}\sum_{kl}a_l^*[\langle z_l|\hat{H}|z_k\rangle + i\hbar\langle\dot{z}_l|z_k\rangle](\Omega^{-1})_{ki}, \tag{4.38b}$$

[iv] Note that the ability to conveniently calculate observables is not lost – while not playing the role of a dynamical variable, D is still available at every time step (it is a simple matter of storing them after the linear system (4.23) is solved).

and identifying the projector $\hat{\Omega} = \sum_{ij} |z_i\rangle (\Omega^{-1})_{ij} \langle z_j|$, we find:

$$\begin{aligned} \frac{dE}{dt} &= \sum_{ij} a_i^* \Big[\langle z_i | (\hat{H} - \hat{H}\hat{\Omega} | \dot{z}_j \rangle + \langle \dot{z}_i | (\hat{H} - \hat{\Omega}\hat{H}) | z_j \rangle \Big] a_j \\ &= 2 \,\mathrm{Re} \sum_{ij} \langle z_i | (\hat{\Omega}\hat{H} - \hat{H}\hat{\Omega}) | \dot{z}_j \rangle D_i^* D_j e^{\frac{i}{\hbar}(S_j - S_i)}. \end{aligned} \tag{4.39}$$

Therefore, the rate of change of E is essentially controlled by the matrix elements $\langle z_i | [\hat{\Omega}, \hat{H}] | \dot{z}_j \rangle$ which, as expected, become identically zero in the limit of a complete basis $\hat{\Omega} \to \hat{1}$.

The intimate relation between energy conservation and the exactness of CCS results has been pointed out by Habershon in Ref. [53]. Thus, by monitoring the value of total energy, one can make an 'on-the-fly' diagnosis as regards to the quality of CCS results. This is illustrated in Chapter 5 with numerical examples.

4.2.6 * Non-unitary case

It may be of interest sometimes – particularly when the system under study has only one or two degrees of freedom – to attempt a more straightforward discrete approximation to the coherent-state closure relation, by writing the basis projector as

$$\hat{\Omega} \approx \sum_{k=1}^{m} |z_k\rangle \lambda_k \langle z_k|, \tag{4.40}$$

with λ_k approximating the integration measure $d\mu(z_k)$ at each phase-space point.

The equation of motion for C in this case can be obtained at once from (4.24) by setting $(\Omega^{-1})_{jk} = \lambda_j \delta_{jk}$, which leads to:

$$i\hbar \, \dot{C}_i = \sum_j \lambda_j \left[\Omega_{ij} \, \Delta_{ij} \, e^{\frac{i}{\hbar}(S_j - S_i)} \right] C_j. \tag{4.41}$$

Similarly, the quantum state in this case is approximated by:

$$|\psi\rangle \approx \sum_k \lambda_k |z_k\rangle C_k e^{\frac{i}{\hbar} S_k}. \tag{4.42}$$

This propagation scheme is computationally less demanding than the standard unitary version of CCS – if the basis-set size is kept the same –, since there is no need to solve a linear system at each time step to get the auxiliary amplitudes D. On the other hand, a larger basis set (usually constructed as a grid in phase space) may be necessary to converge the results if the approximated closure relation (4.40) is employed. Moreover, the norm of the propagated quantum state is not automatically conserved, meaning that results must be normalized on output. Further observations regarding this version of the method in a Gaussian-based framework are made by Shalashilin and Child in Ref. [27].

This non-unitary propagation scheme, as formulated in terms of the bosonic parametriza-

tion of Chapter 2, has been tested in Ref. [28], where it was applied to a model system of interacting bosons trapped in a double-well potential. In that problem, the approach is quite feasible since the phase space has a single degree of freedom. Different dynamical regimes have been studied, with the number of particles N varying in the range $100 - 5000$ (while other parameters were held fixed). All runs used roughly the same number of basis elements and a improvement of results with increasing N was observed, in accordance with the idea that the CCS method is best suited for describing systems evolving under semiclassical conditions – in that case, the classical limit corresponds to the thermodynamical limit, $N \to \infty$ (see Ref. [28] for more details).

4.2.7 The standard form of the generalized CCS method: a few remarks

The propagation scheme whereby the wavefunction, written as

$$|\psi\rangle = \sum_{i=1}^{m} |z_i\rangle D_i e^{\frac{i}{\hbar} S_i}, \tag{4.43}$$

evolves in time according to Eqs. (1.72), (1.74) and (4.26) – with Δ_{ij} and ω_{ij} respectively given by Eqs. (4.18) and (4.25) and – represents the discrete unitary version of the generalized CCS method. This is the standard form of the generalized coherent-state guided-basis approach developed in this work. In what follows we make some additional remarks.

Initial state. In theory, the method is able to propagate any initial state $|\psi_0\rangle$ once a suitable basis set is provided – as we have seen earlier, the initial condition for the C amplitudes is, in this case, $C_0(z_i) = \langle z_{0i}|\psi_0\rangle$. However, sampling a basis set capable of adequately representing an arbitrary quantum state is not an easy task, and this problem often requires a methodology of its own – one example would be the diffusion Monte Carlo strategy developed in Ref. [54]. A throughout examination of such kinds of techniques is out of the scope of the present work, since our interest is towards the time evolution itself. We shall, therefore, avoid altogether the difficulties associated with an arbitrary $|\psi_0\rangle$ by restricting the analysis to the case where the initial state is a coherent state, i.e.

$$|\psi_0\rangle = |z_0\rangle \quad \Rightarrow \quad C_0(z_i) = \langle z_{i0}|z_0\rangle. \tag{4.44}$$

Sampling of basis elements is simpler in this case, for it can be achieved by random generation of z vectors which are accepted or rejected according to criteria based on coherent-state scalar products, $\Omega(z^*, z') = \langle z|z'\rangle$, a quantity whose analytical expression is known. Also, the fact that $|\Omega(z^*, z')|$ decreases fast as $|z - z'|$ grows allows for simple sampling strategies that result in basis elements being mostly concentrated in a neighborhood of the initial state $|z_0\rangle$, a region from where the most important contributions to the integral formula are expected to arise, at least for short times. A general sampling

algorithm, designed for this purpose is presented in §4.4.

It should be mentioned that this restriction on initial states does not necessarily implies a loss of generality, for once an arbitrary $|\psi_0\rangle$ is expressed as a superposition of static coherent states, then each of its components can be independently propagated with the CCS method, and the disjoint solutions can be recombined later to give the complete time-evolved wavefunction.

Classical propagation. Finally, a special case of the generalized CCS method is worth of mention: that whereupon a single coherent-state basis element is employed in the wavefunction representation. If this single basis element is made to coincide with the initial state, which is assumed to be $|\psi_0\rangle = |z_0\rangle$, then, by setting $m = 1$ in the CCS formulas, the approximated quantum state at $t > 0$ is:

$$|\psi(t)\rangle = |z_1(t)\rangle e^{\frac{i}{\hbar}S_1(t)}, \quad \text{with:} \quad z_1(0) = z_0. \tag{4.45}$$

This is so because the right-hand side of Eq. (4.24) vanishes for $m = 1$, implying $\dot{C}_1 = 0$ and hence $C_1(t) = C_1(0) = \langle z_1(0)|z_0\rangle = 1$. Equation (4.45) is nothing but the 'classical propagation scheme' discussed in §1.3.3.

What is to gain by adopting a trajectory-guided methodology? The whole point of using time-dependent basis functions in representing an evolving quantum state is that they are potentially more efficient for such a task than a static basis set would be; this is meant in the sense that an accurate description of the system can be achieved with a lesser number of basis elements if these are allowed to vary with time. Evidently, this claim rests on the assumption that the dynamics of each basis element can be assigned in a such a way as to drive the quantum wavefunction to the most important regions of the Hilbert space – a poor dynamical prescription would only misguide the system (hence the caveat in the first sentence, embodied in the word 'potentially'). This latter requirement is ensured in a full variational treatment, such as that outlined in §1.2.2, by the very nature of the variational principle.

The trajectory-guided technique, on the other hand, further relies on the assumption that, under certain regimes, each optimized basis state is able to capture most of the wavefunction's behavior; in other words, that under the appropriate circumstances the evolution of individual basis states is *qualitatively* similar to that of the entire system. In the generalized coherent-state context, where we have identified single coherent-states as classical approximations, such 'appropriate circumstances' that justify the trajectory-guided strategy constitute what we have called the 'semiclassical regime'.

Thus, if a properly constructed trajectory-guided scheme is implemented for a system that evolves under the adequate dynamical regime, it would not only be more efficient than a traditional static-basis approach – it would also provide results as accurate as those that would have been obtained by a full variational method (at least for a sufficiently short

propagation time), but at a much less expensive computational cost, if the basis set size is the same in both cases.

When is the generalized CCS advantageous? The methodology developed in this section utilizes a time-dependent basis set with m elements to represent the system's wavefunction. In order to carry out the time evolution, a set of differential equations that couples the amplitudes of different basis elements has to be integrated. This integration proceeds step-by-step, and a linear system of size m has be solved at each step. The computational cost of this latter operation (measured in CPU time) scales roughly as $\sim m^3$. Thus we may say that the computational cost of the discrete unitary version of the generalized CCS method goes as $\sim m^3$ per time step.[v]

Meanwhile, the standard numerical approach to quantum problems is based on diagonalization of the matrix representation of the Hamiltonian operator $\hat{H}$ in a complete orthonormal basis, say $|\Phi\rangle$.[vi] If n denotes the size of the Hilbert space in question, the diagonalization procedure has a computational cost which scales as $\sim n^3$. For time-independent Hamiltonians this operation has to be carried out a single time only; once the eigen-energies and eigenstates have been determined any initial wavefunction represented in the $|\Phi\rangle$ basis may be straightforwardly decomposed in terms of the system's eigenstates and propagation is then trivial.

Therefore, in order to be competitive against the traditional approach – judging in terms of CPU time – the overall computational cost of CCS has to be small enough to compensate for the time spent on a *single* diagonalization of the quantum Hamiltonian. Such a condition is quite hard to meet if the dimension of the Hilbert space n is comparable to the CCS basis-set size m.

However, it is a well-know fact that the dimensionality of a quantum problem scales exponentially with the system's size. For definiteness, we may picture a system of N distinguishable and structureless particles moving inside a box. The dimension of the configuration space is $3N$. Suppose we establish that a satisfactory description is achieved if L basis functions are employed for each position variable. In that case, the total size of the Hilbert space is $n = L^{3N}$; it grows exponentially as more particles are added to the system.

Similarly, for systems of indistinguishable particles we have seen that the number of dimensions of the Fock space grows fast (in a factorial fashion) with both the number of particles N and the number of underlying single-particle states K used in the description, as shown by Eq. (2.9) for bosons and by Eq. (3.9) for fermions. Thus, the standard quantum approach easily becomes intractable, even for moderately sized systems.

[v] In asserting this we presume that the linear system, required for computing the amplitude derivative, stands as the computational 'bottleneck' of the method. This is the usual situation encountered in practice. However, other scenarios are possible – see §4.5 for a more throughout discussion.

[vi] In practice one always works with a finite set of basis functions; in other words, here, the term 'complete' should be understood as 'complete for practical purposes'.

At the same time, some systems exhibit an interesting property: depending on the dynamical regime in which they are found, they behave 'more classically' as they grow larger (e.g. bosonic systems approaching the thermodynamical limit). This sort of property invites treatments such as CCS, which has a strong semiclassical character.

Indeed, some of the CCS propagations presented at Chapter 5 (those involving systems of comparatively large sizes) took less overall CPU time than the one-time diagonalization of the quantum Hamiltonian operator.[vii]

Now, leaving aside questions regarding the 'classicality' of the system being described, we may argue that the *true advantage* of the CCS method is revealed when Hamiltonians with explicit time dependence are considered.

This is so because, for time-dependent Hamiltonians, one cannot rely on the concept of stationary states and the exact quantum propagation has to be conducted by means of some kind of short-time evolution operator, $\hat{U}(t+\tau, t)$, where τ denotes a small time displacement.

A popular form of writing the matrix representation of $\hat{U}(t+\tau, t)$ – using the $|\Phi\rangle$ basis, for instance – is according to the Crank-Nicholson recipe:[55]

$$U_{kl}(t+\tau, t) = \sum_{j=1}^{n} \left(I_n + \tfrac{i}{2\hbar} H(t)\tau\right)^{-1}_{kj} \left(I_n - \tfrac{i}{2\hbar} H(t)\tau\right)_{jl}, \tag{4.46}$$

where the entries of the Hamiltonian matrix are $H_{kl}(t) = \langle \Phi_k | \hat{H}(t) | \Phi_l \rangle$. This expression is unitary and correct to order $O(\tau^2)$; it thus leads to a norm-conserving and numerically stable propagation for sufficiently small τ. Under this framework, the wavefunction $\Psi_k(t) = \langle \Phi_k | \Psi(t) \rangle$ is obtained at instants $t = (\tau, 2\tau, 3\tau, \dots)$ by repeated action of $U(t+\tau, t)$:

$$\Psi_k(t+\tau) = \sum_{l=1}^{n} U_{kl}(t+\tau, t) \Psi_l(t).$$

Since the Hamiltonian changes with t, the evolution operator must be reconstructed at every time step of the propagation. As Eq. (4.46) shows, this requires a matrix inversion (or some operation of equivalent complexity) to be carried out at each step, and the computational cost of such operation scales roughly as $\sim n^3$.

Therefore, for systems governed by time-dependent Hamiltonians, the CCS method (whose formulation is, by the way, equally valid in such cases) competes directly with the quantum approach described above, since both schemes are limited by a bottleneck operation that takes place wherever the wavefunction is evolved by a small time interval.

Ignoring other possible technical difficulties, we may assert that the computational cost per time step associated with the short-time evolution operator methodology goes as $\sim n^3$, while that of CCS goes as $\sim m^3$. Now, the Hilbert space size n scales exponentially with system size; in contrast, a much less dramatic increase of the basis set size m is

[vii] These simulations were also aided by a parallelization scheme – cf. §4.5.

expected from CCS, as discussed previously. We thus conclude that, in the majority of problems involving large systems we have: $n^3 \gg m^3$. Therefore, the CCS method is expected to be much more efficient if $\hat{H} = \hat{H}(t)$.

Despite this conclusion, in this thesis we do not perform simulations with time-dependent Hamiltonians. This is because, in order to access the accuracy of the generalized CCS method, all results reported in Chapter 5 are compared against exact quantum calculations. Thus, if we intended to do the same sort of analysis for time-dependent systems, we would also have to carry out the full quantum propagation and face the computational difficulties exposed above; this, in turn, would require the development of sophisticated quantum propagation algorithms, a task which would fall out of the scope of the present work.

4.3 The CCS coupling for specific parametrizations

In this section we provide formulas for the CCS coupling, as computed for the coherent-state descriptions discussed in Chapters 2 and 3, which apply to standard many-particle Hamiltonians with one- and two-body terms. Before giving the equations for the bosonic and fermionic cases, however, let us recover, from the general formulas the expression for Gaussian wavepackets (i.e. Glauber states) – this is for didactic purposes only.

If we substitute in Eq. (4.9) [or its discrete version, Eq. (4.18)] the canonical, flat-geometry ingredients, $(\partial f(z_i^*, z_j)/\partial z_{i\alpha}^*) = z_{j\alpha}$ and $g(z_i^*, z_j)_{\alpha\beta} = \delta_{\alpha\beta}$, we get at once:

$$\begin{aligned}\Delta_{ij} &= E(z_i^*, z_j) - \left[E(z_i^*, z_i) + \sum_{\alpha=1}^{d}(z_j - z_i)_\alpha \frac{\partial E(z^*, z)}{\partial z_\alpha}\right] \\ &= \tfrac{1}{2}\sum_{\alpha\beta}(z_j - z_i)_\alpha \frac{\partial^2 E(z^*, z)}{\partial z_\alpha \partial z_\beta}|_{z_i}(z_j - z_i)_\beta + \ldots \end{aligned} \tag{4.47}$$

showing that the analytical structure of the coupling, seen as a series expansion of z_j around z_i, is such that it starts with a second-order energy term. This result does not exactly extend to other classes of coherent-states; nonetheless, it is demonstrated below that the interpretation of Δ_{ij} as a second-order energy deviation is also possible in the specific boson and fermion systems considered here.

4.3.1 The bosonic case

Let us consider the bosonic parametrization of Chapter 2, and a system whose dynamics is dictated by a prototype Hamiltonian as that of Eq. (2.45). By substituting the relevant quantities in Eq. (4.18) we may work the specific formula of the CCS coupling for this case. This short derivation is delineated below.

It is convenient to introduce a shorthand notation for the analytically-continued one-

density element corresponding to the reference mode $b_0^\dagger$,

$$\Gamma_{00}^{ij} = \frac{\{z_i|b_0^\dagger b_0|z_j\}}{\{z_i|z_j\}} = (1+z_i^* z_j)^{-1} \equiv \gamma_{ij}. \tag{4.48}$$

In this way, the Kähler gradients in (4.18) are abbreviated and the coupling becomes:

$$\Delta_{ij} = (E_{ij} + i\hbar\, N\gamma_{ij}\sum_\nu z_{j\nu}\dot{z}_{i\nu}^*) - (E_{ii} + i\hbar\, N\gamma_{ii}\sum_\nu z_{i\nu}\dot{z}_{i\nu}^*). \tag{4.49}$$

Next, we replace $\dot{z}_i^*$ using the complex-conjugate of the mean-field equation of motion, Eq. (2.57). Adapting the notation, we have:

$$-i\hbar\,\dot{z}_{i\nu}^* = G_{0\nu}^{ii} - G_{00}^{ii} z_{i\nu}^* + \sum_\mu z_{i\mu}^* G_{\mu\nu}^{ii} - \sum_\mu z_{i\mu}^* G_{\mu 0}^{ii} z_{i\nu}^*. \tag{4.50}$$

Let us then evaluate the non-diagonal term involving $\dot{z}_i^*$ – the expression is organized as follows:

$$\begin{aligned} i\hbar\, N\gamma_{ij}\sum_{nu} z_{j\nu}\dot{z}_{i\nu}^* &= N(G_{00}^{ii} + \sum_\mu z_{i\mu}^* G_{\mu 0}^{ii})\sum_\nu z_{j\nu}\gamma_{ij} z_{i\nu}^* \\ &\quad - N\sum_\nu z_{j\nu}\gamma_{ij}\, G_{0\nu}^{ii} - N\sum_{\nu\mu} z_{j\nu}\gamma_{ij} z_{i\mu}^*\, G_{\mu\nu}^{ii}. \end{aligned} \tag{4.51}$$

In the first line of the above equation we put

$$\sum_\nu z_{j\nu}\gamma_{ij} z_{i\nu}^* = \frac{z_i^* z_j}{1+z_i^* z_j} = 1-\gamma_{ij}, \tag{4.52}$$

and proceed with the following identifications,

$$\begin{aligned} i\hbar\, N\gamma_{ij}\sum_{nu} z_{j\nu}\dot{z}_{i\nu}^* &= N(G_{00}^{ii} + \sum_\mu z_{i\mu}^* G_{\mu 0}^{ii}) \\ &\quad - N\gamma_{ij}\, G_{00}^{ii} - N\sum_\nu \gamma_{ij} z_{i\nu}^*\, G_{\nu 0}^{ii} - N\sum_\nu z_{j\nu}\gamma_{ij}\, G_{0\nu}^{ii} - N\sum_{\nu\mu} z_{j\nu}\gamma_{ij} z_{i\mu}^*\, G_{\mu\nu}^{ii} \\ &= N(G_{00}^{ii} + \sum_\mu z_{i\mu}^* G_{\mu 0}^{ii}) - N\Big(\Gamma_{00}^{ij} G_{00}^{ii} + \sum_\nu \Gamma_{0\nu}^{ij} G_{\nu 0}^{ii} + \sum_\nu \Gamma_{\nu 0}^{ij} G_{0\nu}^{ii} + \sum_{\nu\mu} \Gamma_{\nu\mu}^{ij}\, G_{\mu\nu}^{ii}\Big) \\ &= N(G_{00}^{ii} + \sum_\mu z_{i\mu}^* G_{\mu 0}^{ii}) - N\sum_{pq} G_{pq}^{ii}\Gamma_{qp}^{ij}. \end{aligned} \tag{4.53}$$

Meanwhile, the analytically-continued energy function, here conveniently written in terms of the Gross-Pitaevskii matrix and the mean-field matrix (compare Eqs. (2.53) and (2.56)), is:

$$E_{ij} = N\sum_{pq}(G_{pq}^{ij} - \tfrac{1}{2}v_{pq}^{ij})\Gamma_{qp}^{ij}. \tag{4.54}$$

Combining this with the result (4.53) yields:

$$E_{ij}+i\hbar N\gamma_{ij}\sum_{\nu} z_{j\nu}\dot{z}^{*}_{i\nu} = N(G^{ii}_{00}+\sum_{\mu} z^{*}_{i\mu}G^{ii}_{\mu 0})+N\sum_{pq}(G^{ij}_{pq}-G^{ii}_{pq})\Gamma^{ij}_{qp}-\tfrac{1}{2}N\sum_{pq} v^{ij}_{pq}\Gamma^{ij}_{qp}. \quad (4.55)$$

The diagonal form is immediately obtained by setting $j = i$,

$$E_{ii} + i\hbar\, N\gamma_{ii}\sum_{\nu} z_{i\nu}\dot{z}^{*}_{i\nu} = N(G^{ii}_{00} + \sum_{\mu} z^{*}_{i\mu}G^{ii}_{\mu 0}) - \tfrac{1}{2}N\sum_{pq} v^{ii}_{pq}\Gamma^{ii}_{qp}. \quad (4.56)$$

The coupling is simply the difference between (4.55) and (4.56):

$$\Delta_{ij} = N\sum_{pq}(G^{ij}_{pq} - G^{ii}_{pq})\Gamma^{ij}_{qp} - \tfrac{1}{2}N\sum_{pq}(v^{ij}_{pq}\Gamma^{ij}_{qp} - v^{ii}_{pq}\Gamma^{ii}_{qp}). \quad (4.57)$$

Noting that $G^{ij}_{pq}-G^{ii}_{pq} = v^{ij}_{pq}-v^{ii}_{pq}$ (the one-body integrals do not depend on z and therefore they cancel off) the above expression can be reorganized according to:

$$\Delta_{ij} = \tfrac{1}{2}N\sum_{pq}\Big[(v^{ij}_{pq} - v^{ii}_{pq})\Gamma^{ij}_{qp} - v^{ii}_{pq}(\Gamma^{ij}_{qp} - \Gamma^{ii}_{qp})\Big]. \quad (4.58)$$

This can be further reduced by making explicit the z-independent two-body integrals embedded in the mean-fields. The first part gives:

$$\sum_{pq}(v^{ij}_{pq} - v^{ii}_{pq})\Gamma^{ij}_{qp} = (N-1)\sum_{pqrs} U_{pr\cdot qs}(\Gamma^{ij}_{sr} - \Gamma^{ii}_{sr})\Gamma^{ij}_{qp}, \quad (4.59)$$

while the second part can be recast as follows:

$$\begin{aligned}\sum_{pq} v^{ii}_{pq}(\Gamma^{ij}_{qp} - \Gamma^{ii}_{qp}) &= (N-1)\sum_{pq}\sum_{rs} U_{pr\cdot qs}\Gamma^{ii}_{sr}(\Gamma^{ij}_{qp} - \Gamma^{ii}_{qp}) \\ &= (N-1)\sum_{rs}\sum_{pq} U_{rp\cdot sq}(\Gamma^{ij}_{qp} - \Gamma^{ii}_{qp})\Gamma^{ii}_{sr} \\ &= (N-1)\sum_{pqrs} U_{pr\cdot qs}(\Gamma^{ij}_{sr} - \Gamma^{ii}_{sr})\Gamma^{ii}_{qp}, \end{aligned} \quad (4.60)$$

where the interchange symmetry of $U_{pr\cdot qs}$ has been used.

Finally, combining the above relations into Eq. (4.58) we arrive at the desired formula:

$$\Delta_{ij} = \tfrac{1}{2}N(N-1)\sum_{pqrs} U_{pr\cdot qs}(\Gamma^{ij}_{sr} - \Gamma^{ii}_{sr})(\Gamma^{ij}_{qp} - \Gamma^{ii}_{qp}). \quad (4.61)$$

One cannot help noticing the similarity between this expression and a second-order energy variation induced by first-order density fluctuations:

$$E(\Gamma_0 + \delta\Gamma) - E(\Gamma_0) = N\sum_{pq} G(\Gamma_0)_{pq}\,\delta\Gamma_{qp} + \tfrac{1}{2}N(N-1)\sum_{pqrs} U_{pr\cdot qs}\delta\Gamma_{sr}\delta\Gamma_{qp}. \quad (4.62)$$

In this case, the energy change would be that induced by an analytic continuation, $z_i \to z_j$, in the one-density, $\delta\Gamma^{ij} = \Gamma(z_i^*, z_j) - \Gamma(z_i^*, z_i)$, and we identify: $E - E_0 = \delta E + \delta^2 E$, with

$$\delta^2 E_{ij} = \tfrac{1}{2} N(N-1) \sum_{pqrs} U_{pr\cdot qs} \delta\Gamma^{ij}_{sr} \delta\Gamma^{ij}_{qp} = \Delta_{ij}. \tag{4.63}$$

This provides a transparent physical interpretation of the CCS coupling. Later we will simplify this even further by considering simple Hubbard models.

4.3.2 The fermionic case

The CCS coupling for the femionic parametrization of Chapter 3 and Hamiltonians such as (3.54) can also be worked down to a much simpler and physically appealing form. The same kind of manipulations operated in the bosonic case are repeated here.

We begin with the replacement of the Kähler gradients, thus rewriting (4.18) as:

$$\Delta_{ij} = \Big[E_{ij} + i\hbar \,\mathrm{tr}\Big(z_j (I_N + z_i^\dagger z_j)^{-1} \dot{z}_i^\dagger\Big)\Big] - \Big[E_{ii} + i\hbar \,\mathrm{tr}\Big(z_i (I_N + z_i^\dagger z_i)^{-1} \dot{z}_i^\dagger\Big)\Big]. \tag{4.64}$$

Lets us consider the $\dot{z}_i^\dagger$ factor. Taking the adjoint of Eq. (3.80),

$$\dot{z}_i^\dagger = \frac{i}{\hbar} \begin{bmatrix} I_N & z_i^\dagger \end{bmatrix} F^{ii} \begin{bmatrix} -z_i^\dagger \\ I_M \end{bmatrix}, \quad F^{ii} = h + v^{ii}, \tag{4.65}$$

(recall $F^\dagger = F$) and writing

$$z_j = \begin{bmatrix} 0 & I_M \end{bmatrix} \begin{bmatrix} I_N \\ z_j \end{bmatrix}, \tag{4.66}$$

we are able to handle the trace as follows:

$$\begin{aligned} i\hbar \,\mathrm{tr}\Big(z_j (I_N + z_i^\dagger z_j)^{-1} \dot{z}_i^\dagger\Big) &= -\mathrm{tr}\left\{ \begin{bmatrix} 0 & I_M \end{bmatrix} \begin{bmatrix} I_N \\ z_j \end{bmatrix} (I_N + z_i^\dagger z_j)^{-1} \begin{bmatrix} I_N & z_i^\dagger \end{bmatrix} F^{ii} \begin{bmatrix} -z_i^\dagger \\ I_M \end{bmatrix} \right\} \\ &= -\mathrm{tr}\left\{ F^{ii} \begin{bmatrix} 0 & -z_i^\dagger \\ 0 & I_M \end{bmatrix} \Gamma^{ij} \right\} \\ &= \mathrm{tr}(F^{ii}_{11} z_i^\dagger \Gamma^{ij}_{21} - F^{ii}_{12} \Gamma^{ij}_{21}) + \mathrm{tr}(F^{ii}_{21} z_i^\dagger \Gamma^{ij}_{22} - F^{ii}_{22} \Gamma^{ij}_{22}), \end{aligned} \tag{4.67}$$

where the analytically continued one-density, $\Gamma^{ij} = \Gamma(z_i^*, z_j)$, has been identified with the second form given in Eq. (3.57). Next, we note that:

$$z_i^\dagger \Gamma^{ij}_{21} = I_N - \Gamma^{ij}_{11} \quad \text{and} \quad z_i^\dagger \Gamma^{ij}_{22} = z_i^\dagger - \Gamma^{ij}_{12}. \tag{4.68}$$

Putting these relations in the respective traces of Eq. (4.67) we get:

$$\begin{aligned} i\hbar\,\mathrm{tr}\Big(z_j(I_N+z_i^\dagger z_j)^{-1}\dot{z}_i^\dagger\Big) &= \mathrm{tr}(F_{11}^{ii}) - \mathrm{tr}(F_{11}^{ii}\Gamma_{11}^{ij}+F_{12}^{ii}\Gamma_{21}^{ij}) + \mathrm{tr}(F_{21}^{ii}z_i^\dagger) - \mathrm{tr}(F_{21}^{ii}\Gamma_{12}^{ij}+F_{22}^{ii}\Gamma_{22}^{ij}) \\ &= \mathrm{tr}(F_{11}^{ii}+F_{21}^{ii}z_i^\dagger) - \mathrm{tr}(F^{ii}\Gamma^{ij}). \end{aligned} \tag{4.69}$$

Adding the energy factor, conveniently written in terms of the analytically-continued Fock matrix and mean-field matrix as

$$E_{ij} = \mathrm{tr}[(h+\tfrac{1}{2}v^{ij})\Gamma^{ij}] = \mathrm{tr}(F^{ij}\Gamma^{ij}) - \tfrac{1}{2}\mathrm{tr}(v^{ij}\Gamma^{ij}), \tag{4.70}$$

gives the non-diagonal part of (4.64):

$$\begin{aligned} E_{ij} + i\hbar\,\mathrm{tr}\Big(z_j(I_N+z_i^\dagger z_j)^{-1}\dot{z}_i^\dagger\Big) &= \mathrm{tr}(F_{11}^{ii}+F_{21}^{ii}z_i^\dagger) + \mathrm{tr}[(F^{ij}-F^{ii})\Gamma^{ij}] - \tfrac{1}{2}\mathrm{tr}(v^{ij}\Gamma^{ij}) \\ &= \mathrm{tr}(F_{11}^{ii}+F_{21}^{ii}z_i^\dagger) + \tfrac{1}{2}\mathrm{tr}[(v^{ij}-v^{ii})\Gamma^{ij}] - \tfrac{1}{2}\mathrm{tr}(v^{ii}\Gamma^{ij}). \end{aligned} \tag{4.71}$$

Setting $j=i$ yields:

$$E_{ii} + i\hbar\,\mathrm{tr}\Big(z_i(I_N+z_i^\dagger z_i)^{-1}\dot{z}_i^\dagger\Big) = \mathrm{tr}(F_{11}^{ii}+F_{21}^{ii}z_i^\dagger) - \tfrac{1}{2}\mathrm{tr}(v^{ii}\Gamma^{ii}). \tag{4.72}$$

Subtracting (4.72) from (4.71) produces the formula:

$$\Delta_{ij} = \tfrac{1}{2}\mathrm{tr}[(v^{ij}-v^{ii})\Gamma^{ij} - v^{ii}(\Gamma^{ij}-\Gamma^{ii})]. \tag{4.73}$$

Once more, we pursue further simplification by considering the two-body integrals explicitly; the two traces involved in (4.73) are rewritten according to:

$$\mathrm{tr}[(v^{ij}-v^{ii})\Gamma^{ij}] = \sum_{pqrs}(V_{pr\cdot qs}-V_{pr\cdot sq})(\Gamma_{sr}^{ij}-\Gamma_{sr}^{ii})\Gamma_{qp}^{ij}, \tag{4.74}$$

and:

$$\begin{aligned} \mathrm{tr}[v^{ii}(\Gamma^{ij}-\Gamma^{ii})] &= \sum_{pq}\sum_{rs}(V_{pr\cdot qs}-V_{pr\cdot sq})\Gamma_{sr}^{ii}(\Gamma_{qp}^{ij}-\Gamma_{qp}^{ii}) \\ &= \sum_{rs}\sum_{pq}(V_{rp\cdot sq}-V_{rp\cdot qs})(\Gamma_{qp}^{ij}-\Gamma_{qp}^{ii})\Gamma_{sr}^{ii} \\ &= \sum_{pqrs}(V_{pr\cdot qs}-V_{pr\cdot sq})(\Gamma_{sr}^{ij}-\Gamma_{sr}^{ii})\Gamma_{qp}^{ii}, \end{aligned} \tag{4.75}$$

which leads at once to the desired result:

$$\Delta_{ij} = \tfrac{1}{2}\sum_{pqrs}(V_{pr\cdot qs}-V_{pr\cdot sq})(\Gamma_{sr}^{ij}-\Gamma_{sr}^{ii})(\Gamma_{qp}^{ij}-\Gamma_{qp}^{ii}). \tag{4.76}$$

As in the bosonic case this can be interpreted in energy terms; the energy difference due to density fluctuation is found from Eq. (3.75) to be

$$E(\Gamma_0 + \delta\Gamma) - E(\Gamma_0) = \sum_{pq} F(\Gamma_0)_{pq}\, \delta\Gamma_{qp} + \tfrac{1}{2} \sum_{pqrs} (V_{pr\cdot qs} - V_{pr\cdot sq}) \delta\Gamma_{sr} \delta\Gamma_{qp}. \tag{4.77}$$

In this case the energy change would be that induced by an analytic continuation, $z_i \to z_j$, in the one-density, $\delta\Gamma^{ij} = \Gamma(z_i^*, z_j) - \Gamma(z_i^*, z_i)$; writing $E - E_0 = \delta E + \delta^2 E$ we identify:

$$\delta^2 E_{ij} = \tfrac{1}{2} \sum_{pqrs} (V_{pr\cdot qs} - V_{pr\cdot sq}) \delta\Gamma^{ij}_{sr} \delta\Gamma^{ij}_{qp} = \Delta_{ij}. \tag{4.78}$$

This provides the fermionic CCS coupling with a sound physical interpretation. Further specification of $V_{pq\cdot qs}$ (e.g. when the system can be described by simple Hubbard models) allows for an even more reduced expression.

4.4 Sampling protocol

In the remainder of this chapter we shall be concerned with some computational aspects of the discrete unitary CCS method. We begin by outlining a general algorithm for carrying out the first stage of any application – basis set sampling at $t = 0$.

The procedure hereby explained assumes that the initial wavefunction is a coherent state, i.e. $|\psi_0\rangle = |z_0\rangle$, and it applies to any type of coherent-state parametrization $|z\rangle$ once two geometry-dependent ingredients are provided: adequate *sampling coordinates*, $q = f(z)$, with a known inverse, $z = f^{-1}(q)$, and a *weight distribution function* $w(q)$, according to which these coordinates are to be randomly selected. In particular, the coordinate associated with the initial state is denoted by $q_0 = f(z_0)$ and $w(q_0)$ is a global maximum of the weight distribution. The sampling strategy follows a very simple 'one-by-one' protocol, which draws inspiration from previously developed basis set conditioning techniques.[53]

One begins by taking $|z_0\rangle$ (the initial state itself) as the first basis element – the initial state will always be part of the basis set, with the corresponding amplitude having the maximum value, $C(z_0) = 1$. This is crucial for accuracy of short-time results and also secures that the initial norm is unity, regardless of how the remaining basis elements turn out to be distributed in phase space. Then the sampling loop starts – each iteration amounts to three steps:

1. Using the appropriate sampling coordinates q and weight function $w(q)$, randomly select a new basis element $z_i = f^{-1}(q_i)$ and temporarily add $|z_i\rangle$ to the basis set.

2. Compute the overlap matrix Ω and evaluate its *conditioning factor*,

$$\beta(\Omega) = \lambda_{\max}/\lambda_{\min}, \tag{4.79}$$

where $\lambda_{\max}$ and $\lambda_{\min}$ are the largest and smallest eigenvalues of Ω, respectively.[viii]

3. If β is less than some threshold value $\beta_{\lim}$, accept $|z_i\rangle$, permanently adding it to the basis set, whose size increases by unity. Else, discard the selected basis element, in which case the basis-set size does not change. (Additional conditions can be enforced; for instance, one may require minimum/maximum overlap with the initial state or some other, problem-specific restriction, e.g. an energy cut-off). In either case, return to the first step.

The above sequence of operations is then repeated until either a predetermined basis-set size m is achieved or *saturation* occurs, meaning that the algorithm is unable to select a new $|z_i\rangle$ that satisfies the β threshold condition (a certain maximum number of attempts may be stipulated). How fast saturation takes place will depend upon the system's dimensionality, the threshold value $\beta_{\lim}$, the coherent-state parameters and the details of the sampling distribution $w(q)$. Typically, we take $\beta_{\lim} \sim 10^8 - 10^{13}$, and, after some test-runs for determining the threshold size, settle for a basis-set just below the saturation point, thus ensuring a dense swarm of initial conditions (since significant overlapping of basis elements is essential for an accurate propagation) but with a reasonably well-conditioned overlap matrix at $t = 0$.

Although nothing prevents that an initially well-conditioned overlap matrix becomes singular at some later time – a known weakness of methods formulated with non-orthogonal basis sets[56] – we observe in practice that the time-dependent conditioning factor,

$$\beta(\Omega(t)) = \lambda_{\max}(t)/\lambda_{\min}(t), \tag{4.80}$$

– which, together with total energy and norm, is one of the default quantities monitored during propagation – tends to decrease over time, specially for systems with a large number of degrees of freedom (this behavior is nonetheless observed in the two-dimensional system studied at §5.3). This is a consequence of the non-linear dynamics of the z variables: trajectories tend to spread over the phase space, and a sparse basis is likely to yield a small conditioning factor.

This also leads to an interesting observation. A possible scenario is the one where, after a long propagation time, the non-diagonal entries of the overlap matrix Ω become negligible, with $\beta(\Omega(t))$ approaching unity. According to Eq. (4.26) this means that amplitudes decouple and therefore 'freeze' on their current values, say $\bar{C}$ and $\bar{D}$. The result is that the CCS wavefunction reduces to a *incoherent mixture* of classically driven,

[viii] The overlap matrix is hermitian and positive-definite, meaning that its eigenvalues are real and positive, though numerical diagonalization may produce null or very small negative eigenvalues. Alternatively, one could employ a singular value decomposition and carry on the sampling procedure using the singular values rather than the eigenvalues.

independent basis states:

$$|\psi(t)\rangle \to \sum_i \bar{D}_i \, |z_i(t)\rangle e^{\frac{i}{\hbar}S_i(t)}, \quad (d/dt)\bar{D}_i \approx 0, \quad \beta(\Omega(t)) \approx 1.$$

Clearly, under such circumstances, the CCS solution has long ceased to give satisfactory results.

Nonetheless, in the event that Ω becomes singular at some instant $t > 0$ one should take appropriate measures before resuming the time evolution. In this regard, a particularly interesting methodology has been developed by Habershon in Ref. [53]. In that work a 'basis set adaptation' algorithm is designed which simultaneously remedies both the ill-conditioning of the overlap matrix and fixes an eventual poor representation of the wavefunction, by dynamically re-sampling the basis set. Habershon's method is formulated for gaussian wavepackets, but it applies equally well to the generalized coherent-state case.

However, in the model problems considered in Chapter 5, the so-called 'singularity problem', associated with ill-conditioning of the basis set, did not occur. On the other hand, in virtually all simulations performed, the CCS wavefunction was observed to become less accurate for sufficiently long propagation times, precisely due to the spreading of trajectories mentioned earlier – no effort to 'adapt' the basis set was made, though; at this stage we simply terminate the calculation.

Finally, we note that our sampling protocol requires the eigenvalues of the overlap matrix to be computed at every iteration. However, that does not compromise the method's overall efficiency since the initial sampling is performed only once. Moreover, the overlap matrix typically does not grow too large; this assertion holds even for multidimensional systems, as long as the sampling distribution is kept sufficiently localized around the initial-state coordinate z_0, from where the most relevant contributions to the initial value representation formula are expected to originate.

4.5 A 'pave-the-way' parallelization scheme

In this section we put forward a parallelization scheme for the standard CCS method (i.e. the discrete unitary version). The technique developed here was used in the simulations of Chapter 5 and has proved its effectiveness – indeed, results would otherwise have been much harder to obtain.

The methodology is rather unusual in that parallel operations are distributed across the time domain with the help of 'time-chunk' buffers. In order to put ideas into perspective, we begin by highlighting some general aspects of the numerical implementation of

the CCS method. Let us recall the fundamental sizes involved:

$$\begin{cases} m & \text{basis-set size (number of trajectories).} \\ d & \text{degrees of freedom (length of complex } z \text{ vectors).} \\ n & \text{number of time steps.} \end{cases} \tag{4.81}$$

The first thing to be noticed is that propagation of the CCS wavefunction consists of two parts: the evolution of individual orbits z_i, which obey

$$\frac{dz_{i\alpha}}{dt} = -\frac{i}{\hbar}\sum_{\beta=1}^{d} g^{-T}_{\alpha\beta}(z_i^*, z_i)\frac{\partial E(z_i^*, z_i)}{\partial z_{i\beta}^*}, \quad \text{for } 1 \le i \le m, \tag{4.82}$$

and the marching of amplitudes C_i, whose dynamics is governed by the pair of equations:

$$\sum_{k=1}^{m}\omega_{jk}C_k = D_j, \quad \frac{dC_i}{dt} = -\frac{i}{\hbar}\sum_{j=1}^{m}(\omega_{ij}\Delta_{ij})D_j, \tag{4.83}$$

with the overlap matrix ω_{ij} and the CCS coupling Δ_{ij} given by Eqs. (4.25) and (4.18).

Let us then pictorically represent the operations required for advancing the wavefunction by one time step:

1. $\dot{z}_i(t) = f(z_i(t)), \quad z_i(t+h) = g(h, \dot{z}_i(t)), \quad (1 \le i \le m)$;
2. $\dot{\boldsymbol{C}}(t) = \boldsymbol{F}(\boldsymbol{z}(t), \boldsymbol{C}(t)), \quad \boldsymbol{C}(t+h) = \boldsymbol{G}(h, \dot{\boldsymbol{C}}(t))$.

Here, the time increment is h and boldface quantities are m-sized arrays: $\boldsymbol{C} = (C_1, \ldots, C_m)$ and $\boldsymbol{z} = (z_1, \ldots, z_m)$, with each z_i being itself a d-sized vector.

The meaning of the above scheme is as follows. The function f represents the equation of motion (4.82), it takes $z(t)$ as input and returns the time-derivative $\dot{z}(t)$. Meanwhile g symbolizes an ordinary differential equation (ODE) stepper routine, which takes the time increment h and the computed $\dot{z}(t)$ as inputs and returns the time-evolved variable, $z(t+h)$. Similarly, $\boldsymbol{F}$ represents the pair of equations in (4.83); this function, which takes arguments $\boldsymbol{z}(t)$ and $\boldsymbol{C}(t)$, builds the required matrices ω_{ij} and Δ_{ij}, solves the linear system for $\boldsymbol{D}$ and produces the amplitude derivative $\dot{\boldsymbol{C}}(t)$. In turn, the application $\boldsymbol{G}$ uses h and the computed $\dot{\boldsymbol{C}}(t)$ to advance the amplitude, returning $\boldsymbol{C}(t+h)$. The scheme is merely illustrative since stepper routines usually require derivatives to be evaluated at several instants, but it is nevertheless useful for discussing the computational effort involved in each operation.

Integration of Eqs. (4.82) can be made with standard ODE routines equipped with step-size adaptation and error control. Ignoring possible complications associated with unstable orbits, we may assume that the computational effort (measured in CPU time) per trajectory per time step scales linearly with the number of degrees of freedom, d.

Thus, we may say that the cost for advancing all basis elements through operations f and g goes as $\sim md$.

In the majority of situations, the most expensive operation per time step is the intermediate calculation of $\boldsymbol{D}$ amplitudes, which requires solution of the linear system in (4.83). This is achieved by LU decomposition of the overlap matrix and subsequent backward substitution. Ignoring matrix building (which scales as $\sim m^2$), the CPU time expend in this operation goes roughly as $\sim m^3$. Since this procedure is conducted by the function $\boldsymbol{F}$ we attach the computational cost of $\sim m^3$ to the latter – also, we henceforth refer to it as the *bottleneck operation*.

4.5.1 * Implementation types – a few examples

Next, let us provide two basic examples of implementation and make some remarks on how they administer the operations described above. All numerical effort associated with secondary tasks, such as monitoring and diagnosis, calculation of observables and output writing will be ignored.

Simplest approach. The propagation scheme which is perhaps the easiest to program is the one where $\boldsymbol{z}$ and $\boldsymbol{C}$ are treated on the same footing, i.e. derivatives $\dot{\boldsymbol{z}}$ and $\dot{\boldsymbol{C}}$ are computed simultaneously and the entire set of variables is advanced together. In more elaborated versions of CCS, like the gaussian-wavepacket-based multiconfigurational Ehrenfest method (MCE),[57;58] this may be the only viable approach, for in that case trajectories actually couple to their amplitudes. However, it is a poor approach to standard CCS, where the $\boldsymbol{z}$ parameters obey separate equations. This is so because the presence of a single unstable orbit will require more ODE calls, with all derivatives being calculated. Thus many operations will be carried out unnecessarily, including the expensive factorization of the overlap matrix, slowing down the time evolution. Nevertheless, it is simple and the difficulties just mentioned are alleviated when considering a small phase space, few basis elements and short propagation times. It has been successfully used in Ref. [28] in the study of a bosonic triple-well system. The same problem is analyzed in §5.3 with the more sophisticated parallel scheme devised here.

Two-stage approach. The fact that CCS trajectories evolve independently brings the possibility of a two-stage strategy. First, orbits are evolved and their coordinates are saved in hard-disk at predetermined instants. Later, this information is loaded and used to build the require matrices for the propagation of amplitudes. The first-stage can be fully parallelized, and unstable orbits do not pose a problem for the overall efficiency. This approach has the interesting advantage of allowing a more sophisticated 'sampling' of trajectories, since their entire history is known, and one may choose which orbits are more adequate for the problem at hand. However, the bottleneck problem is not addressed under this scheme. There is also a drawback concerning memory usage: for a system with d degrees of freedom, the memory needed for storing m orbits evaluated at n time steps

goes as nmd; this can be huge. Also, loading from hard-disk is slow. Nonetheless, the two-stage methodology is useful when individual trajectories are propagated at a very expensive computational cost. This situation is found when analytical Hamiltonians are not available. This is usual in quantum chemistry problems studied with the Gaussian-based *ab initio* MCE technique,[59–63] where each basis element represents a molecular geometry. In order to determine the forces that act on the system, an electronic structure calculation must be performed at every time step. Indeed, in this kind of problem, the cost per trajectory obliterates everything else – the factorization of the overlap matrix becomes a minor issue.

Let us mention that one possible way of dealing with the bottleneck operation in the standard CCS method is through parallelization of the algorithm used in the factorization of the overlap matrix. This could be implemented with either of the approaches discussed above and the required sub-routines are available in some scientific libraries. If the LU decomposition of ω is performed in a multi-threaded fashion the cost of the operation would be diminished from m^3 to $\sim m^3/p$, where p is the number of processors. The problem is that this becomes advantageous only if m is very large, say $m \sim 10^3$, which leads to other difficulties. Alternative low-level schemes are discussed in Ref. [52].

4.5.2 The three-stage 'pave-the-way' implementation

The discussion so far was meant to give a general idea of the sort of difficulties to be overcome when designing a parallel CCS algorithm. Having prepared the terrain, we now set out to formulate the so called 'pave-the-way' approach.

Let us consider the intermediate situation wherein trajectories are reasonable cheap to compute, so that the operations involved in the integration of Eq. (4.82) can be handled by a single processor. For definiteness we may imagine $d = 10$. Also, we assume a moderate basis-set size; a representative number of basis elements would be $m = 100$. Under these circumstances, the low-level parallelization of the bottleneck operation (mentioned earlier as a possible way of dealing with the problem) is not profitable, hardly compensating for the setting up of the required multi-thread environment. Therefore we must look for alternative solutions.

We propose a three-stage procedure based on parallel tasks distributed over a range of sequential time intervals. This means that the full timespan of the propagation is sliced into pieces of size $n' < n$. Again, for definiteness, let us take the total number of time steps $n = 2000$; we could then work with one-hundred time slices of size $n' = 20$. We call the workspace associated with each time slice a *time chunk*.

Only one time chunk is needed in the program – it is used for propagating time slices one after the other. The time chunk must allocate sufficient memory for storing n' copies of the CCS workspace, which consists essentially of the basis vector array $\boldsymbol{z}$ – of size md – and $m \times m$ matrices $\boldsymbol{\omega}$ and $\boldsymbol{X}$ – the latter being defined through the relation $X_{ij} = \omega_{ij}\Delta_{ij}$,

i.e. it is the matrix that multiplies $\boldsymbol{D}$ in Eq. (4.83). For simplicity we ignore other auxiliary quantities.

Hence the memory required per time step is $\sim (md + 2m^2)$. The memory associated with the time chunk is then $\sim n'(md + 2m^2)$. This can be quite big, but the strategy is already effective for n' of the same order of the number of processors, hereby denoted p, and which is usually ~ 10, so that we do not need a too large time-chunk (though the method is more profitable for larger n'). Also, notice that this refers to RAM memory, meaning that reading and writing operations are fast.

Let us set $p = 10$. The three stages of the 'pave-the-way' scheme are as follows.

1. Basis elements are propagated in parallel during the timespan which is currently contemplated by the time chunk. Let us think this is the first time slice, so the timespan is: $0 \leq t \leq n'h$. As each trajectory evolves its coordinates are stored in the appropriate slots of the $\boldsymbol{z}$ array corresponding to instants $t = 0, h, 2h, \ldots, n'h$. This is straightforward parallelism without any interdependencies whatsoever. The computational cost associated with trajectory propagation is thus reduced from the assumed $\sim md$ to $\sim p^{-1}md$. Moreover, since most orbits behave similarly, the workload is well-balanced among processors.[ix]

2. Once all trajectory information during the interval $0 \leq t \leq n'h$ is stored in the time chunk, each processor is then assigned to work on one of the n' instants, with tasks distributed as in a 'parallel-for' loop. Each thread reads the $\boldsymbol{z}$ array from a specific time instant, builds the matrices $\boldsymbol{\omega}$ and $\boldsymbol{X}$ and, finally, conducts the LU decomposition of the matrix $\boldsymbol{\omega}$, which can be stored in the same matrix space used by the overlap matrix corresponding to that instant. Since a moderate basis-set size m was assumed, this calculation should be handled without difficulty by a single processor. Once again this is dependency-free parallelism with nearly perfect workload balance. The overall effect is that the time required for carrying out the n' bottleneck operations for the current time slice has been reduced from $\sim n'm^3$ to $\sim p^{-1}n'm^3$. In other words, instead of focusing on a single time step, we took advantage of the fact that the z vectors can be independently evolved, in order to conduct the LU decompositions in parallel at adjacent time instants.

3. The last stage concerns propagation of amplitudes during the time chunk's span. This stage is performed in a serial fashion using a forth-order Runge-Kutta stepper routine (the $\boldsymbol{G}$ operations in the 'pictorical scheme').[x] Notice that, with the LU-factorized form of the overlap matrix at our disposal, the $\boldsymbol{D}(t)$ amplitudes at each

[ix] In our codes the evolution of basis elements is performed with the general-purpose 'Runge-Kutta-Fehlberg (4,5)' integrator, with error control and adaptive step size, as implemented in the GNU Scientific Library;[64] however, since coherent-state variables evolve in a classical phase-space, one would perhaps prefer a symplectic integrator.

[x] The general-purpose forth-order Runge-Kutta stepper was chosen because it delivers good balance

instant t are obtained from $\boldsymbol{C}(t)$ by simple backward substitution, with computational cost scaling as $\sim m^2$. The algorithm yields $\boldsymbol{C}(h), \boldsymbol{C}(2h), \boldsymbol{C}(3h), \ldots, \boldsymbol{C}(n'h)$ and the propagation on the current time-slice is completed.

Following this last stage, the time chunk is reseted and propagation on the subsequent time slice begins (the last instant stored in the time chunk is re-allocated, becoming the first instant for the next round).

Below, we provide a descriptive scheme of the three stages enumerated above, as implement with a time chunk of size $n' = 5$, for a wavefunction with $m = 8$ basis elements, and $p = 3$ processors (these are indicated by the letter P). An additional detail, which was left out of the previous explanation is illustrated: the fact that, in the last stage, each integration step usually requires more than one evaluation of the derivative function $\boldsymbol{F}$.

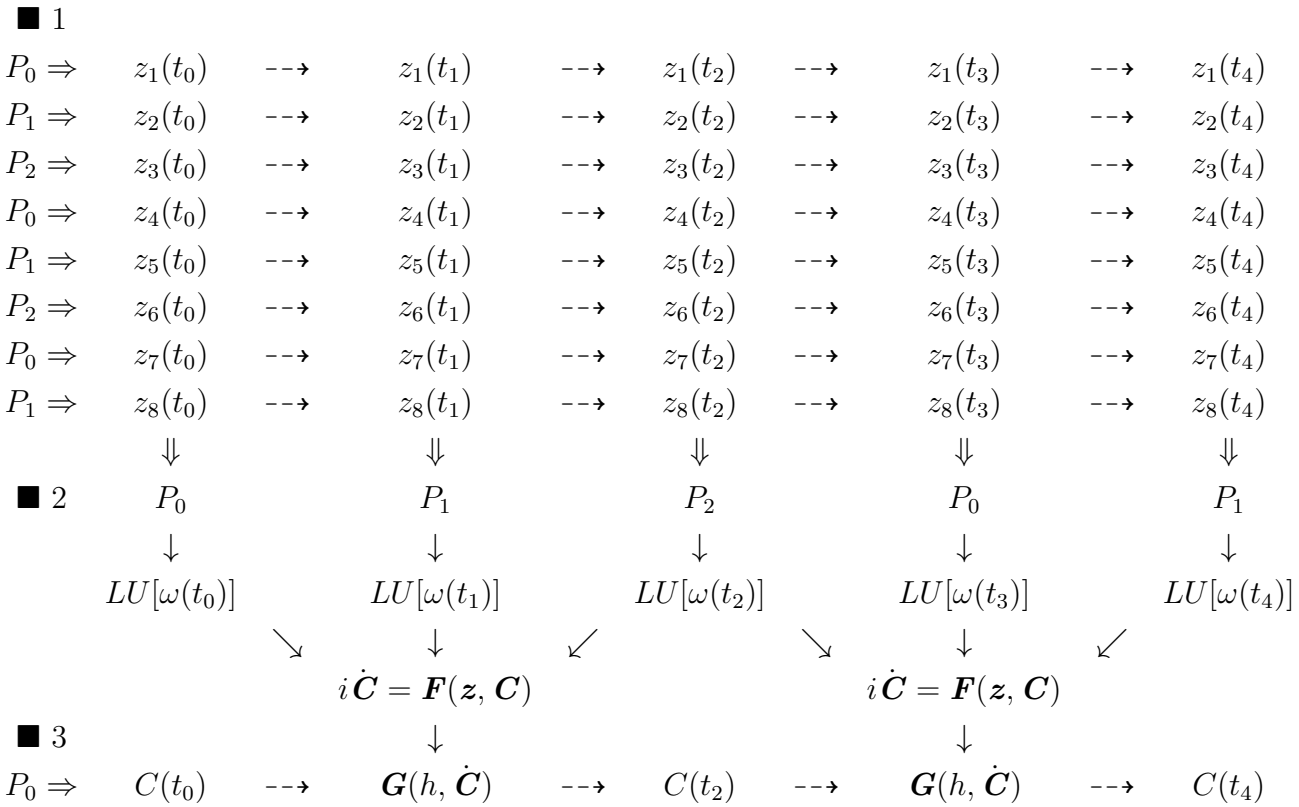

The whole strategy is based on the idea of 'paving the way' for the integration of the amplitude's equation of motion, hence the chosen name. Finally, we emphasize once more that this technique was crucial in accelerating the simulations of Chapter 5.

between simplicity of implementation and overall accuracy – the latter meant in the sense that propagation remains stable even for reasonably large time increments h. Ideally, however, one would prefer a more sophisticated algorithm, specifically designed for propagating quantum states represented in terms of non-orthogonal, time-dependent basis functions; such a scheme is developed in Ref. [65].

4.6 * Extensions of the multiconfigurational method

In this last section we specifically consider the CCS method as formulated with the fermionic coherent states (Thouless determinants) of Chapter 3. Earlier, at §3.3, we analyzed the relation between different Thouless representations (i.e. whose parameters are defined with respect to different reference determinants) of a same physical state and found that the corresponding coherent-state labels are connected by an analytical map [cf. Eq. (3.95)]. We also discussed how such map can be useful in regularizing the coherent-state variables. Here, we shall introduce these ideas in the context of the multiconfigurational formula – the resulting CCS framework, where configurations are allowed to change reference state at any instant during propagation, will be referred to as 'extended'.[xi]

4.6.1 * Extended overlap

Suppose each Thouless configuration participating in the CCS wavefunction is defined with respect to a (possibly) distinct reference state. The first issue that arises concerns the overlap between any two such configurations.

In order to establish the extended formulas we employ the idea of a 'default' reference state, i.e. we presume there exists a set of single-particle operators, c and $c^\dagger$, in terms of which the operators corresponding to the i-th and j-th configurations can be written as

$$c_p^{(i)\dagger} = \sum_q c_q^\dagger \, Y_{qp}^{(i)}, \quad c_p^{(i)} = \sum_q X_{pq}^{(i)} \, c_q; \qquad c_p^\dagger = \sum_q c_q^{(i)\dagger} \, X_{qp}^{(i)}, \quad c_p = \sum_q Y_{pq}^{(i)} \, c_q^{(i)}; \tag{4.84a}$$

$$c_p^{(j)\dagger} = \sum_q c_q^\dagger \, Y_{qp}^{(j)}, \quad c_p^{(j)} = \sum_q X_{pq}^{(j)} \, c_q; \qquad c_p^\dagger = \sum_q c_q^{(j)\dagger} \, X_{qp}^{(j)}, \quad c_p = \sum_q Y_{pq}^{(j)} \, c_q^{(j)}; \tag{4.84b}$$

for $1 \leq i, j \leq m$. The transformation matrices are unitary and, as in §3.3, Y denotes the inverse of X,

$$Y^{(i)} = [X^{(i)}]^{-1} = X^{(i)\dagger}; \quad Y^{(j)} = [X^{(j)}]^{-1} = X^{(j)\dagger}. \tag{4.85}$$

We adopt the following convention: configurations defined in terms of the default set are labeled with the letter z, whereas modified configurations are labeled with the letter w; thus,

$$\langle z_i| \equiv \langle z_i; c|, \;\; |z_j\rangle \equiv |z_j; c\rangle; \quad \text{and} \quad \langle w_i| \equiv \langle w_i; c^{(i)}|, \;\; |w_j\rangle \equiv |w_j; c^{(j)}\rangle, \tag{4.86}$$

and likewise for non-normalized states – to alleviate the notation we omit the operator indication inside *kets* and *bras* from now on.

[xi] A similar scheme may be devised for the bosonic coherent states of Chapter 2, since the transformations involved are entirely analogous to the fermionic case. However, the flexibility brought by the extended framework is much more pertinent to the fermion problem – in order to avoid repetitive arguments, we only discuss the latter.

As we know from previous analysis (cf. §3.3), variables z and w are linked by the relations:

$$w_j = (X_{21}^{(j)} + X_{22}^{(j)} z_j)(X_{11}^{(j)} + X_{12}^{(j)} z_j)^{-1}; \tag{4.87a}$$
$$w_i^\dagger = (Y_{11}^{(i)} + z_i^\dagger Y_{21}^{(i)})^{-1}(Y_{12}^{(i)} + z_i^\dagger Y_{22}^{(i)}); \tag{4.87b}$$

whose inverse form is

$$z_j = (Y_{21}^{(j)} + Y_{22}^{(j)} w_j)(Y_{11}^{(j)} + Y_{12}^{(j)} w_j)^{-1}; \tag{4.88a}$$
$$z_i^\dagger = (X_{11}^{(i)} + w_i^\dagger X_{21}^{(i)})^{-1}(X_{12}^{(i)} + w_i^\dagger X_{22}^{(i)}). \tag{4.88b}$$

In particular, the non-normalized state vectors are connected by

$$|z_j\} = |w_j\}[\det(Y_{11}^{(j)} + Y_{12}^{(j)} w_j)]^{-1}; \tag{4.89a}$$
$$\{z_i| = [\det(X_{11}^{(i)} + w_i^\dagger X_{21}^{(i)})]^{-1}\{w_i|, \tag{4.89b}$$

whence we obtain the scalar product:

$$\{w_i|w_j\} = [\det(X_{11}^{(i)} + w_i^\dagger X_{21}^{(i)})][\det(I_N + z_i^\dagger z_j)][\det(Y_{11}^{(j)} + Y_{12}^{(j)} w_j)]. \tag{4.90}$$

In order to derive a sensible formula we must replace the z's by w's. Using (4.88) we find:

$$\begin{aligned} I_N + z_i^\dagger z_j &= I_N + (X_{11}^{(i)} + w_i^\dagger X_{21}^{(i)})^{-1}(X_{12}^{(i)} + w_i^\dagger X_{22}^{(i)})(Y_{21}^{(j)} + Y_{22}^{(j)} w_j)(Y_{11}^{(j)} + Y_{12}^{(j)} w_j)^{-1} \\ &= (X_{11}^{(i)} + w_i^\dagger X_{21}^{(i)})^{-1}(W_{11}^{(i,j)} + W_{12}^{(i,j)} w_j + w_i^\dagger W_{21}^{(i,j)} + w_i^\dagger W_{22}^{(i,j)} w_j)(Y_{11}^{(j)} + Y_{12}^{(j)} w_j)^{-1}. \end{aligned}$$

Above, a new matrix $W^{(i,j)}$ has been defined in terms of its occupied, virtual and mixed blocks – in full form it is simply the product of transformation matrices belonging to the configurations involved:

$$W^{(i,j)} \equiv X^{(i)} Y^{(j)}. \tag{4.91}$$

Substitution of the latter result into (4.90) leads to:

$$\{w_i|w_j\} = \det(W_{11}^{(i,j)} + W_{12}^{(i,j)} w_j + w_i^\dagger W_{21}^{(i,j)} + w_i^\dagger W_{22}^{(i,j)} w_j), \tag{4.92}$$

whose normalized version is the extended overlap we were seeking:

$$\langle w_i|w_j\rangle = \frac{\det(W_{11}^{(i,j)} + W_{12}^{(i,j)} w_j + w_i^\dagger W_{21}^{(i,j)} + w_i^\dagger W_{22}^{(i,j)} w_j)}{\sqrt{\det(I_N + w_i^\dagger w_i)\det(I_N + w_j^\dagger w_j)}}. \tag{4.93}$$

This derivation provides an idea of the kind of method we intend to formulate.

4.6.2 * Extended configurations

Our goal is to write the CCS wavefunction in terms of extended configurations,

$$|\psi\rangle = \sum_j |z_j\rangle D(z_j) e^{\frac{i}{\hbar}S(z_j)} = \sum_j |w_j\rangle \tilde{D}(w_j) e^{\frac{i}{\hbar}\tilde{S}(w_j)}. \tag{4.94}$$

The next issue to be addressed is how the change of variables $z \to w$ affects the action and amplitude of each basis element. Let us begin with the former. In what follows, transformed quantities will be indicated with a tilde, e.g. $\tilde{S}_j = \tilde{S}(w_j)$ and $\tilde{D}_j = \tilde{D}(w_j)$.

We know from §3.3 that holomorphic transformations of the coherent-state variable such as those exemplified in Eqs. (4.87) and (4.88) result in a relative phase between the corresponding normalized coherent state vectors [cf. Eq. (3.100)],

$$|z\rangle = |w\rangle e^{-i\varphi}, \quad \varphi = \arg[\det(Y_{11} + Y_{12}w)], \tag{4.95}$$

where matrix Y is any of the $Y^{(j)}$ above – for the purposes of this subsection we may focus in a single configuration, omitting the basis set-label.

In a time-dependent scenario, the relative phase leads to an accumulated phase difference between action integrals computed along orbits $z(t)$ and $w(t)$; this phase difference can be found by considering the Lagrangians of each description, which are connected by

$$\begin{aligned} L(z) &= \frac{i\hbar}{2}\Big[\langle z|\dot{z}\rangle - \langle \dot{z}|z\rangle\Big] - \langle z|\hat{H}|z\rangle \\ &= \frac{i\hbar}{2}\Big[\langle w|\dot{w}\rangle - \langle \dot{w}|w\rangle\Big] - \langle w|\hat{H}|w\rangle + \hbar\,\dot{\varphi} = \tilde{L}(w) + \hbar\,\dot{\varphi}. \end{aligned} \tag{4.96}$$

Thus, integrating from t_0 to t, we obtain:

$$S(z;t,t_0) = \tilde{S}(w;t,t_0) + \hbar\varphi(w;t) - \hbar\varphi(w;t_0). \tag{4.97}$$

Notice we have specified the initial and final time instants.

Taking into account both effects – the relative phase between state vectors and accumulated action phase – we find that, at time $t > t_0$, default and extended configurations are related as follows:

$$|z(t)\rangle e^{\frac{i}{\hbar}S(z;t,t_0)} = |w(t)\rangle e^{-i\varphi(w;t)} e^{\frac{i}{\hbar}\tilde{S}(w;t,t_0)} e^{i(\varphi(w;t)-\varphi(w;t_0))} = |w(t)\rangle e^{\frac{i}{\hbar}S(w;t,t_0)} e^{-i\varphi(w;t_0)}. \tag{4.98}$$

We see that the form of the configuration is not preserved, due to the factor $e^{-i\varphi(w;t_0)}$.

At first sight, this would seen to hinder the extended method inviable, since in the CCS wavefunction configurations interfere with one another, meaning that their relative phases are crucial. In other words, transformations of coherent-state variables midway through propagation are only acceptable if the total phase of each configuration is pre-

served. (Notice that this is not an issue in a mean-field description – i.e. where the total wavefunction is represented by a single Thouless determinant – because, in that case, the coherent-state's phase is just an immaterial global phase.)

As it turns out, however, this problem can be easily solved. Consider, from a computational perspective, the following situation. An initial configuration $|z(t_0)\rangle$ is propagated in time. It acquires a phase $S(z;t,t_0)$. This phase is accumulated into a variable $\theta(t)$. At some instant $t_1 > t_0$ the configuration's reference state requires changing and its underlying orbitals are thus subjected to an unitary transformation X. Integration is halted and the new, regularized variables w are obtained from z according to the usual prescription:

$$w = (X_{21} + X_{22}z)(X_{11} + X_{12}z)^{-1} \quad (\text{at } t = t_1). \tag{4.99}$$

At the same time, we cause a discontinuity in the cumulative variable θ, setting:

$$\theta(t_1) \to \theta(t_1) - \hbar\varphi(w;t_1) \quad (\text{at } t = t_1), \tag{4.100}$$

where, in terms of matrix X, the discontinuity angle is $\varphi(w;t_1) = \arg[\det(X_{11}^\dagger + X_{21}^\dagger w(t_1))]$. Integration is then resumed, and $\theta(t)$ now accumulates the action $\tilde{S}(w;t,t_1)$, computed with the new variables w (the equation of motion for w has precisely the same form as that for z, provided the Hamiltonian is transformed as well – see below for more details).

The net result is this: at time $t > t_1$ the accumulated phase is

$$\theta(t) = \tilde{S}(w;t,t_1) + S(z;t_1,t_0) - \hbar\varphi(w;t_1) \quad (\text{at } t > t_1). \tag{4.101}$$

Therefore, after regularization, the state is represented as:

$$|w(t)\rangle e^{\frac{i}{\hbar}\theta(t)} = |z(t)\rangle e^{i\varphi(w;t)}\ e^{\frac{i}{\hbar}(\tilde{S}(w;t,t_1)+S(z;t_1,t_0)-\hbar\varphi(w;t_1))}. \tag{4.102}$$

But, from (4.97) (replacing $t_0 \to t_1$ in that formula),

$$\tilde{S}(w;t,t_1) = S(z;t,t_1) - \hbar\varphi(w;t) + \hbar\varphi(w;t_1). \tag{4.103}$$

Putting this in Eq. (4.102), and recalling the cumulative property of the action integral: $S(z;t,t_0) = S(z;t,t_1) + S(z;t_1,t_0)$, we get:

$$|w(t)\rangle e^{\frac{i}{\hbar}\theta(t)} = |z(t)\rangle e^{\frac{i}{\hbar}S(z;t,t_0)}. \tag{4.104}$$

In other words, provided the '$\theta(t)$-discontinuity' protocol of Eq. (4.100) is enforced, the same configuration will be represented by the new variables, *including its phase*, as if it were computed with the default reference state all along. Clearly, this works just the same if new transformations take place at future instants t_2, t_3, etc., and even if configurations

start off with different reference states.

In short, the fact that a cumulative phase variable $\theta(t)$ is used, which is always computed from the Lagrangian that is currently appropriate for the timespan between transformations, and the fact that a phase discontinuity is introduced by hand at each regularization event – these procedures compensate both the state vector's phase shift induced by the change of variables and the associated action difference. Since in practice we compute $\theta(t)$ rather than $S(t)$, the extended method's configurations will be written as $|w(t)\rangle e^{\frac{i}{\hbar}\theta(t)}$ for the remainder of this section.

4.6.3 * CCS amplitudes in the extended framework

An important conclusion can be immediately drawn from the developments discussed above: amplitudes C and D are not affected by the transformation of coherent-state variables. This is evident since Eq. (4.104) implies:

$$\tilde{C}(w_j) = e^{-\frac{i}{\hbar}\theta_j}\langle w_j|\psi\rangle = e^{-\frac{i}{\hbar}S(z_j)}\langle z_j|\psi\rangle = C(z_j). \tag{4.105}$$

Likewise, for the phased overlap we obtain:

$$\omega_{ij} = e^{-\frac{i}{\hbar}S(z_i)}\langle z_i|z_j\rangle e^{\frac{i}{\hbar}S(z_j)} = e^{-\frac{i}{\hbar}\theta_i}\langle w_i|w_j\rangle e^{\frac{i}{\hbar}\theta_j} = \tilde{\omega}_{ij}. \tag{4.106}$$

These two results combined imply the invariance of D, since

$$\tilde{C}(w_j) = \sum_j \tilde{\omega}_{ij}\tilde{D}(w_j) = \sum_j \omega_{ij}\tilde{D}(w_j) = C(z_j) \quad \Rightarrow \quad \tilde{D}(w_j) = D(z_j). \tag{4.107}$$

Therefore, the CCS wavefunction may be written in terms of extended configurations as

$$|\psi\rangle = \sum_j |z_j\rangle D(z_j) e^{\frac{i}{\hbar}S(z_j)} = \sum_j |w_j\rangle \tilde{D}(w_j) e^{\frac{i}{\hbar}\theta_j}, \tag{4.108}$$

and this equality actually holds term by term. We have thus established the viability of the extended method.

Check. If amplitudes are unmodified in the extended framework, then this can only be true if the coupled equation which they obey is also unaffected by the fact that each configuration is possibly defined in terms of different reference states. In order to confirm this equivalence we need to examine the CCS coupling. Using the raw expression (4.6)

we find that the coupling transforms as follows:

$$\begin{aligned}\Delta_{ij} &= \frac{\langle z_i|\hat{H}|z_j\rangle}{\langle z_i|z_j\rangle} + i\hbar\frac{\langle \dot{z}_i|z_j\rangle}{\langle z_i|z_j\rangle} + L(z_i) \\ &= \frac{e^{i\varphi_i}\langle w_i|\hat{H}|w_j\rangle e^{-i\varphi_j}}{e^{i\varphi_i}\langle w_i|w_j\rangle e^{-i\varphi_j}} + i\hbar\left[\frac{e^{i\varphi_i}\langle \dot{w}_i|w_j\rangle e^{-i\varphi_j}}{e^{i\varphi_i}\langle w_i|w_j\rangle e^{-i\varphi_j}} + i\dot{\varphi}(w)\right] + [\tilde{L}(w_i) + \hbar\dot{\varphi}(w_i)] \\ &= \frac{\langle w_i|\hat{H}|w_j\rangle}{\langle w_i|w_j\rangle} + i\hbar\frac{\langle \dot{w}_k|w_j\rangle}{\langle w_k|w_j\rangle} + \tilde{L}(w_i) = \tilde{\Delta}_{ij}. \end{aligned} \tag{4.109}$$

Then, since $\omega_{ij} = \tilde{\omega}_{ij}$,

$$i\hbar\,\dot{C}_i = \sum_j(\omega_{ij}\Delta_{ij})D_j = \sum_j(\tilde{\omega}_{ij}\tilde{\Delta}_{ij})D_j, \tag{4.110}$$

confirming the invariance of the equation of motion.

4.6.4 * Matrix elements

Even though Eq. (4.109) tells us that the extended CCS coupling assumes the same values as in the default formulation – despite the fact that the fermionic configurations involved might be defined in terms of distinct single-particle orbitals –, the actual expression for matrix elements is different in the latter case. This is because the calculation of non-diagonal quantities, such as $\tilde{E}(w_i^*, w_j)$, is now complicated by the fact that the extended overlap involves the matrix $W^{(i,j)}$ of Eq. (4.91). In particular, the simplified expressions for Δ_{ij} found in §4.3 are *not* valid in the extended framework. Thus, if a workable formula is to be developed, one must start again from the bare definition (4.18) – this subsection is dedicated to that purpose and some useful results are derived along the way.

Let us first consider the extended, analytically-continued one-density matrix,

$$\tilde{\Gamma}(w_i^*, w_j)_{pq} = \frac{\{w_i|{c_p^{(i)}}^\dagger c_q^{(j)}|w_j\}}{\{w_i|w_j\}}. \tag{4.111}$$

An expression for its elements can be obtained by the procedure employed in the default formulation, depicted in Appendix C. That derivation still holds for the present case, provided one replaces the quantity $\varrho(z_i^*, z_j) = I_N + z_i^\dagger z_j$, used in those calculations, by its extended counterpart:

$$\tilde{\varrho}(w_i^*, w_j) = W_{11}^{(i,j)} + W_{12}^{(i,j)}w_j + w_i^\dagger W_{21}^{(i,j)} + w_i^\dagger W_{22}^{(i,j)}w_j = \begin{bmatrix} I_N & w_i^\dagger \end{bmatrix} W^{(i,j)} \begin{bmatrix} I_N \\ w_j \end{bmatrix}, \tag{4.112}$$

which allows the non-normalized extended overlap to be expressed as:

$$\{w_i|w_j\} = \det\tilde{\varrho}(w_i^*, w_j). \tag{4.113}$$

Then, the same steps leading to the expression of the default one-density yield:

$$\tilde{\Gamma}(w_i^*, w_j) = \frac{\{w_i|{c_p^{(i)}}^\dagger c_q^{(j)}|w_j\}}{\{w_i|w_j\}} = \begin{bmatrix} I_N \\ w_j \end{bmatrix} [\tilde{\varrho}(w_i^*, w_j)]^{-1} \begin{bmatrix} I_N & w_i^\dagger \end{bmatrix}. \tag{4.114}$$

These same considerations apply to two-body matrix elements, which are thus given by the general expression:

$$\frac{\{w_i|{c_p^{(i)}}^\dagger {c_r^{(i)}}^\dagger c_s^{(j)} c_q^{(j)}|w_j\}}{\{w_i|w_j\}} = \tilde{\Gamma}_{qp}(w_i^*, w_j)\tilde{\Gamma}_{sr}(w_i^*, w_j) - \tilde{\Gamma}_{qr}(w_i^*, w_j)\tilde{\Gamma}_{sp}(w_i^*, w_j). \tag{4.115}$$

The above formulas permit us to write extended versions for coherent-state expectation values of one- and two-body operators.

Let us consider the one-body operator $\hat{A}$ which, in the default representation, reads:

$$\hat{A} = \sum_{p'q'} A_{p'q'}\, c_{p'}^\dagger c_{q'}, \quad A_{p'q'} = \langle \phi_p|\hat{A}|\phi_q\rangle. \tag{4.116}$$

Using Eqs. (4.84) we obtain:

$$\hat{A} = \sum_{pq} \left[\sum_{p'q'} X_{pp'}^{(i)}\, A_{p'q'}\, Y_{q'q}^{(j)} \right] {c_p^{(i)}}^\dagger c_q^{(j)} = \sum_{pq} \tilde{A}_{pq}^{(i,j)}\, {c_p^{(i)}}^\dagger c_q^{(j)}, \tag{4.117}$$

where the extended form of the one-body integral is:

$$\tilde{A}_{pq}^{(i,j)} = \langle \phi_p^{(i)}|\hat{A}|\phi_q^{(j)}\rangle = \sum_{p'q'} X_{pp'}^{(i)}\, \langle \phi_{p'}|\hat{A}|\phi_{q'}\rangle\, Y_{q'q}^{(j)}. \tag{4.118}$$

Notice that these integrals depend on indexes i, j (because of the transformation matrices attached to each configuration) but not on the labels w_i^*, w_j. The coherent-state expectation value is then immediately found with the help of (4.114):

$$\tilde{A}(w_i^*, w_j) = \frac{\{w_i|\hat{A}|w_j\}}{\{w_i|w_j\}} = \sum_{pq} \tilde{A}_{pq}^{(i,j)}\, \tilde{\Gamma}(w_i^*, w_j)_{qp}. \tag{4.119}$$

Meanwhile, the two-body term will transform according to

$$\hat{B} = \sum_{p,q,r,s} B_{pr\cdot qs}\, c_p^\dagger c_r^\dagger c_s c_q = \sum_{p,q,r,s} \tilde{B}_{pr\cdot qs}^{(i,j)}\, {c_p^{(i)}}^\dagger {c_r^{(i)}}^\dagger c_s^{(j)} c_q^{(j)}, \tag{4.120}$$

where the extended two-body integrals are:

$$\tilde{B}_{pr\cdot qs}^{(i,j)} = \sum_{p'q'r's'} X_{pp'}^{(i)} X_{rr'}^{(i)}\, B_{p'r'\cdot q's'}\, Y_{q'q}^{(j)} Y_{s's}^{(j)}. \tag{4.121}$$

Again, these depend on configuration indexes, but not on the variables w_i and w_j. Using

Eq. (4.115) we obtain:

$$\tilde{B}(w_i^*, w_j) = \frac{\{w_i|\hat{B}|w_j\}}{\{w_i|w_j\}} = \sum_{pqrs} \tilde{B}^{(i,j)}_{pr\cdot qs}\Big[\tilde{\Gamma}_{qp}(w_i^*, w_j)\tilde{\Gamma}_{sr}(w_i^*, w_j) - \tilde{\Gamma}_{qr}(w_i^*, w_j)\tilde{\Gamma}_{sp}(w_i^*, w_j)\Big]$$
$$= \sum_{pqrs}\Big(\tilde{B}^{(i,j)}_{pr\cdot qs} - \tilde{B}^{(i,j)}_{pr\cdot sq}\Big)\tilde{\Gamma}_{qp}(w_i^*, w_j)\tilde{\Gamma}_{sr}(w_i^*, w_j). \tag{4.122}$$

Thus, analytically-continued energy functions $\tilde{E}(w_i^*, w_j)$ can be computed as before, provided the properly transformed density and extended one- and two-body integrals are employed,

$$\tilde{E}(w_i^*, w_j) = \sum_{pq} \tilde{h}^{(i,j)}_{pq}\, \tilde{\Gamma}(w_i^*, w_j)_{qp} + \sum_{pqrs}\Big(\tilde{V}^{(i,j)}_{pr\cdot qs} - \tilde{V}^{(i,j)}_{pr\cdot sq}\Big)\tilde{\Gamma}_{qp}(w_i^*, w_j)\tilde{\Gamma}_{sr}(w_i^*, w_j). \tag{4.123}$$

The other ingredient required for expressing the CCS coupling, as defined by Eq. (4.18), is the extended Kähler potential,

$$\tilde{f}(w_i^*, w_j) = \log[\det \tilde{\varrho}(w_i^*, w_j)], \tag{4.124}$$

or, more specifically, its gradients with respect to w_i^* and w_j. Despite the extra terms introduced by the matrix $W^{(i,j)}$ (implicit in the quantity $\tilde{\varrho}(w_i^*, w_j)$) the calculation is straightforward, leading to:

$$\frac{\partial \tilde{f}(w_i^*, w_j)}{\partial w_{j\cdot\mu\alpha}} = [\tilde{\varrho}(w_i^*, w_j)^{-1}(W_{12}^{(i,j)} + w_i^\dagger W_{22}^{(i,j)})]_{\alpha\mu}, \tag{4.125a}$$
$$\frac{\partial \tilde{f}(w_i^*, w_j)}{\partial w^*_{i\cdot\mu\alpha}} = [(W_{21}^{(i,j)} + W_{22}^{(i,j)} w_j)\tilde{\varrho}(w_i^*, w_j)^{-1}]_{\alpha\mu}. \tag{4.125b}$$

Therefore, with the aid of Eqs. (4.123) and (4.125), we find a workable formula for the extended CCS coupling:

$$\tilde{\Delta}_{ij} = \tilde{E}(w_i^*, w_j) - E(w_i^*, w_i) - i\hbar\,\mathrm{tr}[\, w_i\,(I_N + w_i^\dagger w_i)\,\dot{w}_i^\dagger\,]$$
$$+ i\hbar\,\mathrm{tr}[\,(W_{21}^{(i,j)} + W_{22}^{(i,j)} w_j)\,(W_{11}^{(i,j)} + W_{12}^{(i,j)} w_j + w_i^\dagger W_{21}^{(i,j)} + w_i^\dagger W_{22}^{(i,j)} w_j)^{-1}\,\dot{w}_i^\dagger\,], \tag{4.126}$$

where we have substituted the explicit form of $\tilde{\varrho}(w_i^*, w_j)$, Eq. (4.112). Notice, however, that not all dependence on the transformation matrices is explicit, for $\tilde{E}(w_i^*, w_j)$ is a function of the extended one-density, which depends on $W^{(i,j)}$. The manipulations that earlier led to reduced forms of the coupling in the default formulation become quite cumbersome in the present case and we do not pursue further simplification of the result (4.126).

Lastly, we return to a point raised at §3.3 and left to be addressed later. It concerns the transformation of the Hamiltonian (and possibly other observables) that must accompany

the change of variables $w \leftarrow z$,

$$w = (X_{21} + X_{22}z)(X_{11} + X_{12}z)^{-1},$$

of individual basis elements. The required formulas can be obtained at once from the general analytically-continued results given in this section by setting $i = j$ (therefore rendering the configuration subscript unnecessary). Thus, the transformed energy function is:

$$\tilde{E}(w^*, w) = \sum_{pq} \tilde{h}_{pq}\, \tilde{\Gamma}_{qp} + \sum_{pqrs} \Big(\tilde{V}_{pr\cdot qs} - \tilde{V}_{pr\cdot sq}\Big)\tilde{\Gamma}_{qp}\tilde{\Gamma}_{sr}, \tag{4.127}$$

with one- and two-body integrals given by:

$$\tilde{h}_{pq} = \sum_{p'q'} X_{pp'}\, h_{p'q'}\, Y_{q'q} \quad \text{and} \quad \tilde{V}_{pr\cdot qs} = \sum_{p'q'r's'} X_{pp'} X_{rr'}\, V_{p'r'\cdot q's'}\, Y_{q'q} Y_{s's}. \tag{4.128}$$

Since, for diagonal elements $W = I_K$, the transformed one-density is:

$$\tilde{\Gamma}(w^*, w) = \begin{bmatrix} I_N \\ w \end{bmatrix} \begin{bmatrix} I_N & w^\dagger \end{bmatrix} = X \begin{bmatrix} I_N \\ z \end{bmatrix} \begin{bmatrix} I_N & z^\dagger \end{bmatrix} Y = X\Gamma(z^*, z)Y. \tag{4.129}$$

The second half of this equation can be demonstrated without difficulty using the analytic connections compiled at the end of §3.3. Notice that the last equality shows that the new density $\tilde{\Gamma}(w^*, w)$ can be obtained directly from the old one $\Gamma(z^*, z)$ by a similarity transform, without need of operating with the basic Thouless parameters, z.

As one would expected, the mean-fields transform as one-body operators; this can be straightforwardly deduced from the relations given above:

$$\begin{aligned} \tilde{v}(\tilde{\Gamma})_{pq} &= \sum_{sr} (\tilde{V}_{pr\cdot qs} - \tilde{V}_{pr\cdot sq})\tilde{\Gamma}_{sr} \\ &= \sum_{p'q'} X_{pp'} \Big[\sum_{r's'} (V_{p'r'\cdot q's'} - V_{p'r'\cdot s'q'}) \Big(\sum_{sr} Y_{s's} \tilde{\Gamma}_{sr} X_{rr'} \Big) \Big] Y_{q'q} = \Big(X v(\Gamma) Y \Big)_{pq}, \end{aligned} \tag{4.130}$$

which means that the Fock matrix as a whole transforms according to the recipe:

$$\tilde{F}(\tilde{\Gamma}) = \tilde{h} + \tilde{v}(\tilde{\Gamma}) = X\Big(h + v(\Gamma) \Big)Y = X\, F(\Gamma)\, Y. \tag{4.131}$$

The transformed Fock matrix, by its turn, enters in the equation of motion obeyed by ω,

$$i\hbar\, \dot{w} = \begin{bmatrix} -w & I_M \end{bmatrix} \tilde{F} \begin{bmatrix} I_N \\ w \end{bmatrix}, \tag{4.132}$$

which has precisely the same structure as that for z variables, Eq. (3.80), for the 'machinery' of the time-dependent variational principle is insensitive to the choice of reference state. (The invariance of the mean-field equation of motion can be directly demonstrated

by effecting the $z \leftarrow w$ change of variables, although this is complicated by the time-derivative $\dot{z}$, which must be written in terms of $\dot{w}$ an w). Finally, the same conclusion holds for the action phase, integrated from

$$\dot{S}(w) = -\mathrm{tr}(\tilde{F}_{11}) - \tfrac{1}{2}\mathrm{tr}(\tilde{F}_{12}w + w^{\dagger}\tilde{F}_{21}) + \tfrac{1}{2}\mathrm{tr}(\tilde{v}\tilde{\Gamma}), \tag{4.133}$$

and whose value should be accumulated into a variable $\theta(t)$, as explained earlier. This completes the list of ingredients required for implementation of extended CCS method.

Chapter 5

Applications in test-systems

Overview. The dynamics of individual coherent states as governed by Hubbard-like Hamiltonians is examined. After this preliminary discussion, we proceed to investigate the capability of the multiconfigurational approach developed in Chapter 4. This is done by considering two model problems: first, a system of spinless bosons trapped in a triple-well potential and interacting through contact forces; second, a system of electrons confined to a one-dimensional circular chain of atoms where they experience tight-binding hopping and on-site repulsion, and are further subjected to an external magnetic field. Both problems are studied for various sets of parameter values and general conclusions concerning the effectiveness of the proposed methodology are drawn.

5.1 Mean-field dynamics with Hubbard-like Hamiltonians

In Chapters 2 and 3 we have considered – from a coherent-state perspective – the dynamics of many-particle systems as governed by prototype Hamiltonians containing one- and two-body terms. A wide range of problems, though, can be described by a more simplistic class of Hamiltonians, having the following parametrization:

$$\hat{H} = \sum_{p,q=1}^{K} h_{pq}\, a_p^\dagger a_q + \tfrac{1}{2} \sum_{p,q=1}^{K} u_{pq}\, a_p^\dagger a_q^\dagger a_q a_p, \tag{5.1}$$

i.e. which exhibit a diagonal interaction term. In the above equation [and also, below, at Eq. (5.3)] a and $a^\dagger$ stand for either boson or fermion operators whose associated single-particle basis states are $|\xi_p\rangle = a_p^\dagger|0\rangle$, $1 \leq p \leq K$. If $\hat{H}$ is hermitian then the $K \times K$ matrices h and u must satisfy the requirements:

$$\begin{cases} h_{pq} = h_{qp}^* \\ u_{pq} = u_{qp}^* = u_{qp} = u_{pq}^* \quad (\text{also } u_{pp} = 0 \text{ for fermions}). \end{cases} \tag{5.2}$$

Thus h is complex and hermitian; u is real and symmetric. In the fermionic case, the diagonal elements of u play no role in the dynamics (since the product of creation and annihilation operators gives zero) and we may safely put $u_{pp} = 0$.

Hamiltonians with the particular structure displayed at Eq. (5.1) are interesting because the mean-fields of the coherent-state description are very simple to compute, owing to the fact that costly manipulations of two-body integrals are avoided.

However, in most situations, the single-particle states $|\xi\rangle$ that bring $\hat{H}$ to the form of Eq. (5.1) are very specific; and it is often the case that the coherent-state dynamics should be carried out with a different underlying set, one which conforms to a physically motivated choice of reference state rather than a mathematically convenient one. This precise situation will be encountered later in this chapter, when we apply the generalized CCS methodology to a fermionic model-system; we shall postpone until there this discussion concerning the single-particle basis.

Before proceeding to detailed applications, let us work out the mean-field equations of motion for a *Hubbard-like Hamiltonian* having the special form of Eq. (5.1) – we thus seek specific expressions for the two-body part of the energy function, hereby denoted E_2, according to the following definitions,

$$E = E_1 + E_2, \quad E_1 = \sum_{pq} h_{pq} \langle z | a_p^\dagger a_q | z \rangle, \quad E_2 = \tfrac{1}{2} \sum_{pq} u_{pq} \langle z | \, a_p^\dagger a_q^\dagger a_q a_p \, | z \rangle, \tag{5.3}$$

and also for the CCS coupling Δ_{ij} [cf. Eqs. (4.61) and (4.76)]. This is done next in two short subsections.

5.1.1 Bosonic case

We first consider the Hubbard two-body interaction term for bosons. It is a peculiarity of the bosonic description that the coherent-state expectation value can be arranged in two different manners; denoting the bosonic operators as $b^\dagger$ and b we have:

$$E_2 = \tfrac{1}{2} \sum_{pq} u_{pq} \langle z | \, b_p^\dagger b_q^\dagger b_q b_p \, | z \rangle = \begin{cases} \frac{1}{2} N(N-1) \sum_{pq} u_{pq} \, \Gamma_{pp} \Gamma_{qq} \\ \frac{1}{2} N(N-1) \sum_{pq} u_{pq} \, \Gamma_{pq} \Gamma_{qp} \end{cases} . \tag{5.4}$$

These are equivalent ways of writing E_2 since $\Gamma_{pp}\Gamma_{qq} = \Gamma_{pq}\Gamma_{qp}$, as one easily verifies by inspecting the definition of Γ [cf. Eq. (2.48)]. Consequently there are two different – but physically indistinguishable – ways of expressing the mean-fields:

$$E_2 = \tfrac{1}{2} N \sum_{pq} v_{pq} \Gamma_{qp} \quad \text{with:} \quad v_{pq} = \begin{cases} (N-1) \, (\sum_s u_{ps} \, \Gamma_{ss}) \, \delta_{pq} & \text{(A)} \\ (N-1) \, u_{pq} \, \Gamma_{pq} & \text{(B)} \end{cases} . \tag{5.5}$$

The form (A) is appealing because it is diagonal, whereas (B) is interesting since it is straightforward to compute; both lead to the same equation of motion:

$$i\hbar\,\dot{z}_\mu = h_{\mu 0} + \sum_\nu h_{\mu\nu} z_\nu - \Big(h_{00} + \sum_\nu h_{0\nu} z_\nu\Big) z_\mu \\ + \tfrac{1}{2}(u_{\mu\mu} - u_{00}) z_\mu + (1+|z|^2)^{-1}(N-1)\Big[(u_{\mu 0} - u_{00}) + \sum_\nu (u_{\mu\nu} - u_{0\nu}) z_\nu^* z_\nu\Big]\, z_\mu. \quad (5.6)$$

Finally, combining Eq. (4.61) with the mean-fields of Eq. (5.5) we arrive at the bosonic CCS coupling for the Hubbard model:

$$\Delta_{ij} = \begin{cases} \frac{1}{2}N(N-1)\sum_{pq} u_{pq}(\Gamma^{ij}_{pp} - \Gamma^{ii}_{pp})(\Gamma^{ij}_{qq} - \Gamma^{ii}_{qq}) & \text{(A)} \\ \frac{1}{2}N(N-1)\sum_{pq} u_{pq}(\Gamma^{ij}_{pq} - \Gamma^{ii}_{pq})(\Gamma^{ij}_{qp} - \Gamma^{ii}_{qp}) & \text{(B)} \end{cases}. \quad (5.7)$$

We shall adopt the (A) version, for it is more convenient to work solely with the diagonal elements of the analytically-continued density matrix.

5.1.2 Fermionic case

Let us now consider the Hubbard interaction for fermions. In this case there is no ambiguity as how to write the coherent-state matrix element E_2 (the ambiguity is lifted by the exchange energy, which was absent in the bosonic problem):

$$E_2 = \tfrac{1}{2}\sum_{pq} u_{pq} \langle z|\, c_p^\dagger c_q^\dagger c_q c_p \,|z\rangle = \tfrac{1}{2}\sum_{pq} u_{pq}\,(\Gamma_{pp}\Gamma_{qq} - \Gamma_{pq}\Gamma_{qp}) = \tfrac{1}{2}\sum_{pq} v_{pq}\Gamma_{qp}. \quad (5.8)$$

In the above formula, the mean field is:

$$v_{pq} = (\textstyle\sum_s u_{ps}\Gamma_{ss})\delta_{pq} - u_{pq}\Gamma_{pq} = \begin{cases} \sum_{s\neq p} u_{ps}\Gamma_{ss} & \text{if } \; p = q \\ -u_{pq}\Gamma_{pq} & \text{if } \; p \neq q \end{cases}. \quad (5.9)$$

Note that diagonal entries u_{pp}, even if non-zero, end up not contributing to the mean field – as we pointed out earlier, such terms cannot play a role in the dynamics. Indeed, we may write the two-body part of the Hamiltonian as:

$$\hat{H}_2 = \tfrac{1}{2}\sum_{pq} u_{pq}\, c_p^\dagger c_q^\dagger c_q c_p = \tfrac{1}{2}\sum_{pq} u_{pq}\,\hat{n}_p\hat{n}_q \quad (\text{if } u_{pp} = 0). \quad (5.10)$$

This is a more familiar form, associated with standard fermionic Hubbard models.

Because the Thouless one-density matrix is considerably more complicated than its bosonic counterpart, the mean-field equation of motion for the Hubbard-like Hamiltonian looks no more simple than Eq. (3.80), which was previously derived from the more general $\hat{H}$ studied in Chapter 3. Since it gives no new insights we shall not present the particularized form of the equation.

Finally, combining Eq. (4.76) with the mean-field of Eq. (5.9), one finds the fermionic multiconfigurational coupling for a Hubbard-like Hamiltonian is

$$\Delta_{ij} = \tfrac{1}{2}\sum_{pq} u_{pq}\Big[(\Gamma^{ij}_{pp} - \Gamma^{ii}_{pp})(\Gamma^{ij}_{qq} - \Gamma^{ii}_{qq}) - (\Gamma^{ij}_{pq} - \Gamma^{ii}_{pq})(\Gamma^{ij}_{qp} - \Gamma^{ii}_{qp})\Big]. \tag{5.11}$$

As we shall see later the above expression can be recast in an even more simple form in the case of spin-$\frac{1}{2}$ fermions.

5.2 On the purpose of the results compiled in this work

In what follows we present a compilation of results obtained with the generalized CCS approach for two model systems – the first deals with bosons in a trapping potential, the second with electrons in a one-dimensional ring of atoms.

It is important to make it clear that the results reported here are only meant to exemplify general trends and overall behavior of the proposed methodology. In absolutely no way the content below is to be understood as a throughout investigation of any of the aforementioned model problems – that would require a systematic numerical study and careful analysis of the data; that is to say: it would require another thesis.

The main objective of this work, we emphasize, is the development and validation of the generalized CCS technique as such. From this perspective, the simple application examples that follow have more of an illustrative character and they should be regarded as preliminary tests of the trajectory-guided propagation scheme put forward here.

And hence the reason we opted for *simple* models in the first place: for, being as such, they fulfill a threefold purpose: (i) crude as they are, they provide a context wherein technical aspects of the CCS strategy can be probed; (ii) they avoid eventual complications inherent to more sophisticated models, whose only effect here would be to obscure the discussion; and finally, (iii) their simplicity allows for exact quantum solutions against which we may compare our CCS results. This does not mean, however, that the chosen models are 'trivial' – as a matter of fact, they give rise to rich quantum dynamics whose accurate description proves to be quite challenging.

5.3 Bose-Einstein condensate in a symmetric triple-well

5.3.1 Three-mode approximation

Let us consider a simplified model describing an N-particle Bose-Einstein condensate trapped in a symmetric triple-well potential, where individual bosons are assumed to interact by contact forces – i.e. the interaction energy has the form $U(\mathbf{x},\mathbf{x}') \propto \delta(\mathbf{x}-\mathbf{x}')$. The main ideas involved are as follows: the triple-well trapping potential, under suitable conditions, can be approximated by an harmonic expansion around each of its three

(symmetrically located) minima. The three-fold degenerate fundamental states of this approximated problem can be determined without difficulty. It is then assumed that the dynamical regime is such that the energy eigenspace spanned by these three local modes is sufficiently isolated from the rest of the single-particle spectrum, so that at low temperatures they alone provide an adequate description of the system. For more details on the derivation and particularities of this model, see Refs. [66;67].

Let a_1, a_2 and a_3 denote the annihilation operators associated with the aforementioned fundamental single-particle modes, related to the locally approximated wells. In terms of these bosonic operators, the 'three-mode approximation'[67] to the Hamiltonian is (units are such that $\hbar = 1$):

$$\hat{H} = \Omega \sum_{1 \leq i \neq j \leq 3} a_i^\dagger a_j + \frac{\chi}{N-1} \sum_{i=1}^{3} \hat{n}_i(\hat{n}_i - 1), \quad \hat{n}_i = a_i^\dagger a_i, \tag{5.12}$$

where Ω is the *tunneling rate* between adjacent wells, and χ is the *collision parameter*, that controls the strength of two-body interactions within the same well.[i] Owing to particle number conservation, this system is suitably described in terms of SU(3) bosonic coherent states $|z\rangle = |z_1, z_2\rangle$, which represent a particular case of the coherent states discussed at Chapter 2.

5.3.2 SU(3) bosonic coherent-state description

In the coherent-state description we must choose one of the three modes to be macroscopically occupied in the reference state $|\Phi_0\rangle$. Since the triple-well is symmetric all choices are equivalent; we take mode a_3 as the reference mode and adapt our notation accordingly:

$$(b_1, b_2, b_0) = (a_1, a_2, a_3). \tag{5.13}$$

Thus the reference state is:

$$|\Phi_0\rangle = \frac{(b_0^\dagger)^N}{\sqrt{N!}}|0\rangle. \tag{5.14}$$

Notice that $|\Phi_0\rangle$ is *not* a non-interacting groundstate. On the contrary, it is an stationary state of the interacting part of the Hamiltonian, with energy $E(\Phi_0) = N\chi$.

With the new labeling of modes, the Hamiltonian of Eq. (5.12) reads

$$\hat{H} = \Omega \sum_{0 \leq p \neq q \leq 2} b_p^\dagger b_q + \frac{\chi}{N-1} \sum_{p=0}^{2} b_p^\dagger b_p^\dagger b_p b_p. \tag{5.15}$$

[i] We note that in the triple-well model, the energy difference between the groundstate and doubly degenerate excited eingenstates of the non-interacting Hamiltonian is $|3\Omega|$ – within the three-mode approximation these stationary states span the same eigenspace as the local modes associated with operators a_1, a_2 and a_3.[67] Also, cross-collision terms, which arise from the interaction between bosons in different wells, are neglected in (5.12).

Comparing with (5.1) we identify the basic Hubbard matrices:

$$h = \Omega \begin{bmatrix} 0 & 1 & 1 \\ 1 & 0 & 1 \\ 1 & 1 & 0 \end{bmatrix}, \quad u = \frac{2\chi}{N-1} \begin{bmatrix} 1 & 0 & 0 \\ 0 & 1 & 0 \\ 0 & 0 & 1 \end{bmatrix}. \tag{5.16}$$

In this case u is diagonal and the ambiguity in the definition of mean-fields, discussed at §5.1.1, does not arise – both choices give the same v. The Gross-Pitaevskii matrix G is then found to be:

$$G = h + v(\Gamma) = \Omega \begin{bmatrix} 0 & 1 & 1 \\ 1 & 0 & 1 \\ 1 & 1 & 0 \end{bmatrix} + \frac{2\chi}{1 + z_1^* z_1 + z_2^* z_2} \begin{bmatrix} 1 & 0 & 0 \\ 0 & z_1^* z_1 & 0 \\ 0 & 0 & z_2^* z_2 \end{bmatrix}. \tag{5.17}$$

From (5.6) the equations of motion are:

$$i\dot{z}_1 = \Omega(1 + z_2) - \Omega(z_1 + z_2)z_1 - \frac{2\chi z_1(1 - |z_1|^2)}{1 + |z_1|^2 + |z_2|^2}, \tag{5.18a}$$

$$i\dot{z}_2 = \Omega(1 + z_1) - \Omega(z_1 + z_2)z_2 - \frac{2\chi z_2(1 - |z_2|^2)}{1 + |z_1|^2 + |z_2|^2}, \tag{5.18b}$$

and the action S can be integrated with the help of the Lagrangian given in Eq. (2.58). (Notice that $z = 0$ is not an stationary point of the classical system, even in the absence of collisions).

It is instructive to examine the explicit form of the energy function:

$$E = N\Omega \frac{(z_1^* z_2 + z_2^* z_1 + z_1^* + z_1 + z_2^* + z_2)}{1 + z_1^* z_1 + z_2^* z_2} + N\chi \frac{(z_1^* z_1)^2 + (z_2^* z_2)^2 + 1}{(1 + z_1^* z_1 + z_2^* z_2)^2}. \tag{5.19}$$

Note that the extensive character of E is due to the $(N-1)^{-1}$ scaling of the collision parameter in the two-body term of (5.15). This is also why the equations of motion (5.18) do not depend on N, and hence the classical system is well-defined in the limit $N \to \infty$.

Finally, since u is proportional to the identity matrix, the multiconfigurational coupling (5.7) for this particular problem is very simple to express:

$$\Delta_{ij} = N\chi\Big[(\Gamma^{ij}_{00} - \Gamma^{ii}_{00})^2 + (\Gamma^{ij}_{11} - \Gamma^{ii}_{11})^2 + (\Gamma^{ij}_{22} - \Gamma^{ii}_{22})^2\Big], \tag{5.20}$$

which clearly shows the symmetrical nature of the triple-well potential.

5.3.3 Exact quantum propagation

The CCS results for the triple-well system are compared with exact data obtained by trivial propagation in the eigenstate basis of the quantum Hamiltonian. The latter is

constructed in the bosonic Fock space representation using the basic local modes according to the matrix-element rules presented in Appendix D.2. The initial state, which is taken to be a coherent state (see below), is first projected on Fock space – using the decomposition given in Eq. (2.26) – and then projected onto the eigenstates of $\hat{H}$ (computed during the diagonalization procedure), at which point propagation can be started.

5.3.4 Monitored quantities

In the simulations reported below the following quantities are computed as functions of time: the norm of the CCS wavefunction $\mathcal{N}(\psi)$; the basis-set conditioning factor $\beta(\Omega)$, discussed in §4.4 (this factor depends solely on the overlap matrix Ω); the total energy $E(\psi)$; an the populations $p_0(\psi)$, $p_1(\psi)$ and $p_2(\psi)$ of the local modes (b_0, b_1, b_2). The formulas are:

$$\mathcal{N}(\psi) = \langle\psi|\psi\rangle = \sum_i C_i^* D_i, \tag{5.21a}$$

$$\beta(\Omega) = \lambda_{\max}(\Omega)\lambda_{\min}^{-1}(\Omega), \tag{5.21b}$$

$$E(\psi) = \langle\psi|\hat{H}|\psi\rangle = N\sum_{ij} D_i^*\omega_{ij}D_j \sum_{pq}[h_{pq} + \tfrac{1}{2}v_{pq}(z_i^*, z_j)]\Gamma_{qp}(z_i^*, z_j), \tag{5.21c}$$

$$p_q(\psi) = \langle\psi|b_q^\dagger b_q|\psi\rangle = N\sum_{ij} D_i^*\omega_{ij}D_j\Gamma_{qq}(z_i^*, z_j), \quad q = 0, 1, 2. \tag{5.21d}$$

The expression for the mean-field v_{pq} is found implicit in Eq. (5.17).

Additionally, the auto-correlation function $a(\psi; t)$ (ACF) is computed,

$$a(\psi; t) = \langle\psi_0|\psi_t\rangle = \sum_{j=1}^{m}\langle z_0|z_j\rangle D_j e^{iS_j}. \tag{5.22}$$

As discussed in Appendix E, the spectral density can be obtained from the ACF by a Fourier transform:

$$I_g(\psi; E) = \pi^{-1}\int_0^\infty dt\; g_\tau^{(k)}(t)\;\mathrm{Re}\,[\,a(\psi; t)e^{\frac{i}{\hbar}Et}\,], \tag{5.23}$$

where $g_\tau^{(k)}(t)$ is a window function of the form given in Eq. (E.10). The spectral density indicates which energy eigenstates play a role in the dynamics.

5.3.5 Opposite-phase mode and population imbalance

The classical system defined in (5.18) has three dynamically equivalent invariant subspaces, specified by the constraints: $z_1 = z_2$, $z_1 = 1$ and $z_2 = 1$. These correspond to so-called *twin-condensate regimes*.[67] Let us concentrate on the first subspace ($z_1 = z_2$) and refer to it as the Λ_1 surface.

Now, consider the set of operators $\tilde{b}_0$, $\tilde{b}_1$ and $\tilde{b}_2$, defined by the canonical transformation:

$$\tilde{b}_0 = b_0, \tag{5.24a}$$

$$\tilde{b}_1 = \tfrac{1}{\sqrt{2}}(b_1 + b_2), \tag{5.24b}$$

$$\tilde{b}_2 = \tfrac{1}{\sqrt{2}}(b_1 - b_2). \tag{5.24c}$$

It can be demonstrated that Λ_1 is an SU(2) subspace whose associated single-particle modes are: $\tilde{b}_0$ and $\tilde{b}_1$: the *solitary mode* and the *identical-phase mode*, respectively. Meanwhile, the $\tilde{b}_2$ mode, which is empty at Λ_1, describes an *opposite-phase* oscillation of the twin-condensate.[67]

Under the classical propagation scheme detailed in §1.3.3 – where the system's wavefunction is approximated by a single configuration – any initial SU(3) coherent state prepared at Λ_1 will have zero occupation of the opposite-phase mode $\tilde{b}_2$ for any $t > 0$; as a matter of fact, the expectation value

$$\tilde{p}_2(z) = \langle z|\tilde{b}_2^\dagger \tilde{b}_2|z\rangle = \frac{N}{2}\frac{(z_1^* - z_2^*)(z_1 - z_2)}{1 + z_1^* z_1 + z_2^* z_2}, \tag{5.25}$$

is identically null in the classically invariant surface Λ_1, where $z_1 = z_2$.

This conclusion, however, does not apply to the actual quantum problem: if the initial state $|\psi_0\rangle$ has null occupation in the opposite-phase mode $\tilde{b}_2$, this situation will *not* be preserved as the system evolves in time – while the quantum evolution preserves the equality between the populations of the local modes b_1 and b_2 [that is: $p_1(\psi) = p_2(\psi)$ for all $t > 0$], the populations of the identical-phase and opposite-phase modes change in time.[67] It is precisely this 'non-classical behavior' – i.e. the classically forbidden occupation of the opposite-phase mode, which lies beyond a mean-field description – that we wish to describe using the SU(3) CCS method.

With that goal in mind, we observe that the reference state is precisely located on the classical invariant surface Λ_1; therefore, we may conveniently take $|\Phi_0\rangle$ as the initial state; that is, we put $|\psi_0\rangle = |z_1', z_2'\rangle$, with

$$z_1' = z_2' = 0.$$

This state will be propagated with the discrete unitary method of §4.2.

In view of the above discussion, two other expectation values shall be computed in addition to the quantities listed in (5.21): the *opposite mode population* $\tilde{p}_2(\psi) = \langle\psi|\tilde{b}_2^\dagger \tilde{b}_2|\psi\rangle$,

which in terms of the local-mode variables z is given by

$$\begin{aligned}\tilde{p}_2(\psi) &= \sum_{ij} D_i^* D_j \omega_{ij} \left[\frac{\{z_i|\tilde{b}_2^\dagger \tilde{b}_2|z_j\}}{\{z_i|z_j\}}\right] \\ &= \sum_{ij} D_i^* \omega_{ij} D_j \left[\frac{N}{2}\frac{(z_{i,1}^* - z_{i,2}^*)(z_{j,1} - z_{j,2})}{1 + z_{i,1}^* z_{j,1} + z_{i,2}^* z_{j,2}}\right],\end{aligned} \tag{5.26}$$

and the *population imbalance*[67] between the identical-phase and solitary modes, $\tilde{b}_1$ and $\tilde{b}_0$ respectively, which in terms of the local-mode coherent-state parameters z reads:

$$\begin{aligned}J(\psi) &= N^{-1}\langle\psi|(\tilde{b}_1^\dagger \tilde{b}_1 - \tilde{b}_0^\dagger \tilde{b}_0)|\psi\rangle = N^{-1}\langle\psi|\left[\tfrac{1}{2}(b_1^\dagger b_1 + b_2^\dagger b_2) - b_0^\dagger b_0\right]|\psi\rangle \\ &= \tfrac{1}{2}\sum_{ij} D_i^* \omega_{ij} D_j \left[\frac{(z_{i,1}^* + z_{i,2}^*)(z_{j,1} + z_{j,2}) - 2}{1 + z_{i,1}^* z_{j,1} + z_{i,2}^* z_{j,2}}\right].\end{aligned} \tag{5.27}$$

5.3.6 Basis set sampling

In order to construct the initial CCS basis set, it is necessary to choose adequate sampling variables. In the present case we opt for angular variables $(\theta_1, \phi_1, \theta_2, \phi_2)$ defined by:

$$z_1 = \tan(\theta_1/2)e^{-i\phi_1}, \quad z_2 = \tan(\theta_2/2)e^{-i\phi_2}. \tag{5.28}$$

The initial conditions $z(0)$ are then randomly sampled around the origin from normal distributions expressed in terms of these angular variables; that is, at $t = 0$ each pair of angles (θ, ϕ) is selected according to probabilities:

$$P(\theta) \propto \exp(-\theta^2/2w_\theta^2); \;\; P(\phi) \propto \exp(-\phi^2/2w_\phi^2). \tag{5.29}$$

Notice that the widths of these distributions, w_θ and w_ϕ, are adjustable parameters of the method; in all simulations, the widths are the same for both entries $z_1(0)$ an $z_2(0)$. The actual sampling procedure – which also comprises specific criteria for accepting and neglecting candidate basis elements – was described in §4.4.

5.3.7 A note on dynamical regimes

Before considering the bosonic CCS results we must point out the following: the triple-well dynamics – as observed with the parameter values used in our simulations – experiences a qualitative change after a certain propagation time. In the 'first dynamical regime', as we shall call it, the population imbalance $J(\psi)$ relaxes while the opposite-mode population $\tilde{p}_2(\psi)$ builds up a non-zero value. During this first stage, the local populations oscillate with a natural period of $(2\pi/3|\Omega|) \approx 2.094$ (which is determined by the energy gap of $3|\Omega|$ between the single-particle ground-state and a degenerate pair of excited modes, as computed from first-order perturbation theory on the potential strength, ignoring two-

body interactions – see Ref. [67] for more details). The reference mode population $p_0(\psi)$ decreases while $p_1(\psi)$ and $p_2(\psi)$, which are always equal, increase (in average).

The systems eventually reaches a second dynamical regime, where the three local-mode populations oscillate (with a much larger period) around a mean value which is roughly one-third the total number of particles. This is illustrated in Figs. 5.1 and 5.2, where long-time exact results are shown for the case $N = 100$ (with: $\Omega = -1.0$ and $\chi = -0.50$).

This dynamical change calls for a reformulation of the CCS approach, meaning that probably the best way to proceed beyond the transition point would be to halt the CCS propagation, perform a new basis set sampling and start off again. Since we have not developed the tools required for this 're-adaptation' of the CCS wavefunction as a whole, we shall concentrate in the first dynamical regime, i.e. our simulations are terminated before the dynamical transition is completed.[ii]

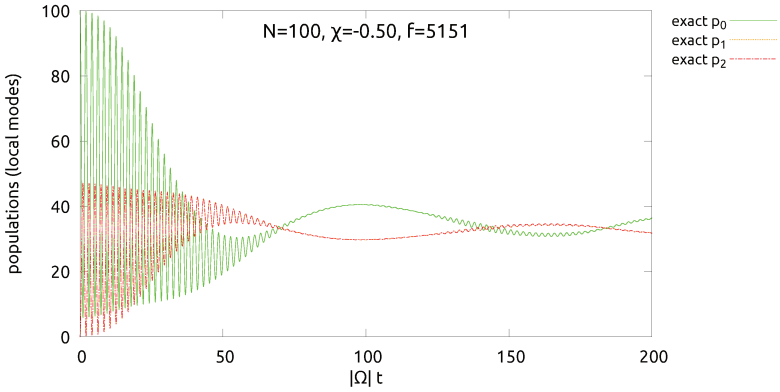

Figure 5.1: Long-time behavior of local populations $p_0(\psi), p_1(\psi), p_2(\psi)$ exemplified for a system with $N = 100$ particles (exact quantum result). The quantum dynamics is such thay $p_1(\psi) = p_2(\psi)$ for all times. In the reference state (also the initial state) all particles occupy the zeroth mode (obs: f denotes the dimension of the bosonic Fock space).

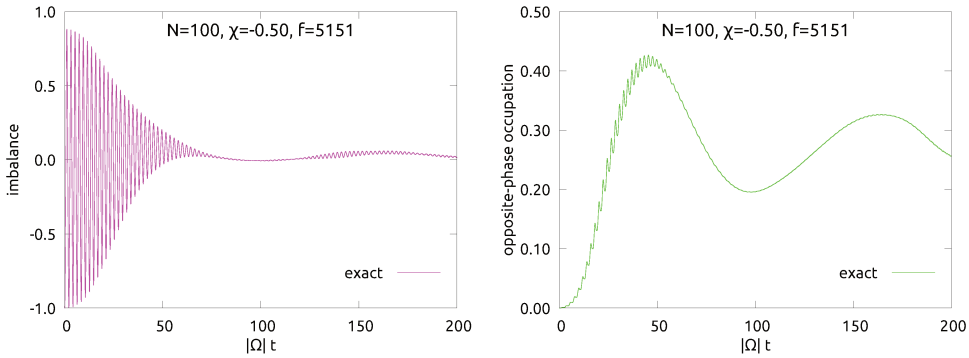

Figure 5.2: Long-time behavior of the population imbalance $J(\psi)$ (left panel) and the opposite-phase mode occupation $\tilde{p}_2(\psi)$ (right panel). Same run as that of Fig. 5.1.

[ii] We should mention that this same triple-well model was studied with the bosonic CCS method in Ref. [28], but only the very short time dynamics was analyzed in that work (up to $|\Omega|t \approx 10, 0$).

5.3.8 Runs: general remarks

The tripe-well simulations presented below, four in total, were all performed with $\Omega = -1.0$ and $\chi = -0.50$; these runs differ in their values of the total particle number, namely: $N = 100,\ 80,\ 70,\ 40$; the size f of the bosonic Fock spaces, in the corresponding order, are: $f = 5151,\ 3321,\ 2556,\ 861$. These values are indicated in the graphs of each run together with the size m of the employed basis set. The sampling was carried out with the same values of the conditioning threshold, which was set to 10^{13}. Additionally, a limiting value for the overlap with the initial state was established: only those initial conditions $z_i(0)$ satisfying $\langle z_i(0)|\Phi_0\rangle < 0.98$ were accepted (see captions for more specific details). The final propagation time was set to $|\Omega|t_{\text{final}} = 80.0$ for all runs.

The overall behavior observed is as follows: a steep drop of the basis-set conditioning factor $\beta(\Omega)$ occurs as soon as propagation starts. This means that trajectories are quickly spreading on the SU(3) phase space. This is not surprising because this is not a perturbative problem, and neither is $|\Phi_0\rangle$ a non-interacting ground-state. As discussed in §4.4, this is a very unfavorable scenario for the CCS method, posing a stringent test to the trajectory-based methodology. The total energy $E(\psi)$ fluctuates, as expected, indicating the inability of the basis set projector $\hat{\Omega}(t)$ of representing the identity operator, as discussed in §4.2.5.

Nevertheless, the CCS method produces accurate results up to $|\Omega|t \approx 40.0$ for all runs. This time should be compared to the natural oscillation period of the first dynamical regime of the system, which, as mentioned earlier, is ≈ 2.094. Thus, during the timespan $0 \leq |\Omega|t \lesssim 40.0$ the system undergoes approximately 19 natural oscillations, and a mostly satisfactory description is maintained during this interval, which is quite reasonable for a trajectory-based technique. In particular, the equality of average populations $p_1(\psi)$ and $p_2(\psi)$, which is guaranteed in the exact quantum propagation, is not enforced by any means in the CCS wavefunction – rather, it depends on a very delicate interference among different configurations. The fact that the populations remain correctly equal after roughly 19 natural oscillations under such unfavorable circumstances is worth of mention. The same can be said regarding the mean values of the population imbalance $J(\psi)$ and the opposite-phase occupation $\tilde{p}_2(\psi)$. To be sure, the run with $N = 40$ is visually less accurate than the others – this is expected since for smaller N the SU(3) coherent states become less localized, and the trajectory picture less appropriate.

The auto-correlation function proves to be an exception to the above observations, for it departs significantly from the exact time signal at a much earlier time, somewhere in the range $20 \lesssim |\Omega|t \lesssim 30$ for different runs. Nevertheless, for all runs the CCS-computed spectral density $I_g(\psi)$ is almost indistinguishable from the exact one.

In the next few pages results are presented without further analysis – some additional information is found in each figure's caption.

5.3.9 Run: $N = 100$

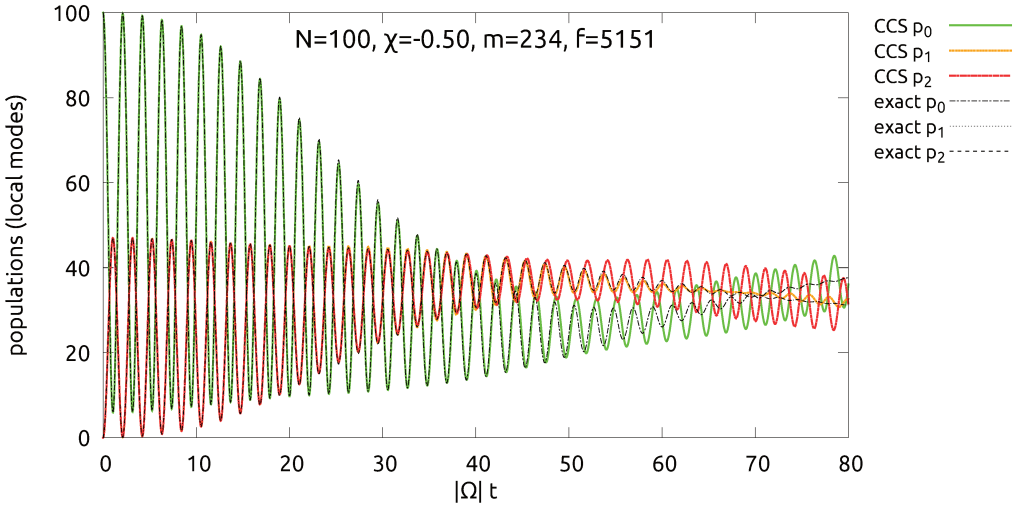

Figure 5.3: Local populations $p_0(\psi), p_1(\psi), p_2(\psi)$, as functions of the dimensionless time $|\Omega|t$. CCS results (solid lines – see legend for color code) are compared to exact data (dashed/dotted lines). In the reference state all particles occupy the zeroth mode; the main parameters for this run are indicated in this and the subsequent graphs.

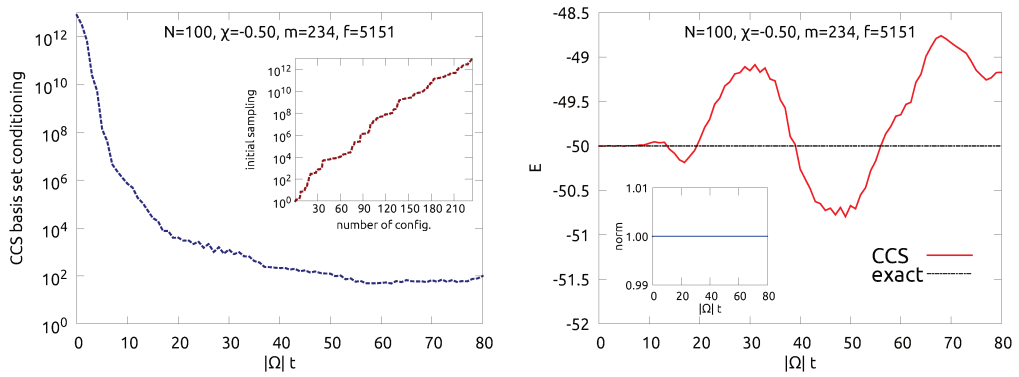

Figure 5.4: Left panel: basis set conditioning $\beta(\Omega)$ during propagation; inset: basis set conditioning increase curve during initial sampling. In this run the widths for the basis set sampling were $(w_\theta, w_\phi) = (0.30\pi, 0.40\pi)$ for both z_1 and z_2; saturation occurred at $m = 234$ basis elements. Right panel: total energy $E(\psi)$; inset: squared norm $N(\psi)$ (both plotted as functions of time).

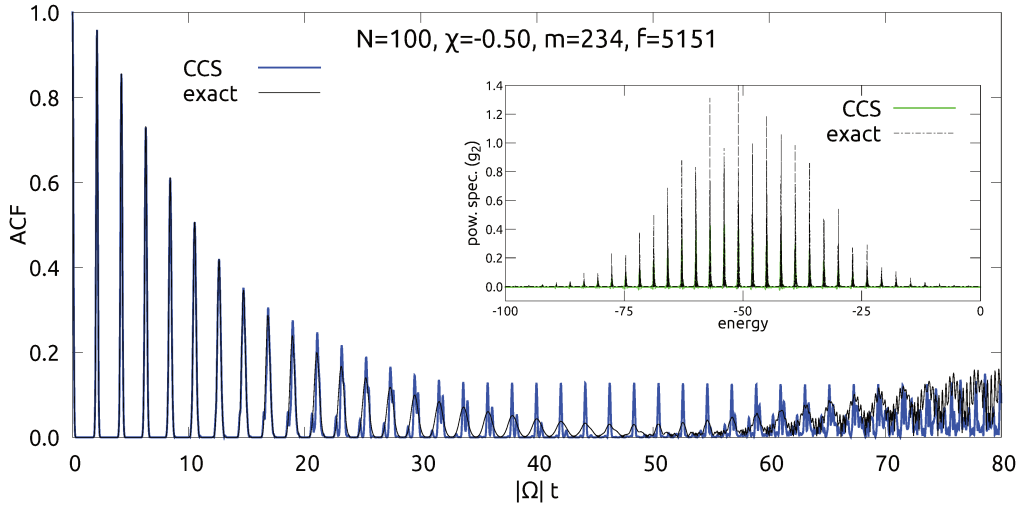

Figure 5.5: Absolute value of the CCS auto-correlation function $a(\psi)$ (blue solid line) compared to the exact time signal (black line). The CCS time increment was $h = 0.020$; propagation was terminated at $|\Omega|t = 80$. Inset: CCS and exact spectral densities $I_g(\psi, E)$ computed from the Fourier transform of the respective ACFs. In this specific run the exact propagation was carried until $|\Omega|t = 400$; this is why the CCS and exact curves display different intensities for the energy peaks.

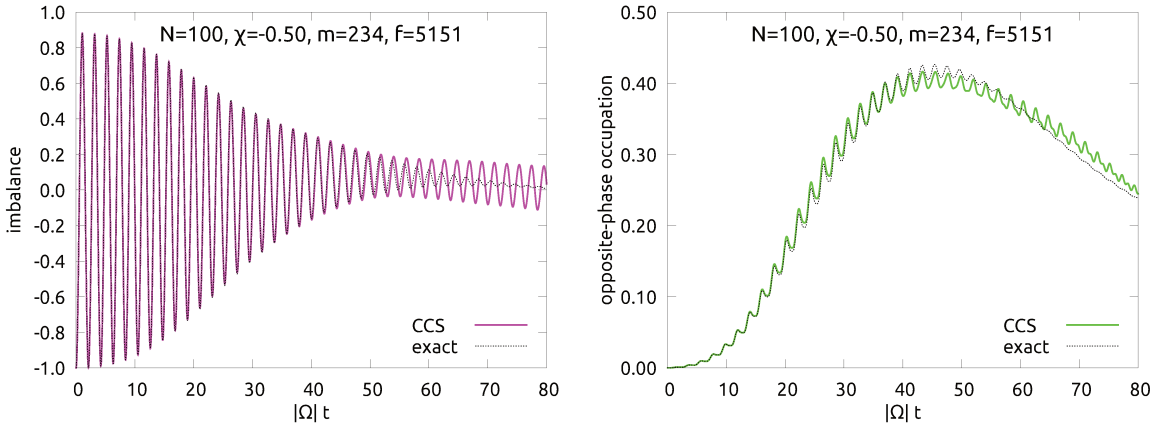

Figure 5.6: Population imbalance $J(\psi)$ (left panel) and opposite-phase mode occupation $\tilde{p}_2(\psi)$ (right panel), both plotted as functions of time during the first dynamical regime of the system. CCS results (solid lines) are compared to exact data (dotted lines).

5.3.10 Run: $N = 80$

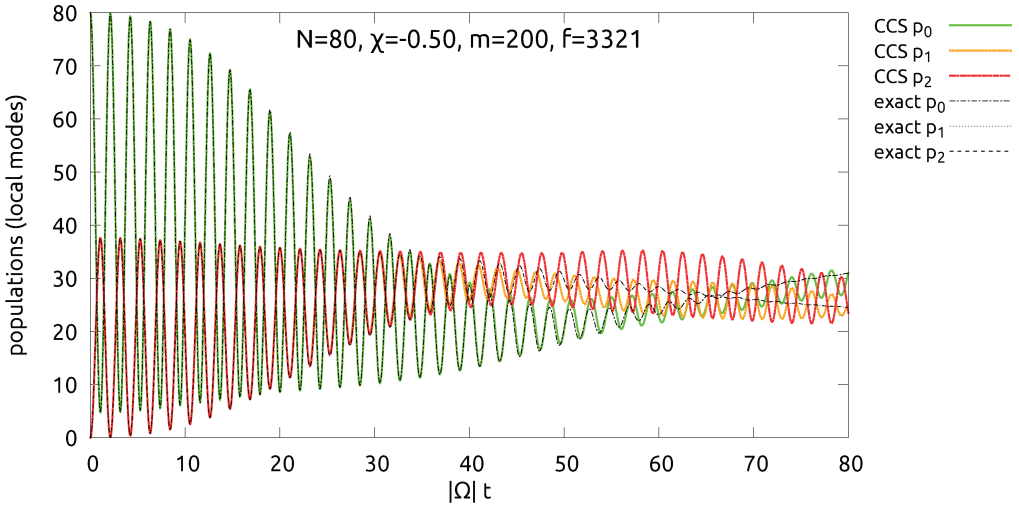

Figure 5.7: Local populations $p_0(\psi), p_1(\psi), p_2(\psi)$, as functions of the dimensionless time $|\Omega|t$. CCS results (solid lines – see legend for color code) are compared to exact data (dashed/dotted lines). In the reference state all particles occupy the zeroth mode; the main parameters for this run are indicated in this and the subsequent graphs.

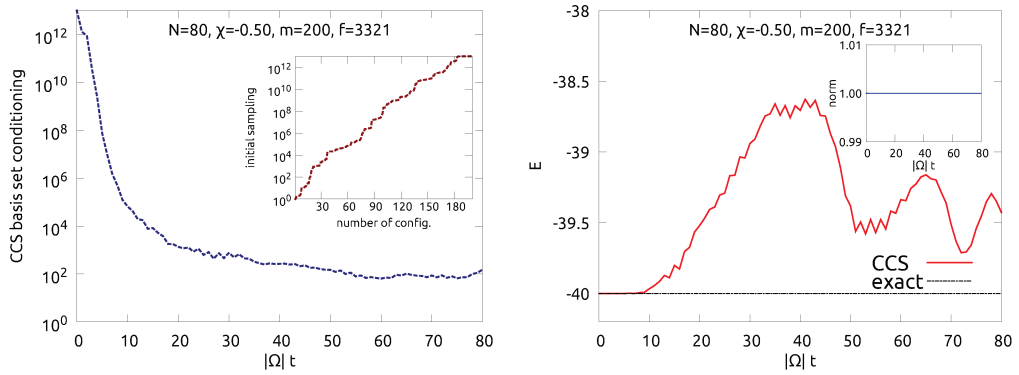

Figure 5.8: Left panel: basis set conditioning $\beta(\Omega)$ during propagation; inset: basis set conditioning increase curve during initial sampling. In this run the widths for the basis set sampling were $(w_\theta, w_\phi) = (0.30\pi, 0.40\pi)$ for both z_1 and z_2; saturation occurred at $m = 200$ basis elements. Right panel: total energy $E(\psi)$; inset: squared norm $N(\psi)$ (both plotted as functions of time).

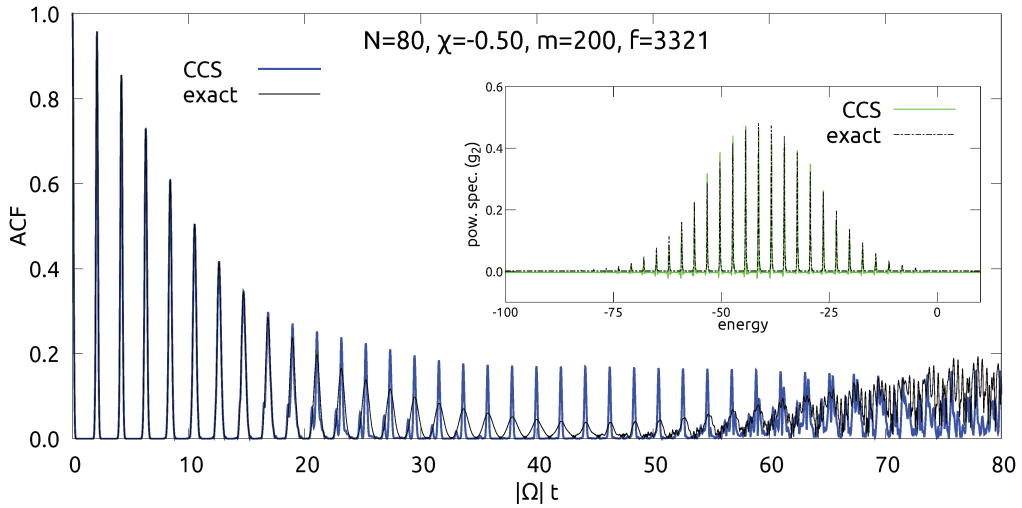

Figure 5.9: Absolute value of the CCS auto-correlation function $a(\psi)$ (blue solid line) compared to the exact time signal (black line). The CCS time increment was $h = 0.020$; propagation was terminated at $|\Omega|t = 80$. Inset: CCS and exact spectral densities $I_g(\psi, E)$ computed from the Fourier transform of the respective ACFs.

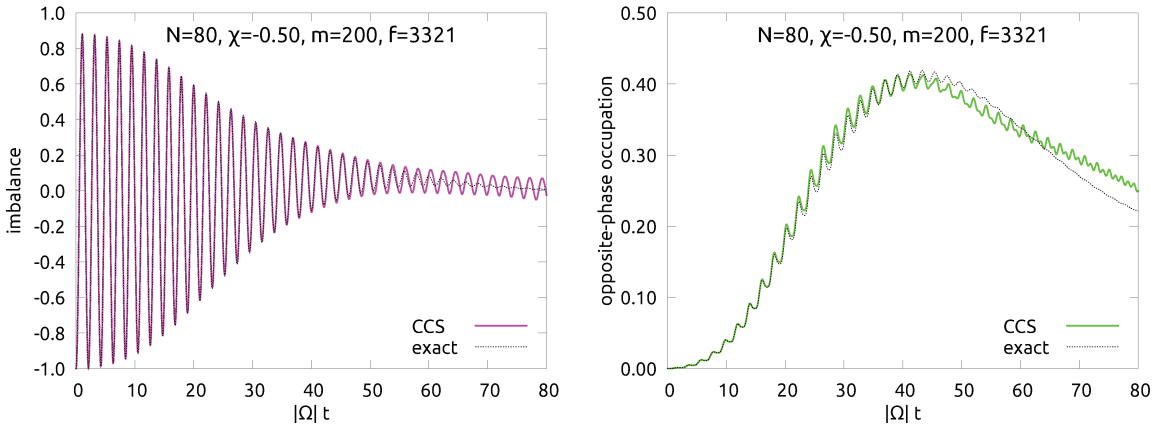

Figure 5.10: Population imbalance $J(\psi)$ (left panel) and opposite-phase mode occupation $\tilde{p}_2(\psi)$ (right panel), both plotted as functions of time during the first dynamical regime of the system. CCS results (solid lines) are compared to exact data (dotted lines).

5.3.11 Run: $N = 70$

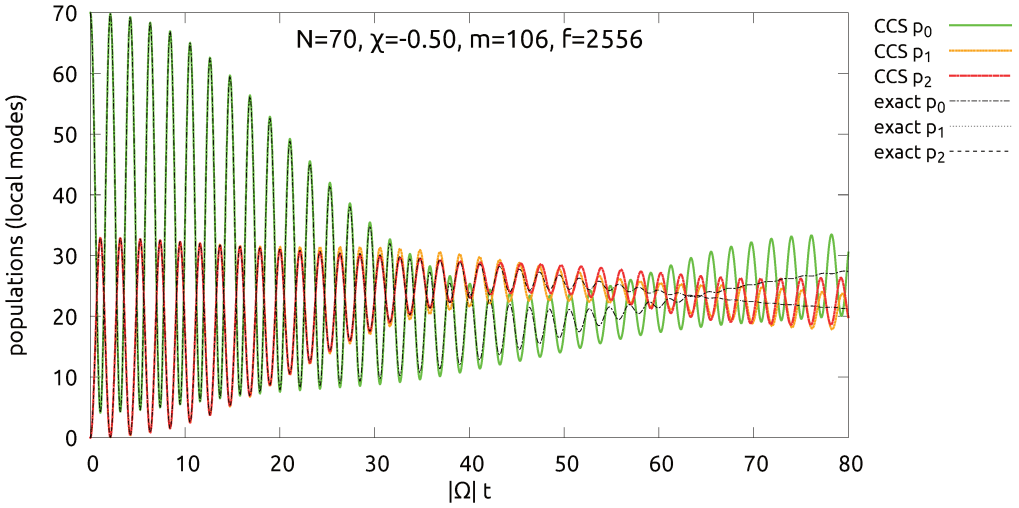

Figure 5.11: Local populations $p_0(\psi), p_1(\psi), p_2(\psi)$, as functions of the dimensionless time $|\Omega|t$. CCS results (solid lines – see legend for color code) are compared to exact data (dashed/dotted lines). In the reference state all particles occupy the zeroth mode; the main parameters for this run are indicated in this and the subsequent graphs.

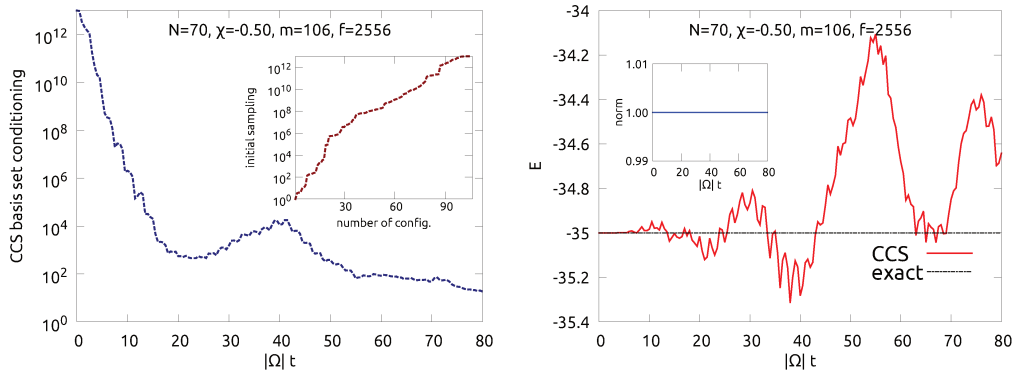

Figure 5.12: Left panel: basis set conditioning $\beta(\Omega)$ during propagation; inset: basis set conditioning increase curve during initial sampling. In this run the widths for the basis set sampling were $(w_\theta, w_\phi) = (0.20\pi, 1.50\pi)$ for both z_1 and z_2; saturation occurred at $m = 106$ basis elements. Right panel: total energy $E(\psi)$; inset: squared norm $N(\psi)$ (both plotted as functions of time).

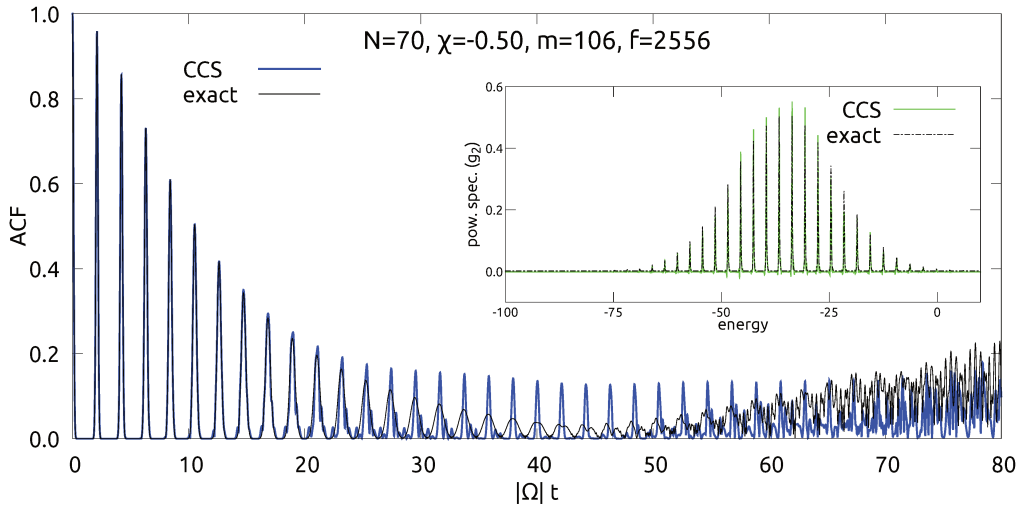

Figure 5.13: Absolute value of the CCS auto-correlation function $a(\psi)$ (blue solid line) compared to the exact time signal (black line). The CCS time increment was $h = 0.010$; propagation was terminated at $|\Omega|t = 80$. Inset: CCS and exact spectral densities $I_g(\psi, E)$ computed from the Fourier transform of the respective ACFs.

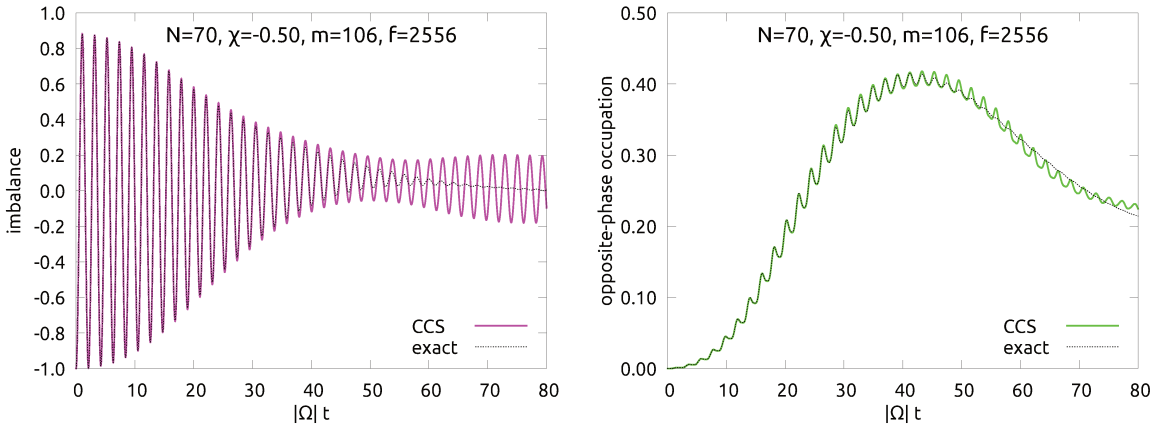

Figure 5.14: Population imbalance $J(\psi)$ (left panel) and opposite-phase mode occupation $\tilde{p}_2(\psi)$ (right panel), both plotted as functions of time during the first dynamical regime of the system. CCS results (solid lines) are compared to exact data (dotted lines).

5.3.12 Run: $N = 40$

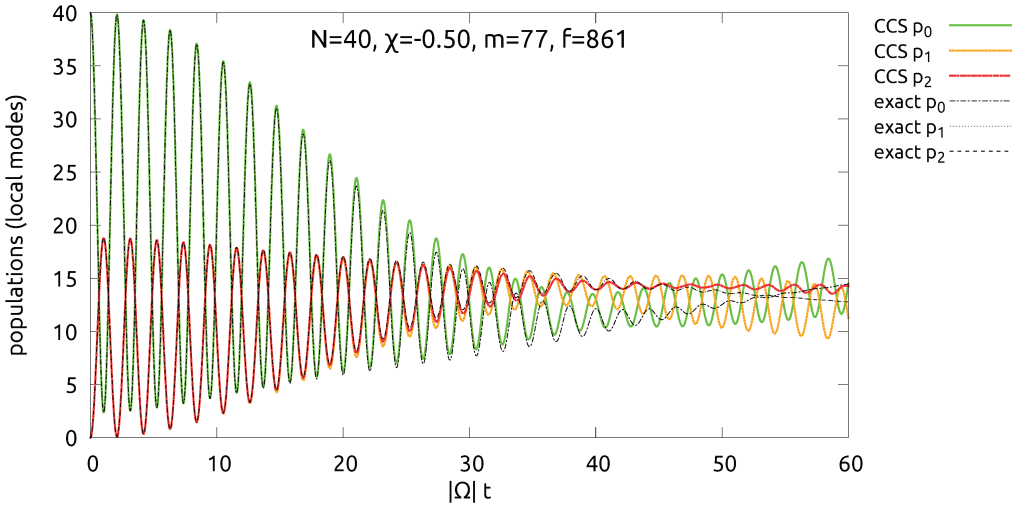

Figure 5.15: Local populations $p_0(\psi), p_1(\psi), p_2(\psi)$, as functions of the dimensionless time $|\Omega|t$. CCS results (solid lines – see legend for color code) are compared to exact data (dashed/dotted lines). In the reference state all particles occupy the zeroth mode; the main parameters for this run are indicated in this and the subsequent graphs.

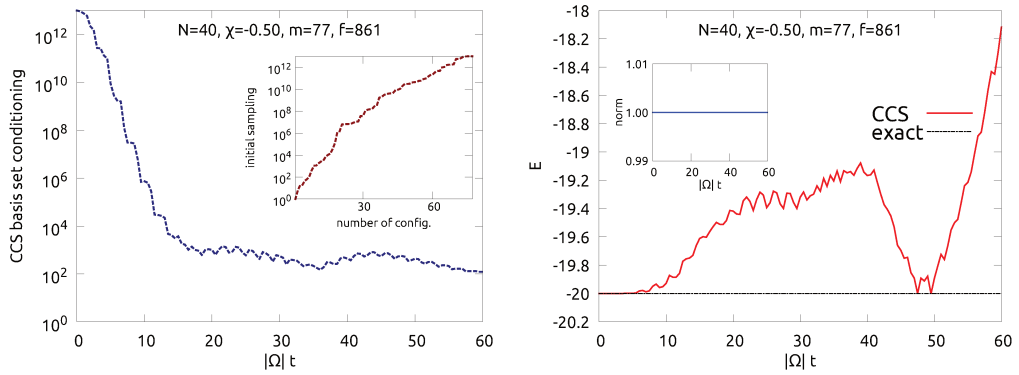

Figure 5.16: Left panel: basis set conditioning $\beta(\Omega)$ during propagation; inset: basis set conditioning increase curve during initial sampling. In this run the widths for the basis set sampling were $(w_\theta, w_\phi) = (0.20\pi, 0.40\pi)$ for both z_1 and z_2; saturation occurred at $m = 77$ basis elements. Right panel: total energy $E(\psi)$; inset: squared norm $N(\psi)$ (both plotted as functions of time).

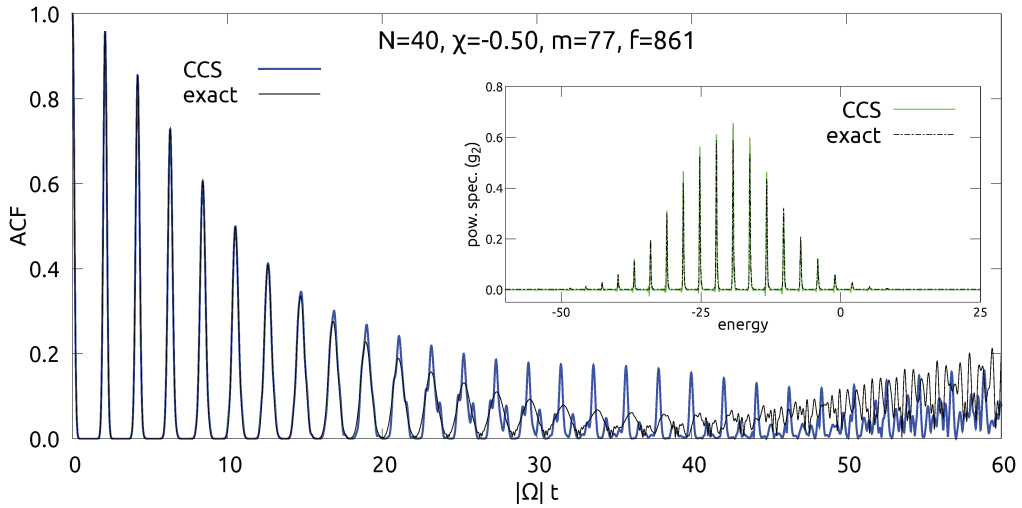

Figure 5.17: Absolute value of the CCS auto-correlation function $a(\psi)$ (blue solid line) compared to the exact time signal (black line). The CCS time increment was $h = 0.010$; propagation was terminated at $|\Omega|t = 80$. Inset: CCS and exact spectral densities $I_g(\psi, E)$ computed from the Fourier transform of the respective ACFs.

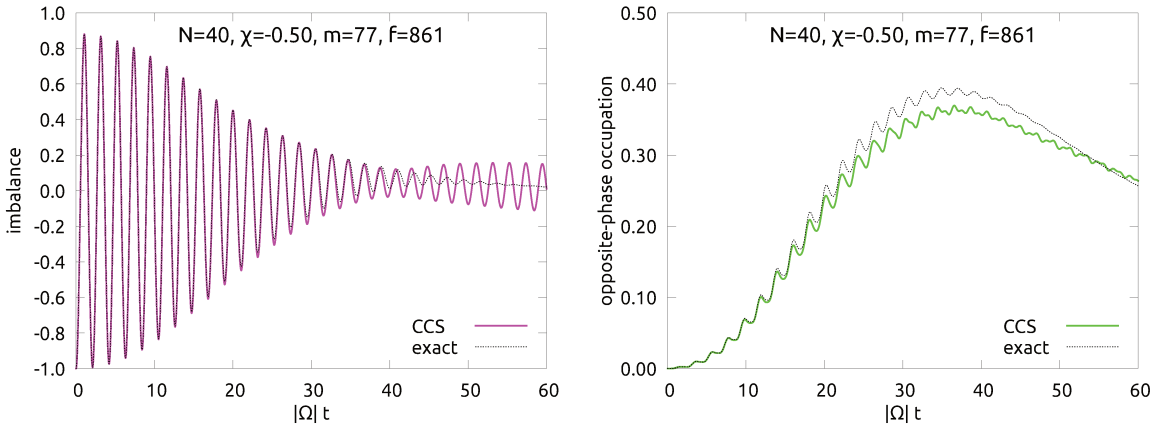

Figure 5.18: Population imbalance $J(\psi)$ (left panel) and opposite-phase mode occupation $\tilde{p}_2(\psi)$ (right panel), both plotted as functions of time during the first dynamical regime of the system. CCS results (solid lines) are compared to exact data (dotted lines).

5.4 Electrons in a Hubbard ring

5.4.1 Lattice space

Let us consider the following crude model for a cyclic molecule. The molecule consists of S atoms of the same kind forming a planar circular ring; for definiteness we assume the ring lies in the xy plane. The atoms are fixed and evenly spaced along the ring and the length of the arc segment connecting each pair is denoted a – the molecular bond-length, denoted b, is then given by the chord formula: $b = (aS/2\pi)\sin(\pi/S)$.

There are N electrons which are free to move in the ring; they are allowed to occupy *localized* molecular orbitals, or Wannier functions, which are constructed from primitive atomic s-type orbitals. Therefore, each molecular orbital comports at most two electrons with opposite spin components (in the z direction), identified by the symbols $\uparrow$ and $\downarrow$. Hence, there are in total of $2S$ possible single-particle states in the system.

Denoting the Wannier functions by $\tilde{\chi}_{\sigma j}(\mathbf{x})$ and assigning them creation operators $\tilde{c}^\dagger_{\sigma j}$, the single-particle basis spanning the electronic active space, its corresponding projector, and the field operator are:

$$|\tilde{\chi}_{\sigma j}\rangle = \tilde{c}^\dagger_{\sigma j}|0\rangle, \quad \hat{P}_{\tilde{\chi}} = \sum_{j=1}^{S}\sum_{\sigma=\uparrow,\downarrow} |\tilde{\chi}_{\sigma j}\rangle\langle\tilde{\chi}_{\sigma j}|, \quad \hat{\psi}_\sigma(\mathbf{x}) = \sum_{j=1}^{S} \tilde{\chi}_{\sigma j}(\mathbf{x})\tilde{c}_{\sigma j}. \tag{5.30}$$

The notational convention for the single-particle description is as follows: the label σ refers to spin; subscripts i, j, ranging from 1 to S, refer to atomic sites – summation ranges are omitted henceforth. The $|\tilde{\chi}_{\sigma j}\rangle$ basis is denominated the *lattice representation*; quantities relating to this basis will be indicated with tildes.

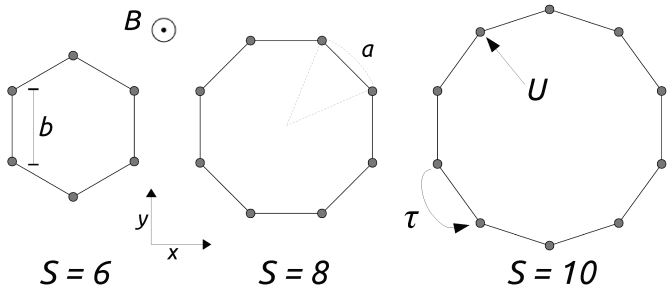

Figure 5.19: Schematics of the Hubbard ring problem: rings with different number of sites are shown and the parameters of the model are indicated.

While the precise spatial shape of the Wannier functions is not relevant for our purposes, the assumption that they can be constructed in such a way as to maintain a local character (i.e. so that they can be associated with individual atoms of the ring) is essential to justify the following dynamical description: electrons are able to tunnel across neighboring atoms of the ring in a tight-binding fashion, with hopping constant τ; electrons

with opposite spins occupying the same localized molecular orbital experience Coulomb repulsion, described '*à la* Hubbard', with strength controlled by a parameter U. Both τ and U are positive and have the dimension of energy. Figure 5.19 illustrates the basic features of the model for rings of different sizes.

The above description amounts to a standard Hubbard Hamiltonian:[68]

$$\hat{H} = -\tau \sum_{j\sigma} (\tilde{c}^{\dagger}_{\sigma j} \tilde{c}_{\sigma(j+1)} + \tilde{c}^{\dagger}_{\sigma(j+1)} \tilde{c}_{\sigma j}) + U \sum_{j} \tilde{n}_{\uparrow j} \tilde{n}_{\downarrow j}, \tag{5.31}$$

where it is understood that $\tilde{c}_{\sigma(S+1)} = \tilde{c}_{\sigma 1}$.

However, we shall introduce a further element: a magnetic field $\mathbf{B} = B\hat{\mathbf{z}}$, perpendicular to the molecular plane. In that case, new terms should be added to the Hamiltonian:[68;69]

$$\hat{H} = -\tau \sum_{j\sigma} (\tilde{c}^{\dagger}_{\sigma j} \tilde{c}_{\sigma(j+1)} e^{-i\theta} + \tilde{c}^{\dagger}_{\sigma(j+1)} \tilde{c}_{\sigma j} e^{i\theta}) - \mu_0 B \sum_{j} (\tilde{n}_{\uparrow j} - \tilde{n}_{\downarrow j}) + U \sum_{j} \tilde{n}_{\uparrow j} \tilde{n}_{\downarrow j}. \tag{5.32}$$

Let us briefly comment on the additional parameters.

The second term in (5.32) accounts for the interaction of each electron's magnetic moment with the field B, giving rise to the well-known Zeeman effect.[42] It lifts the spin degeneracy of each single-particle state. The constant μ_0 is *Bohr's magneton*, which is expressed in terms of $\hbar$, the fundamental electric charge e, and the electron mass m_e:

$$\mu_0 = e\hbar/m_e = 5.788\,382 \times 10^{-5}\ \text{eV} \cdot \text{T}^{-1}. \tag{5.33}$$

The phase θ in the kinetic term of (5.32) is the so-called 'Peierls phase',[68] which originates from the gauge coupling between the magnetic field and the electronic momentum. It depends on the number of sites S and the magnetic flux Φ through the ring – following Ref. [69] this flux is computed as if the ring were a circle, leading to the formula:

$$\theta \equiv \frac{2\pi}{S}(\Phi/\Phi_0) = \frac{a^2 B S}{2\Phi_0}. \qquad \left[\Phi = B \cdot (\text{ring's area}) = B\pi(aS/2\pi)^2\right] \tag{5.34}$$

Here, Φ_0 denotes the *magnetic flux quantum*, a fundamental quantity which is expressed in terms of $\hbar$, e, and the speed of light in vacuum c,

$$\Phi_0 = 2\pi\hbar c/e = 2.067\,834 \times 10^{-15}\ \text{T} \cdot \text{m}^2. \tag{5.35}$$

The Hamiltonian of Eq. (5.32) is the model we shall study. In everything that follows,

the tight-binding hopping constant τ and the arc-length a will be held fix at the values[iii]

$$\tau = 1.00 \text{ eV}, \quad a = 1.40 \times 10^{-10} \text{ m}, \quad \text{(fixed parameters)} \tag{5.36}$$

and we shall investigate a number problems for different values of: the number of sites S, the number of electrons N, the Coulomb strength U, and the magnetic field B.

As indicated in the previous formulas, we take as basic units: Tesla (T), meter (m) and electron-volts (eV). In this system the natural time unit is '$\hbar \cdot \text{eV}^{-1}$', but our results will be reported in femtoseconds; the conversion factor is: $\hbar \cdot \text{eV}^{-1} = 0.6582120$ fs.

Let us now put the Hamiltonian in the standard form of §5.1. For that purpose, we denote the total number of single-particle states by $K = 2S$ and rename the basic operators as follows:

$$\tilde{\chi}_{\sigma j} : (\tilde{c}_{\uparrow 1}, \tilde{c}_{\uparrow 2}, \cdots, \tilde{c}_{\uparrow s}, \tilde{c}_{\downarrow 1}, \tilde{c}_{\downarrow 2}, \cdots, \tilde{c}_{\downarrow s}) \rightarrow \tilde{\chi}_p : (\tilde{c}_1, \tilde{c}_2, \cdots, \tilde{c}_s, \tilde{c}_{s+1}, \tilde{c}_{s+2}, \cdots, \tilde{c}_K). \tag{5.37}$$

Thus, the lattice representation is organized according to spin components, in the way of §3.2.3. We recall that this spin structure should not be confused with the occupied-virtual partitioning of the Thouless determinants, which will be introduced shortly. Notice that, here, the particular ordering of orbitals within spin blocks is unimportant since sites can be interchanged without affecting the Hamiltonian.

The new indexation is also assigned to the basis functions:

$$|\tilde{\chi}_p\rangle = \tilde{c}_p^\dagger |0\rangle, \quad \hat{P}_{\tilde{\chi}} = \sum_{p=1}^{K} |\tilde{\chi}_p\rangle\langle\tilde{\chi}_p|. \tag{5.38}$$

Henceforth, the conventions of Chapter 3 are adopted: subscripts p, q, r, s will always range from 1 to K, and summation limits will be omitted.

In this way we are able to write the Hamiltonian in the lattice representation, with the help of matrices $\tilde{\varepsilon}$ and $\tilde{u}$,

$$\hat{H} = \sum_{pq} (\tilde{\varepsilon}_{pq}\, \tilde{c}_p^\dagger \tilde{c}_q + \tfrac{1}{2} \tilde{u}_{pq}\, \tilde{n}_p \tilde{n}_q), \tag{5.39}$$

as in §5.1.2. These matrices should obey the properties listed in (5.2). In order to illustrate the parametrization, we consider a ring with $S = 4$ ($K = 8$). In this case, the one-body

[iii] For reference, the carbon-carbon bound length in a benzene molecule is ~ 1.400Å; in our problem: $b(S = 6) \sim 1.337$Å, so our 6-site ring is just a bit smaller than a benzene. Although we chose to keep a fixed, and not b, the variation of the latter is very small for $S > 6$; this is compatible with the fixed value of the hopping constant (which is expected to depend on the bond-length).

matrix is:

$$\tilde{\varepsilon} = \begin{bmatrix} -\mu_0 B & -\tau e^{-i\theta} & 0 & -\tau e^{i\theta} & 0 & 0 & 0 & 0 \\ -\tau e^{i\theta} & -\mu_0 B & -\tau e^{-i\theta} & 0 & 0 & 0 & 0 & 0 \\ 0 & -\tau e^{i\theta} & -\mu_0 B & -\tau e^{-i\theta} & 0 & 0 & 0 & 0 \\ -\tau e^{-i\theta} & 0 & -\tau e^{i\theta} & -\mu_0 B & 0 & 0 & 0 & 0 \\ 0 & 0 & 0 & 0 & \mu_0 B & -\tau e^{-i\theta} & 0 & -\tau e^{i\theta} \\ 0 & 0 & 0 & 0 & -\tau e^{i\theta} & \mu_0 B & -\tau e^{-i\theta} & 0 \\ 0 & 0 & 0 & 0 & 0 & -\tau e^{i\theta} & \mu_0 B & -\tau e^{-i\theta} \\ 0 & 0 & 0 & 0 & -\tau e^{-i\theta} & 0 & -\tau e^{i\theta} & \mu_0 B \end{bmatrix}. \tag{5.40}$$

while the interaction matrix is:

$$\tilde{u} = U \begin{bmatrix} 0 & 0 & 0 & 0 & 1 & 0 & 0 & 0 \\ 0 & 0 & 0 & 0 & 0 & 1 & 0 & 0 \\ 0 & 0 & 0 & 0 & 0 & 0 & 1 & 0 \\ 0 & 0 & 0 & 0 & 0 & 0 & 0 & 1 \\ 1 & 0 & 0 & 0 & 0 & 0 & 0 & 0 \\ 0 & 1 & 0 & 0 & 0 & 0 & 0 & 0 \\ 0 & 0 & 1 & 0 & 0 & 0 & 0 & 0 \\ 0 & 0 & 0 & 1 & 0 & 0 & 0 & 0 \end{bmatrix}. \tag{5.41}$$

Notice that the external field does not modify the latter.

The reason why the lattice representation is useful is precisely because matrix $\tilde{u}$ is so simple to express (this leads to a particularly simple mean-field in the lattice representation – see Eq. (5.59) below). However, since we want to describe the weakly interacting regime, where $U \ll \tau$, we must define our coherent states in terms of the reciprocal space representation discussed next.

5.4.2 Reciprocal space

Let us consider the one-body part $\hat{H}_1$ of the Hamiltonian (5.32),

$$\hat{H}_1 = -\tau \sum_{j\sigma} (\tilde{c}^\dagger_{\sigma j} \tilde{c}_{\sigma(j+1)} e^{-i\theta} + \tilde{c}^\dagger_{\sigma(j+1)} \tilde{c}_{\sigma j} e^{i\theta}) - \mu_0 B \sum_j (\tilde{n}_{\uparrow j} - \tilde{n}_{\downarrow j}). \tag{5.42}$$

This operator can be diagonalized by changing to the *reciprocal basis* $|\phi_{\sigma k}\rangle$,

$$|\phi_{\sigma k}\rangle = c^\dagger_{\sigma k}|0\rangle, \quad \hat{P}_\phi = \sum_{k=0}^{S-1} \sum_{\sigma=\uparrow,\downarrow} |\phi_{\sigma k}\rangle\langle\phi_{\sigma k}|, \quad \hat{\psi}_\sigma(\mathbf{x}) = \sum_{k=0}^{S-1} \phi_{\sigma k}(\mathbf{x}) c_{\sigma k}, \tag{5.43}$$

whose associated creation and annihilation operators, $c^\dagger_{\sigma k}$ and $c_{\sigma k}$ (no tildes), are related to the original lattice operators, $\tilde{c}^\dagger_{\sigma j}$ and $\tilde{c}_{\sigma j}$, as follows:[69]

$$\tilde{c}_{j\sigma} = S^{-1/2}\sum_{k=0}^{S-1} c_{k\sigma}e^{i(2\pi/S)kj}, \quad \tilde{c}^\dagger_{j\sigma} = S^{-1/2}\sum_{k=0}^{S-1} c^\dagger_{k\sigma}e^{-i(2\pi/S)kj}. \quad (1 \leq j \leq S) \tag{5.44}$$

Notice that the reciprocal-basis subscript k is defined in the range 0 to $S-1$. Evidently, both lattice and reciprocal orbitals span the same single-particle space.

The transformation (5.44) brings the non-interacting Hamiltonian to the form $\hat{H}_1 = \sum_{k\sigma}\varepsilon_{\sigma k}n_{\sigma k}$ with energies

$$\varepsilon_{\sigma k} = -2\tau\cos\Big(\frac{2\pi k}{S} - \theta\Big) - \sigma\mu_0 B, \tag{5.45}$$

for $k = 0, \ldots, (S-1)$; in the above formula, the spin label should be understood as a sign: $\sigma = (\uparrow, \downarrow) = (+1, -1)$, meaning that the energy of spin-up levels is lowered and that of spin-down levels is raised.

From Eq. (5.45) we see that the presence of a non-zero magnetic field leads to a well-defined hierarchy of levels, for, once the degeneracies are removed, these can be sorted according to their non-interacting energies. (Note that the phase θ is also essential for this purpose.) This fact allows an unambiguous definition of the Thouless reference state, which we shall later take to be the non-interacting ground-state.

Therefore, in contrast to the lattice representation case, the re-labeling of the reciprocal space orbitals $|\phi\rangle$, is based on a specific criterion: labels 1 to K are assigned in *ascending order of the non-interacting energy* $\varepsilon_{\sigma k}$:

$$\phi_{\sigma k} : (c_{\uparrow 0}, \cdots, c_{\uparrow(S-1)}, c_{\downarrow 0}, \cdots, c_{\downarrow(S-1)}) \xrightarrow{\text{sorted}} \phi_p : (c_1, \cdots, c_S, c_{S+1}, \cdots, c_K), \tag{5.46}$$

The new indexation is also enforced upon the basis functions:

$$|\phi_p\rangle = c^\dagger_p|0\rangle, \quad \hat{P}_\phi = \sum_{p=1}^{K}|\phi_p\rangle\langle\phi_p|, \tag{5.47}$$

which are thus organized in such a way that:

$$\varepsilon(\phi_1) < \varepsilon(\phi_2) < \cdots < \varepsilon(\phi_K). \tag{5.48}$$

Let us now look at the interacting part of (5.32) (the Coulomb repulsion term); using the transformation (5.44) we find that it assumes the form:

$$U\sum_j \tilde{n}_{\uparrow j}\tilde{n}_{\downarrow j} = \frac{U}{S}\sum_k\sum_{k'}\sum_l\sum_{l'}(\delta_{k+l,k'+l'})\, c^\dagger_{\uparrow k}c^\dagger_{\downarrow l}c_{\downarrow l'}c_{\uparrow k'}. \tag{5.49}$$

This means that the full reciprocal-space Hamiltonian has the general prototype form studied in Chapter 3 (the only simplification being the diagonal one-body term):

$$\hat{H} = \sum_{pq} \varepsilon_p \, c_p^\dagger c_p + \tfrac{1}{2} \sum_{pqrs} V_{pr\cdot qs} c_p^\dagger c_r^\dagger c_s c_q. \tag{5.50}$$

The two-body matrix elements $V_{pr\cdot qs}$ constitute a sparse array, whose entries are directly related to the Kronecker deltas on the right-hand side of expression (5.49) (where several spin Kronecker deltas are implicit). Still, it is convenient to avoid dealing with the two-body integrals; for this reason we adopt a 'two-representation strategy'.

5.4.3 Two-representation strategy for trajectory propagation

In the case of weak interactions, $U/\tau \ll 1$, the most physically appropriate reference state for the Thouless parametrization is the non-interacting ground-state, which is straightforwardly constructed from creation operators $c^\dagger$ associated with orbitals $|\phi\rangle$ belonging to the reciprocal representation. Following the prescription of Chapter 3, the single-particle space is partitioned into occupied and virtual subspaces, of respective sizes N and $M \equiv K - N$,

$$(c_1, \cdots, c_N, c_{N+1}, \cdots, c_K) \to (a_1, \cdots, a_N, b_1, \cdots, b_M). \tag{5.51}$$

Therefore, the reference state is:

$$|\Phi_0\rangle = a_1^\dagger a_2^\dagger \cdots a_N^\dagger |0\rangle, \tag{5.52}$$

and the (unnormalized) Thouless determinant is written as:

$$|z\} = \exp\Big(\sum_{\alpha} \sum_{\mu} z_{\mu\alpha} b_\mu^\dagger a_\alpha) |\Phi_0\rangle. \tag{5.53}$$

The dynamics of z under Hamiltonians such as that of Eq. (5.50) was examined in detail at Chapter 3; let us recall the essential formulas.[iv]

The key quantity is the reciprocal-space one-density matrix, which is obtained from z according to the recipe:

$$\Gamma = \begin{bmatrix} I_N \\ z \end{bmatrix} \varrho^{-1} \begin{bmatrix} I_N & z^\dagger \end{bmatrix}, \quad \text{with:} \quad \varrho \equiv I_N + z^\dagger z. \tag{5.54}$$

The Fock matrix F depends on the one-density through the mean-fields v; in the reciprocal

[iv] The dynamical equations were given before; they are reproduced here for mere convenience.

space representation their elements are given by

$$F_{pq} = \varepsilon_p \delta_{pq} + v_{pq}(\Gamma), \quad \text{with:} \quad v_{pq} = \sum_{sr} V_{pr\cdot qs} \Gamma_{sr}, \tag{5.55}$$

where ε_p are the sorted eigenvalues of Eq. (5.45) and $V_{pr\cdot qs}$ are the two-body integrals implicit in Eq. (5.50), which should result in the interaction term in the right-hand side of Eq. (5.49) (as we have mentioned, the purpose of the present methodology is precisely to avoid dealing with this quantity). Once the Fock matrix is constructed, the equations of motion for z are expressed as:

$$i\hbar \dot{z} = F_{21} + F_{22} z - F_{11} z - z F_{12} z \tag{5.56}$$

(recall the blockwise occupied/virtual space partitioning of Chapter 3). Finally, the action S is integrated from

$$\dot{S} = -\mathrm{tr}(F_{11}) - \tfrac{1}{2}\mathrm{tr}(F_{12} z + z^\dagger F_{21}) + \tfrac{1}{2}\mathrm{tr}(v\Gamma). \tag{5.57}$$

This summarizes the dynamics for the reciprocal-space Thouless parameters.

Now, while the mean-field v of the reciprocal representation has the general form depicted in (5.55), the lattice representation mean-field, denoted $\tilde{v}$, is particularly easy to compute – the expression is given in Eq. (5.9), where the Hubbard-model matrix $\tilde{u}$ – exemplified for the specific case $S = 4$ in Eq. (5.41) – must be substituted. The simplicity of the resulting formula is best appreciated if the spin structure of the lattice-space one-density matrix, denoted $\tilde{\Gamma}$, is considered; in the manner of §3.2.3, we have

$$\tilde{\Gamma} = \begin{bmatrix} \tilde{\Gamma}_{\uparrow\uparrow} & \tilde{\Gamma}_{\uparrow\downarrow} \\ \tilde{\Gamma}_{\downarrow\uparrow} & \tilde{\Gamma}_{\downarrow\downarrow} \end{bmatrix}, \tag{5.58}$$

where the spin blocks are of size $S \times S$. Then, putting Eq. (5.9) in matrix form, one finds, in the case $S = 3$, for instance, that the lattice-space mean-field matrix is

$$\tilde{v} = U \begin{bmatrix} (\tilde{\Gamma}_{\downarrow\downarrow})_{11} & 0 & 0 & -(\tilde{\Gamma}_{\uparrow\downarrow})_{11} & 0 & 0 \\ 0 & (\tilde{\Gamma}_{\downarrow\downarrow})_{22} & 0 & 0 & -(\tilde{\Gamma}_{\uparrow\downarrow})_{22} & 0 \\ 0 & 0 & (\tilde{\Gamma}_{\downarrow\downarrow})_{33} & 0 & 0 & -(\tilde{\Gamma}_{\uparrow\downarrow})_{33} \\ -(\tilde{\Gamma}_{\downarrow\uparrow})_{11} & 0 & 0 & (\tilde{\Gamma}_{\uparrow\uparrow})_{11} & 0 & 0 \\ 0 & -(\tilde{\Gamma}_{\downarrow\uparrow})_{22} & 0 & 0 & (\tilde{\Gamma}_{\uparrow\uparrow})_{22} & 0 \\ 0 & 0 & -(\tilde{\Gamma}_{\downarrow\uparrow})_{33} & 0 & 0 & (\tilde{\Gamma}_{\uparrow\uparrow})_{33} \end{bmatrix}. \tag{5.59}$$

Evidently, this simple form is due to the uncomplicated nature of the basic Hubbard matrix $\tilde{u}$.

Hence, there is an obvious motivation for seeking a connection between the reciprocal

and lattice mean-fields, $v(\Gamma)$ and $\tilde{v}(\tilde{\Gamma})$, respectively. For that purpose, it is convenient to write the transformation (5.44) in an abbreviated manner, using subscripts p, q in the range 1 to K:

$$\tilde{c}_p^\dagger = \sum_q c_q^\dagger Y_{qp}, \quad \tilde{c}_p = \sum_q X_{pq} c_q \quad \text{or} \quad |\chi_p\rangle = \sum_q |\phi_q\rangle Y_{qp}, \quad \langle\chi_p| = \sum_q X_{pq}\langle\phi_q|, \tag{5.60}$$

where $Y = X^{-1} = X^\dagger$. Notice that the unitary matrices X and Y are constructed from the Fourier coefficients of Eq. (5.44).[v]

Let us first consider the one-body term; using (5.60) we easily find the connection between lattice and reciprocal representations:

$$\sum_{pq} \tilde{\varepsilon}_{pq}\, \tilde{c}_p^\dagger \tilde{c}_q = \sum_{pq} \tilde{\varepsilon}_{pq} \sum_{p'q'} (c_{p'}^\dagger Y_{p'p})(X_{qq'} c_{q'}) = \sum_{p'q'} \Big(\sum_{pq} Y_{p'p} \tilde{\varepsilon}_{pq} X_{qq'} \Big) c_{p'}^\dagger c_{q'} \quad \Rightarrow \quad \varepsilon = Y \tilde{\varepsilon} X, \tag{5.61}$$

which is written in matrix form on the right (since ε is diagonal we see that X is the matrix whose columns are the eigenvectors of $\tilde{\varepsilon}$).

The transformation rule for any two-body operator is easily obtained by a similar calculation; the result is:

$$V_{pr\cdot qs} = \sum_{p'q'r's'} Y_{pp'} Y_{rr'}\, \tilde{V}_{p'r'\cdot q's'}\, X_{q'q} X_{s's}. \tag{5.62}$$

Next, we analyze the one-density. Its transformation rule can be derived in many ways. The most straightforward approach consists of using the connection formulas (3.100), which relate coherent-states $|w\rangle_\chi$ and $|z\rangle_\phi$ defined over distinct sets of single-particle orbitals, $|\chi\rangle$ and $|\phi\rangle$, respectively – this is the precise situation found here. Then, starting from the one-density definition, Eq. (3.56), and using the connection formulas (3.100) together with relations (5.60) we obtain:

$$\tilde{\Gamma}_{qp} = \langle w|\tilde{c}_p^\dagger \tilde{c}_q|w\rangle = \sum_{p'q'} e^{-i\varphi}\langle z|(c_{p'}^\dagger Y_{p'p})(X_{qq'} c_{q'})|z\rangle e^{i\varphi} = \sum_{p'q'} X_{qq'} \Gamma_{q'p'} Y_{p'p},$$

where φ is simply a geometrical phase [cf. §3.3]. In matrix form the above reads:

$$\tilde{\Gamma} = X\, \Gamma\, Y. \tag{5.63}$$

We are now ready to derive the transformation rule for the mean-fields. Starting from

[v] All transformation rules studied in this section were previously obtained, in a more general form, at §4.6; we find, however, that reproducing some of those calculations here, in a more restricted context, is less confusing than to invoke the results derived earlier.

the definition of in the reciprocal representation, we proceed as follows:

$$v_{pq} = \sum_{sr} V_{pr\cdot qs}\Gamma_{sr} = \sum_{p'q'r's'} Y_{pp'}\tilde{V}_{p'r'\cdot q's'}\Big(\sum_{sr} X_{s's}\Gamma_{sr}Y_{rr'}\Big)X_{q'q}$$
$$= \sum_{p'q'} Y_{pp'}\Big(\sum_{r's'} \tilde{V}_{p'r'\cdot q's'}\tilde{\Gamma}_{s'r'}\Big)X_{q'q} = \sum_{p'q'} Y_{pp'}\tilde{v}_{p'q'}X_{q'q},$$

where (5.63) was substituted in passing to the second line. We therefore confirm the expected result that mean-fields transform as one-body operators; in matrix form:

$$v = Y\tilde{v}X. \tag{5.64}$$

The above equation allows the reciprocal-space mean-field v to be obtained from the much more simple lattice-representation $\tilde{v}$, whose expression is exemplified in Eq. (5.59), by a simple similarity transform – this approach to the computation of v is much more efficient than building and handling the two-body integrals of the reciprocal representation.

Thus, the strategy to carry out the time evolution of individual Thouless determinants – which are elements of the guided-basis set employed in the multiconfigurational formula that we shall apply to the Hubbard ring problem – can be summarized as follows:

1. Input: z.

2. Build the one-density matrix in reciprocal representation ϕ:

   $$\Gamma = \begin{bmatrix} I_N \\ z \end{bmatrix} \varrho^{-1} \begin{bmatrix} I_N & z^\dagger \end{bmatrix}$$

   and store both Γ and the auxiliary quantity $\varrho = I_N + z^\dagger z$ for later purposes. The required inverse, ϱ^{-1}, is computed by Cholesky decomposition.[64]

3. Use transformation matrix X (and its hermitian-conjugate Y) to get the one-density in the lattice representation χ:

   $$\tilde{\Gamma} = X\,\Gamma\,Y$$

   and store $\tilde{\Gamma}$ for later purposes.

4. Use the Hubbard model matrix $\tilde{u}$ together with $\tilde{\Gamma}$ to build the mean-field matrix in the lattice representation χ:

   $\tilde{v}_{pq} = (\sum_s \tilde{u}_{ps}\tilde{\Gamma}_{ss})\delta_{pq} - \tilde{u}_{pq}\tilde{\Gamma}_{pq}$

   obs: see matrix form exemplified in Eq. (5.59).

5. Use the reciprocal-space energies ε together with previously computed quantities to construct both the mean-field and Fock matrices in the reciprocal representation ϕ:

   $$v = Y\,\tilde{v}\,X$$

   $$F = \varepsilon + v$$

6. Use F and v and previously computed quantities to evaluate $\dot{z}$ and $\dot{S}$:

$$i\hbar\,\dot{z} = F_{21} + F_{22}z - zF_{11} - zF_{12}z$$
$$\dot{S} = -\mathrm{tr}(F_{11}) - \tfrac{1}{2}\mathrm{tr}(F_{12}z + z^{\dagger}F_{21}) + \tfrac{1}{2}\mathrm{tr}(v\Gamma)$$

This is the basic routine used in the ordinary-differential equation solver that propagates individual Thouless determinants in the fermionic version of the multiconfigurational method. Additionally, as explained in §4.5, each trajectory is independently integrated in a parallel fashion according to the 'pave-the-way' scheme (this is the first stage of the scheme).

5.4.4 Two-representation approach to the multiconfigurational propagation

Let us now describe how the two-representation strategy is implemented with respect to the propagation of quantum amplitudes C in the multiconfigurational method.

We have seen earlier, at §4.6, that some of the basic ingredients of the fermionic CCS method are invariant by unitary transformations of the single-particle orbitals.[vi] In particular, it was established that the CCS coupling matrix Δ has the same numerical value if evaluated in terms of coherent states defined over distinct sets of underlying orbitals – in the case of the lattice and reciprocal representations, which is of our concern here, this property is mathematically stated as follows:

$$\Delta_{ij} = \Delta(z_i^*, z_j) = \tilde{\Delta}(w_i^*, w_j) = \tilde{\Delta}_{ij}. \tag{5.65}$$

This means that, even if the coherent-state basis functions $|z_i\rangle$ are defined in terms of reciprocal space orbitals ϕ, their quantum amplitudes $C_i = \langle z_i|\psi\rangle e^{-\frac{i}{\hbar}S_i}$ can be obtained by means of an 'hybrid' equation of motion:

$$i\hbar\,\dot{C}_i = \sum_j \omega_{ij}\tilde{\Delta}_{ij}D_j, \tag{5.66}$$

where $\tilde{\Delta}_{ij}$ is constructed using the lattice representation χ.

This is of great advantage since the coupling can be easily computed in the lattice representation – starting from the fermionic Hubbard-like expression (5.11), substituting the model matrix $\tilde{u}$ exemplified in Eq. (5.41), and once more invoking the spin structure (5.58) of the lattice-space one-density $\tilde{\Gamma}$, one finds that the matrix elements of $\tilde{\Delta}$ can be obtained from:

$$\Delta_{ij} = U\sum_{n=1}^{S}\Big[(\tilde{\Gamma}^{ij}_{\uparrow\uparrow} - \tilde{\Gamma}^{ii}_{\uparrow\uparrow})_{nn}(\tilde{\Gamma}^{ij}_{\downarrow\downarrow} - \tilde{\Gamma}^{ii}_{\downarrow\downarrow})_{nn} - (\tilde{\Gamma}^{ij}_{\uparrow\downarrow} - \tilde{\Gamma}^{ii}_{\uparrow\downarrow})_{nn}(\tilde{\Gamma}^{ij}_{\downarrow\uparrow} - \tilde{\Gamma}^{ii}_{\downarrow\uparrow})_{nn}\Big]. \tag{5.67}$$

[vi] The discussion at §4.6 addresses the more general scenario where distinct sets of orbitals can be used for *ket* and *bra* coherent states. The situation here is more simple and the results enunciated below are adapted accordingly.

Above, we have abbreviated: $\tilde{\Gamma}^{ij}_{\sigma\sigma'} = \tilde{\Gamma}(w_i^*, w_j)_{\sigma\sigma'}$, where variables w refer to Thouless parameters defined over lattice-space orbitals $|\chi\rangle$ – these auxiliary variables are never handled explicitly since the lattice one-density $\tilde{\Gamma}^{ij}$ can be directly obtained by a similarity transform (see 'step 4' in the algorithm described below). Notice that, in the present context, labels ij refer to the coherent-state basis elements (and *not* to atomic sites as in §5.4.1), ranging from 1 to m (the basis-set size).

The lattice-space coupling (5.67) can be written in an even more compact form if we define a set of auxiliary vectors:

$$\begin{aligned} \delta\tilde{\gamma}^{ij}_{\uparrow\uparrow} &= \mathrm{diag}(\tilde{\Gamma}^{ij}_{\uparrow\uparrow} - \tilde{\Gamma}^{ii}_{\uparrow\uparrow}), \quad \delta\tilde{\gamma}^{ij}_{\uparrow\downarrow} = \mathrm{diag}(\tilde{\Gamma}^{ij}_{\uparrow\downarrow} - \tilde{\Gamma}^{ii}_{\uparrow\downarrow}), \\ \delta\tilde{\gamma}^{ij}_{\downarrow\uparrow} &= \mathrm{diag}(\tilde{\Gamma}^{ij}_{\downarrow\uparrow} - \tilde{\Gamma}^{ii}_{\downarrow\uparrow}), \quad \delta\tilde{\gamma}^{ij}_{\downarrow\downarrow} = \mathrm{diag}(\tilde{\Gamma}^{ij}_{\downarrow\downarrow} - \tilde{\Gamma}^{ii}_{\downarrow\downarrow}), \end{aligned} \tag{5.68}$$

whose components are the diagonals of the spin blocks of the lattice-space difference matrix $\tilde{\Gamma}(w_i^*, w_j) - \tilde{\Gamma}(w_i^*, w_i)$. In this way, Eq. (5.67) reduces to

$$\Delta_{ij} = U(\delta\tilde{\gamma}^{ij}_{\uparrow\uparrow} \cdot \delta\tilde{\gamma}^{ij}_{\downarrow\downarrow} - \delta\tilde{\gamma}^{ij}_{\uparrow\downarrow} \cdot \delta\tilde{\gamma}^{ij}_{\downarrow\uparrow}), \tag{5.69}$$

where the '$\cdot$' denotes a standard S-dimensional scalar vector product. This represents a huge simplification if compared with the general fermionic form of Eq. (4.76). The multiconfigurational algorithm is summarized below, in two separate stages.

Stage 1. The phased overlap and coupling matrices, ω and $\tilde{\Delta}$, are constructed element-wise:

1. Inputs (previously computed during trajectory propagation):

   i) $\{z_i, S_i\}$ and $\{z_j, S_j\}$ (ϕ-representation).

   ii) ϱ_{ii}, ϱ_{jj} (ϕ-representation).

   ii) ϕ and χ diagonal one-densities: $\{\Gamma^{ii}, \Gamma^{jj}\}$ and $\{\tilde{\Gamma}^{ii}, \tilde{\Gamma}^{jj}\}$.

2. Compute mixed density ij entry in ϕ-representation:

   $$\Gamma^{ij} = \begin{bmatrix} I_N \\ z_j \end{bmatrix} \varrho_{ij}^{-1} \begin{bmatrix} I_N & z_i^\dagger \end{bmatrix},$$

   and store auxiliary quantity: $\varrho_{ij} = I_N + z_i^\dagger z_j$. The required inverse $(\varrho_{ij})^{-1}$ is explicitly computed (LU decomposition is used). [vii]

3. Compute ij entry of the phased overlap [LU decomposition is used to evaluate $\det(\varrho_{ij})$]

   $$\omega_{ij} = [\det(\varrho_{ij})/\sqrt{\det(\varrho_{ii})\det(\varrho_{jj})}]\, e^{\frac{i}{\hbar}(S_j - S_i)}.$$

[vii] Explicit inverses should always be avoided; this is a rule of thumb in numerics. However, this operation does not bring difficulties to our simulations, since the size of matrix ϱ is $N \times N$, and we have work with $N \leq 4$.

4. Using X and Y compute the ij entry of the mixed one-density in χ-representation:
   $\tilde{\Gamma}^{ij} = X\,\Gamma^{ij}\,Y$.

5. Using the Hubbard matrix $\tilde{u}$ and the above quantities, compute the ij entry of the CCS coupling:
   $\tilde{\Delta}_{ij} = U(\delta\tilde{\gamma}^{ij}_{\uparrow\uparrow}\cdot\delta\tilde{\gamma}^{ij}_{\downarrow\downarrow} - \delta\tilde{\gamma}^{ij}_{\uparrow\downarrow}\cdot\delta\tilde{\gamma}^{ij}_{\downarrow\uparrow})$,
   where the vectors $\delta\tilde{\gamma}^{ij}$ are defined in Eq. (5.68).

Stage 2. Once ω and $\tilde{\Delta}$ are completed, amplitude propagation is performed in the following way:

1. Input (vector/matrix form):
   $\{C, \omega, \Delta\}$.

2. Compute auxiliary amplitude D by solving linear system:
   $\omega\,D = C$.
   obs: this is done by LU decomposition of ω.

3. Compute $\dot{C}$ from:
   $i\hbar\,\dot{C}_i = \sum_j \Omega_{ij}\,\Delta_{ij}\,D_j$.

The computed derivatives are then used in a fourth-order Runge-Kutta stepper routine. As explained in §4.5, the code additionally implements a 'pave-the-way' parallel scheme.

5.4.5 Initial state and sampling

As discussed earlier, in order to avoid complications associated with the sampling of the initial conditions for a generic initial wavefunction, we shall take the initial state to be itself a coherent state. In the present fermionic context this means that $|\psi_0\rangle$ is simply a Thouless determinant $|z_0\rangle$.

Since we are considering the weak-coupling regime, it would be natural to take the initial state as the reference state $|\Phi_0\rangle = |z_0 = 0\rangle$ for all runs. However, we observe that the ensuing dynamics turns out to be uninteresting, since the wavefunction most often departs very little from the non-interacting ground-state $|z_0 = 0\rangle$. The propagation is simply not challenging enough – it would be a poor way of testing the CCS methodology.

A richer dynamics can be achieved if the initial wavefunction is taken to be a *random* Thouless determinant, with the z_0 variables sampled around the origin; that is, with the initial configuration still rather close to the non-interacting ground-state, but overlaping with a larger number of excited Fock configurations.

This, in turn, raises the question of how to generate the random initial state and the surrounding initial conditions. Adequate coordinates must be chosen for that purpose. We have found that *hyper-spherical angles* propitiate a satisfactory sampling: when these coordinates are employed, a steady increase in the overlap matrix conditioning factor $\beta(\Omega)$ is observed as more basis functions are added, eventually reaching the saturation point, defined by a threshold value of the basis set conditioning. This indicates that the phase-space region in the vicinities of the reference state is being efficiently populated with basis functions.

In our simulations, M-dimensional hyper-spherical parametrizations are used for each column of the Thouless array z, with independent sets of angles being assigned for the real and imaginary parts of the column entries; mathematically:

$$\begin{aligned}
q_{1,\alpha} &= \tan(\Theta_\alpha^{(q)}/2)\cos(\varphi_{1,\alpha}^{(q)}) \\
q_{2,\alpha} &= \tan(\Theta_\alpha^{(q)}/2)\sin(\varphi_{1,\alpha}^{(q)})\cos(\varphi_{2,\alpha}^{(q)}) \\
q_{3,\alpha} &= \tan(\Theta_\alpha^{(q)}/2)\sin(\varphi_{1,\alpha}^{(q)})\sin(\varphi_{2,\alpha}^{(q)})\cos(\varphi_{3,\alpha}^{(q)}) \\
&\vdots \\
q_{M-1,\alpha} &= \tan(\Theta_\alpha^{(q)}/2)\sin(\varphi_{1,\alpha}^{(q)})\sin(\varphi_{2,\alpha}^{(q)})\cdots\sin(\varphi_{M-2,\alpha}^{(q)})\cos(\varphi_{M-1,\alpha}^{(q)}) \\
q_{M,\alpha} &= \tan(\Theta_\alpha^{(q)}/2)\sin(\varphi_{1,\alpha}^{(q)})\sin(\varphi_{2,\alpha}^{(q)})\cdots\sin(\varphi_{M-2,\alpha}^{(q)})\sin(\varphi_{M-1,\alpha}^{(q)}),
\end{aligned}$$

where $q_{\mu\alpha} = \{\mathrm{Re}(z_{\mu\alpha}), \mathrm{Im}(z_{\mu\alpha})\}$, with $1 \leq \mu \leq M$ and $1 \leq \alpha \leq N$. Notice that the hyper-radius of each column α is also parametrized by an angle, $\Theta_\alpha^{(q)}$. The ranges of these 'polar' and 'axial' angles are: $0 \leq \Theta \leq \pi$ and $0 \leq \varphi < 2\pi$.

The same procedure is adopted when generating the initial state angles and the basis set initial conditions; it can be summarized as follows: each angle of the set (Θ, φ), corresponding to either the real or imaginary part of one of the columns of z, is chosen from a normal distribution according to the prescriptions:

$$P(\Theta) \propto \exp\Big[-(\Theta-\Theta_c)^2/2w_\Theta^2\Big], \quad P(\varphi) \propto \exp\Big[-(\varphi-\varphi_c)^2/2w_\varphi^2\Big], \tag{5.70}$$

where $P(\Theta)$ and $P(\varphi)$ stand for the probability of choosing particular values for Θ and φ. The width parameters, w_Θ and w_φ, are the same for all the columns of the z array. For the initial state z_0, which is sampled around the origin, we have: $\Theta_c = 0$ and $\varphi_c = 0$ for all entries. For the initial conditions, which, in turn, are sampled around the initial state, we have $\Theta_c = \Theta_0$ and $\varphi_c = \varphi_0$ for all entries, that is, the central coordinates of the normal distribution are the initial-state angles. The sampling widths w_Θ and w_φ for initial state generation have different values than those employed in the sampling of initial conditions.

The hyper-spherical angles represent the 'adequate' sampling coordinates mentioned in §4.4; the normal distributions shown in (5.70) are the 'weight functions'. The above formulas are implemented within the sampling protocol explained in §4.4.

5.4.6 Exact quantum propagation (Full-CI)

The CCS results are compared with exact quantum data obtained by trivial propagation in the eigenstate basis of the quantum Hamiltonian. The latter is constructed in the lattice representation according to the matrix-element rules presented in §D.1 – this is the so-called 'Full Configuration Interaction' (Full-CI) Hamiltonian. The randomly generated initial Thouless determinant $|z_0\rangle$ is first projected in reciprocal occupation number space, using the Fock decompositon of Eq. (3.27). The resulting Fock state is transformed to lattice occupation number space using the transformation formulas given in §D.1.2. Finally, the lattice-space vector is projected into the Hamiltonian eigenstates, at which point propagation can be started.

5.4.7 Monitored quantities

In the simulations reported below the following quantities are computed as functions of time: the squared norm of the CCS wavefunction $\mathcal{N}(\psi)$; the basis set conditioning factor $\beta(\Omega)$, discussed in §4.4 (which depends solely on the overlap matrix Ω); the total energy $E(\psi)$; and the expectation value of the diagonal entries of the reciprocal-space one-density, i.e. the populations $n_q(\psi)$ of each reciprocal orbital $|\phi_q\rangle$, hereby called the 'tight-binding populations', $n_q(\psi)$. The formulas are:

$$\mathcal{N}(\psi) = \langle\psi|\psi\rangle = \sum_i C_i^* D_i, \tag{5.71a}$$

$$\beta(\Omega) = \lambda_{\max}(\Omega)\lambda_{\min}^{-1}(\Omega), \tag{5.71b}$$

$$E(\psi) = \langle\psi|\hat{H}|\psi\rangle = \sum_{ij} D_i^* \omega_{ij} D_j \sum_{pq} [\varepsilon_p \delta_{pq} + \tfrac{1}{2} v_{pq}(z_i^*, z_j)]\Gamma_{qp}(z_i^*, z_j), \tag{5.71c}$$

$$n_q(\psi) = \langle\psi|c_q^\dagger c_q|\psi\rangle = \sum_{ij} D_i^* \omega_{ij} D_j \Gamma_{qq}(z_i^*, z_j), \quad q = 1, 2, \ldots, K. \tag{5.71d}$$

Additionally, the auto-correlation function $a(\psi; t)$ (ACF) is computed through the formula $a(\psi; t) = \langle\psi_0|\psi_t\rangle = \sum_{j=1}^m \langle z_0|z_j\rangle D_j e^{iS_j}$. As discussed in Appendix E, the spectral density can be obtained from the ACF by a Fourier transform:

$$I_g(\psi; E) = \pi^{-1} \int_0^\infty dt\, g_\tau^{(k)}(t)\, \mathrm{Re}\,[\, a(\psi; t) e^{\frac{i}{\hbar}Et}\,], \tag{5.72}$$

where $g_\tau^{(k)}(t)$ is a window function of the form given in Eq. (E.10). This quantity indicates which energy eigenstates of the quantum system play a role in the dynamics.

5.4.8 Runs: general remarks

We report a total of six runs, organized according to the size of the fermionic Fock space f, which takes the values: $f = 220,\ 495,\ 560,\ 816,\ 2024,\ 4845$; in each of these runs, the number of degrees of freedom on a given CCS basis element is, correspondently: $d = 27,\ 32,\ 39,\ 45,\ 63,\ 64$. The simulations were performed with different settings for most of the system's parameters – these are indicated in the graphs and figure captions, together with the size of the employed CCS basis set m, the phase-space dimension d, and other quantities.

At each run, the number of electrons N is either 3 or 4, and the number of sites S is kept in the range $6 \leq S \leq 12$. These restrictions on the system size were necessary for two reasons: (i) so that exact quantum results could be computed; and (ii) so that the number of basis elements m required for each CCS run did not exceed ≈ 400 – after this threshold the propagation is slow, even when implemented with the 'pave-the-way' parallelization scheme (the machine where calculations were performed had 8 independent cores). Notice that setting $N = 1$ is not interesting since the mean-field approximation is exact in this case. At the same time, systems with only $N = 2$ electrons (for S in the range mentioned earlier) are simply two small: the basis set ends up filling the entire Hilbert space, with $m = f$ at the saturation point, meaning that there is nothing to gain from using the CCS method – hence, we work with $N = 3, 4$. Meanwhile, the Coulomb repulsion strength varies slightly across runs, staying in the range $0.22\ \text{eV} \leq U \leq 0.44\ \text{eV}$. The magnetic field is set to $B = 3000$ T in all but the first and last simulations.

The time increment for the CCS propagation was the same in all runs: $h = 0.020\ \hbar \cdot \text{eV}^{-1} = 1.32 \times 10^{-2}$ fs. Also, the random angular coordinates for real and imaginary parts were selected from normal distributions with the same width (specific sampling details are given in the corresponding figure). In addition to the basis-set conditioning criterion for sampling, initial conditions $z_i(0)$ had to display a minimum overlap with $|z_0\rangle$ in order to be accepted, i.e. they had to satisfy $\langle z_i(0)|z_0\rangle > 10^{-3}$.

The overall behavior is as follows: the basis set retains a high conditioning factor throughout all propagations. This means that basis elements maintain a significant overlap with each other, despite the fact that the phase-space dimensions d involved are quite large – this suggests that fermionic coherent states of the special unitary group, despite their intrinsic minimum uncertainty property, are much more spread-out in phase-space than their bosonic counterparts, at least in the vicinities of the reference state.

In accordance with the above, only small energy fluctuations are observed, meaning that, for each run, the basis set projector is providing a reasonable representation of the identity operator. This is reflected in the accuracy of the average tight-binding populations $n_q(\psi)$ and auto-correlation functions $a(\psi)$; these results are in excellent agreement with those obtained from the Full-CI approach for the runs where the two-body interaction

strength U is weaker, but they are still good for the runs having larger values of this parameter (the less accurate runs were terminated earlier, though) – evidently, this general trend is expected. We observe that, in all runs, tight-binding populations for most of the virtual orbitals are too small to be seen at the corresponding figure's scale.

An interesting comparison is made for the run with $S = 9$ sites and $N = 3$ electrons. Here, CCS results are compared to the mean-field prediction, i.e. results calculated with the 'classical propagation scheme', which, in the present case, is equivalent to a time-dependent Hartree-Fock calculation. The comparison shows how 'beyond mean-field' effects are incorporated into the CCS wavefunction (which, we recall, is constructed from a superposition of mean-field solutions).

In the next few pages results are presented without further analysis – some additional information is found in each figure's caption.

5.4.9 Run: $S = 6$ sites, $N = 3$ electrons.

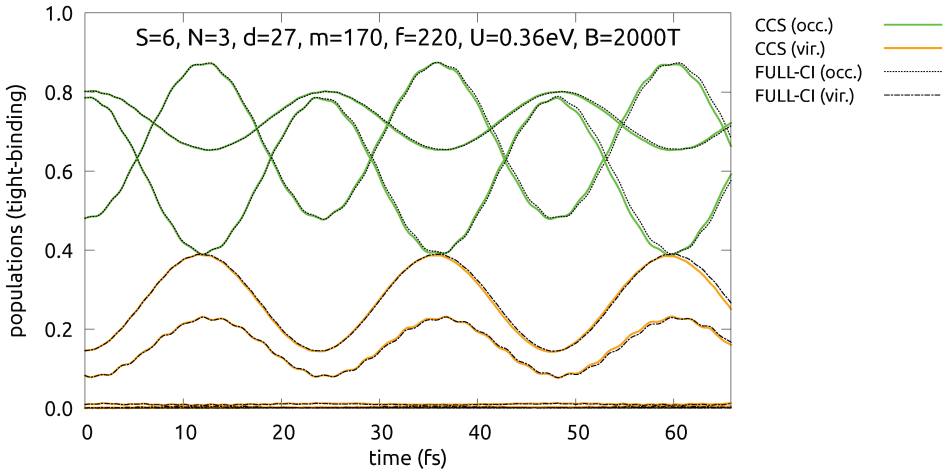

Figure 5.20: Tight-binding populations $n_q(\psi)$, $1 \leq q \leq 12$, as a function of time. CCS results (solid lines) are compared to exact Full-CI data (dashed/dotted lines). CCS populations for $N = 3$ occupied and $M = 9$ virtual orbitals are plotted with different colors (see legend on the right). The number of degrees of freedom in each Thouless determinant is $d = 27$, and the reference state is the non-interacting ground-state; the main parameters for this run are indicated in this and the subsequent graphs (additionally: $\mu_0 B/\tau = 1.157676 \times 10^{-1}$ and $\theta = 5.687111 \times 10^{-2}$).

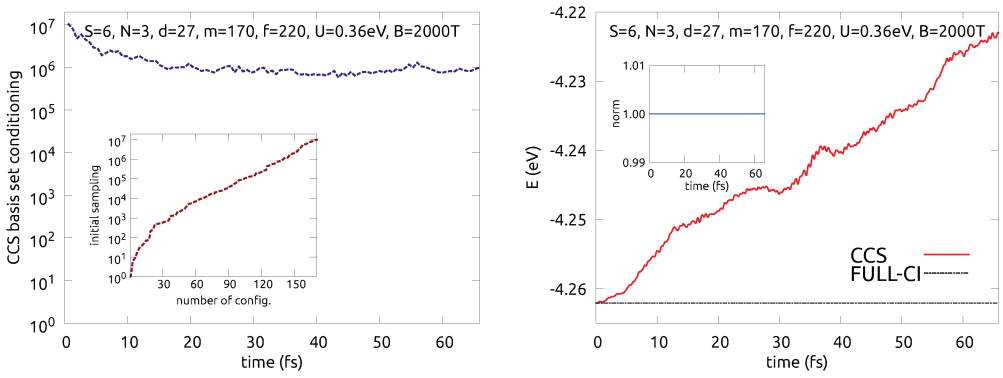

Figure 5.21: Left panel: basis set conditioning $\beta(\Omega)$ during propagation; inset: basis set conditioning increase curve during initial sampling. For this run the random initial state was generated with: $(w_\Theta, w_\varphi) = (0.50\pi, 1.00\pi)$ for polar and axial angles, respectively; the widths for the basis set sampling were $(w_\Theta, w_\varphi) = (0.25\pi, 0.50\pi)$ with conditioning threshold set to 10^7; saturation occurred at $m = 170$ basis elements. Right panel: total energy $E(\psi)$; inset: squared norm $N(\psi)$ (both plotted as functions of time).

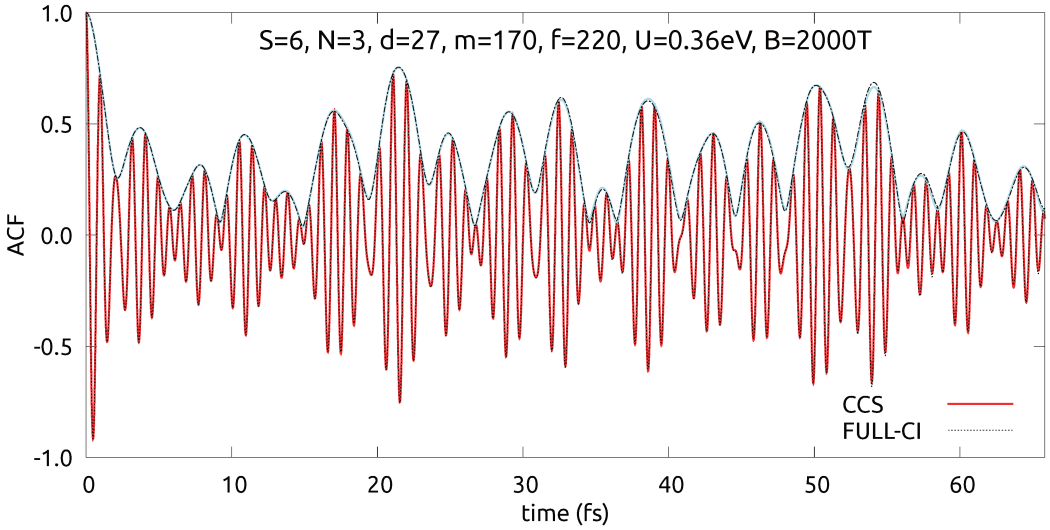

Figure 5.22: CCS auto-correlation function $a(\psi)$ (solid lines – red: real part, light-blue: absolute value) compared to the exact Full-CI time signal (dotted curve). Propagation was terminated at $t = 100\ \hbar \cdot \mathrm{eV}^{-1} = 65.82$ fs.

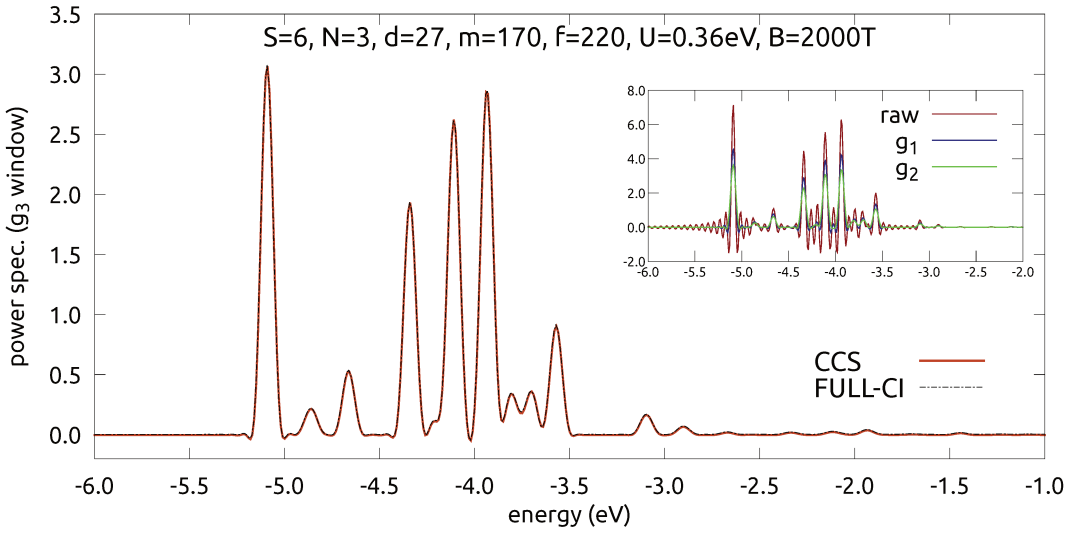

Figure 5.23: Spectral density $I_g(\psi, E)$ computed from the Fourier transform of the ACF $a(\psi)$ using a third-order window function. Spectra obtained from the CCS and Full-CI wavefunctions using the same filter are compared (solid line: CCS – dot-dashed line: Full-CI). Inset: same CCS spectrum computed with different filters.

5.4.10 Run: $S = 6$ sites, $N = 4$ electrons.

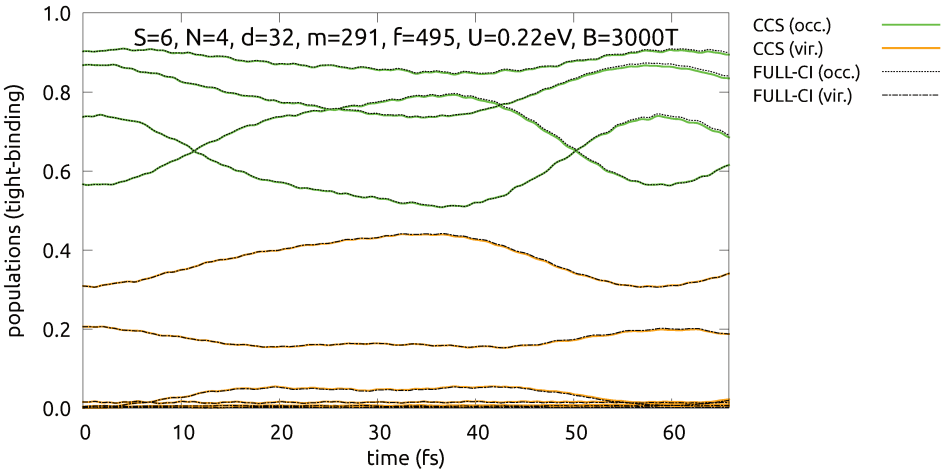

Figure 5.24: Tight-binding populations $n_q(\psi)$, $1 \leq q \leq 12$, as a function of time. CCS results (solid lines) are compared to exact Full-CI data (dashed/dotted lines). CCS populations for $N = 4$ occupied and $M = 8$ virtual orbitals are plotted with different colors (see legend on the right). The number of degrees of freedom in each Thouless determinant is $d = 32$, and the reference state is the non-interacting ground-state; the main parameters for this run are indicated in this and the subsequent graphs (additionally: $\mu_0 B/\tau = 1.736515 \times 10^{-1}$ and $\theta = 8.530666 \times 10^{-2}$).

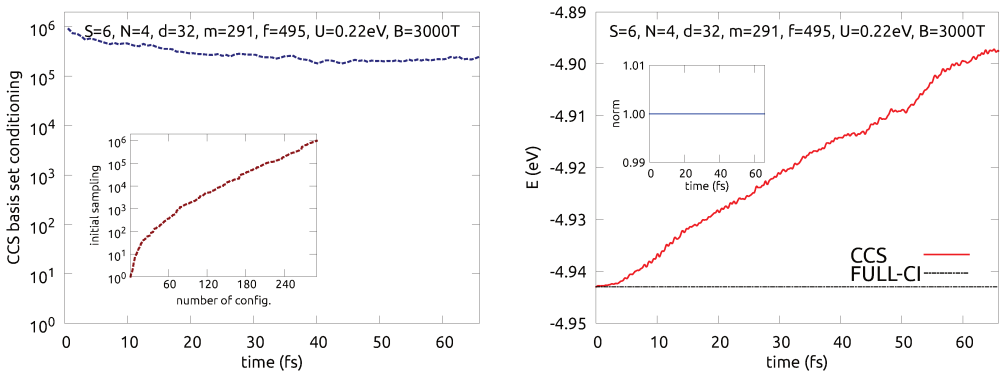

Figure 5.25: Left panel: basis set conditioning $\beta(\Omega)$ during propagation; inset: basis set conditioning increase curve during initial sampling. For this run the random initial state was generated with: $(w_\Theta, w_\varphi) = (0.40\pi, 0.80\pi)$ for polar and axial angles, respectively; the widths for the basis set sampling were $(w_\Theta, w_\varphi) = (0.25\pi, 0.50\pi)$ with conditioning threshold set to 10^6; saturation occurred at $m = 291$ basis elements. Right panel: total energy $E(\psi)$; inset: squared norm $N(\psi)$ (both plotted as functions of time).

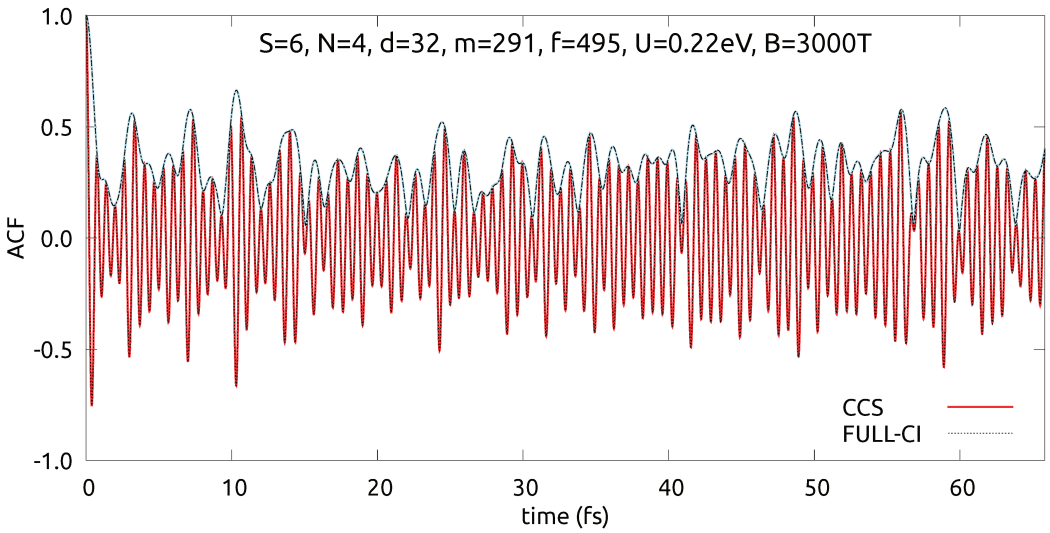

Figure 5.26: CCS auto-correlation function $a(\psi)$ (solid lines – red: real part, light-blue: absolute value) compared to the exact Full-CI time signal (dotted curve). Propagation was terminated at $t = 100\ \hbar \cdot \mathrm{eV}^{-1} = 65.82$ fs.

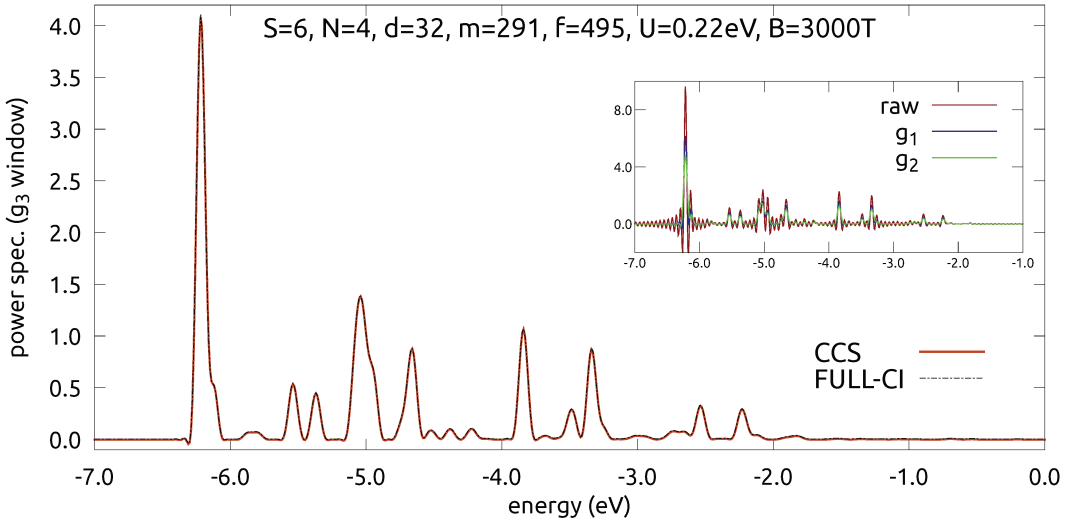

Figure 5.27: Spectral density $I_g(\psi, E)$ computed from the Fourier transform of the ACF $a(\psi)$ using a third-order window function. Spectra obtained from the CCS and Full-CI wavefunctions using the same filter are compared (solid line: CCS – dot-dashed line: Full-CI). Inset: same CCS spectrum computed with different filters.

5.4.11 Run: $S = 8$ sites, $N = 3$ electrons.

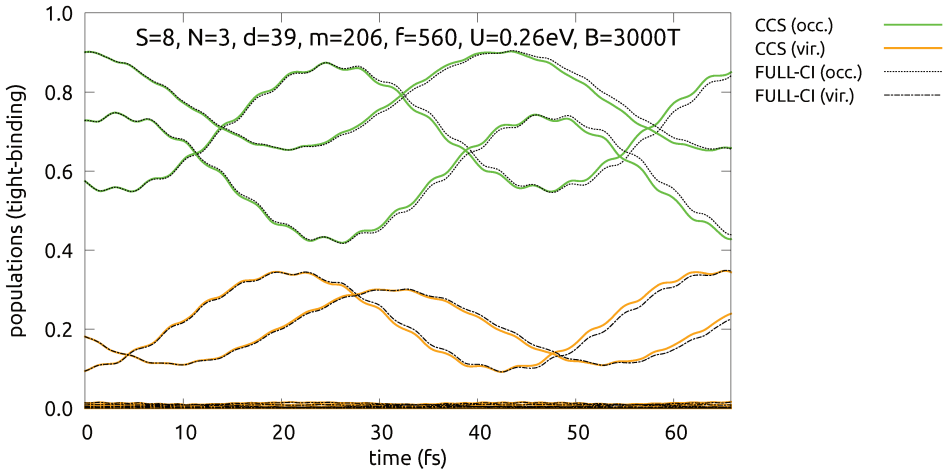

Figure 5.28: Tight-binding populations $n_q(\psi)$, $1 \leq q \leq 16$, as a function of time. CCS results (solid lines) are compared to exact Full-CI data (dashed/dotted lines). CCS populations for $N = 3$ occupied and $M = 15$ virtual orbitals are plotted with different colors (see legend on the right). The number of degrees of freedom in each Thouless determinant is $d = 39$, and the reference state is the non-interacting ground-state; the main parameters for this run are indicated in this and the subsequent graphs (additionally: $\mu_0 B/\tau = 1.736515 \times 10^{-1}$ and $\theta = 1.137472 \times 10^{-1}$).

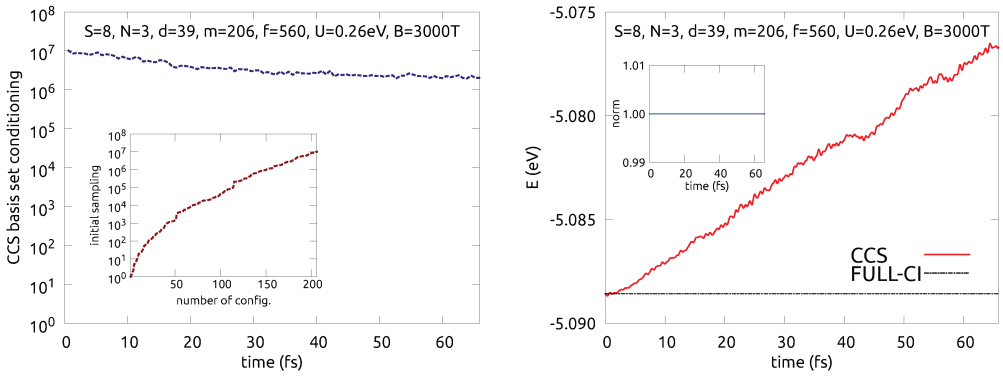

Figure 5.29: Left panel: basis set conditioning $\beta(\Omega)$ during propagation; inset: basis set conditioning increase curve during initial sampling. For this run the random initial state was generated with: $(w_\Theta, w_\varphi) = (0.40\pi, 0.40\pi)$ for polar and axial angles, respectively; the widths for the basis set sampling were $(w_\Theta, w_\varphi) = (0.25\pi, 0.50\pi)$ with conditioning threshold set to 10^7; saturation occurred at $m = 206$ basis elements. Right panel: total energy $E(\psi)$; inset: squared norm $N(\psi)$ (both plotted as functions of time).

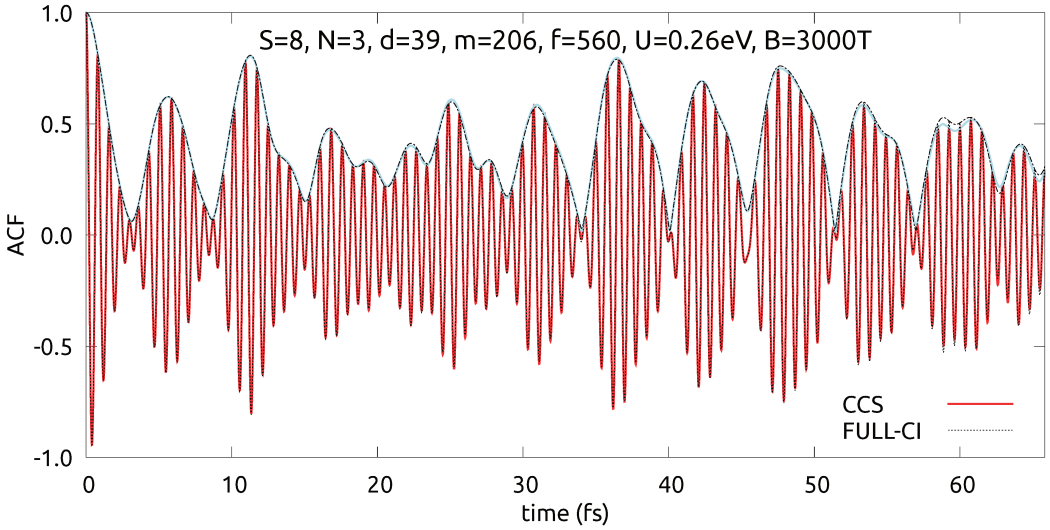

Figure 5.30: CCS auto-correlation function $a(\psi)$ (solid lines – red: real part, light-blue: absolute value) compared to the exact Full-CI time signal (dotted curve). Propagation was terminated at $t = 100\ \hbar \cdot \mathrm{eV}^{-1} = 65.82$ fs.

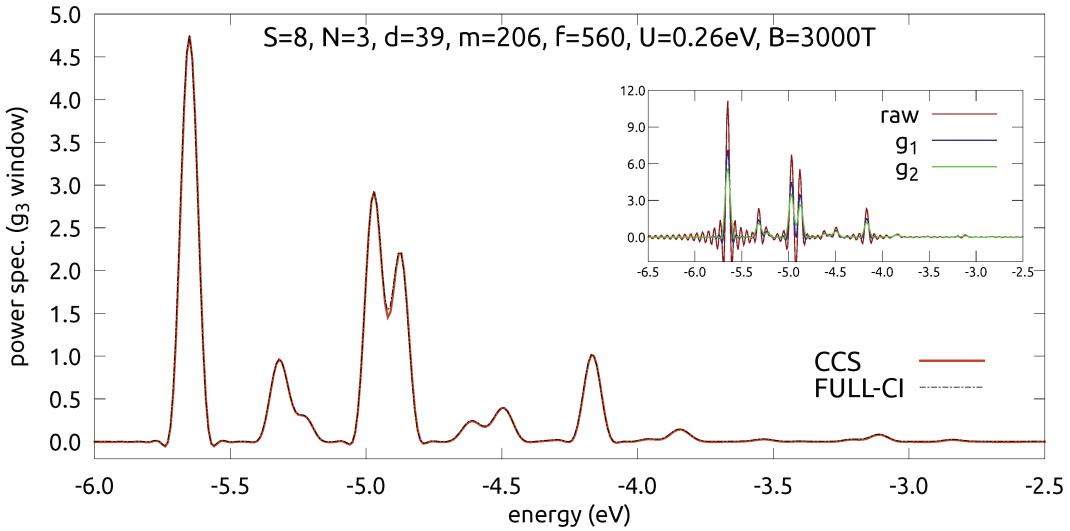

Figure 5.31: Spectral density $I_g(\psi, E)$ computed from the Fourier transform of the ACF $a(\psi)$ using a third-order window function. Spectra obtained from the CCS and Full-CI wavefunctions using the same filter are compared (solid line: CCS – dot-dashed line: Full-CI). Inset: same CCS spectrum computed with different filters.

5.4.12 Run: $S = 9$ sites, $N = 3$ electrons. (CCS vs. mean-field)

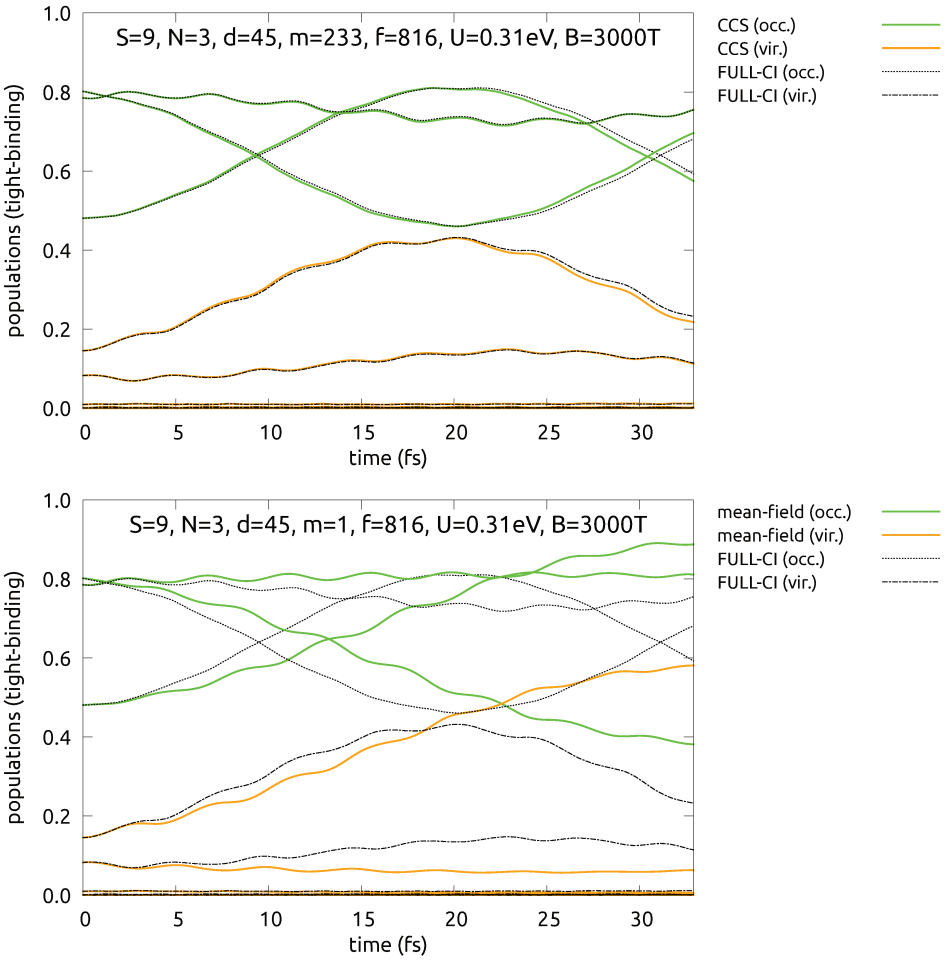

Figure 5.32: Tight-binding populations $n_q(\psi)$, $1 \leq q \leq 18$, as a function of time. CCS results (upper panel – solid lines) and the mean-field prediction (bottom panel – solid lines) are compared to exact Full-CI data (dashed/dotted lines in both panels). CCS and mean-field populations for $N = 3$ occupied and $M = 9$ virtual orbitals are plotted with the same color code (see legends). Populations for most of the virtual orbitals are too small to be seen at each figure's scale. The reference state is the non-interacting ground-state; the main parameters for this run are indicated in this and the subsequent graphs (additionally: $\mu_0 B/\tau = 1.736515 \times 10^{-1}$ and $\theta = 1.279600 \times 10^{-1}$).

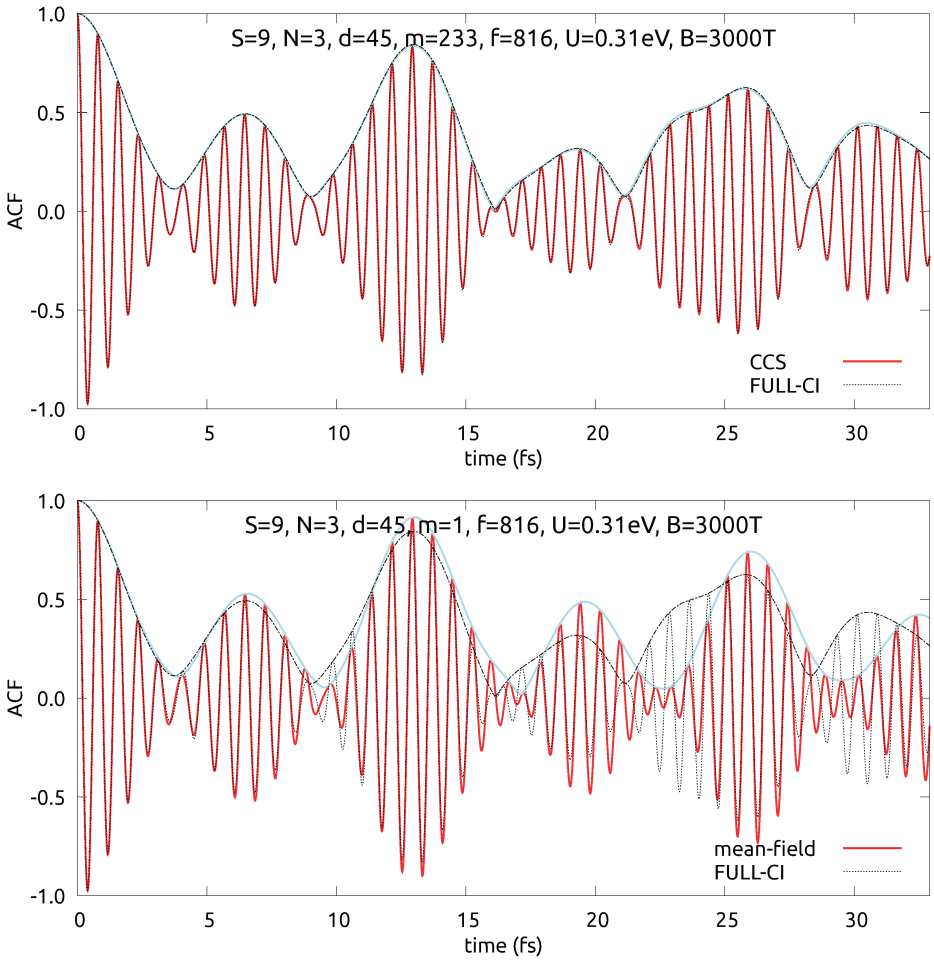

Figure 5.33: CCS (solid lines – upper panel) and mean-field (solid lines – bottom panel) auto-correlation functions $a(\psi)$ compared to the exact Full-CI time signal (dotted curve in both panels). The color code is the same for CCS and mean-field plots: red: real part, light-blue: absolute value. Propagation was terminated at $t = 50\ \hbar \cdot \mathrm{eV}^{-1} = 32.91$ fs.

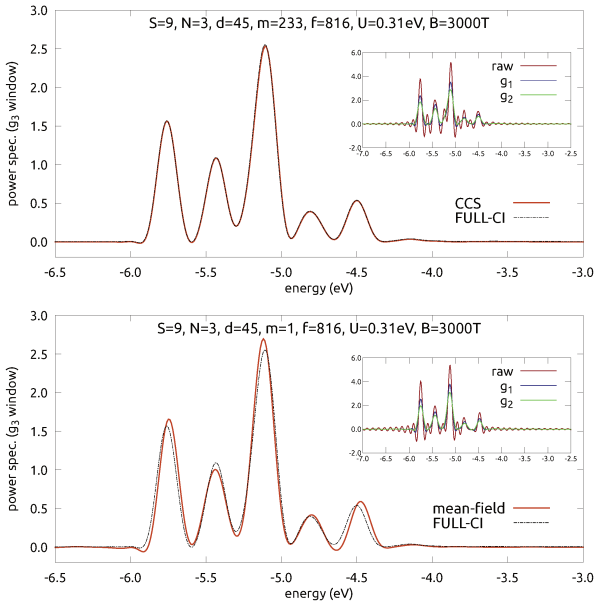

Figure 5.34: Spectral density $I_g(\psi, E)$ computed from the Fourier transform of the ACF $a(\psi)$ using a third-order window function. Spectra obtained from CCS (solid line – upper panel) and mean-field (solid line – bottom panel) wavefunctions are compared to the Full-CI result (dot-dashed line in both panels) using the same filters.

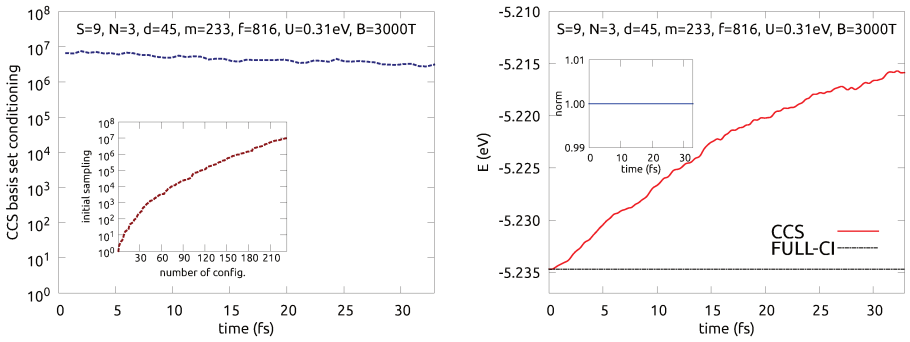

Figure 5.35: Left panel: basis set conditioning $\beta(\Omega)$ during propagation; inset: basis set conditioning increase curve during initial sampling. For this run the random initial state was generated with: $(w_\Theta, w_\varphi) = (0.50\pi, 1.00\pi)$ for polar and axial angles, respectively; the widths for the basis set sampling were $(w_\Theta, w_\varphi) = (0.25\pi, 0.50\pi)$ with conditioning threshold set to 10^7 and minimum overlap with $|z_0\rangle$ set to 10^{-3}; saturation occurred at $m = 170$ basis elements. Right panel: total energy $E(\psi)$; inset: squared norm $N(\psi)$ (both plotted as functions of time).

5.4.13 Run: $S = 12$ sites, $N = 3$ electrons.

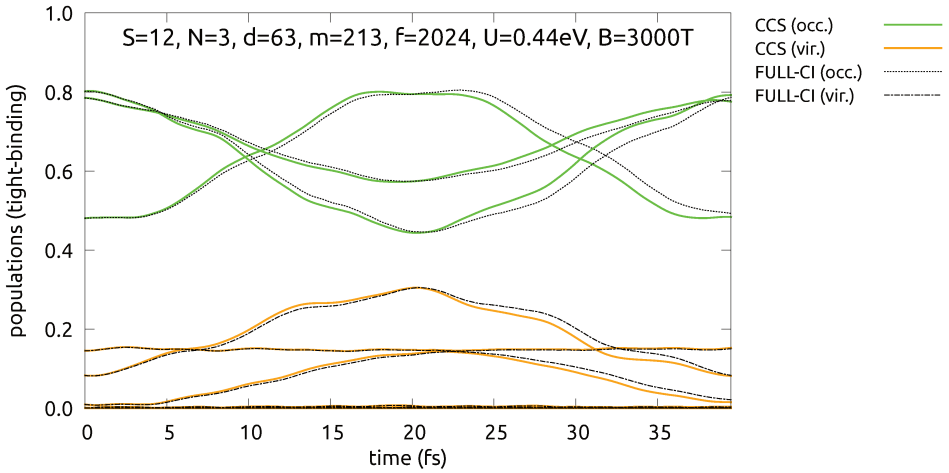

Figure 5.36: Tight-binding populations $n_q(\psi)$, $1 \leq q \leq 24$, as a function of time. CCS results (solid lines) are compared to exact Full-CI data (dashed/dotted lines). CCS populations for $N = 3$ occupied and $M = 21$ virtual orbitals are plotted with different colors (see legend on the right). The number of degrees of freedom in each Thouless determinant is $d = 63$, and the reference state is the non-interacting ground-state; the main parameters for this run are indicated in this and the subsequent graphs (additionally: $\mu_0 B/\tau = 1.736515 \times 10^{-1}$ and $\theta = 1.706133 \times 10^{-1}$).

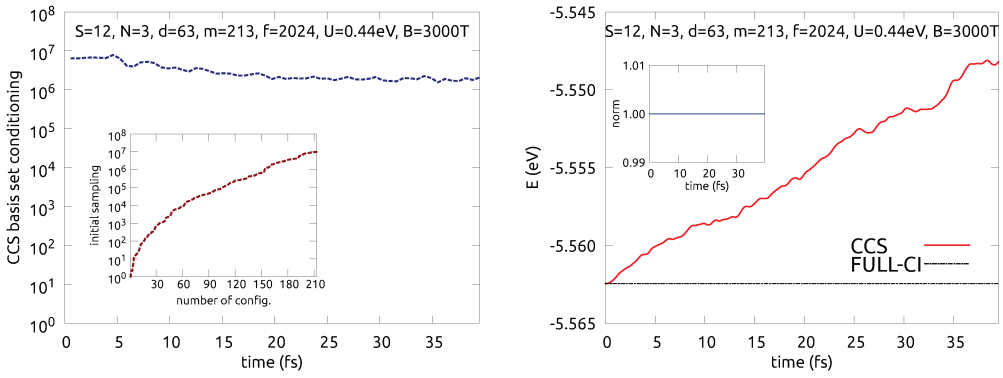

Figure 5.37: Left panel: basis set conditioning $\beta(\Omega)$ during propagation; inset: basis set conditioning increase curve during initial sampling. For this run the random initial state was generated with: $(w_\Theta, w_\varphi) = (0.50\pi, 1.00\pi)$ for polar and axial angles, respectively; the widths for the basis set sampling were $(w_\Theta, w_\varphi) = (0.25\pi, 0.50\pi)$ with conditioning threshold set to 10^7; saturation occurred at $m = 213$ basis elements. Right panel: total energy $E(\psi)$; inset: squared norm $N(\psi)$ (both plotted as functions of time).

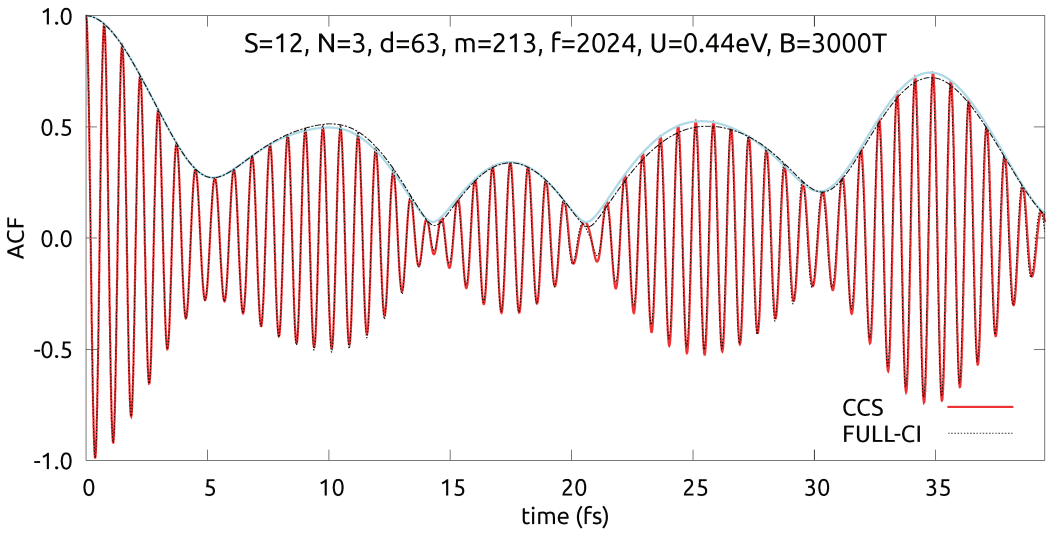

Figure 5.38: CCS auto-correlation function $a(\psi)$ (solid lines – red: real part, light-blue: absolute value) compared to the exact Full-CI time signal (dotted curve). Propagation was terminated at $t = 60\ \hbar \cdot \mathrm{eV}^{-1} = 39.49$ fs.

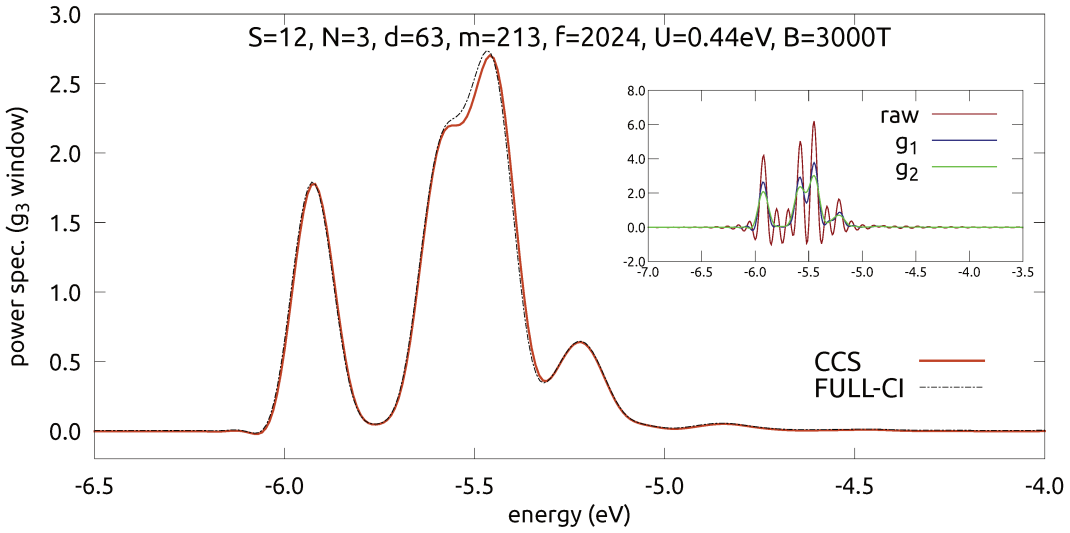

Figure 5.39: Spectral density $I_g(\psi, E)$ computed from the Fourier transform of the ACF $a(\psi)$ using a third-order window function. Spectra obtained from the CCS and Full-CI wavefunctions using the same filter are compared (solid line: CCS – dot-dashed line: Full-CI). Inset: same CCS spectrum computed with different filters.

5.4.14 Run: $S = 10$ sites, $N = 4$ electrons.

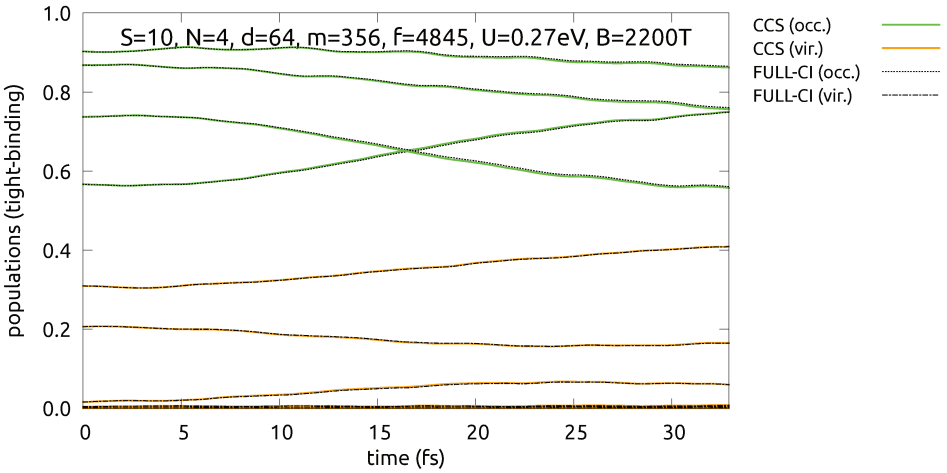

Figure 5.40: Tight-binding populations $n_q(\psi)$, $1 \leq q \leq 20$, as a function of time. CCS results (solid lines) are compared to exact Full-CI data (dashed/dotted lines). CCS populations for $N = 4$ occupied and $M = 16$ virtual orbitals are plotted with different colors (see legend on the right). The number of degrees of freedom in each Thouless determinant is $d = 64$, and the reference state is the non-interacting ground-state; the main parameters for this run are indicated in this and the subsequent graphs (additionally: $\mu_0 B/\tau = 1.273444 \times 10^{-1}$, $\theta = 1.042637 \times 10^{-1}$).

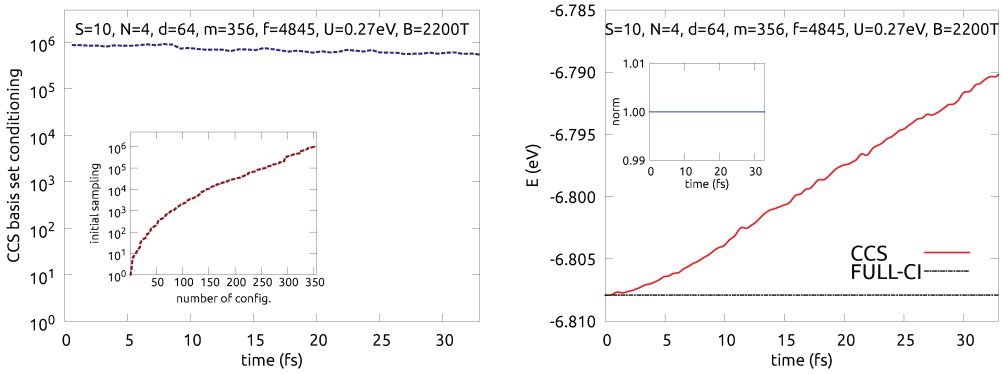

Figure 5.41: Left panel: basis set conditioning $\beta(\Omega)$ during propagation; inset: basis set conditioning increase curve during initial sampling. For this run the random initial state was generated with: $(w_\Theta, w_\varphi) = (0.40\pi, 0.80\pi)$ for polar and axial angles, respectively; the widths for the basis set sampling were $(w_\Theta, w_\varphi) = (0.25\pi, 0.50\pi)$ with conditioning threshold set to 10^6; saturation occurred at $m = 356$ basis elements. Right panel: total energy $E(\psi)$; inset: squared norm $N(\psi)$ (both plotted as functions of time)

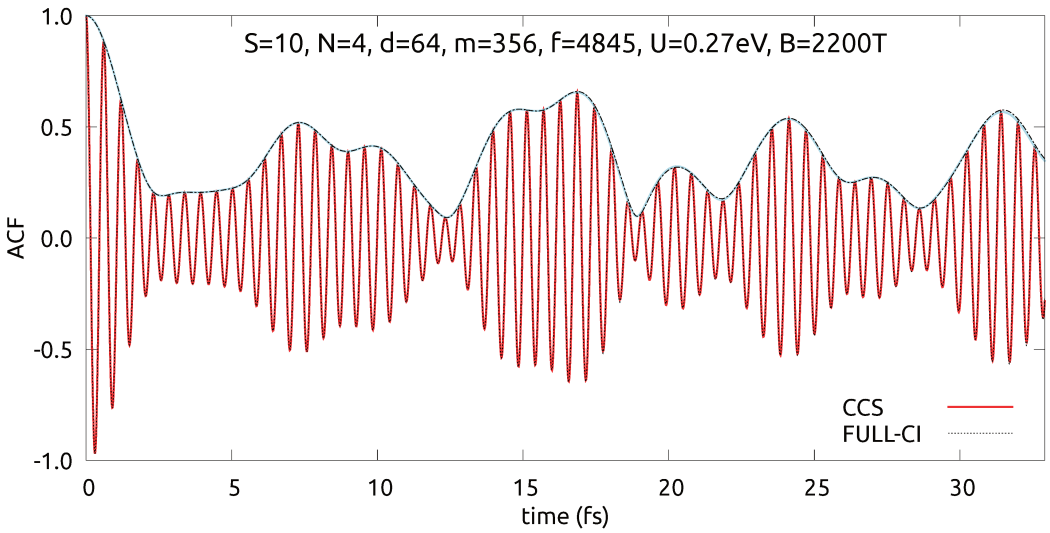

Figure 5.42: CCS auto-correlation function $a(\psi)$ (solid lines – red: real part, light-blue: absolute value) compared to the exact Full-CI time signal (dotted curve). Propagation was terminated at $t = 50\ \hbar \cdot \mathrm{eV}^{-1} = 32.91$ fs.

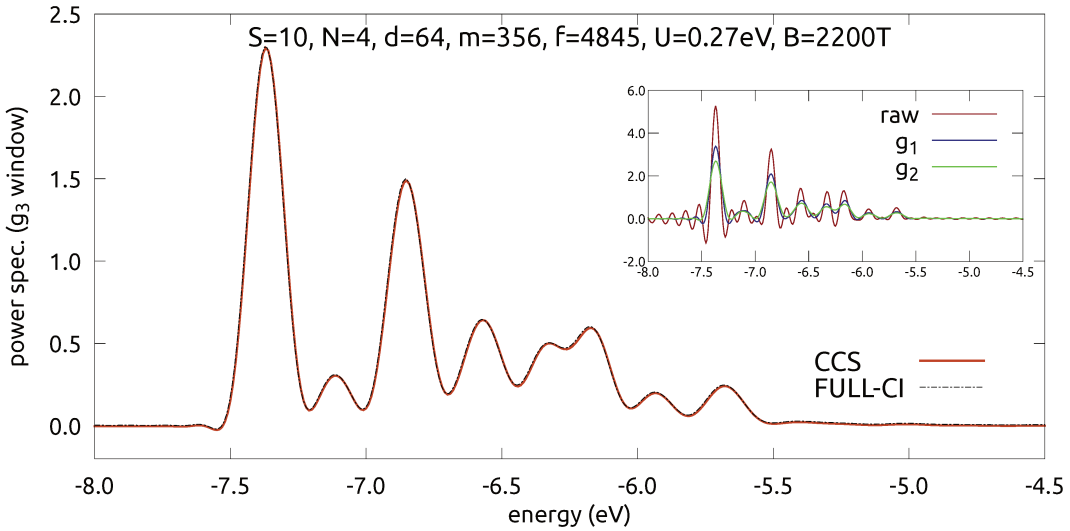

Figure 5.43: Spectral density $I_g(\psi, E)$ computed from the Fourier transform of the ACF $a(\psi)$ using a third-order window function. Spectra obtained from the CCS and Full-CI wavefunctions using the same filter are compared (solid line: CCS – dot-dashed line: Full-CI). Inset: same CCS spectrum computed with different filters.

Chapter 6

Semiclassical initial-value representation

Overview. A semiclassical approximation for the generalized coherent-state propagator is devised. The resulting expression is recognized as a semiclassical initial-value representation formula, which involves a phase-space integral over a swarm of initial conditions, each spawning a classical trajectory with an associated complex amplitude. The overall strategy adopted here is parallel to that of earlier works based on Gaussian wavepackets, particularly Ref. [70]. The present derivation, however, is conducted with a greater level of detail if compared to previous treatments, with emphasis given to certain points which are commonly overlooked. Following this calculation, aspects of the numerical implementation of the semiclassical approach are discussed, and a particularly convenient propagation scheme is advanced.

6.1 The stability matrix

In what follows we shall adopt a 'phase-space flow' picture of classical dynamics, whereupon the coordinates of a given trajectory at time $t > 0$ are seen as functions of the initial conditions at time $t = 0$. For convenience, we introduce the shorthand notation

$$\begin{cases} z_{t\alpha} = z_\alpha(z_0^*, z_0, t) \\ z_{t\alpha}^* = z_\alpha^*(z_0^*, z_0, t) \end{cases} \qquad \text{for} \;\; 1 \leq \alpha \leq d, \tag{6.1}$$

where the time label is indicated as the leftmost subscript. We work with complex notation, treating z and z^* as independent variables.

Roughly stated, the idea of stability relates to the question of how neighbour points in phase space move over time – whether they get closer or farther apart as the flow develops. Let us then inquire on how small deviations of initial conditions $(\delta z_0, \delta z_0^*)$, centred at some reference orbit $z(t)$, evolve into deviations $(\delta z_\tau, \delta z_\tau^*)$ at a later instant τ.

Embracing the flow picture and using the chain rule we obtain:

$$\delta z_{\tau\alpha} = \sum_\beta \frac{\partial z_{\tau\alpha}}{\partial z_{0\beta}} \delta z_{0\beta} + \sum_\beta \frac{\partial z_{\tau\alpha}}{\partial z^*_{0\beta}} \delta z^*_{0\beta},$$
$$\delta z^*_{\tau\alpha} = \sum_\beta \frac{\partial z^*_{\tau\alpha}}{\partial z_{0\beta}} \delta z_{0\beta} + \sum_\beta \frac{\partial z^*_{\tau\alpha}}{\partial z^*_{0\beta}} \delta z^*_{0\beta}.$$

Introducing the column vectors $\delta z = (\delta z_1, \delta z_2, \ldots, \delta z_d)^T$ and $\delta z^* = (\delta z^*_1, \delta z^*_2, \ldots, \delta z^*_d)^T$ the latter can be organized in matrix form:

$$\begin{pmatrix} \delta z_\tau \\ \delta z^*_\tau \end{pmatrix} = M(\tau) \begin{pmatrix} \delta z_0 \\ \delta z^*_0 \end{pmatrix} = \begin{pmatrix} M_{11}(\tau) & M_{12}(\tau) \\ M_{21}(\tau) & M_{22}(\tau) \end{pmatrix} \begin{pmatrix} \delta z_0 \\ \delta z^*_0 \end{pmatrix}, \tag{6.2}$$

where the $2d \times 2d$ matrix M and its $d \times d$ blocks were given an implicit definition.[i] The matrix M is called the *stability matrix* – it connects small deviations at initial and final times and in this way encompasses information about the neighborhood of the reference orbit – this will be better appreciated when we discuss the semiclassical approximation. Evidently, $M(0) = I_{2d}$.

Excluding the case of very simple systems, the elements of the stability matrix cannot be computed explicitly; rather, one must compute them numerically for each individual orbit by integrating, in addition to the orbit's classical equations of motion, a linear system of equations – one that we now proceed to find.

Let us consider the classical equations [cf. Eqs. (1.72)] from the flow perspective:

$$\frac{dz_{t\alpha}}{dt} = -\frac{i}{\hbar} \sum_\gamma g^{-T}_{\alpha\gamma}(z^*_t, z_t) \frac{\partial E(z^*_t, z_t)}{\partial z^*_{t\gamma}} = \dot{z}_\alpha(z^*_0, z_0, t) = \dot{z}_{t\alpha}, \tag{6.3a}$$
$$\frac{dz^*_{t\alpha}}{dt} = \frac{i}{\hbar} \sum_\gamma g^{-1}_{\alpha\gamma}(z^*_t, z_t) \frac{\partial E(z^*_t, z_t)}{\partial z_{t\gamma}} = \dot{z}^*_\alpha(z^*_0, z_0, t) = \dot{z}^*_{t\alpha}. \tag{6.3b}$$

Thus $\dot{z}_{t\alpha}$ and $\dot{z}^*_{t\alpha}$ are also to be understood as implicit functions of the initial conditions through the variables $z_t = z(z^*_0, z_0, t)$ and $z^*_t = z^*(z^*_0, z_0, t)$, and the same abbreviated notation is assigned to these quantities. Next we note that derivatives taken with respect to t commute with those taken with respect to components of either z_0 or z^*_0; so, for example, if we differentiate (6.3a) with respect to $z_{0\beta}$ we obtain:

$$\frac{\partial}{\partial z_{0\beta}} \frac{dz_{t\alpha}}{dt} = \sum_\gamma \frac{\partial \dot{z}_{t\alpha}}{\partial z_{t\gamma}} \frac{\partial z_{t\gamma}}{\partial z_{0\beta}} + \sum_\gamma \frac{\partial \dot{z}_{t\alpha}}{\partial z^*_{t\gamma}} \frac{\partial z^*_{t\gamma}}{\partial z_{0\beta}} = \frac{d}{dt} \frac{\partial z_{t\alpha}}{\partial z_{0\beta}} = \dot{M}_{11}(t)_{\alpha\beta},$$

with the derivatives of $\dot{z}_{t\alpha}$ and $\dot{z}^*_{t\alpha}$ explicitly given by (with time labels momentarily

[i] The convention is that index '1' refers to variable z, whereas index '2' refers to the complex conjugate variable z^*; thus $M_{11}(\tau)_{\alpha\beta} = (\partial z_{\tau\alpha}/\partial z_{0\beta})$, $M_{21}(\tau)_{\alpha\beta} = (\partial z^*_{\tau\alpha}/\partial z_{0\beta})$, and so on. Also, the stability matrix is often called 'tangent matrix' or, if the reference trajectory is periodic, the 'monodromy matrix'.

omitted):

$$\frac{\partial \dot{z}_\alpha}{\partial z_\gamma} = -\frac{i}{\hbar}\sum_{\gamma'}\left(\frac{\partial g^{-T}_{\alpha\gamma'}}{\partial z_\gamma}\frac{\partial E}{\partial z^*_{\gamma'}} + g^{-T}_{\alpha\gamma'}\frac{\partial^2 E}{\partial z^*_{\gamma'}\partial z_\gamma}\right),$$
$$\frac{\partial \dot{z}_\alpha}{\partial z^*_\gamma} = -\frac{i}{\hbar}\sum_{\gamma'}\left(\frac{\partial g^{-T}_{\alpha\gamma'}}{\partial z^*_\gamma}\frac{\partial E}{\partial z^*_{\gamma'}} + g^{-T}_{\alpha\gamma'}\frac{\partial^2 E}{\partial z^*_{\gamma'}\partial z^*_\gamma}\right).$$

Expressions for the time derivatives of the remaining elements of the stability matrix are found in a similar fashion; the complete system is:

$$\dot{M}_{11}(t)_{\alpha\beta} = \sum_\gamma \frac{\partial \dot{z}_{t\alpha}}{\partial z_{t\gamma}} M_{11}(t)_{\gamma\beta} + \sum_\gamma \frac{\partial \dot{z}_{t\alpha}}{\partial z^*_{t\gamma}} M_{21}(t)_{\gamma\beta}, \tag{6.4a}$$
$$\dot{M}_{21}(t)_{\alpha\beta} = \sum_\gamma \frac{\partial \dot{z}^*_{t\alpha}}{\partial z_{t\gamma}} M_{11}(t)_{\gamma\beta} + \sum_\gamma \frac{\partial \dot{z}^*_{t\alpha}}{\partial z^*_{t\gamma}} M_{21}(t)_{\gamma\beta}, \tag{6.4b}$$
$$\dot{M}_{12}(t)_{\alpha\beta} = \sum_\gamma \frac{\partial \dot{z}_{t\alpha}}{\partial z_{t\gamma}} M_{12}(t)_{\gamma\beta} + \sum_\gamma \frac{\partial \dot{z}_{t\alpha}}{\partial z^*_{t\gamma}} M_{22}(t)_{\gamma\beta}, \tag{6.4c}$$
$$\dot{M}_{22}(t)_{\alpha\beta} = \sum_\gamma \frac{\partial \dot{z}^*_{t\alpha}}{\partial z_{t\gamma}} M_{12}(t)_{\gamma\beta} + \sum_\gamma \frac{\partial \dot{z}^*_{t\alpha}}{\partial z^*_{t\gamma}} M_{22}(t)_{\gamma\beta}. \tag{6.4d}$$

The above equations can be integrated alongside the trajectory's equation of motion from a given initial condition (z_0, z_0^*) together with $M(0) = I_{2d}$. Notice that the sub-blocks are coupled only in pairs: M_{11} and M_{21}; M_{12} and M_{22} – this is just a consequence of our choice to work with complex variables, a choice that brings some redundancies, e.g. $M_{22} = M_{11}^*$, and $M_{12} = M_{21}^*$. So, in principle, there are just $2d^2$ free complex parameters in M.

The linear system (6.4) is best expressed in matrix form as:

$$\begin{pmatrix} \dot{M}_{11}(t) & \dot{M}_{12}(t) \\ \dot{M}_{21}(t) & \dot{M}_{22}(t) \end{pmatrix} = \begin{pmatrix} R_{11}(t) & R_{12}(t) \\ R_{21}(t) & R_{22}(t) \end{pmatrix} \begin{pmatrix} M_{11}(t) & M_{12}(t) \\ M_{21}(t) & M_{22}(t) \end{pmatrix}, \tag{6.5}$$

or more succinctly:

$$\dot{M}(t) = R(t)M(t) \quad \text{with} \quad M(0) = I_{2d}, \tag{6.6}$$

with the matrix R and its blocks implicitly defined by (6.4) and (6.5) – R is nothing but the Jacobian matrix of the classical dynamical system. Again, the complex notation brings with it some redundancies; in this case: $R_{22} = R_{11}^*$, and $R_{21} = R_{12}^*$.

6.1.1 Symplectic properties

As a result of the Hamiltonian structure of the equations of motion the stability matrix has a number of interesting properties. For instance, it can be shown to satisfy the constraint:[29]

$$M \begin{pmatrix} 0 & -g_0^{-T} \\ g_0^{-1} & 0 \end{pmatrix} M^T = \begin{pmatrix} 0 & -g_t^{-T} \\ g_t^{-1} & 0 \end{pmatrix}, \tag{6.7}$$

where we abbreviate: $M = M(t)$, $g_0 = g(z_0^*, z_0)$, and $g_t = g(z_t^*, z_t)$. We recognize (6.7) as a curved-phase-space version of the symplectic condition obeyed by the stability matrix of canonical, i.e. flat-phase-space, classical systems (a case which is recovered by putting $g = I_d$).

Relations amongst individual blocks can be directly deduced from (6.7):

$$M_{12}\, g_0^{-1} M_{11}^T - M_{11}\, g_0^{-T} M_{12}^T = 0, \tag{6.8a}$$

$$M_{11}\, g_0^{-T} M_{22}^T - M_{12}\, g_0^{-1} M_{21}^T = g_t^{-T}, \tag{6.8b}$$

showing that there are actually less than $2d^2$ free complex parameters in M. A complementary set of relations can also be found by further manipulating (6.7): multiplying on the left by M^{-1} and on the right by M^{-T}, and subsequently inverting both sides of the resulting equation leads to:

$$M^T \begin{pmatrix} 0 & g_t \\ -g_t^T & 0 \end{pmatrix} M = \begin{pmatrix} 0 & g_0 \\ -g_0^T & 0 \end{pmatrix}, \tag{6.9}$$

which in blockwise form reads:

$$M_{11}^T\, g_t M_{21} - M_{21}^T\, g_t^T M_{11} = 0, \tag{6.10a}$$

$$M_{11}^T\, g_t M_{22} - M_{21}^T\, g_t^T M_{12} = g_0. \tag{6.10b}$$

Moreover, we note that identity (6.7) also unlocks an explicit expression for the inverse of the stability matrix; multiplying on the left by M^{-1} and performing the straightforward inversion of the matrix with off-diagonal blocks $-g_t^{-T}$ and g_t^{-1} we get:

$$M^{-1} = \begin{pmatrix} 0 & -g_0^{-T} \\ g_0^{-1} & 0 \end{pmatrix} M^T \begin{pmatrix} 0 & g_t \\ -g_t^T & 0 \end{pmatrix} \tag{6.11}$$

– that is, the inverse of M can be easily obtained from its transpose.

Lastly, it follows from (6.7) that, even though we cannot, in the general case, obtain explicit expressions for the elements of the stability matrix, its determinant is always given by:

$$\det M(t) = \frac{\det g(z_0^*, z_0)}{\det g(z_t^*, z_t)}. \tag{6.12}$$

This result can also be derived through an alternative approach – see Eq. (A.5) in Appendix A.

6.2 Integral expression for the coherent-state propagator

Our purpose is to find a semiclassical expression for the time evolution operator $\hat{U}(\tau)$, with τ denoting the elapsed time.[ii] The starting point is the coherent-state propagator K, the transition amplitude between two coherent states, here labeled z_0 and w:

$$\begin{aligned} K(w^*, z_0; \tau) &= \langle w|\hat{U}(\tau)|z_0\rangle \\ &= \{w|\hat{U}(\tau)|z_0\}\, e^{-\frac{1}{2}f(w^*,w)-\frac{1}{2}f(z_0^*,z_0)} \equiv \tilde{K}_\tau(w^*, z_0)\, e^{-\frac{1}{2}f(w^*,w)-\frac{1}{2}f(z_0^*,z_0)}. \end{aligned} \tag{6.13}$$

Most of the time we shall find more convenient to work with the quantity $\tilde{K}_\tau(w^*, z_0)$, which is analytic in both its complex arguments – this is just the usual propagator striped from unimportant normalization factors.

In keeping with the spirit of the techniques so far presented we seek to express the propagator in terms of a basis set guided by classical trajectories – i.e. as an initial-value representation. This can be accomplished with the help of the closure relation written in the specific form:

$$\hat{1} = \int d\mu(\zeta_\tau)|\zeta_\tau\rangle\langle\zeta_\tau| = \int d\mu(\zeta_0)|\zeta_\tau\rangle\langle\zeta_\tau|, \tag{6.14}$$

where ζ_τ is a time-dependent coherent-state label, bound to obey the equation of motion (1.72) and evaluated at $t = \tau$, the final propagation time. In accordance with the flow picture discussed previously, this should be understood as $\zeta_\tau = \zeta_\tau(\zeta_0^*, \zeta_0)$. As indicated, the integral is to be performed with the phase-space measure evaluated at initial time $t = 0$. Since the measure is invariant under the classical flow this change of integration domain comes at no expense – i.e. the Jacobian of the transformation from $d\mu(\zeta_\tau)$ to $d\mu(\zeta_0)$ is unity – cf. Appendix A.

We then proceed by inserting the identity (6.14) into the matrix element that defines $\tilde{K}$ in Eq. (6.13) and performing the following sequence of manipulations:

$$\begin{aligned} \tilde{K}_\tau(w^*, z_0) &= \int d\mu(\zeta_0)\{w|\zeta_\tau\rangle\langle\zeta_\tau|\hat{U}(\tau)|z_0\} \\ &= \int d\mu(\zeta_0)\{w|\zeta_\tau\rangle\Big[\frac{\langle\zeta_\tau|\hat{U}(\tau)|z_0\}}{\langle\zeta_0|z_0\}}\Big]\langle\zeta_0|z_0\} \equiv \int d\mu(\zeta_0)\{w|\zeta_\tau\rangle\, \mathcal{U}_\tau(z_0; \zeta_0^*, \zeta_0)\, \langle\zeta_0|z_0\}. \end{aligned} \tag{6.15}$$

The implicitly defined function $\mathcal{U}_\tau(z_0; \zeta_0^*, \zeta_0)$ – analytic in z_0 and independent of the end-point variable w^* – will be the object of our considerations henceforth.

[ii] For brevity we write the time operator with a single time label, $\hat{U}(\tau)$, or sometimes even '$\exp(-\frac{i}{\hbar}\hat{H}\tau)$'. However, the derivation is also valid for Hamiltonians with explicit time dependence.

6.2.1 * Classical propagator and zeroth-order semiclassical approximation

In order to gain some insight, let us momentarily consider the case of a Hamiltonian $\hat{H}_0$ which is a linear function of the group generators of the chosen coherent-state representation – for both bosonic and fermionic representations that were studied in detail in previous chapters, this translates to the case of a non-interacting Hamiltonian.

In such systems the time evolution operator, denoted $\hat{U}^{(0)}(\tau) = \exp(-\frac{i}{\hbar}\hat{H}_0\tau)$, is in fact an element of the coherent-state's group, and we have seen at Chapter 1 that the effect of $\hat{U}^{(0)}(\tau)$ upon an initial coherent state $|\zeta_0\rangle$ is exactly given by:

$$\hat{U}^{(0)}(\tau)|\zeta_0\rangle = |\zeta_\tau(\zeta_0)\rangle e^{\frac{i}{\hbar}S_\tau(\zeta)}, \tag{6.16}$$

with ζ_τ being a holomorphic function of ζ_0 and the accumulated phase $S_\tau(\zeta)$ being precisely the classical action (1.74) evaluated over the trajectory $\zeta_\tau(\zeta_0)$. Concrete examples of this kind of dynamics were discussed in §2.2.3 and §3.2.5.

Using the unitary property of the evolution operator the latter equation may be rewritten as $\langle\zeta_\tau|\hat{U}^{(0)}(\tau) = e^{\frac{i}{\hbar}S_\tau(\zeta)}\langle\zeta_0|$, whence we find

$$\frac{[\langle\zeta_\tau|\hat{U}^{(0)}(\tau)]\cdot|z_0\}}{\langle\zeta_0|z_0\}} = \frac{e^{\frac{i}{\hbar}S_\tau(\zeta)}\langle\zeta_0|z_0\}}{\langle\zeta_0|z_0\}} \quad\Rightarrow\quad \mathcal{U}^{(0)}_\tau(\zeta_0^*,\zeta_0) = e^{\frac{i}{\hbar}S_\tau(\zeta)}. \tag{6.17}$$

Check. Before commenting on this result let us evaluate the consistency of the integral expression (6.15) for this particular scenario – according to (6.16) we must obtain $K^{(0)}(w^*,z_0;\tau) = \langle w|\hat{U}^{(0)}(\tau)|z_0\rangle = \langle w|z_\tau(z_0)\rangle e^{\frac{i}{\hbar}S_\tau(z)}$. For this purpose we write the (unnormalized) non-interacting propagator as

$$\tilde{K}^{(0)}_\tau(w^*,z_0) = \int d\mu(\zeta_0)\Upsilon(w^*;\zeta)\{\zeta_0|z_0\}e^{-f(\zeta_0^*,\zeta_0)}, \tag{6.18}$$

where we have defined the auxiliary quantities:

$$\Upsilon(w^*;\zeta) = \{w|\zeta_\tau(\zeta_0)\}\, e^{\gamma(\zeta)} \quad\text{and}\quad \gamma(\zeta) = \frac{i}{\hbar}A_\tau(\zeta_\tau^*,\zeta_0) - f(\zeta_\tau^*,\zeta_\tau), \tag{6.19}$$

with $A_\tau(\zeta_\tau^*,\zeta_0)$ being the complex action of Eq. (1.67), whose derivatives are listed in Eq. (1.71). We notice that consistency will be ensured through the reproducing kernel property (1.62b) as long as $\Upsilon(w^*;\zeta)$ is analytic on the variable ζ_0. Since in the present case we know $\zeta_\tau(\zeta_0)$ is holomorphic – and therefore so is $\{w|\zeta_\tau(\zeta_0)\}$ – it remains to be checked whether the phase $\gamma(\zeta)$ shares this attribute. And, as it turns out, its derivatives with respect to the components of the complex conjugate vector ζ_0^* all vanish identically:

$$\frac{\partial\gamma(\zeta)}{\partial\zeta^*_{0\mu}} = \sum_\nu\left[\left(\frac{i}{\hbar}\frac{\partial A_\tau(\zeta_\tau^*,\zeta_0)}{\partial\zeta^*_{\tau\nu}} - \frac{\partial f(\zeta_\tau^*,\zeta_\tau)}{\partial\zeta^*_{\tau\nu}}\right)\frac{\partial\zeta^*_{\tau\nu}}{\partial\zeta^*_{0\mu}} - \frac{\partial f(\zeta_\tau^*,\zeta_\tau)}{\partial\zeta_{\tau\nu}}\frac{\partial\zeta_{\tau\nu}}{\partial\zeta^*_{0\mu}}\right] = 0, \tag{6.20}$$

for the terms inside the parenthesis cancel due to (1.71) and the last term disappears because we know $(\partial\zeta_\tau/\partial\zeta_0^*) = 0$. Thus $\Upsilon(w^*;\zeta)$ is analytic in ζ_0 and by the reproducing kernel property the integral (6.18) reduces to:

$$\tilde{K}_\tau^{(0)}(w^*, z_0) = \Upsilon(w^*;\zeta_0)|_{\zeta_0=z_0}\,. \tag{6.21}$$

The expression for the non-interacting propagator $K_\tau^{(0)}(w^*, z_0;\tau)$ is then obtained by inserting normalization factors and reorganizing the exponentials:

$$\begin{aligned} K_\tau^{(0)}(w^*, z_0;\tau) &= [\{w|z_\tau(z_0)\}e^{\frac{i}{\hbar}A_\tau(z_\tau^*,z_0)-f(z_\tau^*,z_\tau)}]\; e^{-\frac{1}{2}f(w^*,w)-\frac{1}{2}f(z_0^*,z_0)} \\ &= e^{-\frac{1}{2}f(w^*,w)}\{w|z_\tau(z_0)\}e^{-\frac{1}{2}f(z_\tau^*,z_\tau)}e^{\frac{i}{\hbar}A_\tau(z_\tau^*,z_0)-\frac{1}{2}f(z_\tau^*,z_\tau)-\frac{1}{2}f(z_0^*,z_0)} \\ &= \langle w|z_\tau(z_0)\rangle e^{\frac{i}{\hbar}S_\tau(z)}, \end{aligned} \tag{6.22}$$

which is in agreement with the result expected from (6.16).

We now come back and explore Eq. (6.17). In Chapter 1, single coherent-state trial functions have been identified as classical approximations [cf. §1.3.3] (as previously mentioned, in the context of the bosonic and fermionic coherent states analyzed at Chapters 2 and 3, this is the same as identifying the mean-field description as a classical approximation). In conformity with this view, we define the *classical propagator* K^{cl}, as an approximated propagator for a *general* system:

$$K^{cl}(w^*, z_0;\tau) = \langle w|z_\tau(z_0)\rangle e^{\frac{i}{\hbar}S_\tau(z)}. \quad \text{(classical propagator)} \tag{6.23}$$

Thus the digression made earlier showed that whenever the Hamiltonian is linear in the group generators the exact propagator reduces to the classsical one (this is just another way of explaining what we mean by 'classical').

Now, consider the following possibility. One may attempt a new approximative scheme by replacing the function $\mathcal{U}$ appearing inside the generally valid integral expression (6.15) by the 'non-interacting' result (6.17) – this procedure gives rise to a slightly more sophisticated formula which we shall denominate (in lack of a better term) the *'zeroth-order' semiclassical propagator*:

$$K^{sc-0}(w^*, z_0;\tau) = \int d\mu(\zeta_0)\langle w|\zeta_\tau\rangle e^{\frac{i}{\hbar}S_\tau(\zeta)}\langle\zeta_0|z_0\rangle. \quad \text{(semiclassical, zeroth-order)} \tag{6.24}$$

Of course, the reproducing kernel property cannot be invoked here since for general systems ζ_τ depends on both ζ_0 and ζ_0^*. An interesting feature of (6.24) is that $\langle w|$ and $|z_0\rangle$ can be deleted leading to a 'zeroth-order' semiclassical approximation for the time evolution operator itself:

$$\hat{U}(\tau) \approx \hat{U}^{sc-0}(\tau) = \int d\mu(\zeta_0)|\zeta_\tau\rangle e^{\frac{i}{\hbar}S_\tau(\zeta)}\langle\zeta_0|. \tag{6.25}$$

This latter result is reminiscent of Heller's 'frozen Gaussian' propagator,[45] a well-known approach of wavepacket-based semiclassical theory. The result (6.25), particularized for the case of fermionic coherent states, has been studied by Suzuki in the context of nuclear dynamics.[18]

6.3 Semiclassical amplitude

The significance of the result (6.17) lies in the fact that it strongly hints on the form and properties that the function $\mathcal{U}$ must possess in the semiclassical regime which we are interested. In other words, the semiclassical formula we wish to develop for the propagator should represent an improvement over the result expressed in Eq. (6.24). Thus we set out to look for a semiclassical expression for $\mathcal{U}$ by means of the following *ansatz*:

$$\mathcal{U}_\tau(z_0;\zeta_0^*,\zeta_0) = \frac{\langle\zeta_\tau|\hat{U}(\tau)|z_0\rangle}{\langle\zeta_0|z_0\rangle} = D_\tau(z_0;\zeta_0^*,\zeta_0)e^{\frac{i}{\hbar}S_\tau(\zeta_0^*,\zeta_0)}, \tag{6.26}$$

where the new and key element is the complex amplitude, henceforth abbreviated $D_\tau(z_0;\zeta)$, which is assigned to each orbit that participates in the integral expression (6.15) of the propagator.

It should be emphasized that this does not amount to a meaningless redefinition of $\mathcal{U}$; the crucial point here is that, in a semiclassical context, and in view of the considerations made earlier, the amplitude $D_\tau(z_0;\zeta)$ – i.e. the specific combination of factors that it stands for as in (6.26) – can be regarded as a *smooth function* of the initial conditions (ζ_0^*,ζ_0) (at least during a sufficiently short interval $0 \leq t \leq \tau$) thus providing a route to conduct the required approximations.

In preparation for the subsequent stages of our derivation, we use (6.26) to organize the integral expression (6.15) in the following way:

$$\begin{aligned}\tilde{K}_\tau(w^*,z_0) &= \int d\mu(\zeta_0) D_\tau(z_0;\zeta)\{w|\zeta_\tau\rangle\langle\zeta_0|z_0\}e^{\frac{i}{\hbar}S_\tau(\zeta)} \\ &= \int d\mu(\zeta_0) D_\tau(z_0;\zeta)\{w|\zeta_\tau\}\{\zeta_0|z_0\}e^{\frac{i}{\hbar}A_\tau(\zeta_\tau^*,\zeta_0)-f(\zeta_\tau^*,\zeta_\tau)-f(\zeta_0^*,\zeta_0)} \\ &= \int d\mu(\zeta_0) D_\tau(z_0;\zeta)e^{F_\tau(z_0,w^*;\zeta)}.\end{aligned} \tag{6.27}$$

Here, things have been arranged so as to make the complex action $A_\tau(\zeta_\tau^*,\zeta_0)$ appear explicitly, since we intent to take advantage of its well-defined properties – recall the relation between $S_\tau(\zeta)$ and $A_\tau(\zeta_\tau^*,\zeta_0)$, displayed at Eq. (1.67). Also, at the last line, all factors multiplying $D_\tau(z_0;\zeta)$ have been combined into a complex phase F,

$$F_\tau(z_0,w^*;\zeta) = \frac{i}{\hbar}A_\tau(\zeta_\tau^*,\zeta_0) + f(w^*,\zeta_\tau) - f(\zeta_\tau^*,\zeta_\tau) + f(\zeta_0^*,z_0) - f(\zeta_0^*,\zeta_0). \tag{6.28}$$

So far we know that the amplitude $D_\tau(z_0;\zeta)$ should comply with a few requirements:

it must be unity at initial time – so that $K(w^*, z_0; 0)$ correctly reduces to $\langle w|z_0\rangle$; it must remain unity whenever the Hamiltonian is linear in the coherent-state's group generators – hence its time derivative must vanish identically in those cases; and, finally, it must be a smooth function of the initial variables (ζ_0^*, ζ_0). The next step is to enforce a dynamical condition upon $D_\tau(z_0; \zeta)$.

6.3.1 Equation of motion for the amplitude

As is well-known, the exact time-evolution operator satisfies Schrödinger's equation:

$$\frac{d\hat{U}(\tau)}{d\tau} + \frac{i}{\hbar}\hat{H}\,\hat{U}(\tau) = 0. \tag{6.29}$$

In terms of the non-normalized propagator the above reads:

$$\frac{d\tilde{K}_\tau(w^*, z_0)}{d\tau} = \{w|\frac{d\hat{U}(\tau)}{d\tau}|z_0\} = -\frac{i}{\hbar}\{w|\hat{H}\,\hat{U}(\tau)|z_0\}. \tag{6.30}$$

By enforcing this condition, and using the propagator's integral expression (6.27), we shall derive an equation of motion for the amplitude $D_\tau(z_0; \zeta)$.

Inserting the closure relation (6.14) on the right-hand side of the latter equation, we find:

$$\begin{aligned}
\frac{d\tilde{K}_\tau(w^*, z_0)}{d\tau} &= -\frac{i}{\hbar}\int d\mu(\zeta_0)\{w|\hat{H}|\zeta_\tau\rangle\langle\zeta_\tau|\hat{U}(\tau)|z_0\rangle \\
&= -\frac{i}{\hbar}\int d\mu(\zeta_0)\{w|\zeta_\tau\rangle\langle\zeta_0|z_0\}\Big[\frac{\{w|\hat{H}|\zeta_\tau\}}{\{w|\zeta_\tau\}}\Big]\Big[\frac{\langle\zeta_\tau|\hat{U}(\tau)|z_0\rangle}{\langle\zeta_0|z_0\rangle}\Big] \\
&= -\frac{i}{\hbar}\int d\mu(\zeta_0)\{w|\zeta_\tau\rangle\langle\zeta_0|z_0\}E(w^*, \zeta_\tau)D_\tau(z_0; \zeta)e^{\frac{i}{\hbar}S_\tau(\zeta)} \\
&= -\frac{i}{\hbar}\int d\mu(\zeta_0)E(w^*, \zeta_\tau)D_\tau(z_0; \zeta)e^{F_\tau(z_0, w^*; \zeta)},
\end{aligned} \tag{6.31}$$

where $E(w^*, \zeta_\tau)$ is the off-diagonal energy function, obtained by analytic continuation of its real-valued counterpart (a quantity which we are acquainted with from previous chapters).

On the other hand, differentiating with respect to τ under the integral sign of (6.27), we get:

$$\frac{d\tilde{K}_\tau(w^*, z_0)}{d\tau} = \int d\mu(\zeta_0)\left[\dot{D}_\tau(z_0; \zeta) + \dot{F}_\tau(z_0, w^*; \zeta)D_\tau(z_0; \zeta)\right]e^{F_\tau(z_0, w^*; \zeta)}, \tag{6.32}$$

where the total time derivative of the phase F [cf. Eq. (6.28)] is computed using the

complex action's properties (1.71) and applying the chain rule as follows:

$$\begin{aligned}\dot{F}_\tau(z_0,w^*;\zeta) &= \frac{i}{\hbar}\frac{\partial A_\tau(\zeta_\tau^*,\zeta_0)}{\partial\tau} + \frac{i}{\hbar}\sum_\alpha \frac{\partial A_\tau(\zeta_\tau^*,\zeta_0)}{\partial\zeta_{\tau\alpha}^*}\dot{\zeta}_{\tau\alpha}^* \\ &\quad + \sum_\alpha\left[\frac{\partial f(w^*,\zeta_\tau)}{\partial\zeta_{\tau\alpha}}\dot{\zeta}_{\tau\alpha} - \frac{\partial f(\zeta_\tau^*,\zeta_\tau)}{\partial\zeta_{\tau\alpha}}\dot{\zeta}_{\tau\alpha} - \frac{\partial f(\zeta_\tau^*,\zeta_\tau)}{\partial\zeta_{\tau\alpha}^*}\dot{\zeta}_{\tau\alpha}^*\right] \\ &= -\frac{i}{\hbar}E(\zeta_\tau^*,\zeta_\tau) + \sum_\alpha\left[\frac{\partial f(w^*,\zeta_\tau)}{\partial\zeta_{\tau\alpha}} - \frac{\partial f(\zeta_\tau^*,\zeta_\tau)}{\partial\zeta_{\tau\alpha}}\right]\dot{\zeta}_{\tau\alpha}. \end{aligned} \tag{6.33}$$

Finally, equating (6.31) and (6.32), and substituting (6.33), we arrive at the desired expression:

$$i\hbar\int d\mu(\zeta_0)\dot{D}_\tau(z_0;\zeta)e^{F_\tau(z_0,w^*;\zeta)} = \int d\mu(\zeta_0)\Delta'(w^*;\zeta_\tau^*,\zeta_\tau)D_\tau(z_0;\zeta)e^{F_\tau(z_0,w^*;\zeta)}, \tag{6.34}$$

where the coupling kernel Δ' has emerged:

$$\Delta'(w^*;\zeta_\tau^*,\zeta_\tau) = E(w^*,\zeta_\tau) - E(\zeta_\tau^*,\zeta_\tau) - i\hbar\sum_\alpha\left[\frac{\partial f(w^*,\zeta_\tau)}{\partial\zeta_{\tau\alpha}} - \frac{\partial f(\zeta_\tau^*,\zeta_\tau)}{\partial\zeta_{\tau\alpha}}\right]\dot{\zeta}_{\tau\alpha}, \tag{6.35}$$

which is precisely the coupling Δ' of Eq. (4.35), that arises when the CCS method is considered from a variational perspective [cf. §4.2.4].

Before proceeding we must bring attention to a detail which, in what follows, will have a pivotal role: the fact that the amplitude $D_\tau(z_0;\zeta)$, as defined in Eq. (6.26), is independent of the propagator's end-point label w^*. In other words, solutions to (6.34) are the same for different end-points and therefore we are free to choose w^* at our convenience – we shall find that by exercising this freedom our equations can be greatly simplified.

6.4 Semiclassical approximation

The basic idea underlying the semiclassical approximation is very intuitive: it is assumed that, in the semiclassical regime, the important contributions to the integrals over initial conditions (ζ_0^*,ζ_0) appearing in both sides of Eq. (6.34) come from the immediate neighborhood of the point (z_0^*,z_0). The trajectory spawned by this specific point is therefore special and shall be henceforth denominated the *reference trajectory*:

$$\zeta_0 = z_0,\quad \zeta_0^* = z_0^*,\quad \text{with}\quad \zeta(z_0^*,z_0,t) = z_t. \qquad \text{(reference trajectory)} \tag{6.36}$$

Furthermore, in view of the arguments presented earlier, we suppose that under semiclassical conditions both the amplitude D and its time derivative $\dot{D}$ are sufficiently smooth functions of (ζ_0^*,ζ_0), so that within the neighborhood of (z_0^*,z_0), and during the timespan

$0 \leq t \leq \tau$, they can be approximated by its reference-trajectory value:

$$D_\tau(z_0;\zeta) \approx D_\tau(z_0;\zeta)|_{\zeta=z} = D_\tau(z); \tag{6.37}$$

$$\dot{D}_\tau(z_0;\zeta) \approx \dot{D}_\tau(z_0;\zeta)\Big|_{\zeta=z} = \dot{D}_\tau(z). \tag{6.38}$$

If these assumptions hold then it is legitimate to expand both the phase and prefactors of the integrands in (6.34) around (z_0^*, z_0). The expansions are to be carried out up to second order in the deviations

$$\eta_0 = \zeta_0 - z_0, \quad \eta_0^* = \zeta_0^* - z_0^*, \tag{6.39}$$

leading to Gaussian integrals whose explicit solution is known. The procedure, however, is not completely straightforward – there is a certain protocol one must follow in order to maintain the consistency of the approximation; this is explained next in detail.

6.4.1 The expansion protocol

The protocol is based on two 'guiding principles'. The first is that deviations from the reference trajectory at different time instants are to be treated at the level of linearized dynamics; thus the final and initial deviations are related through:

$$\zeta_{\tau\mu}(\zeta_0^*,\zeta_0) \approx z_{\tau\mu}(z_0^*,z_0) + \frac{\partial\zeta_{\tau\mu}(\zeta_0^*,\zeta_0)}{\partial\zeta_{0\nu}}|_r(\zeta_{0\nu}-z_{0\nu}) + \frac{\partial\zeta_{\tau\mu}(\zeta_0^*,\zeta_0)}{\partial\zeta_{0\nu}^*}|_r(\zeta_{0\nu}^*-z_{0\nu}^*), \tag{6.40}$$

$$\zeta_{\tau\mu}^*(\zeta_0^*,\zeta_0) \approx z_{\tau\mu}^*(z_0^*,z_0) + \frac{\partial\zeta_{\tau\mu}^*(\zeta_0^*,\zeta_0)}{\partial\zeta_{0\nu}}|_r(\zeta_{0\nu}-z_{0\nu}) + \frac{\partial\zeta_{\tau\mu}^*(\zeta_0^*,\zeta_0)}{\partial\zeta_{0\nu}^*}|_r(\zeta_{0\nu}^*-z_{0\nu}^*), \tag{6.41}$$

where quantities evaluated at (z_0^*, z_0) are indicated with the right-sided bar '$|_r$' – a convention that is adopted hereon. The above relations can be organized as

$$\begin{pmatrix}\eta_\tau\\ \eta_\tau^*\end{pmatrix} = \begin{pmatrix}M_{11}(\tau) & M_{12}(\tau)\\ M_{21}(\tau) & M_{22}(\tau)\end{pmatrix}\begin{pmatrix}\eta_0\\ \eta_0^*\end{pmatrix} = M(\tau)\begin{pmatrix}\eta_0\\ \eta_0^*\end{pmatrix}, \quad \text{with} \quad \begin{cases}\eta_\tau = \zeta_\tau - z_\tau\\ \eta_\tau^* = \zeta_\tau^* - z_\tau^*\end{cases}, \tag{6.42}$$

where M denotes the stability matrix associated with the reference trajectory $z_\tau(z_0^*, z_0)$.

Essentially, this means that the same stability matrix is assigned to all orbits whose initial conditions are located within the neighborhood of the reference trajectory; or, translating into practical terms: while performing the required expansions, whenever one encounters derivatives of ζ_τ or ζ_τ^* with respect to either ζ_0 or ζ_0^*, these should be understood as

$$\frac{\partial\zeta_\tau}{\partial\zeta_0} \approx \frac{\partial\zeta_\tau}{\partial\zeta_0}|_r = \frac{\partial z_\tau}{\partial z_0} = M_{11}(\tau), \quad \frac{\partial\zeta_\tau}{\partial\zeta_0^*} \approx \frac{\partial\zeta_\tau}{\partial\zeta_0^*}|_r = \frac{\partial z_\tau}{\partial z_0^*} = M_{12}(\tau), \quad \text{etc;} \tag{6.43}$$

i.e. they should be approximated to zeroth order and, therefore, second-order derivatives

of this kind should be neglected – this gives our first rule, mathematically expressed as:

$$\frac{\partial^2\zeta_\tau}{\partial\zeta_0\partial\zeta_0}\approx 0,\quad \frac{\partial^2\zeta_\tau}{\partial\zeta_0\partial\zeta_0^*}\approx 0,\quad \frac{\partial^2\zeta_\tau}{\partial\zeta_0^*\partial\zeta_0^*}\approx 0,\quad \text{etc.}\qquad \text{(rule one)}$$

The second principle is that a certain hierarchy should be observed when considering the second-order expansion of the integrands of (6.34). Consider, for example, the Kähler potential $f(\zeta^*,\zeta)$; its second-order expansion around (z^*,z) reads:

$$\begin{aligned} f(\zeta^*,\zeta)\approx f(z^*,z)+\sum_\mu\frac{\partial f}{\partial z_\mu}(\zeta-z)_\mu+\sum_\mu\frac{\partial f}{\partial z_\mu^*}(\zeta^*-z^*)_\mu+\sum_{\mu\nu}(\zeta-z)_\mu\frac{\partial^2 f}{\partial z_\mu\partial z_\nu^*}(\zeta^*-z^*)_\nu\\ +\frac{1}{2}\sum_{\mu\nu}(\zeta-z)_\mu\frac{\partial^2 f}{\partial z_\mu\partial z_\nu}(\zeta-z)_\nu+\frac{1}{2}\sum_{\mu\nu}(\zeta^*-z^*)_\mu\frac{\partial^2 f}{\partial z_\mu^*\partial z_\nu^*}(\zeta^*-z^*)_\nu \end{aligned}\qquad (6.44)$$

where all derivatives are computed at (z^*,z) – the time label is not important for developing the present argument since different instants are connected by the stability matrix evaluated at the reference trajectory. The point to be noticed is that, amidst the various quantities composing the integrands in (6.34), we find some which are written in terms of derivatives of f, such as the metric matrix g and the gradients appearing in the coupling kernel Δ'. Thus, if we let f belong to a certain category of functions whose phase-space derivatives up to second order should not be discarded, then, according to (6.44), first-order gradients of f should be approximated as:

$$\frac{\partial f(\zeta^*,\zeta)}{\partial\zeta_\mu}\approx\frac{\partial f(z^*,z)}{\partial z_\mu}+\sum_\nu\frac{\partial^2 f(z^*,z)}{\partial z_\mu\partial z_\nu}(\zeta-z)_\nu+\sum_\nu\frac{\partial^2 f(z^*,z)}{\partial z_\mu\partial z_\nu^*}(\zeta^*-z^*)_\nu \qquad (6.45)$$

$$\frac{\partial f(\zeta^*,\zeta)}{\partial\zeta_\mu^*}\approx\frac{\partial f(z^*,z)}{\partial z_\mu^*}+\sum_\nu\frac{\partial^2 f(z^*,z)}{\partial z_\mu^*\partial z_\nu}(\zeta-z)_\nu+\sum_\nu\frac{\partial^2 f(z^*,z)}{\partial z_\mu^*\partial z_\nu^*}(\zeta^*-z^*)_\nu, \qquad (6.46)$$

whereas second-order gradients should be approximated as

$$\frac{\partial^2 f(\zeta^*,\zeta)}{\partial\zeta_\mu\partial\zeta_\nu}\approx\frac{\partial^2 f(z^*,z)}{\partial z_\mu\partial z_\nu},\quad \frac{\partial^2 f(\zeta^*,\zeta)}{\partial\zeta_\mu\partial\zeta_\nu^*}\approx\frac{\partial^2 f(z^*,z)}{\partial z_\mu\partial z_\nu^*},\quad \frac{\partial^2 f(\zeta^*,\zeta)}{\partial\zeta_\mu^*\partial\zeta_\nu^*}\approx\frac{\partial^2 f(z^*,z)}{\partial z_\mu^*\partial z_\nu^*}. \qquad (6.47)$$

Moreover, when expanding the integrands in (6.34), whenever higher-order derivatives of f are encountered they should be neglected, providing us with a second expansion rule:

$$\frac{\partial^3 f(\zeta^*,\zeta)}{\partial\zeta_\gamma\partial\zeta_\mu\partial\zeta_\nu}\approx 0,\quad \frac{\partial^3 f(\zeta^*,\zeta)}{\partial\zeta_\gamma^*\partial\zeta_\mu\partial\zeta_\nu^*}\approx 0,\quad \text{etc.}\qquad \text{(rule two)}$$

An immediate consequence is that the metric matrix elements shall be approximated to order zero:

$$g(\zeta_0^*,\zeta_0)_{\alpha\beta}=\frac{\partial^2 f(\zeta_0^*,\zeta_0)}{\partial\zeta_{0\alpha}\partial\zeta_{0\beta}^*}\approx\frac{\partial^2 f(z_0^*,z_0)}{\partial z_{0\alpha}\partial z_{0\beta}^*}=g(z_0^*,z_0)_{\alpha\beta}, \qquad (6.48)$$

which implies that the determinant of $g(\zeta_0^*, \zeta_0)$ is to be approximated as:

$$\det g(\zeta_0^*, \zeta_0) \approx \det g(z_0^*, z_0). \tag{6.49}$$

Besides the Kähler potential f, other quantities pertaining to such category of functions – those whose derivatives up to second-order are to be accounted for in the expansions – are the complex action A and the energy function E. The defining characteristic of all these quantities being the fact that they are on the same footing as the phase F with regards to phase-space derivatives, as suggested by Eqs. (6.28) and (1.71).

Thus, consider next the $\dot{\zeta}_\tau$ appearing in the definition of Δ', Eq. (6.35). Its explicit expression (written below without time labels) involves the metric matrix g as well as a first-order gradient of the energy function E, and therefore it is to be understood as

$$\begin{aligned}\dot{\zeta}_\alpha &= -\frac{i}{\hbar}\sum_\gamma g^{-T}_{\alpha\gamma}(\zeta^*,\zeta)\frac{\partial E(\zeta^*,\zeta)}{\partial z^*_\gamma} \\ &\approx -\frac{i}{\hbar}\sum_\gamma g^{-T}_{\alpha\gamma}(z^*,z)\left[\frac{\partial E(z^*,z)}{\partial z^*_\gamma} + \sum_\nu \frac{\partial^2 E(z^*,z)}{\partial z^*_\gamma \partial z_\nu}(\zeta - z)_\nu + \sum_\nu \frac{\partial^2 E(z^*,z)}{\partial z^*_\gamma \partial z^*_\nu}(\zeta^* - z^*)_\nu\right].\end{aligned} \tag{6.50}$$

Hence, should we encounter derivatives of $\dot{\zeta}_\tau$ with respect to either ζ_τ or ζ^*_τ, these are to be regarded as zeroth-order approximations:

$$\frac{\partial \dot{\zeta}_{\tau\alpha}}{\partial \zeta_{\tau\beta}} \approx -\frac{i}{\hbar}\sum_\gamma g^{-T}_{\alpha\gamma}(z^*_\tau, z_\tau)\frac{\partial^2 E(z^*_\tau, z_\tau)}{\partial z^*_{\tau\gamma}\partial z_{\tau\beta}}, \tag{6.51}$$

$$\frac{\partial \dot{\zeta}_{\tau\alpha}}{\partial \zeta^*_{\tau\beta}} \approx -\frac{i}{\hbar}\sum_\gamma g^{-T}_{\alpha\gamma}(z^*_\tau, z_\tau)\frac{\partial^2 E(z^*_\tau, z_\tau)}{\partial z^*_{\tau\gamma}\partial z^*_{\tau\beta}}, \tag{6.52}$$

which means that higher-order derivatives of this kind must also be neglected, giving a third rule:

$$\frac{\partial^2 \dot{\zeta}_\alpha}{\partial \zeta_\beta \partial \zeta_\gamma} \approx 0, \quad \frac{\partial^2 \dot{\zeta}_\alpha}{\partial \zeta_\beta \partial \zeta^*_\gamma} \approx 0. \qquad \text{(rule three)}$$

In the previous section we established that the amplitude D defined in (6.26) should be approximated by its value on the reference trajectory; for the sake of completeness we now incorporate that fact into our expansion protocol, translating it as the following rule:

$$\frac{\partial D_\tau(z_0;\zeta)}{\partial \zeta_0} \approx 0, \quad \frac{\partial D_\tau(z_0;\zeta)}{\partial \zeta^*_0} \approx 0; \text{ and } \frac{\partial \dot{D}_\tau(z_0;\zeta)}{\partial \zeta_0} \approx 0, \quad \frac{\partial \dot{D}_\tau(z_0;\zeta)}{\partial \zeta^*_0} \approx 0. \quad \text{(rule zero)}$$

Finally, let us rewrite the equation of motion (6.34) in view of the observations made so far. From (6.49) the measure $d\mu(\zeta_0)$ appearing on both sides of (6.34) is approximated

according to [recalling the definitions given in Eqs. (1.60) and (1.61)]:

$$\begin{aligned} d\mu(\zeta_0) &= \kappa\ \det g(\zeta_0^*,\zeta_0)\ \prod_{\alpha=1}^{d}\frac{d\zeta_{0\alpha}d\zeta_{0\alpha}^*}{2\pi i} \\ &\approx \kappa\ \det g(z_0^*,z_0)\ \prod_{\alpha=1}^{d}\frac{d\eta_{0\alpha}d\eta_{0\alpha}^*}{2\pi i} \\ &\equiv (2\pi i)^{-d}\,\kappa\ \det g(z_0^*,z_0)\ d^2\eta_0, \end{aligned} \tag{6.53}$$

where integration variables have been changed from (ζ_0,ζ_0^*) to the deviations (η_0,η_0^*) defined in (6.39), and the abbreviation $d^2\eta_0$ has been introduced to denote the $2d$-dimensional area element. This, together with 'rule zero', reduces the equation of motion (6.34) to the form:

$$i\hbar\,\dot{D}_\tau^{sc}(z)\Big[\int d^2\eta_0\, e^{F_\tau(z_0,w^*;\zeta)}\Big] = D_\tau^{sc}(z)\Big[\int d^2\eta_0\,\Delta'(w^*;\zeta_\tau^*,\zeta_\tau)e^{F_\tau(z_0,w^*;\zeta)}\Big] \tag{6.54}$$

– notice how constant factors multiplying both sides have been canceled out of the expression. Henceforth we begin denoting the semiclassical amplitude with a superscript indication, $D_\tau^{sc}(z)$. The task now is to expand Δ' and F under the integral signs, observing the rules stated above.

6.4.2 First order derivatives and tuning of w

The first order derivatives of the phase F, viz. Eq. (6.28), with respect to phase-space variables ζ_0 and ζ_0^* are computed as follows:

$$\begin{aligned} \frac{\partial F_\tau(z_0,w^*;\zeta)}{\partial\zeta_{0\mu}} &= \sum_\alpha \frac{i}{\hbar}\frac{\partial A_\tau(\zeta_\tau^*,\zeta_0)}{\partial\zeta_{\tau\alpha}^*}\frac{\partial\zeta_{\tau\alpha}^*}{\partial\zeta_{0\mu}} + \frac{i}{\hbar}\frac{\partial A(\zeta_\tau^*,\zeta_0)}{\partial\zeta_{0\mu}} - \frac{\partial f(\zeta_0^*,\zeta_0)}{\partial\zeta_{0\mu}} \\ &\quad + \sum_\alpha\left[\frac{\partial f(w^*,\zeta_\tau)}{\partial\zeta_{\tau\alpha}}\frac{\partial\zeta_{\tau\alpha}}{\partial\zeta_{0\mu}} - \frac{\partial f(\zeta_\tau^*,\zeta_\tau)}{\partial\zeta_{\tau\alpha}}\frac{\partial\zeta_{\tau\alpha}}{\partial\zeta_{0\mu}} - \frac{\partial f(\zeta_\tau^*,\zeta_\tau)}{\partial\zeta_{\tau\alpha}^*}\frac{\partial\zeta_{\tau\alpha}^*}{\partial\zeta_{0\mu}}\right] \\ &= \sum_\alpha \frac{\partial\zeta_{\tau\alpha}}{\partial\zeta_{0\mu}}\left[\frac{\partial f(w^*,\zeta_\tau)}{\partial\zeta_{\tau\alpha}} - \frac{\partial f(\zeta_\tau^*,\zeta_\tau)}{\partial\zeta_{\tau\alpha}}\right], \end{aligned} \tag{6.55a}$$

$$\begin{aligned} \frac{\partial F_\tau(z_0,w^*;\zeta)}{\partial\zeta_{0\mu}^*} &= \sum_\alpha \frac{i}{\hbar}\frac{\partial A_\tau(\zeta_\tau^*,\zeta_0)}{\partial\zeta_{\tau\alpha}^*}\frac{\partial\zeta_{\tau\alpha}^*}{\partial\zeta_{0\mu}^*} + \frac{\partial f(\zeta_0^*,z_0)}{\partial\zeta_{0\mu}^*} - \frac{\partial f(\zeta_0^*,\zeta_0)}{\partial\zeta_{0\mu}^*} \\ &\quad + \sum_\alpha\left[\frac{\partial f(w^*,\zeta_\tau)}{\partial\zeta_{\tau\alpha}}\frac{\partial\zeta_{\tau\alpha}}{\partial\zeta_{0\mu}^*} - \frac{\partial f(\zeta_\tau^*,\zeta_\tau)}{\partial\zeta_{\tau\alpha}}\frac{\partial\zeta_{\tau\alpha}}{\partial\zeta_{0\mu}^*} - \frac{\partial f(\zeta_\tau^*,\zeta_\tau)}{\partial\zeta_{\tau\alpha}^*}\frac{\partial\zeta_{\tau\alpha}^*}{\partial\zeta_{0\mu}^*}\right] \\ &= \sum_\alpha \frac{\partial\zeta_{\tau\alpha}}{\partial\zeta_{0\mu}^*}\left[\frac{\partial f(w^*,\zeta_\tau)}{\partial\zeta_{\tau\alpha}} - \frac{\partial f(\zeta_\tau^*,\zeta_\tau)}{\partial\zeta_{\tau\alpha}}\right] + \frac{\partial f(\zeta_0^*,z_0)}{\partial\zeta_{0\mu}^*} - \frac{\partial f(\zeta_0^*,\zeta_0)}{\partial\zeta_{0\mu}^*}. \end{aligned} \tag{6.55b}$$

The properties of the complex action, listed in Eqs. (1.71), have been employed in both of the above calculations.

Derivatives of Δ' with respect to the initial points ζ_0 and ζ_0^*, in turn, are obtained

from derivatives with respect to ζ_τ and ζ_τ^* through the chain rule:

$$\frac{\partial\Delta'(w^*;\zeta_\tau^*,\zeta_\tau)}{\partial\zeta_{0\nu}} = \sum_\mu \left[\frac{\partial\Delta'(w^*;\zeta_\tau^*,\zeta_\tau)}{\partial\zeta_{\tau\mu}}\frac{\partial\zeta_{\tau\mu}}{\partial\zeta_{0\nu}} + \frac{\partial\Delta'(w^*;\zeta_\tau^*,\zeta_\tau)}{\partial\zeta_{\tau\mu}^*}\frac{\partial\zeta_{\tau\mu}^*}{\partial\zeta_{0\nu}}\right],$$
$$\frac{\partial\Delta'(w^*;\zeta_\tau^*,\zeta_\tau)}{\partial\zeta_{0\nu}^*} = \sum_\mu \left[\frac{\partial\Delta'(w^*;\zeta_\tau^*,\zeta_\tau)}{\partial\zeta_{\tau\mu}}\frac{\partial\zeta_{\tau\mu}}{\partial\zeta_{0\nu}^*} + \frac{\partial\Delta'(w^*;\zeta_\tau^*,\zeta_\tau)}{\partial\zeta_{\tau\mu}^*}\frac{\partial\zeta_{\tau\mu}^*}{\partial\zeta_{0\nu}^*}\right]$$

– from (6.35), we have:

$$\begin{aligned}\frac{\partial\Delta'(w^*;\zeta_\tau^*,\zeta_\tau)}{\partial\zeta_{\tau\mu}} &= \frac{\partial E(w^*,\zeta_\tau)}{\partial\zeta_{\tau\mu}} - \frac{\partial E(\zeta_\tau^*,\zeta_\tau)}{\partial\zeta_{\tau\mu}} - i\hbar\sum_\alpha\left[\frac{\partial^2 f(w^*,\zeta_\tau)}{\partial\zeta_{\tau\alpha}\partial\zeta_{\tau\mu}} - \frac{\partial^2 f(\zeta_\tau^*,\zeta_\tau)}{\partial\zeta_{\tau\alpha}\partial\zeta_{\tau\mu}}\right]\dot\zeta_{\tau\alpha} \\ &\quad - i\hbar\sum_\alpha\left[\frac{\partial f(w^*,\zeta_\tau)}{\partial\zeta_{\tau\alpha}} - \frac{\partial f(\zeta_\tau^*,\zeta_\tau)}{\partial\zeta_{\tau\alpha}}\right]\frac{\partial\dot\zeta_{\tau\alpha}}{\partial\zeta_{\tau\mu}}, \qquad (6.56a)\\ \frac{\partial\Delta'(w^*;\zeta_\tau^*,\zeta_\tau)}{\partial\zeta_{\tau\mu}^*} &= -\frac{\partial E(\zeta_\tau^*,\zeta_\tau)}{\partial\zeta_{\tau\mu}^*} + i\hbar\sum_\alpha\frac{\partial^2 f(\zeta_\tau^*,\zeta_\tau)}{\partial\zeta_{\tau\mu}^*\partial\zeta_{\tau\alpha}}\dot\zeta_{\tau\alpha} - i\hbar\sum_\alpha\left[\frac{\partial f(w^*,\zeta_\tau)}{\partial\zeta_{\tau\alpha}} - \frac{\partial f(\zeta_\tau^*,\zeta_\tau)}{\partial\zeta_{\tau\alpha}}\right]\frac{\partial\dot\zeta_{\tau\alpha}}{\partial\zeta_{\tau\mu}^*} \\ &= -i\hbar\sum_\alpha\left[\frac{\partial f(w^*,\zeta_\tau)}{\partial\zeta_{\tau\alpha}} - \frac{\partial f(\zeta_\tau^*,\zeta_\tau)}{\partial\zeta_{\tau\alpha}}\right]\frac{\partial\dot\zeta_{\tau\alpha}}{\partial\zeta_{\tau\mu}^*}. \qquad (6.56b)\end{aligned}$$

In this last expression the first couple of terms on the upper line add to zero by virtue of the equation of motion (6.3a).

The above derivatives are to be evaluated at the reference trajectory. We find, however, that no significant simplification of these expressions is achieved by setting $\zeta_0 = z_0$; for instance, Eqs. (6.55a) and (6.55b) assume the form:

$$\frac{\partial F_\tau(z_0,w^*;\zeta)}{\partial\zeta_{0\mu}}|_r = \sum_\alpha (M_{11}^T)_{\mu\alpha}\left[\frac{\partial f(w^*,z_\tau)}{\partial z_{\tau\alpha}} - \frac{\partial f(z_\tau^*,z_\tau)}{\partial z_{\tau\alpha}}\right],$$
$$\frac{\partial F_\tau(z_0,w^*;\zeta)}{\partial\zeta_{0\mu}^*}|_r = \sum_\alpha (M_{12}^T)_{\mu\alpha}\left[\frac{\partial f(w^*,z_\tau)}{\partial z_{\tau\alpha}} - \frac{\partial f(z_\tau^*,z_\tau)}{\partial z_{\tau\alpha}}\right],$$

the only noticeable change being the cancellation of the last terms in (6.55b). The same goes to Eqs. (6.56a) and (6.56b) – they experience no simplifications whatsoever.

Now, this situation, albeit undesirable, does not prevent one from performing the required integrals – explicit solutions for Gaussian integrals with non-zero linear terms, on both the exponent and prefactor, are available – though they are somewhat cumbersome.

Fortunately, as argued earlier, we have the freedom to choose the propagator's end-point w^* at our convenience, since the amplitude D does not depend on its value; and it is easy to see that by tuning this parameter with the choice:

$$w^* = z_\tau^*(z_0^*, z_0), \qquad \text{(parameter tuning)} \qquad (6.57)$$

all of the above derivatives vanish.[iii] Indeed, since it leads to the vanishing of the expo-

[iii] One detail has been left out here. The choice $w^* = z_\tau^*$ makes the propagator's end point τ-dependent,

nent's first-order derivatives:

$$\frac{\partial F_\tau(z_0, z_\tau^*; \zeta)}{\partial \zeta_{0\mu}}|_r = 0, \qquad \frac{\partial F_\tau(z_0, z_\tau^*; \zeta)}{\partial \zeta_{0\mu}^*}|_r = 0, \tag{6.58}$$

such a choice for w^* makes the reference trajectory's initial condition (z_0^*, z_0) a stationary point of the integrands in (6.34). Simultaneously, both Δ' and its first-order derivatives die off:

$$\Delta'(z_\tau^*; \zeta_\tau^*, \zeta_\tau)|_r = 0, \qquad \frac{\partial \Delta'(z_\tau^*; \zeta_\tau^*, \zeta_\tau)}{\partial \zeta_{0\mu}}|_r = 0, \qquad \frac{\partial \Delta'(z_\tau^*; \zeta_\tau^*, \zeta_\tau)}{\partial \zeta_{0\mu}^*}|_r = 0. \tag{6.59}$$

These two facts combined enormously simplify the subsequent calculations – therefore, in everything else that follows, the parameter tuning expressed in (6.57) is adopted.[iv]

In this way, the semiclassical expansions around the reference orbit yield the following expression for the phase F:

$$F_\tau(z_0, z_\tau^*; \zeta) \approx \frac{i}{\hbar} A_\tau(z_\tau^*, z_0) - \frac{1}{2} \begin{pmatrix} \eta_0^T & \eta_0^{*T} \end{pmatrix} \begin{pmatrix} U_{11} & U_{12} \\ U_{21} & U_{22} \end{pmatrix} \begin{pmatrix} \eta_0 \\ \eta_0^* \end{pmatrix}, \tag{6.60}$$

where the second-order derivatives of F with respect to ζ_0 and ζ_0^* have been organized into the implicitly defined matrix U – the minus sign in its definition is just a convenience. Similarly, for the coupling Δ' we have:

$$\Delta'(z_\tau^*; \zeta_\tau^*, \zeta_\tau) \approx \frac{1}{2} \begin{pmatrix} \eta_\tau^T & \eta_\tau^{*T} \end{pmatrix} \begin{pmatrix} V_{11} & V_{12} \\ V_{21} & V_{22} \end{pmatrix} \begin{pmatrix} \eta_\tau \\ \eta_\tau^* \end{pmatrix} = \frac{1}{2} \begin{pmatrix} \eta_0^T & \eta_0^{*T} \end{pmatrix} \left[M^T \begin{pmatrix} V_{11} & V_{12} \\ V_{21} & V_{22} \end{pmatrix} M \right] \begin{pmatrix} \eta_0 \\ \eta_0^* \end{pmatrix}, \tag{6.61}$$

where the matrix V contains the second-order derivatives of Δ' with respect to ζ_τ and ζ_τ^*, and M denotes the stability matrix, which connects the deviations (η_τ, η_τ^*) and (η_0, η_0^*) at final and initial times. All of the above matrices – M, U and V – are calculated at the reference orbit $z(t)$.

The resulting complex Gaussian integral can be solved explicitly,[43] leading to:

$$i\hbar\, \dot{D}^{sc}(z) = \tfrac{1}{2}\mathrm{tr}(U^{-T} M^T V M)\, D^{sc}(z). \tag{6.62}$$

This is the 'raw form' of the equation of motion satisfied by the semiclassical amplitude, with initial condition $D_0^{sc} = 1$. (In what follows we omit the time variable). All left to do

meaning that the total derivatives of Eqs. (6.31) and (6.32) should have operated on w^* as well. However, the new terms arising from $\{\dot{w}|$ and $\sum_\nu \dot{w}_\nu^* (\partial F_\tau / \partial w_\nu^*)$ cancel off, and one is led again to Eq. (6.34).

[iv] One may object that, although D, as defined in (6.26), is assuredly independent of w^*, this ceases to be true once the approximations that shape the semiclassical formula are introduced. It is not difficult to show though, that the semiclassical amplitude's first-order derivatives with respect to w^* vanish for w^* arbitrary but close to z_τ^* – as long as the extra 'interpolation terms' that arise in the approximated formula are also consistently expanded around z_τ^*. This, however, is a lengthy and unnecessary calculation and we prefer not to include it here.

is to compute matrices U and V.

6.4.3 * Second-order derivatives

The second-order derivatives of F, computed with the tuning (6.57), are:

$$\frac{\partial^2 F_\tau(z_0,z_\tau^*;\zeta)}{\partial\zeta_{0\mu}\partial\zeta_{0\nu}} = \sum_{\alpha\beta}\frac{\partial\zeta_{\tau\alpha}}{\partial\zeta_{0\mu}}\left[\left(\frac{\partial^2 f(z_\tau^*,\zeta_\tau)}{\partial\zeta_{\tau\alpha}\partial\zeta_{\tau\beta}}-\frac{\partial^2 f(\zeta_\tau^*,\zeta_\tau)}{\partial\zeta_{\tau\alpha}\partial\zeta_{\tau\beta}}\right)\frac{\partial\zeta_{\tau\beta}}{\partial\zeta_{0\nu}}-\frac{\partial^2 f(\zeta_\tau^*,\zeta_\tau)}{\partial\zeta_{\tau\alpha}\partial\zeta_{\tau\beta}^*}\frac{\partial\zeta_{\tau\beta}^*}{\partial\zeta_{0\nu}}\right], \tag{6.63a}$$

$$\frac{\partial^2 F_\tau(z_0,z_\tau^*;\zeta)}{\partial\zeta_{0\mu}\partial\zeta_{0\nu}^*} = \sum_{\alpha\beta}\frac{\partial\zeta_{\tau\alpha}}{\partial\zeta_{0\mu}}\left[\left(\frac{\partial^2 f(z_\tau^*,\zeta_\tau)}{\partial\zeta_{\tau\alpha}\partial\zeta_{\tau\beta}}-\frac{\partial^2 f(\zeta_\tau^*,\zeta_\tau)}{\partial\zeta_{\tau\alpha}\partial\zeta_{\tau\beta}}\right)\frac{\partial\zeta_{\tau\beta}}{\partial\zeta_{0\nu}^*}-\frac{\partial^2 f(\zeta_\tau^*,\zeta_\tau)}{\partial\zeta_{\tau\alpha}\partial\zeta_{\tau\beta}^*}\frac{\partial\zeta_{\tau\beta}^*}{\partial\zeta_{0\nu}^*}\right], \tag{6.63b}$$

$$\begin{aligned}\frac{\partial^2 F_\tau(z_0,z_\tau^*;\zeta)}{\partial\zeta_{0\mu}^*\partial\zeta_{0\nu}^*} &= \sum_{\alpha\beta}\frac{\partial\zeta_{\tau\alpha}}{\partial\zeta_{0\mu}^*}\left[\left(\frac{\partial^2 f(z_\tau^*,\zeta_\tau)}{\partial\zeta_{\tau\alpha}\partial\zeta_{\tau\beta}}-\frac{\partial^2 f(\zeta_\tau^*,\zeta_\tau)}{\partial\zeta_{\tau\alpha}\partial\zeta_{\tau\beta}}\right)\frac{\partial\zeta_{\tau\beta}}{\partial\zeta_{0\nu}^*}-\frac{\partial^2 f(\zeta_\tau^*,\zeta_\tau)}{\partial\zeta_{\tau\alpha}\partial\zeta_{\tau\beta}^*}\frac{\partial\zeta_{\tau\beta}^*}{\partial\zeta_{0\nu}^*}\right]\\ &\quad+\frac{\partial^2 f(\zeta_0^*,z_0)}{\partial\zeta_{0\mu}^*\partial\zeta_{0\nu}^*}-\frac{\partial^2 f(\zeta_0^*,\zeta_0)}{\partial\zeta_{0\mu}^*\partial\zeta_{0\nu}^*}.\end{aligned} \tag{6.63c}$$

Notice how some terms have been neglected in accordance with 'rule one' established earlier. Evaluating the above expressions at the reference orbit and accounting for the minus sign in (6.60), we obtain the elements of matrix U:

$$(U_{11})_{\mu\nu} = -\frac{\partial^2 F_\tau(z_0,z_\tau^*;\zeta)}{\partial\zeta_{0\mu}\partial\zeta_{0\nu}}|_r = \sum_{\alpha\beta}\frac{\partial z_{\tau\alpha}}{\partial z_{0\mu}}\frac{\partial^2 f(z_\tau^*,z_\tau)}{\partial z_{\tau\alpha}\partial z_{\tau\beta}^*}\frac{\partial z_{\tau\beta}^*}{\partial z_{0\nu}} = (M_{11}^T g_\tau M_{21})_{\mu\nu}, \tag{6.64a}$$

$$(U_{12})_{\mu\nu} = -\frac{\partial^2 F_\tau(z_0,z_\tau^*;\zeta)}{\partial\zeta_{0\mu}\partial\zeta_{0\nu}^*}|_r = \sum_{\alpha\beta}\frac{\partial z_{\tau\alpha}}{\partial z_{0\mu}}\frac{\partial^2 f(z_\tau^*,z_\tau)}{\partial z_{\tau\alpha}\partial z_{\tau\beta}^*}\frac{\partial z_{\tau\beta}^*}{\partial z_{0\nu}^*} = (M_{11}^T g_\tau M_{22})_{\mu\nu} = (U_{21})_{\nu\mu}, \tag{6.64b}$$

$$(U_{22})_{\mu\nu} = -\frac{\partial^2 F_\tau(z_0,z_\tau^*;\zeta)}{\partial\zeta_{0\mu}^*\partial\zeta_{0\nu}^*}|_r = \sum_{\alpha\beta}\frac{\partial z_{\tau\beta}^*}{\partial z_{0\mu}^*}\frac{\partial^2 f(z_\tau^*,z_\tau)}{\partial z_{\tau\beta}^*\partial z_{\tau\alpha}}\frac{\partial z_{\tau\alpha}}{\partial z_{0\nu}^*} = (M_{22}^T g_\tau^T M_{12})_{\mu\nu}. \tag{6.64c}$$

In turn, the second-order derivatives of Δ' – again embodying (6.57) – are worked out below:

$$\begin{aligned}\frac{\partial^2\Delta'(z_\tau^*,\zeta_\tau)}{\partial\zeta_{\tau\mu}\partial\zeta_{\tau\nu}} &= \frac{\partial^2 E(z_\tau^*,\zeta_\tau)}{\partial\zeta_{\tau\mu}\partial\zeta_{\tau\nu}}-\frac{\partial^2 E(\zeta_\tau^*,\zeta_\tau)}{\partial\zeta_{\tau\mu}\partial\zeta_{\tau\nu}}-i\hbar\sum_\alpha\left[\frac{\partial^2 f(z_\tau^*,\zeta_\tau)}{\partial\zeta_{\tau\alpha}\partial\zeta_{\tau\mu}}-\frac{\partial^2 f(\zeta_\tau^*,\zeta_\tau)}{\partial\zeta_{\tau\alpha}\partial\zeta_{\tau\mu}}\right]\frac{\partial\dot\zeta_{\tau\alpha}}{\partial\zeta_{\tau\nu}}\\ &\quad-i\hbar\sum_\alpha\left[\frac{\partial^2 f(z_\tau^*,\zeta_\tau)}{\partial\zeta_{\tau\alpha}\partial\zeta_{\tau\nu}}-\frac{\partial^2 f(\zeta_\tau^*,\zeta_\tau)}{\partial\zeta_{\tau\alpha}\partial\zeta_{\tau\nu}}\right]\frac{\partial\dot\zeta_{\tau\alpha}}{\partial\zeta_{\tau\mu}},\end{aligned} \tag{6.65a}$$

$$\frac{\partial^2\Delta'(z_\tau^*,\zeta_\tau)}{\partial\zeta_{\tau\mu}^*\partial\zeta_{\tau\nu}} = -i\hbar\sum_\alpha\left[\frac{\partial^2 f(z_\tau^*,\zeta_\tau)}{\partial\zeta_{\tau\alpha}\partial\zeta_{\tau\nu}}-\frac{\partial^2 f(\zeta_\tau^*,\zeta_\tau)}{\partial\zeta_{\tau\alpha}\partial\zeta_{\tau\nu}}\right]\frac{\partial\dot\zeta_{\tau\alpha}}{\partial\zeta_{\tau\mu}^*}, \tag{6.65b}$$

$$\frac{\partial^2\Delta'(z_\tau^*,\zeta_\tau)}{\partial\zeta_{\tau\mu}^*\partial\zeta_{\tau\nu}^*} = i\hbar\sum_\alpha\frac{\partial^2 f(\zeta_\tau^*,\zeta_\tau)}{\partial\zeta_{\tau\alpha}\partial\zeta_{\tau\nu}^*}\frac{\partial\dot\zeta_{\tau\alpha}}{\partial\zeta_{\tau\mu}^*}. \tag{6.65c}$$

Once more, notice how we have employed the protocol – namely, 'rule two' and 'rule three'

–, neglecting various derivatives. Evaluating at the reference orbit we find:

$$(V_{11})_{\mu\nu} = \frac{\partial^2 \Delta'(z^*_\tau, \zeta_\tau)}{\partial \zeta_{\tau\mu} \partial \zeta_{\tau\nu}}|_r = 0, \tag{6.66a}$$

$$(V_{12})_{\mu\nu} = \frac{\partial^2 \Delta'(z^*_\tau, \zeta_\tau)}{\partial \zeta_{\tau\mu} \partial \zeta^*_{\tau\nu}}|_r = (V_{21})_{\nu\mu} = 0, \tag{6.66b}$$

$$(V_{22})_{\mu\nu} = \frac{\partial^2 \Delta'(z^*_\tau, \zeta_\tau)}{\partial \zeta^*_{\tau\mu} \partial \zeta^*_{\tau\nu}}|_r = i\hbar \sum_\alpha \frac{\partial^2 f(z^*_\tau, z_\tau)}{\partial z^*_{\tau\nu} \partial z_{\tau\alpha}} \frac{\partial \dot{z}_{\tau\alpha}}{\partial z^*_{\tau\mu}} = i\hbar \, (g_\tau^T \, R_{12})_{\nu\mu} \tag{6.66c}$$

– i.e. the matrix V displays only a single nonzero block, which leads to a particularly simple expression for the trace in Eq. (6.62), as we shall soon verify.

At this point all ingredients needed for writing the equation of motion satisfied by the semiclassical amplitude are available. Before proceeding though, and for the sake of transparency, we conduct simple checks on the mixed derivatives of F and Δ'.

Check 1. We got to (6.63b) starting from (6.55a) and differentiating with respect to $\zeta^*_{0\nu}$. The same answer, with transposed indexes, must be obtained if we calculate the mixed derivative in the opposite order, starting from (6.55b) and deriving with respect to $\zeta_{0\nu}$; the latter procedure yields:

$$\begin{aligned} \frac{\partial^2 F_\tau(z_0, z^*_\tau; \zeta)}{\partial \zeta^*_{0\mu} \partial \zeta_{0\nu}} = & \sum_{\alpha\beta} \frac{\partial \zeta_{\tau\alpha}}{\partial \zeta^*_{0\mu}} \left(\frac{\partial^2 f(z^*_\tau, \zeta_\tau)}{\partial \zeta_{\tau\alpha} \partial \zeta_{\tau\beta}} - \frac{\partial^2 f(\zeta^*_\tau, \zeta_\tau)}{\partial \zeta_{\tau\alpha} \partial \zeta_{\tau\beta}} \right) \frac{\partial \zeta_{\tau\beta}}{\partial \zeta_{0\nu}} \\ & - \sum_{\alpha\beta} \frac{\partial \zeta_{\tau\alpha}}{\partial \zeta^*_{0\mu}} \frac{\partial^2 f(\zeta^*_\tau, \zeta_\tau)}{\partial \zeta_{\tau\alpha} \partial \zeta^*_{\tau\beta}} \frac{\partial \zeta^*_{\tau\beta}}{\partial \zeta_{0\nu}} - \frac{\partial^2 f(\zeta^*_0, \zeta_0)}{\partial \zeta^*_{0\mu} \partial \zeta_{0\nu}}. \end{aligned} \tag{6.67}$$

This result is exactly equivalent to (6.63b), even though this is not obvious at first sight. The equivalence rests on one of the identities satisfied by the stability matrix elements – namely, the transposed version of Eq. (6.10b), $(g_0^T + M_{12}^T g_\tau M_{21})_{\mu\nu} = (M_{22}^T g_\tau^T M_{11})_{\mu\nu}$, which in terms of ζ reads:

$$\frac{\partial^2 f(\zeta^*_0, \zeta_0)}{\partial \zeta^*_{0\mu} \partial \zeta_{0\nu}} + \sum_{\alpha\beta} \frac{\partial \zeta_{\tau\alpha}}{\partial \zeta^*_{0\mu}} \frac{\partial^2 f(\zeta^*_\tau, \zeta_\tau)}{\partial \zeta_{\tau\alpha} \partial \zeta^*_{\tau\beta}} \frac{\partial \zeta^*_{\tau\beta}}{\partial \zeta_{0\nu}} = \sum_{\alpha\beta} \frac{\partial \zeta^*_{\tau\alpha}}{\partial \zeta^*_{0\mu}} \frac{\partial^2 f(\zeta^*_\tau, \zeta_\tau)}{\partial \zeta^*_{\tau\alpha} \partial \zeta_{\tau\beta}} \frac{\partial \zeta_{\tau\beta}}{\partial \zeta_{0\nu}}.$$

The last pair of terms in (6.67) can be replaced by the right-hand side of the latter expression, leading to (after some rearrangement):

$$\frac{\partial^2 F_\tau(z_0, z^*_\tau; \zeta)}{\partial \zeta^*_{0\mu} \partial \zeta_{0\nu}} = \sum_{\alpha\beta} \frac{\partial \zeta_{\tau\beta}}{\partial \zeta_{0\nu}} \left[\left(\frac{\partial^2 f(z^*_\tau, \zeta_\tau)}{\partial \zeta_{\tau\beta} \partial \zeta_{\tau\alpha}} - \frac{\partial^2 f(\zeta^*_\tau, \zeta_\tau)}{\partial \zeta_{\tau\beta} \partial \zeta_{\tau\alpha}} \right) \frac{\partial \zeta_{\tau\alpha}}{\partial \zeta^*_{0\mu}} - \frac{\partial^2 f(\zeta^*_\tau, \zeta_\tau)}{\partial \zeta_{\tau\beta} \partial \zeta^*_{\tau\alpha}} \frac{\partial \zeta^*_{\tau\alpha}}{\partial \zeta^*_{0\mu}} \right], \tag{6.68}$$

which is precisely Eq. (6.63b), only with indexes μ and ν interchanged.

Check 2. The same procedure is applied to the coupling Δ' – the result (6.65b) was obtained from (6.56b) by taking the second derivative with respect to $\zeta_{\tau\nu}$; now we start

from (6.56a) and differentiate with respect to $\zeta^*_{\tau\nu}$:

$$\begin{aligned}\frac{\partial^2\Delta'(z^*_\tau,\zeta_\tau)}{\partial\zeta_{\tau\mu}\partial\zeta^*_{\tau\nu}} &= -\frac{\partial^2 E(\zeta^*_\tau,\zeta_\tau)}{\partial\zeta_{\tau\mu}\partial\zeta^*_{\tau\nu}} - i\hbar\sum_\alpha\left[\frac{\partial^2 f(z^*_\tau,\zeta_\tau)}{\partial\zeta_{\tau\alpha}\partial\zeta_{\tau\mu}} - \frac{\partial^2 f(\zeta^*_\tau,\zeta_\tau)}{\partial\zeta_{\tau\alpha}\partial\zeta_{\tau\mu}}\right]\frac{\partial\dot\zeta_{\tau\alpha}}{\partial\zeta^*_{\tau\nu}} + i\hbar\sum_\alpha\frac{\partial^2 f(\zeta^*_\tau,\zeta_\tau)}{\partial\zeta_{\tau\alpha}\partial\zeta^*_{\tau\nu}}\frac{\partial\dot\zeta_{\tau\alpha}}{\partial\zeta_{\tau\mu}}\\ &= -i\hbar\sum_\alpha\left[\frac{\partial^2 f(z^*_\tau,\zeta_\tau)}{\partial\zeta_{\tau\alpha}\partial\zeta_{\tau\mu}} - \frac{\partial^2 f(\zeta^*_\tau,\zeta_\tau)}{\partial\zeta_{\tau\alpha}\partial\zeta_{\tau\mu}}\right]\frac{\partial\dot\zeta_{\tau\alpha}}{\partial\zeta^*_{\tau\nu}}\\ &+ \frac{\partial}{\partial\zeta_{\tau\mu}}\left[i\hbar\sum_\alpha\frac{\partial^2 f(\zeta^*_\tau,\zeta_\tau)}{\partial\zeta_{\tau\alpha}\partial\zeta^*_{\tau\nu}}\dot\zeta_{\tau\alpha} - \frac{\partial E(\zeta^*_\tau,\zeta_\tau)}{\partial\zeta^*_{\tau\nu}}\right] - i\hbar\sum_\alpha\frac{\partial^3 f(\zeta^*_\tau,\zeta_\tau)}{\partial\zeta_{\tau\mu}\partial\zeta_{\tau\alpha}\partial\zeta^*_{\tau\nu}},\end{aligned}$$

where, in passing to the second line, we have factored out $(\partial/\partial\zeta_{\tau\mu})$ – the term between brackets, the one upon which this derivative thereafter operates, vanishes identically in view of the equation of motion (6.3a) for ζ. At the same time, the last term is a third-order derivative of the function f and should be neglected according to our expansion protocol. This leaves only the first term, in complete agreement with (6.65b) (again, with indexes μ and ν interchanged).

6.5 The semiclassical time-evolution operator

Having the second-order matrices computed we now seek to determine a workable expression for the trace in the amplitude's equation of motion, Eq. (6.62). Henceforth, except when otherwise indicated, all quantities are evaluated at time t, being computed on the reference trajectory $z(t)$. We first note that the matrix U, whose individual blocks are given in Eqs. (6.64), can be written in the form of a product:

$$U = \begin{pmatrix} M_{11}^T & 0 \\ 0 & M_{22}^T \end{pmatrix}\begin{pmatrix} 0 & g \\ g^T & 0 \end{pmatrix}\begin{pmatrix} M_{11} & M_{12} \\ M_{21} & M_{22} \end{pmatrix}. \tag{6.69}$$

In this way, the required inverse-transpose is easy to express:

$$U^{-1} = M^{-1}\begin{pmatrix} 0 & g^{-T} \\ g^{-1} & 0 \end{pmatrix}\begin{pmatrix} M_{11}^{-T} & 0 \\ 0 & M_{22}^{-T} \end{pmatrix} \;\Rightarrow\; U^{-T} = \begin{pmatrix} M_{11}^{-1} & 0 \\ 0 & M_{22}^{-1} \end{pmatrix}\begin{pmatrix} 0 & g^{-T} \\ g^{-1} & 0 \end{pmatrix} M^{-T}. \tag{6.70}$$

Now, in a most crucial step, the inverse-transpose of the stability matrix M^{-T} (which springs from U^{-T}, as shown above) is compensated by the M^T in the matrix product $U^{-T}M^TVM$ appearing in (6.62). This striking simplification, together with the fact that the matrix V – depicted in Eqs. (6.66) – has a very simple structure,

$$V = \begin{pmatrix} 0 & 0 \\ 0 & i\hbar\, g^T R_{12} \end{pmatrix}, \tag{6.71}$$

results in a straightforward evaluation of the aforementioned product:

$$U^{-T}M^{T}VM = i\hbar \begin{pmatrix} R_{12}M_{21}M_{11}^{-1} & R_{12}M_{21}M_{22}^{-1} \\ 0 & 0 \end{pmatrix}. \tag{6.72}$$

Tracing this last matrix we arrive at the desired form of the equation of motion:

$$\dot{D}^{sc} = \tfrac{1}{2}\mathrm{tr}(R_{12}M_{21}M_{11}^{-1})D^{sc}, \tag{6.73}$$

which can be numerically integrated from the initial condition $D^{sc}(0) = 1$, together with Eqs. (6.3a) and (6.6), with $M_{21}(0) = 0_d$ and $M_{11}(0) = I_d$.

Owing to the linearity of (6.73) explicit expressions for the semiclassical amplitude can be worked out analytically; a particularly interesting form is found by noticing that, from (6.4a),

$$\dot{M}_{11} = R_{11}M_{11} + R_{12}M_{21} \quad \Rightarrow \quad R_{12}M_{21}M_{11}^{-1} = \dot{M}_{11}M_{11}^{-1} - R_{11}; \tag{6.74}$$

hence we may write, as long as the determinant of M_{11} does not vanish,

$$\dot{D}^{sc} = \tfrac{1}{2}\mathrm{tr}(\dot{M}_{11}M_{11}^{-1} - R_{11})D^{sc}, \tag{6.75}$$

whose time-integrated form (at final instant τ) is:

$$D_{\tau}^{sc}(z) = (\det M_{11}(\tau))^{1/2} \exp\left[-\tfrac{1}{2}\int_0^{\tau} dt\, \mathrm{tr}(R_{11}(t))\right]. \tag{6.76}$$

This is the sought semiclassical amplitude, here expressed in closed form.

In applications, however, it is more practical to numerically integrate Eq. (6.73) rather than employ the latter formula. The reason for this stems from the fact that phase correlations among basis elements are crucial in the IVR formula, and it is therefore essential that the overall phase associated with each element be a continuous function of time. Now, if one chooses to compute the semiclassical amplitude at specific instants using Eq. (6.76), one must keep track of the phase of the complex determinant 'det(M_{11})' in order to make sure that the correct branch of the square root is followed, so that the phase can be later 'unwrapped' into a continuous function of time. This requires evaluation of the determinant at short time intervals, which can be computationally demanding for systems with a large number of degrees of freedom.

Such difficulties are avoided if, instead, the amplitude is integrated from the initial condition $D_0^{sc}(z) = 1$ using the differential equation (6.73), although in that case one must deal with the inverse M_{11}^{-1}, which has to be computed at every evaluation of the amplitude's derivative – a potentially effective way of handling this problem is discussed

in §6.6 below.[v] Nevertheless, Eq. (6.76) enables direct inspection of some of the properties of the semiclassical amplitude, as we shall see in a moment.

As a final and important step, the semiclassical result, specifically obtained for the reference trajectory $z(t)$, is *extended for all orbits* $\zeta(t)$ that participate in the propagator's $\tilde{K}(w^*, z_0)$ integral expression, Eq. (6.27). This can be mathematically stated as follows:

$$D_\tau(z_0;\zeta) \approx D_\tau^{sc}(z)\big|_{z=\zeta} = D_\tau^{sc}(\zeta) \quad \text{[in Eq. (6.27)]}. \tag{6.77}$$

Therefore, the integral form of the semiclassical coherent-state propagator becomes (adding the appropriate normalization factors):

$$K_\tau^{sc}(w^*, z_0) = \int d\mu(\zeta_0)\langle w|\zeta_\tau\rangle\, D_\tau^{sc}(\zeta)\, \langle\zeta_0|z_0\rangle e^{\frac{i}{\hbar}S_\tau(\zeta)}, \tag{6.78}$$

which, together with the prescription (6.73), summarizes the semiclassical approximation. We now proceed to discuss some of its properties.

The first thing to note is that, since the amplitude depends neither on w^* or z_0, we might erase $\langle w|$ and $|z_0\rangle$ from this expression (just like in the 'zeroth-order' case of §6.2.1) leading to an initial-value representation for the semiclassical time-evolution operator itself:

$$\hat{U}^{sc}(\tau) = \int d\mu(\zeta_0)|\zeta_\tau\rangle D_\tau^{sc}(\zeta) e^{\frac{i}{\hbar}S_\tau(\zeta)}\langle\zeta_0|. \tag{6.79}$$

This approximated operator is not unitary,

$$[\hat{U}^{sc}(\tau)]^\dagger \hat{U}^{sc}(\tau) \neq \hat{1}, \tag{6.80}$$

except in simple cases where the time evolution amounts to a group transformation.

In the particular case of Glauber coherent states (Gaussian wavepackets – cf. §1.3.4) the result expressed in Eq. (6.79) reduces to Solari's propagator,[11] which is a Q-form version[vi] of the more popular Herman-Kluk formula.[72–74] The same result was found by Martin-Fierro and Llorente.[75] In these works, strategies completely different than the one followed here were used. The generalized result (6.79) has been derived by Viscondi starting from a primitive, 'duplicated phase-space' propagator[29] (see §6.5.1 for additional remarks on this regard). The derivation presented here may be seen as complementary to the latter, thus providing support to a point emphasized by Kay in Ref. [44]: that semiclassical IVR formulas, although fundamentally connected to primitive root-search propagators, stand as semiclassical approximations in their own right.

[v] A strategy for dealing with the phase unwrapping problem, which is also based on solving a differential equation rather than computing the semiclassical amplitude directly, is developed in Ref. [71].

[vi] The energy function defined as $E(z^*, z) = \langle z|\hat{H}|z\rangle$ is known as the 'Q-symbol' of the Hamiltonian. Solari uses this form of the energy function (the same we employ everywhere in this work). On the other hand, the Herman-Kluk propagator is formulated with a symmetrized version of the energy function, known as the 'Weyl-symbol' – see Ref. [43] for more details on this subject.

Let us now make some comments regarding the amplitude $D^{sc}_{\tau}(z)$, which is the distinguishing object of the semiclassical time-evolution operator of Eq. (6.79).

Consistency. According to the adopted expansion protocol, derivatives of D^{sc} with respect to initial conditions z_0 and z_0^* should be proportional to high-order terms; from Eq. (6.76) we get:

$$\frac{\partial D^{sc}_{\tau}(z)}{\partial z_{0\gamma}} = \frac{1}{2} D^{sc}_{\tau}(z) \sum_{\alpha\beta} \left\{ (M_{11}^{-1})_{\alpha\beta} \frac{\partial^2 z_{\tau\beta}}{\partial z_{0\alpha} \partial z_{0\gamma}} + \int_0^{\tau} dt \left[\frac{\partial^2 \dot{z}_{t\alpha}}{\partial z_{t\alpha} \partial z_{t\beta}} (M_{11})_{\beta\gamma} + \frac{\partial^2 \dot{z}_{t\alpha}}{\partial z_{t\alpha} \partial z^*_{t\beta}} (M_{21})_{\beta\gamma} \right] \right\}.$$

Consistency is therefore ensured by rules 'one' and 'three' of §6.4.1, for they state that the mixed derivatives on the right-hand side should be ignored during the semiclassical expansion. The same holds for $\partial D^{sc}_{\tau}(z)/\partial z^*_{0\gamma}$; similar analysis shows that $\partial \dot{D}^{sc}_{\tau}(z)/\partial z_{0\gamma}$ and $\partial \dot{D}^{sc}_{\tau}(z)/\partial z^*_{0\gamma}$ are also high-order, which is consistent with the zeroth order approximation for the amplitude's time derivative.

Focal points. A major feature of traditional (Gaussian-based) semiclassical IVR formulas is the fact that they are not directly affected by 'focal points' of the classical flow. This also holds for the generalized coherent-state propagator of Eq. (6.78). In the present context, focal points are phase-space points where $|\det(M_{11})| \to 0$. The time-integrated form of the amplitude [Eq. (6.76)] reveals that $D^{sc}_{\tau}(z) \to 0$ as $|\det(M_{11})| \to 0$, meaning that trajectories going through a focal point end up giving a negligible contribution to the integral formula for that particular instant τ, despite the indeterminate character exhibited by the equation of motion (6.73) at such instant (because of the inverse matrix block M_{11}^{-1}). Below, at §6.6, we briefly comment on how focal points may indirectly affect the integration of the semiclassical amplitude.

Linear Hamiltonians. We known from §6.2.1 that the classical propagator is exact for Hamiltonians which are linear in the coherent-state's group generators. Hence, for such systems, it must result from the more general semiclassical scheme that $D^{sc}_{\tau}(z) = 1$ for all $\tau > 0$ (for then the classical formula is recovered). This means that the right-hand side of (6.73) must vanish identically in those cases (recall the initial condition on amplitudes: $D^{sc}_{0}(z) = 1$). This is exemplified in the context of the bosonic and fermionic parametrizations of Chapters 2 and 3: in the case of linear Hamiltonians, both Fock and Gross-Pitaevskii matrices – F and G, respectively – figuring in the equations of motion (2.57) and (3.52) reduce to the z-independent one-body matrix h. Both equations take the general form

$$i\hbar\, \dot{z} = h_{21} + h_{22} z - z h_{11} - z h_{12} z,$$

whence we immediately conclude that $R_{12} = \partial \dot{z}/\partial z^* = 0$; therefore $(d/dt) D^{sc}_{t}(z) = 0$, as expected.

6.5.1 * Alternative expression

The integral expression (6.79) for the semiclassical time-evolution operator was previously derived via a different approach by Viscondi.[29] His starting point is a generalized coherent-state semiclassical propagator formulated in terms of complex trajectories – i.e. trajectories that live in an analytically-continued phase space, with twice the number of degrees of freedom. This latter 'root-search' propagator, in turn, is obtained by a coherent-state path-integral formulation followed by a stationary phase approximation. The fact that the result displayed at Eqs. (6.79) and (6.76) can also be found by means of such well-established techniques strengthens our more pedestrian derivation.[vii]

However, the time-integrated version of the semiclassical amplitude presented here differs in appearance from the one given in Viscondi's thesis. It is quite simple, though, to demonstrate the equivalence of both expressions; to end this section we perform this little calculation.

Starting from (6.76) we notice that, since $\mathrm{tr}(R) = \mathrm{tr}(R_{11} + R_{22})$, we may write:

$$\exp\left[-\tfrac{1}{2}\int_0^\tau dt\,\mathrm{tr}(R_{11})\right] = \exp\left[-\tfrac{1}{4}\int_0^\tau dt\,\mathrm{tr}(R)\right]\exp\left[\tfrac{1}{4}\int_0^\tau dt\,\mathrm{tr}(R_{22}-R_{11})\right]. \tag{6.81}$$

On the other hand, Eq. (A.4) (cf. appendix A), which is reproduced below, relates the trace of R with determinants of the metric matrix g:

$$\frac{d}{dt}\log(\det g) = -\mathrm{tr}(R) \quad\Rightarrow\quad \exp\left[-\int_0^\tau dt\,\mathrm{tr}(R)\right] = \frac{\det g(\tau)}{\det g(0)}.$$

Using this in (6.81) and taking the resulting formula into (6.76) one finds that the semiclassical amplitude at final time τ may be written as:

$$D^{sc}_\tau(z) = \left[\frac{\det g(\tau)}{\det g(0)}\right]^{1/4}(\det M_{11}(\tau))^{1/2}\exp\left[\tfrac{1}{4}\int_0^\tau dt\,\mathrm{tr}(R_{11}(t)-R_{22}(t))\right], \tag{6.82}$$

exactly as in Ref. [29]. This is also how Solari writes the semiclassical amplitude of his SU(2) coherent-state propagator.[12] When dealing with real trajectories, as opposed to analytically continued ones, this way of expressing D^{sc} has the advantage that, since $R_{22} = R^*_{11}$ and the metric matrix g is hermitian (meaning that its determinant is real) a explicit polar form is obtained:

$$D^{sc}_\tau(z) = \left[\frac{\det g(\tau)}{\det g(0)}\right]^{1/4}|\det M_{11}(\tau)|^{1/2}\exp\left[\tfrac{i}{2}\Big(\sigma_{11}(\tau) + \mathrm{Im}\int_0^\tau dt\,\mathrm{tr}\,R_{11}(t)\Big)\right], \tag{6.83}$$

[vii] Interestingly, the hypothesis $\kappa \to 1$ (κ being the normalization constant of the coherent state closure relation), which is required in Ref. [29] in order to get a convergent expression for the preliminary 'root-search' form of the semiclassical propagator, and which is therefore built-in the final integral expression for the time-evolution operator, was not needed in our derivation, since all constant factors stemming from the phase-space integrals in Eq. (6.34) cancel off.

where $\sigma_{11} = \arg(\det M_{11})$ must be evaluated in such a way as to make the semiclassical amplitude a continuous function of time.

6.6 The Z matrix

Looking back at the equation of motion (6.73) we realize that the time-dependent trace, which 'drives' the dynamics of D^{sc}, depends not on the stability matrix as a whole but only on the specific quotient of its two independent blocks, $M_{21}M_{11}^{-1}$. Here we explore this idea; we shall find that this observation allows an alternative approach to the semiclassical equation that potentially leads to significant computational savings when implementing the method. Since there is no longer any chance for confusion, we will drop the superscript 'sc' of the semiclassical amplitude from now on.

We begin with Eq. (6.73), where a new dynamical quantity, the $d \times d$ matrix Z, is defined:

$$\dot{D} = \tfrac{1}{2}\mathrm{tr}(R_{12}Z)D; \quad Z \equiv M_{21}M_{11}^{-1}. \tag{6.84}$$

Clearly, since at initial time $M_{21}(0) = 0_d$ an $M_{11}(0) = I_d$, we have $Z(0) = 0_d$. Moreover, an equation of motion for Z is easily found by differentiating the above definition with respect to t:

$$\begin{aligned}\frac{d}{dt}M_{21}M_{11}^{-1} &= \dot{M}_{21}M_{11}^{-1} - M_{21}M_{11}^{-1}\dot{M}_{11}M_{11}^{-1} \\ &= (R_{21}M_{11} + R_{22}M_{21})M_{11}^{-1} - M_{21}M_{11}^{-1}(R_{11}M_{11} + R_{12}M_{21})M_{11}^{-1} \\ &= R_{21} + R_{22}(M_{21}M_{11}^{-1}) - (M_{21}M_{11}^{-1})R_{11} - (M_{21}M_{11}^{-1})R_{12}(M_{21}M_{11}^{-1}).\end{aligned} \tag{6.85}$$

where Eqs. (6.5) have been used in substituting $\dot{M}_{11}$ and $\dot{M}_{21}$. From this we conclude that Z obeys the following first-order nonlinear equation:

$$\dot{Z} = R_{21} + R_{22}Z - ZR_{11} - ZR_{12}Z, \tag{6.86}$$

which, together with $Z(0) = 0_d$, can be integrated by standard numerical techniques. Thus the amplitude can be simultaneously evolved alongside with the Z matrix, rather than with the pair of independent stability matrix blocks, M_{11} and M_{21}. This brings two advantages. First, the system is half the size: Z has d^2 complex entries, whereas M_{11} and M_{21} combined have $2d^2$ complex entries. Secondly, direct integration of Z avoids the troublesome inversion of M_{11} (or some alternative procedure of equivalent complexity), an operation that has to be carried out at each time step in order to get $\dot{D}$ from Eq. (6.73).

There is a possible drawback, though, concerning the numerical stability of Eq. (6.86). Due to the nonlinearity of this equation, Z is expected to behave in a more complicated way than M_{21} and M_{11} (which, in contrast, obey linear dynamics). Also, the existence of focal points, where M_{11} becomes singular, is bound to lead to instabilities during the

integration of Z [however, this sort of obstacle also occurs if Eq. (6.73) is employed]. And, although such difficulties end up being alleviated, since $D \to 0$ when $\det(M_{11}) \to 0$, as discussed earlier, there might be some problems when trajectories go through regions near the focal point. We have not had the opportunity to investigate these issues more profoundly – this is why the reserved statement was made earlier, that the present scheme 'potentially' leads to savings in computational effort.

6.6.1 * Semiclassical phase correction and modulation

So far two different time-integrated expressions for the semiclassical amplitude have been discussed, Eqs. (6.76) and (6.82). Yet, perhaps the most straightforward way of writing D is:

$$D(\tau) = \exp\left[\tfrac{1}{2}\int_0^\tau dt\, \mathrm{tr}(R_{12}Z)\right]. \tag{6.87}$$

From this perspective, it is interesting to separate the real and imaginary parts of the complex phase. In order to do so, we introduce the following definitions:

$$Z = X + iY, \quad R_{11} = A_{11} + iB_{11}, \quad \text{and} \quad R_{12} = A_{12} + iB_{12}, \tag{6.88}$$

by means of which Eq. (6.87) assumes the form:

$$D(\tau) = \exp\left[\tfrac{1}{2}\int_0^\tau dt\, \mathrm{tr}(A_{12}X - B_{12}Y)\right] \exp\left[\tfrac{i}{2}\int_0^\tau dt\, \mathrm{tr}(A_{12}Y + B_{12}X)\right] \tag{6.89}$$

$$\equiv \exp\Big[i\theta(\tau) + \gamma(\tau)\Big], \tag{6.90}$$

where two real dimensionless quantities, θ and γ, have been implicitly defined. The first is simply a phase correction, whereas the second gives a logarithmic modulation factor which can be either positive or negative.

Meanwhile, by splitting the real and imaginary parts of Eq. (6.86) one finds:

$$\begin{aligned}\dot{X} = \;& A_{12} + (A_{11}X - XA_{11}) + (B_{11}Y + YB_{11}) \\ & - (XA_{12} - YB_{12})X + (XB_{12} + YA_{12})Y, \end{aligned} \tag{6.91a}$$

$$\begin{aligned}\dot{Y} = \;& -B_{12} + (A_{11}Y - YA_{11}) - (B_{11}X + XB_{11}) \\ & - (XA_{12} - YB_{12})Y - (XB_{12} + YA_{12})X, \end{aligned} \tag{6.91b}$$

where the relations $R_{21} = R_{12}^*$ and $R_{22} = R_{11}^*$ have been used. The initial condition $Z(0) = 0_d$ implies $X(0) = 0_d$ and $Y(0) = 0_d$. At the same time, the factors θ and γ can be integrated from:

$$\dot{\theta} = \tfrac{1}{2}\mathrm{tr}(A_{12}Y + B_{12}X), \tag{6.92a}$$

$$\dot{\gamma} = \tfrac{1}{2}\mathrm{tr}(A_{12}X - B_{12}Y), \tag{6.92b}$$

with initial conditions $\theta(0) = 0$ and $\gamma(0) = 0$.

Under this scheme, the semiclassical time evolution operator is simply expressed as:

$$\hat{U}(\tau) = \int d\mu(z_0)|z_\tau\rangle\, e^{\gamma_\tau} e^{\frac{i}{\hbar}(S_\tau + \hbar\,\theta_\tau)}\, \langle z_0|. \tag{6.93}$$

6.7 * Invariance under group transformations

The semiclassical amplitude D features a very appealing property: it is invariant under restricted group transformations of the coherent-state, where by 'restricted' we mean that the transformation has no explicit time-dependence. In Chapters 2 and 3, we saw examples of such transformations, where they were shown to materialize as holomorphic maps of the coherent-state label. Thus, in order to prove the invariance property, we consider two different descriptions, in which states are labeled by complex vectors z and w, and we suppose both sets of variables are related by an invertible map as follows:[viii]

$$\begin{cases} w = w(z) & \text{with } \partial w/\partial z^* = 0 \text{ and } \partial w/\partial t = 0, \\ z = z(w) & \text{with } \partial z/\partial w^* = 0 \text{ and } \partial z/\partial t = 0. \end{cases} \quad \text{(holomorphic and restricted).} \tag{6.94}$$

Several relations follow immediately from (6.94). For instance, in the context of the flow picture, where $w = w_\tau(w_0^*, w_0)$ and $z = z_\tau(z_0^*, z_0)$, derivatives of w with respect to w_0 and w_0^* can be expressed in terms of similar derivatives belonging to the z-label description:

$$\frac{\partial w_{\tau\alpha}}{\partial w_{0\beta}} = \sum_{\gamma\gamma'} \frac{\partial w_{\tau\alpha}}{\partial z_{\tau\gamma}} \frac{\partial z_{\tau\gamma}}{\partial z_{0\gamma'}} \frac{\partial z_{0\gamma'}}{\partial w_{0\beta}}, \quad \frac{\partial w^*_{\tau\alpha}}{\partial w_{0\beta}} = \sum_{\gamma\gamma'} \frac{\partial w^*_{\tau\alpha}}{\partial z^*_{\tau\gamma}} \frac{\partial z^*_{\tau\gamma}}{\partial z_{0\gamma'}} \frac{\partial z_{0\gamma'}}{\partial w_{0\beta}}, \tag{6.95a}$$

$$\frac{\partial w_{\tau\alpha}}{\partial w^*_{0\beta}} = \sum_{\gamma\gamma'} \frac{\partial w_{\tau\alpha}}{\partial z_{\tau\gamma}} \frac{\partial z_{\tau\gamma}}{\partial z^*_{0\gamma'}} \frac{\partial z^*_{0\gamma'}}{\partial w^*_{0\beta}}, \quad \frac{\partial w^*_{\tau\alpha}}{\partial w^*_{0\beta}} = \sum_{\gamma\gamma'} \frac{\partial w^*_{\tau\alpha}}{\partial z^*_{\tau\gamma}} \frac{\partial z^*_{\tau\gamma}}{\partial z^*_{0\gamma'}} \frac{\partial z^*_{0\gamma'}}{\partial w^*_{0\beta}}. \tag{6.95b}$$

Notice how these expressions owe their remarkable simplicity to the analytic property of the maps $w(z)$ and $z(w)$. The above relations become more manageable if we introduce the transformation's Jacobian matrix Λ (and its inverse) through:

$$\Lambda_{\alpha\beta} = \frac{\partial w_\alpha}{\partial z_\gamma}, \quad \Lambda^{-1}_{\alpha\beta} = \frac{\partial z_\alpha}{\partial w_\gamma}. \tag{6.96}$$

Thence, if we denote by M the z-label stability matrix and, correspondingly, by $\tilde{M}$ the w-label stability matrix, Eqs. (6.95) read:

$$\tilde{M}_{11} = \Lambda_\tau M_{11} \Lambda_0^{-1}, \quad \tilde{M}_{21} = \Lambda^*_\tau M_{21} \Lambda_0^{-1}, \quad \tilde{M}_{12} = \Lambda_\tau M_{12} \Lambda_0^{*-1}, \quad \tilde{M}_{22} = \Lambda^*_\tau M_{22} \Lambda_0^{*-1}; \tag{6.97}$$

[viii] If the map $z \to w$ is parametrized by a set of s parameters, collectively denoted by a, as in $w = w(z; a)$, then the explicit time-dependence is encoded in the partial derivative $\partial w/\partial t = \sum_{j=1}^{s} (\partial w/\partial a_j)\dot{a}_j$; thus the 'restricted' condition translates into: $\dot{a}_j = 0$, for $1 \le j \le s$; the nomenclature is borrowed from the classical theory of canonical transformations.

i.e. they tell us how the stability matrix transforms under the map $z \to w$. In what follows, we carry on with this notation: a tilde is used to indicate quantities belonging to the w-label description, whereas 'untilded' quantities refer to the z-label description.

Our goal is to show that $\tilde{D} = D$. For that purpose we shall consider the quantity '$\mathrm{tr}(ZR_{12})$' figuring in Eq. (6.84) – if this trace is unchanged by the transformation then it follows that the amplitudes in both descriptions are equal, since in that case they satisfy the same equation of motion with the same initial condition.

We begin with matrix Z – using (6.97) together with the definition (6.84) one easily finds:

$$\tilde{Z} = \tilde{M}_{21}\tilde{M}_{11}^{-1} = (\Lambda_\tau^* M_{21}\Lambda_0^{-1})(\Lambda_0 M_{11}^{-1}\Lambda_\tau^{-1}) = \Lambda_\tau^*(M_{21}M_{11}^{-1})\Lambda_\tau^{-1} = \Lambda_\tau^* Z \Lambda_\tau^{-1}. \tag{6.98}$$

Next we inquire about the system's Jacobian matrix block R_{12}; let us consider its w-label description, i.e. $(\tilde{R}_{12})_{\alpha\beta} = (\partial \dot{w}_\alpha / \partial w_\beta^*)$. The first thing to notice is that the time derivative $\dot{w}$ does not inherit the transformation's holomorphic property; nevertheless, it can be expressed as a function of z and z^* in a tractable manner:

$$\frac{d}{dt}w_\alpha = \sum_\gamma \frac{\partial w_\alpha}{\partial z_\gamma}\dot{z}_\gamma \quad \Rightarrow \quad \dot{w} = \dot{w}(\Lambda(z), \dot{z}(z^*, z)) \tag{6.99}$$

(remember: $\partial w/\partial t = 0$). This enables application of the chain rule in the following way:

$$\begin{aligned}\frac{\partial \dot{w}_\alpha}{\partial w_\beta^*} &= \sum_\gamma \frac{\partial w_\alpha}{\partial z_\gamma}\frac{\partial \dot{z}_\gamma}{\partial w_\beta^*} + \sum_\gamma \dot{z}_\gamma \frac{\partial^2 w_\alpha}{\partial z_\gamma \partial w_\beta^*} \\ &= \sum_{\gamma\gamma'} \frac{\partial w_\alpha}{\partial z_\gamma}\Big(\frac{\partial \dot{z}_\gamma}{\partial z_{\gamma'}}\underbrace{\frac{\partial z_{\gamma'}}{\partial w_\beta^*}}_{0} + \frac{\partial \dot{z}_\gamma}{\partial z_{\gamma'}^*}\frac{\partial z_{\gamma'}^*}{\partial w_\beta^*}\Big) + \sum_\gamma \dot{z}_\gamma \frac{\partial}{\partial z_\gamma}\Big(\underbrace{\frac{\partial w_\alpha}{\partial w_\beta^*}}_{0}\Big) = \sum_{\gamma\gamma'} \frac{\partial w_\alpha}{\partial z_\gamma}\frac{\partial \dot{z}_\gamma}{\partial z_{\gamma'}^*}\frac{\partial z_{\gamma'}^*}{\partial w_\beta^*}\end{aligned} \tag{6.100}$$

(note how the independence of w and w^* eliminates the second-order derivative). The transformation relations for the remaining R blocks can be found in a similar fashion; the result is:

$$\tilde{R}_{11} = \Lambda_\tau R_{11}\Lambda_\tau^{-1}, \quad \tilde{R}_{12} = \Lambda_\tau R_{12}\Lambda_\tau^{*-1}, \quad \tilde{R}_{21} = \Lambda_\tau^* R_{21}\Lambda_\tau^{-1}, \quad \tilde{R}_{22} = \Lambda_\tau^* R_{22}\Lambda_\tau^{*-1}. \tag{6.101}$$

Finally, combining (6.97) and (6.101), we find that under the map $z \to w$ the trace term at issue behaves as follows:

$$\mathrm{tr}(\tilde{Z}\tilde{R}_{12}) = \mathrm{tr}(\Lambda_\tau^* Z \Lambda_\tau^{-1} \cdot \Lambda_\tau R_{12}\Lambda_\tau^{*-1}) = \mathrm{tr}(ZR_{12}), \tag{6.102}$$

showing that $\dot{\tilde{D}} = \dot{D}$. Therefore, in view of the reasons mentioned earlier, the semiclassical amplitude is invariant: $\tilde{D} = D$, as we intended to demonstrate.

Check. The fact that D is unaffected by the map $z \to w$ can also be proved by consid-

ering the time-integrated form of the semiclassical amplitude, as displayed in Eq. (6.76). We shall present this alternative proof as a check, but also because it brings attention to an interesting property of the class of transformations depicted in (6.94).

Looking at expression (6.76) we see that the terms that must be examined are 'det(M_{11})' and 'tr(R_{11})'. The latter is easily shown to be invariant; with the help of (6.101) we obtain:

$$\mathrm{tr}(\tilde{R}_{11}) = \mathrm{tr}(\Lambda_\tau R_{11} \Lambda_\tau^{-1}) = \mathrm{tr}(R_{11}). \tag{6.103}$$

On the other hand, from (6.97) we deduce that the determinant term transforms according to:

$$\det(\tilde{M}_{11}) = \det(\Lambda_\tau M_{11} \Lambda_0^{-1}) = \det(M_{11}) \cdot \det(\Lambda_\tau)[\det(\Lambda_0)]^{-1}. \tag{6.104}$$

Thus in order to confirm the amplitude's invariance we must show that the product of the last two determinants on the right side of the above formula is unity.

For that purpose let us compute the following time derivative:

$$\frac{d}{dt}\det(\Lambda) = \det(\Lambda)\mathrm{tr}(\dot{\Lambda}\Lambda^{-1}) \tag{6.105}$$

– as it turns out, a detailed analysis of the trace factor reveals that:

$$\begin{aligned}
(\dot{\Lambda}\Lambda^{-1})_{\alpha\beta} &= \sum_\gamma \Big[\frac{d}{dt}\left(\frac{\partial w_\alpha}{\partial z_\gamma}\right)\Big]\frac{\partial z_\gamma}{\partial w_\beta} = \sum_{\gamma\gamma'}\Big[\frac{\partial^2 w_\alpha}{\partial z_\gamma \partial z'_\gamma}\dot{z}_{\gamma'}\Big]\frac{\partial z_\gamma}{\partial w_\beta} \\
&= \sum_{\gamma'}\dot{z}_{\gamma'}\Big[\frac{\partial}{\partial z_{\gamma'}}\left(\sum_\gamma \frac{\partial w_\alpha}{\partial z_\gamma}\frac{\partial z_\gamma}{\partial w_\beta}\right) - \sum_\gamma \frac{\partial w_\alpha}{\partial z_\gamma}\frac{\partial^2 z_\gamma}{\partial w_\beta \partial z_{\gamma'}}\Big] \\
&= \sum_{\gamma'}\dot{z}_{\gamma'}\Big[\frac{\partial}{\partial z_{\gamma'}}\underbrace{\sum_\gamma \Lambda_{\alpha\gamma}(\Lambda^{-1})_{\gamma\beta}}_{\delta_{\alpha\beta}} - \sum_\gamma \frac{\partial w_\alpha}{\partial z_\gamma}\frac{\partial}{\partial w_\beta}\Big(\underbrace{\frac{\partial z_\gamma}{\partial z_{\gamma'}}}_{\delta_{\gamma\gamma'}}\Big)\Big] = 0.
\end{aligned} \tag{6.106}$$

Hence we conclude that transformations of the type described in Eqs. (6.94) have the interesting property that the determinant of their Jacobian matrix Λ does not change with time, implying that their value at any given instant τ is the same as at $t = 0$, or: $\det(\Lambda_\tau) = \det(\Lambda_0)$. Therefore, Eq. (6.104) actually states that:

$$\det(\tilde{M}_{11}) = \det(M_{11}); \tag{6.107}$$

and this, together with (6.103) – and in view of Eq. (6.76) – confirms that the semiclassical amplitude D is the precisely the same in both descriptions.

Extended semiclassical initial-value representation. We have seen earlier that the multiconfigurational method of Chapter 4, when constructed in terms of fermionic basis states (Thouless determinants), admits an 'extended' formalism wherein configurations may be subjected to group transformations at specific instants during the propagation – which

have the purpose of regularizing their dynamics (cf. §3.3 and §4.6). In particular, we have introduced the notion of 'extended configurations': basis states carrying an action phase that changes discontinuously when a group transformation is applied to the state, in such a way that geometrical phases acquired in the process are balanced out; and we have demonstrated that quantum amplitudes associated with such configurations are unaffected by the group transformation. What we have shown now is that the semiclassical amplitude inherits this 'invariance' property. Therefore, the same kind of extended formalism is also possible in a semiclassical context. In other words, the content of this section lays the ground for an extended (fermionic) semiclassical initial-value representation; one based on Thouless determinants that can be independently regularized during their time evolution without compromising the delicate phase correlations of the integral formula.

6.8 Semiclassical IVR: complete scheme

In this final section, we delineate a general scheme for implementing the semiclassical method; for future reference, we compile its basic equations in an organized manner.

Let us assume, for the sake of definiteness, that one seeks to obtain an approximation to a correlation function of the following type:

$$C_{ab}(t) = \langle \psi_a | \hat{U}(t) | \psi_b \rangle, \tag{6.108}$$

where $\langle \psi_a |$ and $| \psi_b \rangle$ are fixed, arbitrary states. In the above formula, we shall substitute the quantum time evolution operator $\hat{U}(t)$ for its semiclassical approximation. In practice, the phase-space integral over initial conditions, figuring on Eq. (6.79), should be replaced with a discrete sum. Leaving aside technical details concerning the basis-set construction, the semiclassical version of (6.108) used in applications reads:

$$C^{sc}_{ab}(t) = n_t \sum_{k=1}^{m} \lambda_k \langle \psi_a | z_{tk} \rangle \, e^{\gamma_k + i\theta_k} e^{\frac{i}{\hbar} S_k} \, \langle z_{0k} | \psi_b \rangle, \tag{6.109}$$

where m is the number of basis elements. We chose to represent the semiclassical amplitude in the way of §6.6.1, in terms of 'phase correction' and 'modulation' variables, θ and γ respectively. In writing (6.109), we have resorted to the same kind of discretization employed in §4.2.6, where the weight λ_k associated with each orbit is supposed to approximate the invariant measure evaluated at the point z_{0k}, that is $\lambda_k \approx d\mu(z_{0k})$ (this is straightforward when initial conditions are arranged on a regular grid, but more involved options – e.g. based on Monte Carlo sampling – are possible). As we have seen earlier, the unitary property of the time evolution is lost within the semiclassical framework. For that reason, the above formula contains an overall time-dependent factor n_t whose purpose is

to normalize any results obtained from $C_{ab}^{sc}(t)$.

The differential equations needed for computing the ingredients that go into Eq. (6.109) are scattered along the present chapter. In what follows, we merely display them in a more comprehensible way. For porpuses of diversity, however, we shall give such equations in terms of real variables. In order to do so, we decompose each coherent-state parameter vector z into its (dimensionless) real and imaginary parts, according to

$$z_\alpha = (q_\alpha + ip_\alpha)/\sqrt{2}, \quad 1 \leq \alpha \leq d \tag{6.110}$$

(the basis-set subscript will be omitted when referring to individual trajectories). The form of this latter expression, as well as the (q, p) notation, are reminiscent from the canonical coherent-state case, where these real parameters reduce to familiar coordinate and momentum variables – evidently, this interpretation is devoid of meaning in a generalized description.

Let us begin by considering the energy function $E(z^*, z)$. Since this function is real, writing it in terms of (q, p) amounts to relabeling its arguments:

$$E(z^*, z) = \langle z|\hat{H}|z\rangle \to E(q, p). \tag{6.111}$$

The same goes for the Kähler potential $f(z^*, z) = \log\{z|z\}$; we simply reinterpret it as:

$$f(z^*, z) \to f(q, p). \tag{6.112}$$

The remaining geometrical ingredients are easily recast in terms of (q, p). Using (6.110) and the chain rule, the complex gradients of f become:

$$\frac{\partial f(z^*, z)}{\partial z_\alpha} = \frac{1}{\sqrt{2}}\left(\frac{\partial f(q, p)}{\partial q_\alpha} - i\frac{\partial f(q, p)}{\partial p_\alpha}\right), \quad \frac{\partial f(z^*, z)}{\partial z_\alpha^*} = \frac{1}{\sqrt{2}}\left(\frac{\partial f(q, p)}{\partial q_\alpha} + i\frac{\partial f(q, p)}{\partial p_\alpha}\right). \tag{6.113}$$

Meanwhile, the phase-space metric $g(z^*, z)$ is split into real and imaginary parts, which are conveniently named $g_R(q, p)$ and $g_I(q, p)$ – these are implicitly defined below; starting from (1.58) and using the chain rule we get (arguments are omitted for brevity):

$$g_{\alpha\beta} = \frac{1}{2}\left(\frac{\partial^2 f}{\partial q_\alpha \partial q_\beta} + \frac{\partial^2 f}{\partial p_\alpha \partial p_\beta}\right) + \frac{i}{2}\left(\frac{\partial^2 f}{\partial q_\alpha \partial p_\beta} - \frac{\partial^2 f}{\partial p_\alpha \partial q_\beta}\right) \equiv (g_R + ig_I)_{\alpha\beta}. \tag{6.114}$$

Since g is hermitian, it follows that g_R is a symmetric matrix, whereas g_I is antisymmetric. We are now ready to list the basic equations of the semiclassical approach.

In terms of the real-valued coherent-state parameters (q, p) the classical equations of

motion [cf. Eq.(1.69)] can be put in the following matrix form:

$$\hbar \begin{pmatrix} \dot{q} \\ \dot{p} \end{pmatrix} = \begin{pmatrix} g_R & g_I \\ -g_I & g_R \end{pmatrix}^{-1} \begin{pmatrix} \partial E/\partial p \\ -\partial E/\partial q \end{pmatrix}, \tag{6.115}$$

with each trajectory being spawned from one of the initial points $z_{0k} = (q_{0k}, p_{0k})$, for $1 \leq k \leq m$. Notice that, here, all quantities are dimensionless, except for the energy function E and the time variable t (with $\hbar$ connecting the time and energy scales).

The action phase, in turn, is integrated from

$$\dot{S} = \frac{\hbar}{2} \sum_{\alpha=1}^{d} \left(\frac{\partial f}{\partial p_\alpha} \dot{q}_\alpha - \frac{\partial f}{\partial q_\alpha} \dot{p}_\alpha \right) - E, \tag{6.116}$$

the right-hand side being simply the (q, p)-version of the Lagrangian defined in Eq. (1.66).

The phase θ and modulation γ, related to the semiclassical amplitude (6.87), depend on the 'second-order dynamics' built into the matrix Z, introduced in §6.6. The required real and imaginary parts of the Jacobian matrices R_{11} and R_{12} – the quantities $\{A_{11}, B_{11}, A_{12}, B_{12}\}$ defined in Eq. (6.88) – can be computed from:

$$(A_{11})_{\alpha\beta} = \frac{1}{2} \left(\frac{\partial \dot{q}_\alpha}{\partial q_\beta} + \frac{\partial \dot{p}_\alpha}{\partial p_\beta} \right), \quad (B_{11})_{\alpha\beta} = \frac{1}{2} \left(\frac{\partial \dot{p}_\alpha}{\partial q_\beta} - \frac{\partial \dot{q}_\alpha}{\partial p_\beta} \right), \tag{6.117a}$$

$$(A_{12})_{\alpha\beta} = \frac{1}{2} \left(\frac{\partial \dot{q}_\alpha}{\partial q_\beta} - \frac{\partial \dot{p}_\alpha}{\partial p_\beta} \right), \quad (B_{12})_{\alpha\beta} = \frac{1}{2} \left(\frac{\partial \dot{q}_\alpha}{\partial p_\beta} + \frac{\partial \dot{p}_\alpha}{\partial q_\beta} \right). \tag{6.117b}$$

In order to express the equations of motion for X and Y – the real and imaginary parts of Z, as denoted in Eq. (6.88) – it is convenient to define the following auxiliary matrices:

$$F_1 = \quad A_{12} + A_{11}X - XA_{11} + B_{11}Y + YB_{11}, \tag{6.118a}$$

$$F_2 = -B_{12} + A_{11}Y - YA_{11} - B_{11}X - XB_{11}, \tag{6.118b}$$

$$G_1 = XA_{12} - YB_{12}, \tag{6.118c}$$

$$G_2 = YA_{12} + XB_{12}. \tag{6.118d}$$

Then, according to (6.91), X and Y can be integrated from:

$$\dot{X} = F_1 - G_1X + G_2Y, \tag{6.119a}$$

$$\dot{Y} = F_2 - G_1Y - G_2X, \tag{6.119b}$$

with initial conditions $X_0 = Y_0 = 0$.

The auxiliary quantities G_1 and G_2 of (6.118) can then be re-utilized in the equations

of motion for the semiclassical corrections, θ and γ, in which case Eq. (6.92) reads:

$$\dot{\gamma} = \tfrac{1}{2}\mathrm{tr}(G_1), \tag{6.120a}$$

$$\dot{\theta} = \tfrac{1}{2}\mathrm{tr}(G_2). \tag{6.120b}$$

These variables should be initialized to zero: $\gamma_0 = \theta_0 = 0$.

Finally, the semiclassical correlation function can be compactly expressed if we put

$$J_k(a,b) = \langle \psi_a | z_{tk} \rangle \langle z_{0k} | \psi_b \rangle, \tag{6.121}$$

which encloses all dependence on the boundary states ψ_b and ψ_a. In this way, the end result takes the form:

$$C_{ab}^{sc}(t) = n_t \sum_{k=1}^{m} \lambda_k \, J_k(a,b) \, e^{\gamma_k + i\theta_k} e^{\frac{i}{\hbar} S_k}. \tag{6.122}$$

This completes the raw scheme of the semiclassical initial-value representation method for generalized coherent-states.

Concluding remarks

In this work we have formulated a multiconfigurational, trajectory-guided quantum propagation scheme whose distinctive feature consists in employing generalized coherent states as basis elements. In this sense, the technique is seen as a natural extension of the coupled coherent states method of Shalashilin and Child[25–27] whereupon frozen Gaussians are replaced by more general configurations. At the same time, the main qualities of the original CCS are retained: quantum amplitudes obey an integro-differential equation (or a linear matrix equation, in the case of discrete basis sets) where the strength of their mutual coupling is controled by a localized overlap function; moreover, these amplitudes present a smooth time dependence, owing to their oscillatory behavior being partially compensated by the classical motion of the basis elements and their action phases.

The preparatory exposition of Chapters 1, 2 and 3 was deliberately constructed in such a way that no deep understanding of group-theory concepts was necessary, neither to derive the basic equations of the method nor to implement it numerically – we have seen that all geometrical ingredients that enter the basic formulas can be straightforwardly evaluated from the coherent-state overlap function alone. Also, the single-configurational dynamics of both bosonic and fermionic systems, formulated in terms of coherent states of the special unitary group, were identified with well-known mean-field theories.

At Chapter 4, three versions of the generalized CCS method have been devised: continuum, non-unitary and unitary. The continuum version most evidently displays the novel elements due to the non-Euclidean geometry associated with the generalized coherent states and it serves primarily as a starting point for a number of possible analytical approximations. The non-unitary version, which is only briefly discussed in this work, can be understood as a direct attempt to reproduce the continuum formulas by reducing phase-space integrals into finite sums.

The discrete unitary version, meanwhile, is the standard form of the method, being the most adequate for the majority of practical applications. Its working equations do not differ in overall structure from their analogue expressions of the original gaussian-wavepacket approach. This is due to the fact that all information concerning distinct coherent-state geometries is encoded in a small number of key elements, namely: the overlap, the phase-space metric and the classical equations of motion – a most desirable feature for programming purposes, for it means that the core subroutines of the method

are essentially independent of the particular type of coherent-state parametrization chosen for the problem at hand.

The discrete version was studied in great detail and several aspects of its numerical implementation were examined. In particular, an interesting parallelization scheme was proposed and its efficiency validated.

In Chapter 5 we have illustrated the general aspects of the proposed technique with applications to simple models of bosonic and fermionic systems, governed by prototype Hubbard-like Hamiltonians. The generalized trajectory-based methodology proved to be a viable numerical approach for solving both model problems.

Finally, the results of Chapter 6 can be immediately combined with the coherent-state parametrizations studied in Chapters 2 and 3. This leads to a trajectory-based semiclassical approach to bosonic and fermionic systems – one which properly accounts for particle interchange symmetry. This opens a wide range of possible applications in what concerns time-dependent many-body problems, provided these can be suitably treated from a semiclassical perspective. For bosons, this adequacy is found in systems composed of a large number of particles. For fermions, on the other hand, such 'classicality' criteria seem to involve considerations of a more complicated sort.[76] We may nevertheless conjecture that, whenever mean-field calculations are capable of producing reasonably accurate results for a given Fermi system, then a semiclassical treatment (in this case, constructed from a swarm of such mean-field solutions) will most likely be justified. In this work, however, we do not explore such possibilities – they are delegated to future investigation.

Bibliography

[1] Nancy Makri. Time-dependent quantum methods for large systems. *Annual Review of Physical Chemistry*, 50(1):167, 1999. URL https://doi.org/10.1146/annurev.physchem.50.1.167.

[2] W. H. Miller and K. A. White. Classical models for electronic degrees of freedom: The second-quantized many-electron Hamiltonian. *The Journal of Chemical Physics*, 84(9):5059, 1986. URL https://doi.org/10.1063/1.450655.

[3] A. Kirrander and D. V. Shalashilin. Quantum dynamics with fermion coupled coherent states: Theory and application to electron dynamics in laser fields. *Physical Review A*, 84(3):033406, 2011. URL https://doi.org/10.1103/PhysRevA.84.033406.

[4] F. Grossmann, M. Buchholz, E. Pollak, and M. Nest. Spin effects and the Pauli principle in semiclassical electron dynamics. *Physical Review A*, 89(3):032104, 2014. URL https://doi.org/10.1103/PhysRevA.89.032104.

[5] H. Feldmeier and J. Schnack. Molecular dynamics for fermions. *Reviews of Modern Physics*, 72(3):655, 2000. URL https://doi.org/10.1103/RevModPhys.72.655.

[6] Peter Kramer and Marcos Saraceno. *Geometry of the Time-Dependent Variational Principle in Quantum Mechanics*. Springer-Verlag, New York, 1981. URL https://doi.org/10.1007/3-540-10579-4.

[7] Robert Delbourgo. Minimal uncertainty states for the rotation and allied groups. *Journal of Physics A: Mathematical and General*, 10(11):1837, 1977. URL http://iopscience.iop.org/article/10.1088/0305-4470/10/11/012.

[8] R. Delbourgo and J. R. Fox. Maximum weight vectors possess minimal uncertainty. *Journal of Physics A: Mathematical and General*, 10(12):L233, 1977. URL http://iopscience.iop.org/article/10.1088/0305-4470/10/12/004.

[9] W.-M. Zhang, D. H. Feng, and R. Gilmore. Coherent states: Theory and some applications. *Reviews of Modern Physics*, 62(4):867, 1990. URL https://doi.org/10.1103/RevModPhys.62.867.

[10] T. Van Voorhis and D. R. Reichman. Semiclassical representations of electronic structure and dynamics. *The Journal of Chemical Physics*, 120(2):579, 2004. URL https://doi.org/10.1063/1.1630963.

[11] Hernan G. Solari. Glauber coherent states and the semiclassical propagator. *Journal of Mathematical Physics*, 27(5):1351, 1986. URL http://dx.doi.org/10.1063/1.527142.

[12] Hernan G. Solari. Semiclassical treatment of spin system by means of coherent states. *Journal of Mathematical Physics*, 28(5):1097, 1987. URL http://dx.doi.org/10.1063/1.527554.

[13] T. F. Viscondi, A. Grigolo, and M. A. M. de Aguiar. Semiclassical propagator in the generalized coherent-state representation. (arXiv:1510.05952/quant-ph). URL https://arxiv.org/abs/1510.05952.

[14] David J. Thouless. Stability conditions and nuclear rotations in the Hartree-Fock theory. *Nuclear Physics*, 21:225–232, 1960. URL http://www.sciencedirect.com/science/article/pii/0029558260900481.

[15] E. Deumens and Y. Öhrn. Time-dependent dynamics of a determinantal state. *Journal of Molecular Structure (Theochem)*, 199:23, 1989. URL http://dx.doi.org/10.1016/0166-1280(89)80039-9.

[16] E. Deumens, A. Diz, H. Taylor, and Y. Öhrn. Time-dependent dynamics of electrons and nuclei. *The Journal of Chemical Physics*, 96(9):6820, 1992. URL http://dx.doi.org/10.1063/1.462571.

[17] E. Deumens, A. Diz, R. Longo, and Y. Öhrn. Time-dependent theoretical treatments of the dynamics of electrons and nuclei in molecular systems. *Reviews of Modern Physics*, 66(3):917, 1994. URL http://dx.doi.org/10.1103/RevModPhys.66.917.

[18] Toru Suzuki. Classical and quantum mechanical aspects of time-dependent Hartree-Fock trajectories. *Nuclear Physics A*, 398:557, 1983. URL http://dx.doi.org/10.1016/0375-9474(83)90302-0.

[19] H. Kuratsuji and T. Suzuki. Path integral approach to many-nucleon systems and time-dependent Hartree-Fock. *Physics Letters B*, 92:19, 1980. URL https://doi.org/10.1016/0370-2693(80)90293-2.

[20] H. Kuratsuji and T. Suzuki. Path integral approach to many-body systems and classical quantization of time-dependent mean field. *Supplement of the Progress of Theoretical Physics*, 74-75:209, 1983. URL https://doi.org/10.1143/PTPS.74.209.

[21] T. F. Viscondi and M. A. M. de Aguiar. Semiclassical propagator for SU(n) coherent states. *Journal of Mathematical Physics*, 52(5):052104, 2011. URL https://doi.org/10.1063/1.3583996.

[22] T. F. Viscondi and M. A. M. de Aguiar. Initial value representation for the SU(n) semiclassical propagator. *The Journal of Chemical Physics*, 134(23):234105, 2011. URL https://doi.org/10.1063/1.3601344.

[23] T. Van Voorhis and E. J. Heller. Nearly real trajectories in complex semiclassical dynamics. *Physical Review A*, 66(5):050501, 2002. URL https://doi.org/10.1103/PhysRevA.66.050501.

[24] T. Van Voorhis and E. J. Heller. Similarity transformed semiclassical dynamics. *The Journal of Chemical Physics*, 119(23):12153, 2003. URL https://doi.org/10.1063/1.1626621.

[25] D. V. Shalashilin and M. S. Child. Time dependent quantum propagation in phase space. *The Journal of Chemical Physics*, 113(22):10028, 2000. URL https://doi.org/10.1063/1.1322075.

[26] D. V. Shalashilin and M. S. Child. Multidimensional quantum propagation with the help of coupled coherent states. *The Journal of Chemical Physics*, 115(12):5367, 2001. URL https://doi.org/10.1063/1.1394939.

[27] D. V. Shalashilin and M. S. Child. The phase space CCS approach to quantum and semiclassical molecular dynamics for high-dimensional systems. *Chemical Physics*, 304:103, 2004. URL https://doi.org/10.1016/j.chemphys.2004.06.013.

[28] A. Grigolo, T. F. Viscondi, and M. A. M. de Aguiar. Multiconfigurational quantum propagation with trajectory-guided generalized coherent states. *The Journal of Chemical Physics*, 144(9):094106, 2016. URL http://dx.doi.org/10.1063/1.4942926.

[29] Thiago. F. Viscondi. *Propagação Semiclássica na Representação de Estados Coerentes*. PhD thesis, Universidade Estadual de Campinas, Brazil, 2013. URL http://www.bibliotecadigital.unicamp.br/document/?code=000904028&opt=4&lg=en_US. (available in Portuguese).

[30] Marcus A. M. de Aguiar. *Tópicos de Mecânica Clássica*. São Paulo: Editora Livraria da Física – Rio de Janeiro: Centro Brasileiro de Pesquisas Físicas, 2011.

[31] M. A. M. de Aguiar, S. A. Vitiello, and A. Grigolo. An initial value representation for the coherent state propagator with complex trajectories. *Chemical Physics*, 370: 42, 2010. URL https://doi.org/10.1016/j.chemphys.2010.01.020.

[32] J. A. Green, A. Grigolo, M. Ronto, and D. V. Shalashilin. A two-layer approach to the coupled coherent states method. *The Journal of Chemical Physics*, 144(2): 024111, 2016. URL http://dx.doi.org/10.1063/1.4939205.

[33] Katsuhisa Ohta. Time-dependent variational principle with constraints. *Chemical Physics Letters*, 329(3):248–254, 2000. URL http://dx.doi.org/10.1016/S0009-2614(00)01016-2.

[34] J. Broeckhove, L. Lathouwers, E. Kesteloot, and P. Van Leuven. On the equivalence of time-dependent variational principles. *Chemical Physics Letters*, 149(5-6):547–550, 1988. URL http://dx.doi.org/10.1016/0009-2614(88)80380-4.

[35] P.-O. Löwdin and P. K. Mukherjee. Some comments on the time-dependent variation principle. *Chemical Physics Letters*, 14(1):1–7, 1972. URL http://dx.doi.org/10.1016/0009-2614(72)87127-6.

[36] M. Beck, A. Jäckle, G. A. Worth, and H.-D. Meyer. The multiconfiguration time-dependent Hartree (MCTDH) method: A highly efficient algorithm for propagating wavepackets. *Physics Reports*, 324(1):1–105, 2000. URL http://dx.doi.org/10.1016/S0370-1573(99)00047-2.

[37] Askold M. Perelomov. *Generalized coherent states and their applications*. Springer Science & Business Media, 2012. URL http://dx.doi.org/10.1007/978-3-642-61629-7.

[38] Askold M. Perelomov. Coherent states for arbitrary Lie group. *Communications in Mathematical Physics*, 26(3):222–236, 1972. URL http://dx.doi.org/10.1007/BF01645091.

[39] Askold M. Perelomov. Generalized coherent states and some of their applications. *Physics-Uspekhi*, 20(9):703–720, 1977. URL http://dx.doi.org/10.1070/PU1977v020n09ABEH005459.

[40] Roy J. Glauber. Coherent and incoherent states of the radiation field. *Physical Review*, 131(6):2766, 1963. URL https://doi.org/10.1103/PhysRev.131.2766.

[41] Roy J. Glauber. Classical behavior of systems of quantum oscillators. *Physics Letters*, 21(6):650–652, 1966. URL http://dx.doi.org/10.1016/0031-9163(66)90111-9.

[42] Eugen Merzbacher. *Quantum Mechanics*. John Wiley & Sons Inc., 3rd edition, 1998.

[43] M. Baranger, M. A. M. de Aguiar, F. Keck, H. J. Korsch, and B. Schellhaaß. Semiclassical approximations in phase space with coherent states. *Journal of Physics A: Mathematical and General*, 34:7227, 2001. URL https://doi.org/10.1088/0305-4470/34/36/309.

[44] Kenneth G. Kay. Semiclassical initial value treatments of atoms and molecules. *Annual Review of Physical Chemistry*, 56:255–280, 2005. URL http://dx.doi.org/10.1146/annurev.physchem.56.092503.141257.

[45] Eric J. Heller. Frozen Gaussians: A very simple semiclassical approximation. *The Journal of Chemical Physics*, 75(6):2923, 1981. URL http://dx.doi.org/10.1063/1.442382.

[46] Alexander L. Fetter and John D. Walecka. *Quantum Theory of Many-Particle Systems*. McGraw-Hill, New York, 1971.

[47] Attila Szabo and Neil S. Ostlund. *Modern Quantum Chemistry: Introduction to Advanced Electronic Structure Theory*. Dover publications, 1996.

[48] Per-Olov Löwdin. Quantum theory of many-particle systems. I. Physical interpretations by means of density matrices, natural spin-orbitals, and convergence problems in the method of configurational interaction. *Physical Review*, 97:1474–1489, 1955. URL http://link.aps.org/doi/10.1103/PhysRev.97.1474.

[49] D. V. Shalashilin and M. S. Child. Basis set sampling in the method of coupled coherent states: Coherent state swarms, trains, and pancakes. *The Journal of Chemical Physics*, 128(5):054102, 2008. URL http://dx.doi.org/10.1063/1.2828509.

[50] M. Ceotto, S. Atahan, G. F. Tantardini, and A. Aspuru-Guzik. Multiple coherent states for first-principles semiclassical initial value representation molecular dynamics. *The Journal of Chemical Physics*, 130(23):234113, 2009. URL http://dx.doi.org/10.1063/1.3155062.

[51] Lev D. Landau and Evgeny M. Lifshitz. *Course of Theoretical Physics Volume 3: Quantum Mechanics (Non-relativistic Theory)*. Butterworth-Heineman, Oxford, 3rd edition, 1977.

[52] Sergi S. Gòdia. Parallelisation of the coupled coherent states quantum dynamics simulation. Master's thesis, The University of Edinburgh, United Kingdom, 2014. URL https://www.epcc.ed.ac.uk/msc/programmes/programme-structure/dissertation/2013-2014.

[53] Scott Habershon. Linear dependence and energy conservation in Gaussian wavepacket basis sets. *The Journal of Chemical Physics*, 136(1):014109, 2012. URL https://doi.org/10.1063/1.3671978.

[54] D. V. Shalashilin and M. S. Child. A version of diffusion Monte Carlo method based on random grids of coherent states. II. Six-dimensional simulation of electronic states of H2. *The Journal of chemical physics*, 122(22):224109, 2005. URL https://doi.org/10.1063/1.1926269.

[55] Hans De Raedt. Product formula algorithms for solving the time dependent Schrödinger equation. *Computer Physics Reports*, 7(1):1–72, 1987. URL http://dx.doi.org/10.1016/0167-7977(87)90002-5.

[56] Kenneth G. Kay. The matrix singularity problem in the time-dependent variational method. *Chemical Physics*, 137:165, 1989. URL https://doi.org/10.1016/0301-0104(89)87102-2.

[57] Dmitrii V. Shalashilin. Quantum mechanics with the basis set guided by Ehrenfest trajectories: Theory and application to spin-boson model. *The Journal of Chemical Physics*, 130(24):244101, 2009. URL http://dx.doi.org/10.1063/1.3153302.

[58] S.-Y. Ye, D. V. Shalashilin, and A. Serafini. Modeling of quantum-information processing with Ehrenfest guided trajectories: A case study with spin-boson-like couplings. *Physical Review A*, 86(3):032312, 2012. URL http://link.aps.org/doi/10.1103/PhysRevA.86.032312.

[59] K. Saita and D. V. Shalashilin. On-the-fly ab initio molecular dynamics with multiconfigurational Ehrenfest method. *The Journal of Chemical Physics*, 137(22):22A506, 2012. URL https://doi.org/10.1063/1.4734313.

[60] K. Saita, M. G. D. Nix, and D. V. Shalashilin. Simulation of ultrafast photodynamics of pyrrole with a multiconfigurational Ehrenfest method. *Physical Chemistry Chemical Physics*, 15(38):16227, 2013. URL http://xlink.rsc.org/?DOI=c3cp51199e.

[61] D. V. Makhov, W. J. Glover, T. J. Martínez, and D. V. Shalashilin. Ab initio multiple cloning algorithm for quantum nonadiabatic molecular dynamics. *The Journal of Chemical Physics*, 141(5):054110, 2014. URL http://scitation.aip.org/content/aip/journal/jcp/141/5/10.1063/1.4891530.

[62] D. V. Makhov, K. Saita, T. J. Martínez, and D. V. Shalashilin. Ab initio multiple cloning simulations of pyrrole photodissociation: TKER spectra and velocity map imaging. *Physical Chemistry Chemical Physics*, 17:3316–3325, 2015. URL http://dx.doi.org/10.1039/C4CP04571H.

[63] A. Kirrander, K. Saita, and D. V. Shalashilin. Ultrafast x-ray scattering from molecules. *Journal of Chemical Theory and Computation*, 12(3):957–967, 2016. URL http://dx.doi.org/10.1021/acs.jctc.5b01042.

[64] M. Galassi, J. Davies, J. Theiler, B. Gough, G. Jungman, M. Booth, and F. Rossi. *GNU Scientific Library: Reference Manual*. Network Theory Ltd., 3rd edition, 2003. URL http://www.worldcat.org/isbn/0954161734.

[65] E. Artacho and D. D. O'Regan. Quantum mechanics in an evolving hilbert space. *Phys. Rev. B*, 95:115155, 2017. doi: 10.1103/PhysRevB.95.115155. URL https://link.aps.org/doi/10.1103/PhysRevB.95.115155.

[66] T. F. Viscondi, K. Furuya, and M. C. de Oliveira. Phase transition, entanglement and squeezing in a triple-well condensate. *EPL (Europhysics Letters)*, 90:10014, 2010. URL https://doi.org/10.1209/0295-5075/90/10014.

[67] T. F. Viscondi and K. Furuya. Dynamics of a Bose-Einstein condensate in a symmetric triple-well trap. *Journal of Physics A: Mathematical and Theoretical*, 44:175301, 2011. URL https://doi.org/10.1088/1751-8113/44/17/175301.

[68] Fabian H. L. Essler, Holger Frahm, Frank Göhmann, Andreas Klümper, and Vladimir E. Korepin. *The one-dimensional Hubbard model*. Cambridge University Press, 2005. URL http://www.cambridge.org/gb/knowledge/isbn/item1168749/?site_locale=en_GB.

[69] Thaís V. Trevisan. Estados transportadores de corrente em 'moléculas' simples. Master's thesis, Universidade Estadual de Campinas, Brazil, 2015. URL http://www.bibliotecadigital.unicamp.br/document/?code=000951981&opt=4&lg=en_US. (available in Portuguese).

[70] M. S. Child and D. V. Shalashilin. Locally coupled coherent states and Herman–Kluk dynamics. *The Journal of Chemical Physics*, 118(5):2061, 2003. URL http://dx.doi.org/10.1063/1.1531997.

[71] R. Gelabert, X. Giménez, M. Thoss, H. Wang, and W. H. Miller. A log-derivative formulation of the prefactor for the semiclassical Herman-Kluk propagator. *The Journal of Physical Chemistry A*, 104(45):10321–10327, 2000. URL http://dx.doi.org/10.1021/jp0012451.

[72] M. F. Herman and E. Kluk. A semiclassical justification for the use of non-spreading wavepackets in dynamics calculations. *Chemical physics*, 91:27, 1984. URL http://dx.doi.org/10.1016/0301-0104(84)80039-7.

[73] E. Kluk, M. F. Herman, and H. L. Davis. Comparison of the propagation of semiclassical frozen Gaussian wave functions with quantum propagation for a highly excited anharmonic oscillator. *The Journal of Chemical Physics*, 84(1):326, 1986. URL http://dx.doi.org/10.1063/1.450142.

[74] Kenneth G. Kay. The Herman-Kluk approximation: Derivation and semiclassical corrections. *Chemical Physics*, 322:3, 2006. URL https://doi.org/10.1016/j.chemphys.2005.06.019.

[75] E. Martín-Fierro and J. M. G. Llorente. Derivation of semiclassical asymptotic initial value representations of the quantum propagator. *Chemical Physics*, 322(1–2):13 – 22, 2006. URL http://dx.doi.org/10.1016/j.chemphys.2005.07.022.

[76] Y. Öhrn and O. Goscinski. Analysis of the Thouless coherent state using the 1/K expansion. *Physical Review A*, 48(2):1093–1097, 1993. URL https://doi.org/10.1103/PhysRevA.48.1093.

[77] Laurence G. Yaffe. Large n limits as classical mechanics. *Reviews of Modern Physics*, 54:407–435, 1982. URL http://link.aps.org/doi/10.1103/RevModPhys.54.407.

[78] Jean-Christophe Pain. Commutation relations of operator monomials. *Journal of Physics A: Mathematical and Theoretical*, 46(3):035304, 2013. URL http://stacks.iop.org/1751-8121/46/i=3/a=035304.

[79] Carl D. Meyer. *Matrix analysis and applied linear algebra*. Siam, 2000.

[80] Hans-Dieter Meyer. *Introduction to MCTDH*. Universität Heidelberg, 2010. URL http://www.pci.uni-heidelberg.de/cms/mctdh.html. (lecture notes).

Appendix A

Phase-space volume conservation and properties of the complex action

A.1 Invariance of the phase-space measure under classical flow

Let us consider the phase-space metric at two distinct instants, t and 0; since the Jacobian matrix of the transformation from $z(t)$ to $z(0)$ is the stability matrix $M(t)$ itself, we have:

$$d\mu(z(t)) = \kappa \, \det g(t) \prod_{\alpha=1}^{d} \frac{dz_\alpha(t) dz_\alpha^*(t)}{2\pi i} = \kappa \, \det g(t) \, \det M(t) \prod_{\alpha=1}^{d} \frac{dz_\alpha(0) dz_\alpha^*(0)}{2\pi i}. \quad \text{(A.1)}$$

Recall that M satisfies the linear equation

$$\dot{M}(t) = R(t) M(t), \quad M(0) = I_{2d},$$

with the time-dependent matrix R defined according to Eqs. (6.4) and (6.5); therefore, differentiating the determinant's logarithm with respect to t we get:

$$\frac{d}{dt} \log (\det M) = \mathrm{Tr}(M^{-1}\dot{M}) = \mathrm{Tr}\, R. \quad \text{(A.2)}$$

On the other hand, the metric's time derivative can be written as follows:

$$\begin{aligned}
\dot{g}_{\alpha\beta} &= \sum_\gamma \left(\frac{\partial g_{\alpha\beta}}{\partial z_\gamma} \dot{z}_\gamma + \frac{\partial g_{\alpha\beta}}{\partial z_\gamma^*} \dot{z}_\gamma^* \right) \\
&= \sum_\gamma \left(\frac{\partial (\dot{z}_\gamma g_{\gamma\beta})}{\partial z_\alpha} + \frac{\partial (g_{\alpha\gamma} \dot{z}_\gamma^*)}{\partial z_\beta^*} - \frac{\partial \dot{z}_\gamma}{\partial z_\alpha} g_{\gamma\beta} - g_{\alpha\gamma} \frac{\partial \dot{z}_\gamma^*}{\partial z_\beta^*} \right) \\
&= -\frac{i}{\hbar} \left(\frac{\partial^2 E}{\partial z_\alpha \partial z_\beta^*} - \frac{\partial^2 E}{\partial z_\beta^* \partial z_\alpha} \right) - \sum_\gamma \left(\frac{\partial \dot{z}_\gamma}{\partial z_\alpha} g_{\gamma\beta} + g_{\alpha\gamma} \frac{\partial \dot{z}_\gamma^*}{\partial z_\beta^*} \right),
\end{aligned}$$

where – and this is the crucial step – the classical equations of motion (6.3) have been substituted in the second line. Evidently, the second-order derivatives of the energy cancel

off leaving:

$$\dot{g} = -(R_{11}^T g + g R_{22}) \quad \Rightarrow \quad g^{-1}\dot{g} = -(g^{-1} R_{11} g + R_{22}). \tag{A.3}$$

Tracing this last equation yields:

$$\mathrm{Tr}(g^{-1}\dot{g}) = -(\mathrm{Tr}\, R_{11} + \mathrm{Tr}\, R_{22}) = -\mathrm{Tr}\, R \quad \Rightarrow \quad \frac{d}{dt}\log(\det g) = -\mathrm{Tr}\, R. \tag{A.4}$$

Thence, we may connect formulas (A.2) and (A.4), establishing the relation:

$$\frac{d}{dt}\log(\det M) = -\frac{d}{dt}\log(\det g).$$

Integrating from 0 to t, exponentiating and using the fact that $\det M(0) = 1$, we conclude:

$$\log\left[\frac{\det M(t)}{\det M(0)}\right] = -\log\left[\frac{\det g(t)}{\det g(0)}\right] \quad \Rightarrow \quad \det M(t) = \frac{\det g(0)}{\det g(t)}. \tag{A.5}$$

Finally, using this result in (A.1) we see that:

$$d\mu(z(t)) = d\mu(z(0)), \tag{A.6}$$

which proves our claim that phase-space volume is preserved under the generalized classical dynamics. Notice that this is true even in the case of driven systems, when the Hamiltonian displays explicit time dependence. This result can also be reached in a different way, cf. Appendix C of Ref. [29].

A.2 The complex action

The complex action of Eq. (1.67), computed over a classical trajectory $z(t)$ that obeys the classical equations (1.72), has a interesting functional structure, as shown by the derivatives listed in Eqs. (1.71). Here, for the sake of completeness, we shall demonstrate those relations, but in a slightly more general form: we will allow for specific initial and final time arguments, labeled t_a and t_b respectively, in which case the complex action reads

$$A(z; t_b, t_a) = \int_{t_a}^{t_b} dt\, L(z) - \frac{i\hbar}{2}\Big[f(z_b^*, z_b) + f(z_a^*, z_a)\Big], \tag{A.7}$$

where $z_a = z(t_a)$ and $z_b = z(t_b)$. The calculation follows that given at Chapter 3 of Ref. [29].

Let us first consider the variation of the action when the end-points of the trajectory $(z(t), z^*(t))$ are displaced by small amounts, $(\delta z_a', \delta z_a^{*\prime})$ at t_a and $(\delta z_b', \delta z_b^{*\prime})$ at t_b. During this preliminary calculation we shall hold the time interval fixed, i.e. the time instants t_b and t_a are kept frozen (this is similar to what we do when deriving the Euler-Lagrange

equations). Denoting this variation by $\delta A'$, the usual procedure gives:[i]

$$\delta A' = -\frac{i\hbar}{2}\Big[\frac{\partial f(z_b^*, z_b)}{\partial z_b}\delta z_b' + \frac{\partial f(z_b^*, z_b)}{\partial z_b^*}\delta z_b^{*\prime}\Big] - \frac{i\hbar}{2}\Big[\frac{\partial f(z_a^*, z_a)}{\partial z_a}\delta z_a' + \frac{\partial f(z_a^*, z_a)}{\partial z_a^*}\delta z_a^{*\prime}\Big]$$
$$+ \frac{\partial L}{\partial \dot{z}}\delta z'\Big|_{t_a}^{t_b} + \frac{\partial L}{\partial \dot{z}^*}\delta z^{*\prime}\Big|_{t_a}^{t_b} + \int_{t_a}^{t_b} dt\,\Big[\Big(\frac{\partial L}{\partial z} - \frac{d}{dt}\frac{\partial L}{\partial \dot{z}}\Big)\delta z' + \Big(\frac{\partial L}{\partial z^*} - \frac{d}{dt}\frac{\partial L}{\partial \dot{z}^*}\Big)\delta z^{*\prime}\Big]. \quad \text{(A.8)}$$

Since the Euler-Lagrange equations are satisfied along the classical trajectory, the terms inside the integral vanish. Moreover, substituting the derivatives of L in the surface terms we find without difficulty:

$$\frac{i}{\hbar}\delta A' = \frac{\partial f(z_b^*, z_b)}{\partial z_b^*}\delta z_b^{*\prime} + \frac{\partial f(z_a^*, z_a)}{\partial z_a}\delta z_a'. \quad \text{(A.9)}$$

As expected, the action is stationary under *virtual* displacements, as long as the boundary conditions $\delta z_b^{*\prime} = \delta z_a' = 0$ are met.

Next we consider the scenario where only the initial and final instants are altered by small amounts, δt_a and δt_b, respectively. Due to their time-dependence, variables z and z^* cannot remain fixed under such displacements and the following changes are induced upon them: $\delta z_a'' = \dot{z}_a \delta t_a$ and $\delta z_b'' = \dot{z}_b \delta t_b$, and likewise for the complex conjugates. Denoting the corresponding variation in the action function by $\delta A''$ we get:

$$\delta A'' = L(z_b)\,\delta t_b - L(z_a)\,\delta t_a$$
$$- \frac{i\hbar}{2}\Big[\frac{\partial f(z_b^*, z_b)}{\partial z_b}\dot{z}_b + \frac{\partial f(z_b^*, z_b)}{\partial z_b^*}\dot{z}_b^*\Big]\delta t_b - \frac{i\hbar}{2}\Big[\frac{\partial f(z_a^*, z_a)}{\partial z_a}\dot{z}_a + \frac{\partial f(z_a^*, z_a)}{\partial z_a^*}\dot{z}_a^*\Big]\delta t_a, \quad \text{(A.10)}$$

and substituting the Lagrangians $L(z_b)$ and $L(z_a)$, computed at different times, we get:

$$\frac{i}{\hbar}\delta A'' = \Big[\frac{\partial f(z_a^*, z_a)}{\partial z_a}\dot{z}_a + \frac{i}{\hbar}E(z_a^*, z_a)\Big]\delta t_a + \Big[\frac{\partial f(z_b^*, z_b)}{\partial z_b^*}\dot{z}_b^* - \frac{i}{\hbar}E(z_b^*, z_b)\Big]\delta t_a. \quad \text{(A.11)}$$

Now, the total variation of the action δA, which contemplates small changes in the initial and final instants followed by small and independent virtual displacements of the end-points of the trajectory, is the sum of $\delta A'$ and $\delta A''$:

$$\frac{i}{\hbar}\delta A = \frac{\partial f(z_b^*, z_b)}{\partial z_b^*}\delta z_b^{*\prime} + \frac{\partial f(z_a^*, z_a)}{\partial z_a}\delta z_a'$$
$$+ \Big[\frac{\partial f(z_a^*, z_a)}{\partial z_a}\dot{z}_a + \frac{i}{\hbar}E(z_a^*, z_a)\Big]\delta t_a + \Big[\frac{\partial f(z_b^*, z_b)}{\partial z_b^*}\dot{z}_a^* - \frac{i}{\hbar}E(z_b^*, z_b)\Big]\delta t_b.$$

However, here we are not interested in virtual displacements $(\delta z', \delta z^{*\prime})$. We want to know how the action changes when dynamical variations $(\delta z, \delta z^*)$ take place; to first order, both

[i] Here a vector notation is used.

types of perturbations are related as:

$$\begin{cases} \delta z_a = \delta z_a' + \dot{z}_a \delta t_a \\ \delta z_a^* = \delta z_a^{*\prime} + \dot{z}_a^* \delta t_a \end{cases}, \quad \begin{cases} \delta z_b = \delta z_b' + \dot{z}_b \delta t_b \\ \delta z_b^* = \delta z_b^{*\prime} + \dot{z}_b^* \delta t_b \end{cases}. \tag{A.12}$$

Putting these relations in the previous equation yields:

$$\frac{i}{\hbar}\delta A = \frac{\partial f(z_b^*, z_b)}{\partial z_b^*}\delta z_b^* + \frac{\partial f(z_a^*, z_a)}{\partial z_a}\delta z_a + \frac{i}{\hbar}E(z_a^*, z_a)\delta t_a - \frac{i}{\hbar}E(z_b^*, z_b)\delta t_b, \tag{A.13}$$

which reveals that the functional structure of the complex action is $A = A(z_b^*, z_a; t_b, t_a)$.

Equation (A.13) gives the partial derivatives of the complex action; they are:

$$\frac{i}{\hbar}\frac{\partial A(z_b^*, z_a; t_b, t_a)}{\partial z_{b\gamma}^*} = \frac{\partial f(z_b^*, z_b)}{\partial z_{b\gamma}^*}, \quad \frac{i}{\hbar}\frac{\partial A(z_b^*, z_a; t_b, t_a)}{\partial z_{a\gamma}} = \frac{\partial f(z_a^*, z_a)}{\partial z_{a\gamma}}, \tag{A.14}$$

and

$$\frac{\partial A(z_b^*, z_a; t_b, t_a)}{\partial t_b} = -E(z_b^*, z_b), \quad \frac{\partial A(z_b^*, z_a; t_b, t_a)}{\partial t_a} = E(z_a^*, z_a). \tag{A.15}$$

Furthermore,

$$\frac{\partial A(z_b^*, z_a; t_b, t_a)}{\partial z_{a\gamma}^*} = 0, \quad \frac{\partial A(z_b^*, z_a; t_b, t_a)}{\partial z_{b\gamma}} = 0. \tag{A.16}$$

It is useful to clarify that, if (z_b^*, z_a) are chosen as independent arguments, the quantities on the right-hand side of Eqs. (A.14) should also be understood as functions of these arguments; for instance, ignoring the time parameters and subscripts, the first of Eqs. (A.14) should be read as:

$$\frac{i}{\hbar}\frac{\partial A(z_b^*, z_a)}{\partial z_b^*} = \frac{\partial f(z_b^*, z_b(z_b^*, z_a))}{\partial z_b^*},$$

This seems a bit exotic since we always treat complex conjugate variables computed at the same instant as independent quantities. Nevertheless, relations (A.14) are still helpful when more usual situations are considered. For example, if we take (z_a^*, z_a) (the initial conditions) as basic variables derivatives can be computed using the chain rule in the following way,

$$\begin{aligned} \frac{i}{\hbar}\frac{\partial A(z_b^*, z_a)}{\partial z_a} &= \frac{i}{\hbar}\left[\frac{\partial A(z_b^*, z_a)}{\partial z_b^*}\frac{\partial z_b^*}{\partial z_a} + \frac{\partial A(z_b^*, z_a)}{\partial z_a}\right] = \frac{\partial f(z_b^*, z_b)}{\partial z_b^*}\frac{\partial z_b^*}{\partial z_a} + \frac{\partial f(z_a^*, z_a)}{\partial z_a} \\ \frac{i}{\hbar}\frac{\partial A(z_b^*, z_a)}{\partial z_a^*} &= \frac{i}{\hbar}\left[\frac{\partial A(z_b^*, z_a)}{\partial z_b^*}\frac{\partial z_b^*}{\partial z_a^*}, + \frac{\partial A(z_b^*, z_a)}{\partial z_a^*}\right] = \frac{\partial f(z_b^*, z_b)}{\partial z_b^*}\frac{\partial z_b^*}{\partial z_a^*}. \end{aligned}$$

where $z_b = z_b(z_a^*, z_a)$ and $z_b^* = z_b^*(z_a^*, z_a)$, whose derivatives with respect to the indicated initial conditions are nothing but elements of the stability matrix introduced in Chapter 6.

Appendix B

Bosonic coherent states: survey

B.1 Condensate density matrix

The explicit form of the one-body density matrix for a system of N bosons allowed to occupy K modes, conveniently defined as the normalized mean-value:

$$\Gamma_{qp}(z^*, z) \equiv N^{-1}\langle z|b_p^\dagger b_q|z\rangle = N^{-1}\frac{\{z|b_p^\dagger b_q|z\}}{\{z|z\}}, \quad 0 \leq p, q \leq d \equiv K-1, \tag{B.1}$$

is straightforwardly obtained by considering the action of a p-mode bosonic annihilator b_p upon an N-particle (non-normalized) coherent state $|N; z\}$. With help of the formula

$$[b_p, (\zeta_0^\dagger)^n] = \theta_p n(\zeta_0^\dagger)^{n-1}, \quad \theta_p = \begin{cases} 1 & \text{if } p = 0 \\ z_\mu & \text{if } p = \mu = 1, \ldots, d \end{cases} \tag{B.2}$$

– easily proved by induction from the basic commutators listed in (2.22) – we find:

$$b_p|N; z\} = b_p\frac{(\zeta_0^\dagger)^N}{\sqrt{N!}}|0\rangle = \theta_p N\frac{(\zeta_0^\dagger)^{N-1}}{\sqrt{N!}}|0\rangle = \sqrt{N}\theta_p|N-1; z\}, \tag{B.3}$$

where θ_p is defined according to (B.2). As one would expect, b_p removes one particle from the condensate, giving a factor of $\sqrt{N}$ times the amplitude associated with the p-th mode in the linear combination that parametrizes the macroscopically occupied state (the action of a creation operator $b_p^\dagger$ upon $|N; z\}$ is, however, not trivial).

B.1.1 One-body density

The above result, together with its conjugate version, allows us to write:

$$\langle z|b_p^\dagger b_q|z\rangle = \frac{\{N; z|b_p^\dagger b_q|N; z\}}{\{N; z|N; z\}} = N\theta_q\theta_p^*\frac{\{N-1; z|N-1; z\}}{\{N; z|N; z\}};$$

and, since $\{N;z|N;z\} = (1+z^*z)^N$, it follows immediately that the elements of the one-density matrix are expressed in terms of z as:

$$\Gamma_{qp}(z^*,z) = \frac{\theta_q\theta_p^*}{1+z^*z},$$

with θ_q and θ_p^* again defined according to Eq. (B.2). In matrix form this is simply:

$$\Gamma(z^*,z) = \frac{1}{1+z^*z}\begin{bmatrix} 1 & z^* \\ z & zz^* \end{bmatrix} \qquad (\text{obs: } (zz^*)_{\mu\nu} = z_\mu z_\nu^*). \tag{B.4}$$

B.1.2 Two-body matrix element

Next we consider the action of a second annihilation operator upon the condensate state $|N;z\}$ – employing Eq. (B.3) twice we get:

$$b_s b_q|N;z\} = \sqrt{N}\theta_q \cdot b_s|N-1;z\} = \sqrt{N(N-1)}\,\theta_q\theta_s|N-2;z\}.$$

This immediately gives the coherent-state's mean-value for the two-body interaction term:

$$\langle z|b_p^\dagger b_r^\dagger b_s b_q|z\rangle = N(N-1)\theta_q\theta_s\theta_r^*\theta_p^*\frac{\{N-2;z|N-2;z\}}{\{N;z|N;z\}} = N(N-1)\frac{\theta_q\theta_s\theta_r^*\theta_p^*}{(1+z^*z)^2},$$

which can be simply expressed in terms of the one-body density:

$$\langle z|b_p^\dagger b_r^\dagger b_s b_q|z\rangle = N(N-1)\,\Gamma_{qp}\Gamma_{sr} = N(N-1)\,\Gamma_{qr}\Gamma_{sp}. \tag{B.5}$$

B.1.3 Gradients of the density matrix

For completeness we also list the gradients of the density matrix which are required in deriving the bosonic mean-field equations of motion. Straightforward differentiation with respect to components of the complex vector z yields:

$$\frac{\partial\Gamma_{00}}{\partial z_\nu} = -\frac{z_\nu^*}{(1+z^*z)^2}, \tag{B.6a}$$

$$\frac{\partial\Gamma_{0\eta'}}{\partial z_\nu} = -\frac{z_\nu^* z_{\eta'}^*}{(1+z^*z)^2}, \tag{B.6b}$$

$$\frac{\partial\Gamma_{\eta 0}}{\partial z_\nu} = \frac{(1+z^*z)\delta_{\nu\eta} - z_\nu^* z_\eta}{(1+z^*z)^2} = \frac{\{(I_d+zz^*)^{-1}\}_{\eta\nu}}{1+z^*z}, \tag{B.6c}$$

$$\frac{\partial\Gamma_{\eta\eta'}}{\partial z_\nu} = \frac{z_{\eta'}^*[(1+z^*z)\delta_{\nu\eta} - z_\nu^* z_\eta]}{(1+z^*z)^2} = \frac{z_{\eta'}^*\{(I_d+zz^*)^{-1}\}_{\eta\nu}}{1+z^*z}. \tag{B.6d}$$

Similarly, differentiation with respect to z^* leads to:

$$\frac{\partial \Gamma_{00}}{\partial z^*_\nu} = -\frac{z_\nu}{(1+z^*z)^2}, \tag{B.7a}$$

$$\frac{\partial \Gamma_{0\eta'}}{\partial z^*_\nu} = \frac{(1+z^*z)\delta_{\nu\eta'} - z_\nu z^*_{\eta'}}{(1+z^*z)^2} = \frac{\{(I_d + zz^*)^{-1}\}_{\nu\eta'}}{1+z^*z}, \tag{B.7b}$$

$$\frac{\partial \Gamma_{\eta 0}}{\partial z^*_\nu} = -\frac{z_\nu z_\eta}{(1+z^*z)^2}, \tag{B.7c}$$

$$\frac{\partial \Gamma_{\eta\eta'}}{\partial z^*_\nu} = \frac{[(1+z^*z)\delta_{\nu\eta'} - z_\nu z^*_{\eta'}]z_\eta}{(1+z^*z)^2} = \frac{\{(I_d + zz^*)^{-1}\}_{\nu\eta'} z_\eta}{1+z^*z}. \tag{B.7d}$$

In these sets of equations the identity (2.40) has been used in recognizing the elements of the inverse matrix $(I_d + zz^*)^{-1}$.

B.2 Normalization of the bosonic closure relation

The constant κ that normalizes the bosonic closure relation, is most easily computed by sandwiching the identity (1.59) with the reference state $|\Phi_0\rangle$; since $\langle\Phi_0|z\} = 1$ we get:

$$\kappa^{-1} = \int [\textstyle\prod_\mu (d^2 z_\mu/\pi)] \det g(z^*, z) e^{-f(z^*,z)}.$$

Using the determinant given in Eq. (2.38), together with $e^{-f(z^*,z)} = (1+z^*z)^{-N}$, we get a simplified expression for κ:

$$\kappa^{-1} = N^{K-1} \times \pi^{-K+1} \int (d^2 z_1 d^2 z_2 \ldots d^2 z_{K-1})(1+z^*z)^{-(K+N)}. \tag{B.8}$$

Since a similar integral also comes up in the process of calculating the closure's normalization constant in the fermionic case, we will find convenient to define:

$$\mathcal{I}(m,l) \equiv \pi^{-m} \int (d^2 w_1 d^2 w_2 \ldots d^2 w_m)(1+|w_1|^2+|w_2|^2+\cdots+|w_m|^2)^{-l}, \;\; l > m \geq 1, \tag{B.9}$$

which accounts for an arbitrary number of complex variables m and exponent $l > m$ (this last condition assures convergence).

The integral (B.9) is solved by changing to real variables (u, φ) defined as: $w_\mu = \sqrt{u_\mu} e^{i\varphi_\mu}$, (for $1 \leq \mu \leq m$), with each u ranging from 0 to ∞ and each φ ranging from 0 to 2π. The angular integrals are trivial, with π^{-m} times the transformation's Jacobian canceling the 2π factors; meanwhile the radial part can be solved through the following

recursive technique:

$$\begin{aligned}
\mathcal{I}(m,l) &= \int du_m \ldots \int du_1 (1+u_1+\ldots+u_m)^{-l} \\
&= \int du_m \ldots \int du_2 \left[-\frac{(1+u_1+\ldots+u_m)^{-(l-1)}}{(l-1)} \right]_{u_1=0}^{u_1=\infty} \\
&= (l-1)^{-1} \int du_m \ldots \int du_2 (1+u_2+\ldots+u_m)^{-(l-1)} \\
&= [(l-1)(l-2)]^{-1} \int du_m \ldots \int du_3 (1+u_3+\ldots+u_m)^{-(l-2)} \\
&= [(l-1)(l-2)\ldots(l-m+1)]^{-1} \int du_m (1+u_m)^{-(l-m+1)} \\
&= [(l-1)(l-2)\ldots(l-m)]^{-1},
\end{aligned}$$

hence establishing the desired identity:

$$\mathcal{I}(m,l) = \frac{(l-m-1)!}{(l-1)!}. \tag{B.10}$$

In Eq. (B.8) we have the case $m = K-1$ and $l = K+N$; thus:

$$\kappa = \frac{(N+K-1)!}{N^{K-1}N!}, \tag{B.11}$$

which is the result we were seeking.

It is interesting to examine the behavior of κ for large N; abbreviating $d = K-1$, taking the logarithm and employing Stirling's formula we find:

$$\begin{aligned}
\log\kappa &= \log(N+d)! - \log N! - \log N^d \\
&\approx (N+d)\log(N+d) - (N+d) - N\log N + N - d\log N \quad (\text{for } N \gg 1) \\
&= N\left(1+\frac{d}{N}\right)\log\left(1+\frac{d}{N}\right) - d \approx \frac{d^2}{N} = \frac{(K-1)^2}{N}. \quad (\text{for } N \gg K)
\end{aligned}$$

We thus see that, in the limit $N \gg K$, '$\log\kappa$' goes to zero, meaning that κ itself approaches unit:

$$\kappa \to 1 \quad \text{for} \quad N \gg K. \tag{B.12}$$

This conclusion applies to the thermodynamic limit, when $N \to \infty$ (with K finite).[77]

B.3 Fock projection of a condensate state

In deriving the Fock projection of a bosonic coherent state we shall rely heavily on the following identity, valid for any two operators whose commutator is proportional to the identity operator through a complex number c:[78]

$$\text{if } [\hat{A},\hat{B}] = c\,\hat{1} \text{ and } n,m \geq 1 \quad \Rightarrow \quad [\hat{A}^m,\hat{B}^n] = \sum_{k=1}^{\min(n,m)} k!\, c^k \binom{m}{k}\binom{n}{k}\, \hat{B}^{n-k}\,\hat{A}^{m-k}. \tag{B.13}$$

The identity holds when considering the annihilators $b_0, b_1, \ldots, b_d$, of the K single-particle modes that span the bosonic Fock space (recall: $d = K-1$) together with the creation operator $\zeta_0^\dagger$ of the condensate's macroscopic mode, since $[b_0,\zeta_0^\dagger] = 1$ and $[b_\nu,\zeta_0^\dagger] = z_\nu$, for $\nu = 1,\ldots,d$. Thus, for any $m_0, m_\nu \geq 1$, Eq. (B.13) gives:

$$b_0^{m_0}(\zeta_0^\dagger)^n = \frac{n!}{(n-m_0)!}(\zeta_0^\dagger)^{n-m_0} + (\zeta_0^\dagger)^n b_0^{m_0} + \sum_{k\neq m_0}^{\min(n,m_0)} k!\binom{m_0}{k}\binom{n}{k}(\zeta_0^\dagger)^{n-k} b_0^{m_0-k},$$

$$b_\nu^{m_\nu}(\zeta_0^\dagger)^n = \frac{n!\, z_\nu^{m_\nu}}{(n-m_\nu)!}(\zeta_0^\dagger)^{n-m_\nu} + (\zeta_0^\dagger)^n b_\nu^{m_\nu} + \sum_{k\neq m_\nu}^{\min(n,m_\nu)} k!\, z_\nu^k \binom{m_\nu}{k}\binom{n}{k}(\zeta_0^\dagger)^{n-k} b_\nu^{m_\nu-k}.$$

These expressions have been organized in a suggestive way: in both formulas, the first term on the right-hand side, which has been singled-out from the summation, is free of annihilation operators; the remaining terms, in turn, display rightmost annihilators. This means that the products on the left-hand side, when acting on the vacuum, give a straightforward result:

$$b_0^{m_0}(\zeta_0^\dagger)^n|0\rangle = \frac{n!}{(n-m_0)!}(\zeta_0^\dagger)^{n-m_0}|0\rangle, \tag{B.14a}$$

$$b_\nu^{m_\nu}(\zeta_0^\dagger)^n|0\rangle = \frac{n!\, z_\nu^{m_\nu}}{(n-m_\nu)!}(\zeta_0^\dagger)^{n-m_\nu}|0\rangle, \tag{B.14b}$$

that is also explicitly valid for the trivial cases, $m_0 = 0$ and $m_\nu = 0$.

In order to compute the projection of the non-normalized coherent state $|z\} = \frac{1}{\sqrt{N!}}(\zeta_0^\dagger)^N|0\rangle$ onto the occupation number eigenstate

$$|m\rangle = |m_0,m_1,m_2,\ldots,m_d\rangle = \frac{(b_0^\dagger)^{m_0}(b_1^\dagger)^{m_1}(b_2^\dagger)^{m_2}\ldots(b_d^\dagger)^{m_d}}{\sqrt{m_0!\,m_1!\,m_2!\,\ldots\,m_d!}}|0\rangle, \quad N = \sum_{j=0}^{d} m_j,$$

all we have to do is employ Eqs. (B.14a) and (B.14b) recursively, as follows:

$$\begin{aligned}
\sqrt{m_0!\,\ldots\,m_d!}\,\langle m|z\} &= \tfrac{1}{\sqrt{N!}}\langle 0|(b_d^{m_d}\cdots b_1^{m_1})\cdot b_0^{m_0}(\zeta_0^\dagger)^N|0\rangle \\
&= \frac{1}{\sqrt{N!}}\frac{N!}{(N-m_0)!}\langle 0|(b_d^{m_d}\cdots b_2^{m_2})\cdot b_1^{m_1}(\zeta_0^\dagger)^{N-m_0}|0\rangle \\
&= \frac{\sqrt{N!}}{(N-m_0)!}\frac{(N-m_0)!\,z_1^{m_1}}{(N-m_0-m_1)!}\,\langle 0|(b_d^{m_d}\cdots b_3^{m_3})\cdot b_2^{m_2}(\zeta_0^\dagger)^{N-m_0-m_1}|0\rangle \\
&= \frac{\sqrt{N!}\,z_1^{m_1}z_2^{m_2}}{(N-m_0-m_1-m_2)!}\,\langle 0|(b_d^{m_d}\cdots b_4^{m_4})\cdot b_3^{m_3}(\zeta_0^\dagger)^{N-m_0-m_1-m_2}|0\rangle \\
&\;\;\vdots \\
&= \frac{\sqrt{N!}\,z_1^{m_1}z_2^{m_2}\cdots z_d^{m_d}}{(N-m_0-\ldots-m_d)!}\,\langle 0|(\zeta_0^\dagger)^{N-m_0-\ldots-m_d}|0\rangle = \sqrt{N!}\,z_1^{m_1}z_2^{m_2}\cdots z_d^{m_d}
\end{aligned}$$

– hence the projection is:

$$\langle m|z\} = \left(\frac{N!}{m_0!\,m_1!\,\cdots\,m_d!}\right)^{\frac{1}{2}}\,z_1^{m_1}z_2^{m_2}\cdots z_d^{m_d}, \tag{B.15}$$

and the complete expansion for a normalized coherent state $|z\rangle$ reads:

$$|z\rangle = \sum_{|m|=N}|m_0,m_1,\ldots,m_d\rangle\,\sqrt{N!}\,(1+z^*z)^{-\frac{N}{2}}\,\frac{z_1^{m_1}z_2^{m_2}\ldots z_d^{m_d}}{\sqrt{m_0!\,m_1!\,\cdots\,m_d!}}. \tag{B.16}$$

Check. The overlap between bosonic coherent states expressed in Eq. (2.25), which was previously computed by second-quantization techniques, can be obtained at once from (B.15); using the completeness of the occupation number states we have:

$$\begin{aligned}
\{z|z'\} &= \sum_{|m|=N}\{z|m_0,\ldots,m_d\rangle\langle m_0,\ldots,m_d|z'\} \\
&= \sum_{|m|=N}\binom{N}{m_0\cdots m_d}\left[1^{m_0}\cdot(z_1^*z_1')^{m_1}(z_2^*z_2')^{m_2}\cdots(z_d^*z_d')^{m_d}\right] \\
&= (1+z_1^*z_1'+z_2^*z_2'+\ldots+z_d^*z_d')^N = (1+z^*z')^N,
\end{aligned}$$

where the multinomial theorem has been used in reverse in the last passage.

Appendix C

Fermionic coherent states: survey

C.1 Thouless density matrix

Let us start by systematically expressing anti-commutation rules (3.24) in terms of a rectangular matrix θ of size $K \times N$:

$$\{c_p, \zeta_\alpha^\dagger\} = \theta_{p\alpha}, \quad \theta = \begin{bmatrix} I_N \\ z \end{bmatrix}. \tag{C.1}$$

It also proves convenient to introduce the matrix ϱ,

$$\varrho \equiv (I_N + z^\dagger z), \quad \{z|z\} = \det \varrho, \tag{C.2}$$

whose determinant is precisely the overlap between two non-normalized Thouless states.

C.1.1 One-body density

Let us evaluate the action of an annihilator c_p upon $|z\} = \zeta_1^\dagger \zeta_2^\dagger \cdots \zeta_N^\dagger |0\rangle$; using (C.1) we obtain:

$$\begin{aligned} c_q|z\} &= \textstyle\sum_\gamma \theta_{q\gamma}(-)^{\gamma-1}(\ldots[\zeta_\gamma^\dagger]\ldots)|0\rangle, \\ \{z|c_p^\dagger &= \textstyle\sum_{\gamma'} \langle 0|(\ldots[\zeta_{\gamma'}]\ldots)(-)^{\gamma'-1}\theta_{p\gamma'}^*, \end{aligned}$$

where a special notation is introduced to indicate those operators left out of a given product, i.e. $(\ldots[\zeta_\gamma^\dagger]\ldots) \equiv \zeta_1^\dagger \ldots \zeta_{\gamma-1}^\dagger \zeta_{\gamma+1}^\dagger \ldots \zeta_N^\dagger$ and $(\ldots[\zeta_\gamma]\ldots) \equiv \zeta_N \ldots \zeta_{\gamma+1}\zeta_{\gamma-1}\ldots\zeta_1$.

The latter formulas enable calculation of the mean-value $\{z|c_p^\dagger c_q|z\}$; the sequence of

steps is depicted below:

$$\begin{aligned}\{z|c_p^\dagger c_q|z\} &= \textstyle\sum_{\gamma\gamma'}(\theta_{q\gamma}\theta^*_{p\gamma'})\langle 0|(\ldots[\zeta_{\gamma'}]\ldots)(\ldots[\zeta_\gamma^\dagger]\ldots)|0\rangle(-)^{\gamma+\gamma'}\\ &= \textstyle\sum_{\gamma\gamma'}(\theta_{q\gamma}\theta^*_{p\gamma'})\mathrm{Minor}(\varrho)_{\gamma';\gamma}(-)^{\gamma+\gamma'}\\ &= \textstyle\sum_{\gamma\gamma'}(\theta_{q\gamma}\theta^*_{p\gamma'})(\det\varrho)\varrho^{-1}_{\gamma\gamma'}\\ &= \{z|z\}\textstyle\sum_{\gamma\gamma'}\theta_{q\gamma}\varrho^{-1}_{\gamma\gamma'}\theta^\dagger_{\gamma' p}.\end{aligned} \tag{C.3}$$

Here, '$\mathrm{Minor}(\varrho)_{\gamma';\gamma}$' denotes the determinant of the sub-matrix of ϱ obtained by removal of line γ' and column γ; in going from the second to the third line we made use of 'Cramer's rule',

$$\mathrm{Minor}(A)_{i;j} = (\det A)(A^{-1})_{ji}(-)^{i+j},$$

which holds for any invertible matrix A; at the last passage, '$\det\varrho$' has been identified as the coherent-state overlap $\{z|z\}$.

Finally, substitution of Eqs. (C.1) and (C.2) into (C.3) yields the desired result:

$$\Gamma_{qp}(z^*,z) = \langle z|c_p^\dagger c_q|z\rangle = \textstyle\sum_{\gamma\gamma'}\theta_{q\gamma}\varrho^{-1}_{\gamma\gamma'}\theta^\dagger_{\gamma' p} = \left\{\begin{bmatrix} I_N \\ z\end{bmatrix}(I_N + z^\dagger z)^{-1}\begin{bmatrix} I_N & z^\dagger\end{bmatrix}\right\}_{qp}. \tag{C.4}$$

C.1.2 Two-body matrix element

In order to compute the two-body mean-value $\{z|c_p^\dagger c_r^\dagger c_s c_q|z\}$ a similar reasoning is employed. We begin by establishing the relations:

$$c_s c_q|z\} = \textstyle\sum_{\gamma\delta}\theta_{s\delta}\theta_{q\gamma}[\pm^{\gamma>\delta}_{\gamma<\delta}](-)^{\gamma+\delta}(\ldots[\zeta_\delta^\dagger\zeta_\gamma^\dagger]\ldots)|0\rangle, \tag{C.5}$$

$$\{z|c_p^\dagger c_r^\dagger = \textstyle\sum_{\gamma'\delta'}\langle 0|(\ldots[\zeta_{\gamma'}\zeta_{\delta'}]\ldots)[\pm^{\gamma'>\delta'}_{\gamma'<\delta'}](-)^{\gamma'+\delta'}\theta^*_{p\gamma'}\theta^*_{r\delta'}, \tag{C.6}$$

which, of course, presuppose $s \neq q$ and $p \neq r$; the notation $(\ldots[\zeta_{\gamma'}\zeta_{\delta'}]\ldots)$ means that both $\zeta_{\gamma'}$ and $\zeta_{\delta'}$ are absent from the product. There is now one additional detail to be accounted for: in (C.5), the second annihilation operator to act upon $|z\}$, while making its way towards the vacuum state, will have to go over a gap left in the product of $\zeta^\dagger$'s due to the action of the first operator, and hence an extra negative sign appears which depends on the orbital indexations; this is why a new symbol is introduced, $[\pm^{\gamma>\delta}_{\gamma<\delta}]$, meaning $(+1)$ if $\gamma > \delta$ and (-1) if $\gamma < \delta$. Similar considerations apply to (C.6).

With the help of these new relations we are able to perform the following manipula-

tions:

$$\begin{aligned}
\{z|c_p^\dagger c_r^\dagger c_s c_q|z\} &= \textstyle\sum_{\gamma'\delta'\delta\gamma}(\theta^*_{p\gamma'}\theta^*_{r\delta'}\theta_{s\delta}\theta_{q\gamma})[\pm^{\gamma>\delta}_{\gamma<\delta}][\pm^{\gamma'>\delta'}_{\gamma'<\delta'}]\langle 0|\cdot[\zeta_{\gamma'}\zeta_{\delta'}]\cdot[\zeta^\dagger_\delta\zeta^\dagger_\gamma]\cdot|0\rangle(-)^{\gamma+\gamma'+\delta+\delta'} \\
&= \textstyle\sum_{\gamma'\delta'\delta\gamma}(\theta^*_{p\gamma'}\theta^*_{r\delta'}\theta_{s\delta}\theta_{q\gamma})[\pm^{\gamma>\delta}_{\gamma<\delta}][\pm^{\gamma'>\delta'}_{\gamma'<\delta'}]\mathrm{Minor}(\varrho)_{\delta'\gamma';\delta\gamma}(-)^{\gamma+\gamma'+\delta+\delta'} \\
&= \textstyle\sum_{\gamma'\delta'\delta\gamma}(\theta^*_{p\gamma'}\theta^*_{r\delta'}\theta_{s\delta}\theta_{q\gamma})(\det\varrho)(\varrho^{-1}_{\delta\delta'}\varrho^{-1}_{\gamma\gamma'}-\varrho^{-1}_{\delta\gamma'}\varrho^{-1}_{\gamma\delta'}) \\
&= \{z|z\}\Big[(\textstyle\sum_{\gamma\gamma'}\theta_{q\gamma}\varrho^{-1}_{\gamma\gamma'}\theta^\dagger_{\gamma' p})(\sum_{\delta\delta'}\theta_{s\delta}\varrho^{-1}_{\delta\delta'}\theta^\dagger_{\delta' r})\ldots \\
&\qquad\qquad -(\textstyle\sum_{\gamma\delta'}\theta_{q\gamma}\varrho^{-1}_{\gamma\delta'}\theta^\dagger_{r\delta'})(\sum_{\delta\gamma'}\theta_{s\delta}\varrho^{-1}_{\delta\gamma'}\theta^\dagger_{p\gamma'})\Big] \\
&= \{z|z\}(\Gamma_{qp}\Gamma_{sr}-\Gamma_{qr}\Gamma_{sp}).
\end{aligned} \tag{C.7}$$

At the second line, 'Minor$(\varrho)_{\delta'\gamma';\delta\gamma}$' stands for the determinant of the sub-matrix of ϱ obtained by removing the pair of lines δ',γ' and the pair of columns δ,γ; in going from the second to the third line we made use of the identity[i]

$$[\pm^{i>j}_{i<j}][\pm^{k>l}_{k<l}]\mathrm{Minor}[A_{(i,j);(k,l)}] = (\det A)[(A^{-1})_{ki}(A^{-1})_{lj}-(A^{-1})_{kj}(A^{-1})_{li}](-)^{i+j+k+l};$$

then, after collecting terms, we recognize at the last passage the one-body density matrices' elements.

From (C.7) we immediately arrive at the result:

$$\langle z|c_p^\dagger c_r^\dagger c_s c_q|z\rangle = \Gamma_{qp}\Gamma_{sr}-\Gamma_{qr}\Gamma_{sp}. \tag{C.8}$$

C.1.3 Gradients of the density matrix

Gradients of $\Gamma(z^*,z)$ with respect to either z^* or z are more easily computed if, instead of directly differentiating its explicit form (C.4), we start from the bare definition of $|z\}$ and note that:

$$|z\} = \exp\Big(\sum_\beta\sum_\nu z_{\nu\beta}b^\dagger_\nu a_\beta\Big)|\Phi_0\rangle \quad\Rightarrow\quad \frac{\partial|z\}}{\partial z_{\mu\alpha}} = b^\dagger_\mu a_\alpha|z\}, \quad \frac{\partial\{z|}{\partial z^*_{\mu\alpha}} = \{z|a^\dagger_\alpha b_\mu. \tag{C.9}$$

[i] Both determinantal identities employed in this section are particular cases of the 'generalized Cramers' rule'.

Thus if the derivative of element Γ_{qp} with respect to $z^*_{\mu\alpha}$ is to be taken, it is possible, with help of the above relations, to proceed as follows:

$$\begin{aligned}
\frac{\partial \Gamma_{qp}}{\partial z^*_{\mu\alpha}} &= \frac{\partial \{z|}{\partial z^*_{\mu\alpha}} \frac{c_p^\dagger c_q |z\}}{\{z|z\}} - \frac{\{z|c_p^\dagger c_q|z\}}{\{z|z\}^2} \frac{\partial \{z|}{\partial z^*_{\mu\alpha}} |z\} \\
&= \langle z|a_\alpha^\dagger b_\mu c_p^\dagger c_q|z\rangle - \langle z|c_p^\dagger c_q|z\rangle \langle z|a_\alpha^\dagger b_\mu|z\rangle \\
&= \langle z|a_\alpha^\dagger \{b_\mu, c_p^\dagger\} c_q|z\rangle + \langle z|c_p^\dagger a_\alpha^\dagger b_\mu c_q|z\rangle - \langle z|c_p^\dagger c_q|z\rangle \langle z|a_\alpha^\dagger b_\mu|z\rangle \\
&= \Gamma_{q\alpha} I_{\mu p} + (\Gamma_{qp}\Gamma_{\mu\alpha} - \Gamma_{q\alpha}\Gamma_{\mu p}) - \Gamma_{qp}\Gamma_{\mu\alpha} \\
&= \Gamma_{q\alpha}(I_{\mu p} - \Gamma_{\mu p}),
\end{aligned} \tag{C.10}$$

where I stands for the $K \times K$ identity matrix (with $I_{\mu p} = \left\{ \begin{bmatrix} 0 & I_M \end{bmatrix} \right\}_{\mu p}$) and the two-body matrix element at the third line has been replaced by the result (C.8). In matrix form Eq. (C.10) reads:

$$\frac{\partial \Gamma_{qp}}{\partial z^*_{\mu\alpha}} = \left\{ \begin{bmatrix} \Gamma_{11} \\ \Gamma_{21} \end{bmatrix} \right\}_{q\alpha} \cdot \left\{ \begin{bmatrix} -\Gamma_{21} & (I_M - \Gamma_{22}) \end{bmatrix} \right\}_{\mu p}. \tag{C.11}$$

Rewriting the blocks of Γ according to

$$\begin{aligned}
\Gamma_{11} &= (I_N + z^\dagger z)^{-1}, \\
\Gamma_{21} &= z(I_N + z^\dagger z)^{-1} = (I_M + zz^\dagger)^{-1} z, \\
\Gamma_{22} &= z(I_N + z^\dagger z)^{-1} z^\dagger = I_M - (I_M + zz^\dagger)^{-1},
\end{aligned}$$

and rearranging terms, we are finally able to express the result in its most useful form:

$$\frac{\partial \Gamma_{qp}}{\partial z^*_{\mu\alpha}} = \left\{ \begin{bmatrix} I_N \\ z \end{bmatrix} (I_N + z^\dagger z)^{-1} \right\}_{q\alpha} \cdot \left\{ (I_M + zz^\dagger)^{-1} \begin{bmatrix} -z & I_M \end{bmatrix} \right\}_{\mu p}. \tag{C.12}$$

The procedure works similarly if differentiation is with respect to $z_{\mu\alpha}$; alternatively one may use the hermitian property of Γ to establish the relation

$$\frac{\partial \Gamma_{qp}}{\partial z_{\mu\alpha}} = \left(\frac{\partial \Gamma_{pq}}{\partial z^*_{\mu\alpha}} \right)^*,$$

and hence conclude from (C.12) that:

$$\frac{\partial \Gamma_{qp}}{\partial z_{\mu\alpha}} = \left\{ \begin{bmatrix} -z^\dagger \\ I_M \end{bmatrix} (I_M + zz^\dagger)^{-1} \right\}_{q\mu} \cdot \left\{ (I_N + z^\dagger z)^{-1} \begin{bmatrix} I_N & z^\dagger \end{bmatrix} \right\}_{\alpha p}. \tag{C.13}$$

C.2 Normalization of the fermionic closure relation

In the same manner as in the bosonic case (cf. B.2), the normalization constant for the fermionic closure relation is computed by sandwiching the identity with the reference state $|\Phi_0\rangle$:

$$\kappa^{-1} = \int [\prod_\alpha \prod_\mu (d^2 z_{\mu\alpha}/\pi)] \det g(z^*, z) e^{-f(z^*,z)}.$$

The metric (3.42) can be written in direct product form:

$$g = (I_M + zz^\dagger)^{-1} \otimes (I_N + z^\dagger z)^{-1},$$

and by means of the identity: $\det(A \otimes B) = (\det A)^m (\det B)^n$, valid for arbitrary matrices A and B of sizes $n \times n$ and $m \times m$, respectively, we conclude that:

$$\det g = [\det(I_M + zz^\dagger)]^{-N} [\det(I_N + zz^\dagger)]^{-M} = [\det(I_N + z^\dagger z)]^{-K}, \tag{C.14}$$

where Sylvester's determinant theorem has been employed (viz. arguments leading to Eq. (2.38) at Chapter 2). Then since $e^{-f(z^*,z)} = [\det(I_N + z^\dagger z)]^{-1}$ we have:

$$\kappa^{-1} = \int [\prod_\alpha \prod_\mu (d^2 z_{\mu\alpha}/\pi)] [\det(I_N + z^\dagger z)]^{-(K+1)}. \tag{C.15}$$

The integration is going to be carried out through a systematic change of variables, which involves manipulation of individual columns of the $M \times N$ matrix z. For this purpose it is convenient to introduce new notation; denoting by v_α the α-th column of z we write this matrix as:

$$z = [v_1, v_2, \ldots, v_N], \tag{C.16}$$

with an obvious meaning. Furthermore, we introduce N rectangular matrices τ defined according to the recipe:

$$\tau_\alpha \equiv [v_\alpha, v_{\alpha+1}, \ldots, v_N] \ , \ 1 \leq \alpha \leq N; \tag{C.17}$$

i.e. τ_α is the sub-matrix of z constructed by removing columns 1 to $\alpha - 1$. Thus $\tau_1 = z$ is of size $M \times N$; then τ_2 is a matrix of size $M \times (N-1)$, and so on; the last matrix $\tau_N = v_N$ is just a vector of size $M \times 1$.

Using this new notation, expression (C.15) reads:

$$\kappa^{-1} = \int [\prod_{\alpha=1}^N (\pi^{-M} \, d^{2M} v_\alpha)] [\det(I_N + \tau_1^\dagger \tau_1)]^{-s} \quad \text{with} \quad s \equiv K + 1, \tag{C.18}$$

where the determinant's exponent has been abbreviated to s. A sequential transformation

of variables $v \to w$ that disentangles the integral is the one given below:

$$\begin{cases} w_1 & = (I_M + [v_2, \ldots, v_N][v_2, \ldots, v_N]^\dagger)^{-\frac{1}{2}} v_1 = (I_M + \tau_2\tau_2^\dagger)^{-\frac{1}{2}} v_1 \\ w_2 & = (I_M + [v_3, \ldots, v_N][v_3, \ldots, v_N]^\dagger)^{-\frac{1}{2}} v_2 = (I_M + \tau_3\tau_3^\dagger)^{-\frac{1}{2}} v_2 \\ \vdots & \\ w_{N-2} & = (I_M + [v_{N-1}, v_N][v_{N-1}, v_N]^\dagger)^{-\frac{1}{2}} v_{N-2} = (I_M + \tau_{N-1}\tau_{N-1}^\dagger)^{-\frac{1}{2}} v_{N-2} \\ w_{N-1} & = (I_M + v_N v_N^*)^{-\frac{1}{2}} v_{N-1} = (I_M + \tau_N\tau_N^\dagger)^{-\frac{1}{2}} v_{N-1} \\ w_N & = v_N \end{cases} . \tag{C.19}$$

Its inverse can be computed by the algorithm:

$$\begin{cases} v_N & = w_N \\ v_{N-1} & = (I_M + v_N v_N^*)^{\frac{1}{2}} w_{N-1} = (I_M + \tau_N\tau_N^\dagger)^{\frac{1}{2}} w_{N-1} \\ v_{N-2} & = (I_M + [v_{N-1}, v_N][v_{N-1}, v_N]^\dagger)^{\frac{1}{2}} w_{N-2} = (I_M + \tau_{N-1}\tau_{N-1}^\dagger)^{\frac{1}{2}} w_{N-2} \\ \vdots & \\ v_2 & = (I_M + [v_3, \ldots, v_N][v_3, \ldots, v_N]^\dagger)^{\frac{1}{2}} w_2 = (I_M + \tau_3\tau_3^\dagger)^{\frac{1}{2}} w_2 \\ v_1 & = (I_M + [v_2, \ldots, v_N][v_2, \ldots, v_N]^\dagger)^{\frac{1}{2}} w_1 = (I_M + \tau_2\tau_2^\dagger)^{\frac{1}{2}} w_1 \end{cases} \tag{C.20}$$

– notice that operations must be performed according to the indicated order.

The trick is to change variables one at a time – starting with the v_1 subspace:

$$\kappa^{-1} = \int [\textstyle\prod_{\alpha=2}^N (\pi^{-M}\, d^{2M} v_\alpha)] \cdot \int (\pi^{-M}\, d^{2M} v_1) [\det(I_N + \tau_1^\dagger \tau_1)]^{-s}. \tag{C.21}$$

Noticing that

$$I_N + \tau_1^\dagger \tau_1 = \begin{bmatrix} 1 + v_1^* v_1 & v_1^* \tau_2 \\ \tau_2^\dagger v_1 & I_{N-1} + \tau_2^\dagger \tau_2 \end{bmatrix},$$

we may, with the help of the identity

$$\det \begin{bmatrix} A & B \\ C & D \end{bmatrix} = \det D \times \det(A - BD^{-1}C),$$

separate the integrand's determinant as follows:

$$\begin{aligned} \det(I_N + \tau_1^\dagger \tau_1) &= \det(I_{N-1} + \tau_2^\dagger \tau_2) \times (1 + v_1^* v_1 - v_1^* \tau_2 (I_{N-1} + \tau_2^\dagger \tau_2)^{-1} \tau_2^\dagger v_1) \\ &= \det(I_{N-1} + \tau_2^\dagger \tau_2) \times [1 + v_1^* (I_M - \tau_2 (I_{N-1} + \tau_2^\dagger \tau_2)^{-1} \tau_2^\dagger) v_1] \\ &= \det(I_{N-1} + \tau_2^\dagger \tau_2) \times [1 + v_1^* (I_M + \tau_2 \tau_2^\dagger)^{-1} v_1] \\ &= \det(I_{N-1} + \tau_2^\dagger \tau_2) \times (1 + w_1^* w_1), \end{aligned}$$

where identities (3.40) have been used, as well as the definition of w_1. Next, we compute the Jacobian of the $v_1 \to w_1$ transformation, bearing in mind that all other variables remain fixed during this integration (this is an important and subtle point of the procedure) – then, since:

$$(\partial v_1/\partial w_1) = (\partial w_1/\partial v_1)^{-1} = (I_M + \tau_2\tau_2^\dagger)^{\frac{1}{2}},$$

we have (once more invoking Sylvester's theorem):

$$d^{2M}v_1 = |\det(\partial v_1/\partial w_1)|^2\, d^{2M}w_1 = \det(I_{N-1} + \tau_2^\dagger\tau_2)\, d^{2M}w_1. \tag{C.23}$$

Combining the above ingredients we find that the w_1 integral has been successfully disentangled:

$$\kappa^{-1} = \int [\textstyle\prod_{\alpha=2}^N (\pi^{-M}\, d^{2M}v_\alpha)][\det(I_{N-1} + \tau_2^\dagger\tau_2)]^{-s+1} \cdot \int (\pi^{-M}\, d^{2M}w_1)(1 + w_1^* w_1)^{-s}. \tag{C.24}$$

This integral, in turn, is of the same kind encountered when computing the bosonic closure's normalization constant at §B.2; in fact, using the formula given in Eq. (B.9), we see that:

$$\int (\pi^{-M}\, d^{2M}w_1)(1 + w_1^* w_1)^{-s} = \mathcal{I}(M, s),$$

which conforms with the condition $s > M \geq 1$, since $s = K + 1 = M + N + 1$.

The thing to be notice is that the same operations used to disentangle this first integral can now be applied to the next, and so on. Thus the remaining variables are disentangled, one at a time, with the exponent s decreasing at each step of the iterative process. This leads to a sequence of simplifications which is delineated below:

$$\begin{aligned}
\kappa^{-1} &= \mathcal{I}(M, s) \cdot \int [\textstyle\prod_{\alpha=2}^N (\pi^{-M}\, d^{2M}v_\alpha)][\det(I_{N-1} + \tau_2^\dagger\tau_2)]^{-(s-1)} \\
&= \mathcal{I}(M, s) \cdot \int (\pi^{-M} d^{2M}w_2)\, (1 + w_2^* w_2)^{-(s-1)} \cdot \int [\textstyle\prod_{\alpha=3}^N (\pi^{-M}\, d^{2M}v_\alpha)][\det(I_{N-2} + \tau_3^\dagger\tau_3)]^{-(s-2)} \\
&\;\;\vdots \\
&= \mathcal{I}(M, s) \cdot \mathcal{I}(M, s-1) \cdots \mathcal{I}(M, s-N+2) \cdot \int [(\pi^{-M}\, d^{2M}v_N)](1 + w_N^* w_N)^{-(s-N+1)} \\
&= \mathcal{I}(M, s) \cdot \mathcal{I}(M, s-1) \cdots \mathcal{I}(M, s-N+2) \cdot \mathcal{I}(M, s-N+1).
\end{aligned} \tag{C.25}$$

Notice how the convergence condition is respected all the way through the last integral, where the exponent modulus is $(s - N + 1) = M + 2$, and thus still greater than M.

Finally, invoking Eq. (B.10) and reorganizing expression (C.25) we reach the result:

$$\kappa = \prod_{n=1}^{N} \frac{(K - n + 1)!}{(N - n + 1)!}. \tag{C.26}$$

Unlike the bosonic case, there is no well-defined limit for this normalization constant

when N grows large (recall that the Pauli principle imposes the condition $K \geq N$). A proper understanding of the classical limit of Thouless states seems to require a more sophisticated approach; an instructive analysis in this direction is presented be Öhrn and Deumens in Ref. [76].

C.3 Fock projection of a Thouless state

Any particular N-electron Fock state, defined over a set of K single-particle spin-orbitals, can be generated from a reference determinant $|\Phi_0\rangle$ by moving l electrons from its occupied to its virtual space. If the size of the virtual space, given by $M = K - N$, is larger than the number of electrons, then l ranges from 0 to N (with $l = 0$ the reference state is recovered).[ii] Adding up all possible electron reallocations – $\binom{N}{l}$ ways of selecting electrons from the occupied space orbitals and $\binom{M}{l}$ ways of placing them into the virtual space orbitals – we find, with the help of 'Vandermonde's identity', a total of

$$\sum_{l=0}^{N} \binom{N}{l}\binom{M}{l} = \binom{K}{N} \tag{C.27}$$

possible states, in agreement with the fact that $\binom{K}{N}$ is precisely the dimension of the Fock space.

Fock configurations may be labeled by simply listing their filled orbitals; in order to distinguish between those orbitals belonging to the occupied and virtual spaces of $|\Phi_0\rangle$, we introduce ordered arrays x and y, whose respective lengths are $N - l$ and l,

$$1 \leq (x_1 < x_2 < \cdots < x_{N-l}) \leq N, \quad 1 \leq (y_1 < y_2 < \cdots < y_l) \leq M, \tag{C.28}$$

with x being a member of the set C^N_{N-l}, of all possible combinations of N objects taken $N-l$ at a time; and y, similarly, being a member of the set C^M_l, of all possible combination of M objects taken l at a time. Using this scheme we may write any given occupation number eigenstate as:

$$|n_1, n_2, \ldots, n_K\rangle = |n(x,y)_l\rangle = a^\dagger_{x_1} a^\dagger_{x_2} \ldots a^\dagger_{x_{N-l}} b^\dagger_{y_1} b^\dagger_{y_2} \ldots b^\dagger_{y_l} |0\rangle, \quad 0 \leq l \leq N. \tag{C.29}$$

Notice that the label l establishes a hierarchy of Fock states – with respect to $|\Phi_0\rangle$, usually a lowest energy configuration, states with the same l are referred to as 'l-tuply excited determinants'.

We proceed by introducing the complementary array $\bar{x}$, build from the l occupied-space

[ii] In the less usual case where $M < N$ then l ranges from 0 to M and everything derived here works the same.

indexes absent from x:

$$\bar{x} \cap x = \emptyset : \quad 1 \leq (\bar{x}_1 < \bar{x}_2 < \cdots < \bar{x}_l) \leq N. \tag{C.30}$$

Thus, $\bar{x}$ is a member of the set C_l^N of possible combinations of N objects taken l at a time, and every x defines a unique $\bar{x}$.[iii]

The last ingredient we require is the N-element permutation $\pi(x)$, constructed via juxtaposition of x and its corresponding $\bar{x}$:

$$\pi(x) = \begin{pmatrix} 1 & 2 & \dots & N-l & N-l+1 & \dots & N-1 & N \\ x_1 & x_2 & \dots & x_{N-l} & \bar{x}_1 & \dots & \bar{x}_{l-1} & \bar{x}_l \end{pmatrix}. \tag{C.31}$$

The signature of this permutation can be obtained from the formula:

$$\pi(x) = \textstyle\sum_{i=1}^{N-l} \dim\{\bar{x} \mid \bar{x} < x_i\} = \sum_{i=1}^{N-l} (x_i - i), \tag{C.32}$$

i.e. by counting the number of entries of $\bar{x}$ which are smaller than a given component of x, and adding up these numbers while going through all components of x (the second equality gives the explicit result).

The permutation $\pi(x)$, connected to a given Fock state $|n(x,y)\rangle$, is interesting because it rearranges the anti-commuting operators $\zeta^\dagger$ of a Thouless configuration in a very useful way:

$$|z\} = (\zeta_1^\dagger \dots \zeta_N^\dagger)|0\rangle = (-)^{\pi(x)} (\zeta_{x_1}^\dagger \dots \zeta_{x_{N-l}}^\dagger)(\zeta_{\bar{x}_1}^\dagger \dots \zeta_{\bar{x}_l}^\dagger)|0\rangle.$$

This, in turn, allows us to write its Fock projection as below:

$$\langle n(x,y)_l|z\} = (-)^{\pi(x)} \langle 0|(b_{y_l} \dots b_{y_1})(a_{x_{N-l}} \dots a_{x_2} a_{x_1} \zeta_{x_1}^\dagger \zeta_{x_2}^\dagger \dots \zeta_{x_{N-l}}^\dagger)(\zeta_{\bar{x}_1}^\dagger \dots \zeta_{\bar{x}_l}^\dagger)|0\rangle.$$

Now, the product of operators at the center of this expression can be effectively replaced by unity because $a_{x_1}\zeta_{x_1}^\dagger = 1 - \zeta_{x_1}^\dagger a_{x_1}$ (since $1 \leq x_1 \leq N$) and, once at the right side of $\zeta_{x_1}^\dagger$, the annihilation operator a_{x_1} will anti-commute its way towards the vacuum, and that term will give no contribution. Next, the same will happen with $a_{x_2}\zeta_{x_2}^\dagger$, and so forth. Thus, the expression simplifies to:

$$\langle n(x,y)_l|z\} = (-)^{\pi(x)} \langle 0|(b_{y_l} \dots b_{y_1})(\zeta_{\bar{x}_1}^\dagger \dots \zeta_{\bar{x}_l}^\dagger)|0\rangle = (-)^{\pi(x)} \det\langle \phi_{(y_1,\dots,y_l)}|\zeta_{(\bar{x}_1,\dots,\bar{x}_l)}\}.$$

Finally, using the fact that $\langle \phi_\mu|\zeta_\alpha\} = z_{\mu\alpha}$, we arrive at:

$$\langle n(x,y)_l|z\} = \det[z_{(y_1,y_2,\dots,y_l)(\bar{x}_1,\bar{x}_2,\dots,\bar{x}_l)}](-)^{\pi(x)}, \tag{C.33}$$

[iii] In the quantum chemistry literature 'l-tuply excited' Fock configurations are most commonly denoted in terms of $\bar{x}$ and y; for instance, the state in Eq. (C.29) – apart from a possible sign – would be written as $|\Phi^{(y_1,y_2,\dots,y_l)}_{(\bar{x}_1,\bar{x}_2,\dots,\bar{x}_l)}\rangle$.

with the signature computed by means of Eq. (C.32). Hence the projection of a Thouless configuration, defined over a reference state $|\Phi_0\rangle$, into an 'l-tuply excited' Fock state is related to an l-sized sub-determinant of the z matrix.

The complete Fock-space expansion for a normalized Thouless configuration reads:

$$|z\rangle = \sum_{l=0}^{N} \sum_{\bar{x}\in C_l^N} \sum_{y\in C_l^M} |n(x,y)_l\rangle (-)^{\pi(x)} \frac{\det[z_{(y_1,y_2,\ldots,y_l)(\bar{x}_1,\bar{x}_2,\ldots,\bar{x}_l)}]}{\sqrt{\det(I_N + z^\dagger z)}}. \tag{C.34}$$

Check. Eq. (C.33) provides an alternative way of calculating the fermionic coherent-state overlap $\{z|z'\}$, as expressed in Eq. (3.26); using the completeness of the occupation number basis we write:

$$\begin{aligned}
\{z|z'\} &= \sum_{l=0}^{N} \sum_{\bar{x}\in C_l^N} \sum_{y\in C_l^M} \{z|n(x,y)_l\rangle\langle n(x,y)_l|z'\} \\
&= \sum_{l=0}^{N} \sum_{\bar{x}\in C_l^N} \sum_{y\in C_l^M} \det[z^*_{(y_1,y_2,\ldots,y_l)(\bar{x}_1,\bar{x}_2,\ldots,\bar{x}_l)}] \det[z'_{(y_1,y_2,\ldots,y_l)(\bar{x}_1,\bar{x}_2,\ldots,\bar{x}_l)}] \\
&= \sum_{l=0}^{N} \sum_{\bar{x}\in C_l^N} \Big\{ \sum_{y\in C_l^M} \det[z^\dagger_{(\bar{x}_1,\bar{x}_2,\ldots,\bar{x}_l)(y_1,y_2,\ldots,y_l)}] \det[z'_{(y_1,y_2,\ldots,y_l)(\bar{x}_1,\bar{x}_2,\ldots,\bar{x}_l)}] \Big\} \\
&= \sum_{l=0}^{N} \sum_{\bar{x}\in C_l^N} \det[(z^\dagger z')_{(\bar{x}_1,\bar{x}_2,\ldots,\bar{x}_l)(\bar{x}_1,\bar{x}_2,\ldots,\bar{x}_l)}].
\end{aligned}$$

where a general property of minors[79] ensures the validity of the last step.

The above formula involves the principal minors of the $N \times N$ matrix $(z^\dagger z')$ – the innermost sum is over all principal minors of a given rank l; the outermost sum is over all possible ranks, from 0 to N (the $l = 1$ term is the trace while the $l = N$ term is the determinant of the full matrix; the $l = 0$ term is defined as unity). Now, for any given $n \times n$ matrix A the following holds[79]

$$\det(I + A) = \sum_{l=0}^{n} \sum_{x\in C_l^n} \det[A_{(x_1,x_2,\ldots x_l)\cdot(x_1,x_2\ldots,x_l)}],$$

and this identity leads us straight to:

$$\{z|z'\} = \det(I_N + z^* z'),$$

in agreement with the result obtained in Chapter 3.

Appendix D

Hubbard model – standard diagonalization

Overview. Exact dynamical solutions to the simple Hubbard models discussed in this work are straightforwardly obtained by the standard expedient: (1) compute the Hamiltonian's eigenvalues and eigenvectors; (2) project the initial state onto the eigenvector basis; and (3) perform a trivial time evolution. The first step is to write the Hamiltonian matrix in Fock representation. The rules for computing matrix elements of the Hubbard Hamiltonian between Fock states of both Fermi and Bose systems are given below. Also, the transformation of Fock configurations induced by an unitary transformation of the underlying single-particle states is derived for both cases.

D.1 Fermi systems

A Fock configuration of N fermions occupying K single-particle orbitals is labeled by a K-sized binary string $n = (n_1, n_2, \ldots, n_K)$ (i.e. each n_p is either 0 or 1) and is expressed in terms of the creation operators $c^\dagger$, associated with a definite set of single-particle orbitals,

$$|n^i\rangle = (c_1^\dagger)^{n_1^i}(c_2^\dagger)^{n_2^i}\cdots(c_K^\dagger)^{n_K^i}|0\rangle, \quad \text{with} \quad \sum_{p=1}^{K} n_p^i = N, \quad \text{for} \quad 1 \leq i \leq \tfrac{K!}{N!(K-N)!}. \tag{D.1}$$

These configurations are thus simultaneous eigenstates of the operators $\hat{n}_p = c_p^\dagger c_p$, for $1 \leq p \leq K$, and are orthonormal $\langle n^i|n^j\rangle = \delta_{ij}$.

D.1.1 Matrix elements

We consider the specific family of Hubbard Hamiltonians, with one- and two-body terms, parame-trized according to

$$\hat{H} = \hat{H}_1 + \hat{H}_2, \quad \text{with:} \quad \hat{H}_1 = \sum_{pq} \varepsilon_{pq}\, c_p^\dagger c_q, \quad \hat{H}_2 = \tfrac{1}{2}\sum_{pq} u_{pq}\, c_p^\dagger c_q^\dagger c_q c_p = \tfrac{1}{2}\sum_{pq} u_{pq}\, \hat{n}_p\hat{n}_q, \tag{D.2}$$

where, without loss of generality, the condition $u_{pp} = 0$ is assumed for the interacting part.

Diagonal matrix elements of the one-body part are trivial since orthogonality of the Fock states ensures that $\langle n^i|c_p^\dagger c_q|n^i\rangle$ is zero except if $p = q$, hence:

$$\langle n^i|\hat{H}_1|n^i\rangle = \sum_p \varepsilon_{pp}\, n_p^i. \quad \text{(one-body, diagonal)} \tag{D.3}$$

In order to compute non-diagonal one-body elements we introduce the notion of 'neighbor configurations' and 'linking state': $|n^i\rangle$ and $|n^j\rangle$ are neighbor configurations when they differ by the placement of one fermion and are in this way linked by an unique $(N-1)$-particle state $|\tilde{n}\rangle$; thus $|n^i\rangle = (-)^{\sigma_r}\, c_r^\dagger\, |\tilde{n}\rangle$ and $|n^j\rangle = (-)^{\sigma_s}\, c_s^\dagger\, |\tilde{n}\rangle$. Here σ_r and σ_s account for the sign chance due to the anti-commutations needed to factor out the creation operators of the differing orbitals – note that both orbitals s and r must be empty in $|\tilde{n}\rangle$. This means that

$$\langle n^i|\hat{H}_1|n^j\rangle = (-)^{\sigma_r+\sigma_s} \sum_{pq} \varepsilon_{pq} \langle\tilde{n}|\, c_r c_p^\dagger c_q c_s^\dagger\, |\tilde{n}\rangle, \tag{D.4}$$

and, with $r \neq s$ (otherwise n^i and n^j would coincide), there is only a single non-vanishing contraction:

$$\sum_{pq} \varepsilon_{pq} \langle\tilde{n}|\, \overbrace{c_r c_p^\dagger} \overbrace{c_q c_s^\dagger}\, |\tilde{n}\rangle = \varepsilon_{rs} \langle\tilde{n}|(1-\hat{n}_r)(1-\hat{n}_s)|\tilde{n}\rangle = \varepsilon_{rs}.$$

Thus we arrive at the following recipe for non-diagonal matrix elements of the non-interacting part of the Hamiltonian:

$$\text{if } \begin{cases} |n^i\rangle = (-)^{\sigma_r}\, c_r^\dagger\, |\tilde{n}\rangle \\ |n^j\rangle = (-)^{\sigma_s}\, c_s^\dagger\, |\tilde{n}\rangle \end{cases} \quad \Rightarrow \quad \langle n^i|\hat{H}_1|n^j\rangle = \varepsilon_{rs}(-)^{\sigma_r+\sigma_s}. \quad \text{(one-body, off-diagonal)} \tag{D.5}$$

The two-body interacting part is trivially evaluated since the Fock configurations are eigenstates of the occupation number operators in the chosen representation:

$$\langle n^i|\hat{H}_2|n^i\rangle = \tfrac{1}{2} \sum_{pq} u_{pq}\, n_p^i n_q^i. \quad \text{(two-body, diagonal)} \tag{D.6}$$

D.1.2 Transformation of fermionic Fock states

Using the above formulas the Hamiltonian matrix for the Hubbard model can be constructed in the particular representation where the two-body interaction term is diagonal. It is sometimes useful, however, to work with a different set of underlying single-particle orbitals related to the original set by an unitary transformation. The question then arises on how the many-body configurations transform as a consequence of the change of single-particle basis.

Let us consider the single-particle transformation $\chi \to \phi$, induced by an unitary matrix

X of size $K \times K$. In terms of the corresponding creation operators we have:

$$\text{if } \; |\phi_p\rangle = c_p^\dagger|0\rangle \;\text{ and }\; |\chi_p\rangle = d_p^\dagger|0\rangle, \;\; \text{then: } \; |\phi_p\rangle = \textstyle\sum_q |\chi_q\rangle X_{qp} \;\Rightarrow\; c_p^\dagger = \sum_q d_q^\dagger X_{qp}. \quad \text{(D.7)}$$

In what follows it is convenient to employ the following 'filled-orbital' notational scheme when referring to the many-body states:

$$|\kappa\rangle_\phi = |\kappa_1, \kappa_2, \cdots, \kappa_N\rangle = c_{\kappa_1}^\dagger c_{\kappa_2}^\dagger \cdots c_{\kappa_N}^\dagger |0\rangle, \quad \text{(D.8a)}$$

$$|\eta\rangle_\chi = |\eta_1, \eta_2, \cdots, \eta_N\rangle = d_{\eta_1}^\dagger d_{\eta_2}^\dagger \ldots d_{\eta_N}^\dagger |0\rangle, \quad \text{(D.8b)}$$

where the array κ lists the N occupied ϕ-orbitals in a given Fock state; likewise η lists the N occupied χ-orbitals in a specific configuration.

Using the transformation rule (D.7) we are able to write $|\kappa\rangle$ as follows:

$$|\kappa\rangle_\phi = c_{\kappa_1}^\dagger c_{\kappa_2}^\dagger \cdots c_{\kappa_N}^\dagger |0\rangle = \sum_{j_1} \sum_{j_2} \cdots \sum_{j_N} d_{j_1}^\dagger d_{j_2}^\dagger \ldots d_{j_N}^\dagger |0\rangle \, X_{j_1\kappa_1} X_{j_2\kappa_2} \ldots X_{j_N\kappa_N},$$

where each of the j indexes runs over the whole range, from 1 to K. At each term of the above sum the product of $d^\dagger$ operators appears in no particular order, and several terms involve the same combination of operators. If the factors multiplying identical combinations are assembled together, with the corresponding operators permuted to the conventional order, we arrive at:

$$|\kappa\rangle_\phi = \sum_{\eta_1 < \eta_2 < \cdots < \eta_N} d_{\eta_1}^\dagger d_{\eta_2}^\dagger \ldots d_{\eta_N}^\dagger |0\rangle \sum_{P \in S_N} (-)^P X_{\eta_{P_1}\kappa_1} X_{\eta_{P_2}\kappa_2} \ldots X_{\eta_{P_N}\kappa_N},$$

where the second sum is over all permutations P of N objects. This sum, which involves products of X-matrix elements, is nothing but the determinant of the $N \times N$ sub-matrix of X build out from rows $(\eta_1, \eta_2, \ldots, \eta_N)$ and columns $(\kappa_1, \kappa_2, \ldots, \kappa_N)$. At the same time, the ordered product of $d^\dagger$ operators constitutes the Fock configuration $|\eta\rangle$; therefore we establish the result:

$$|\kappa_1, \kappa_2, \cdots, \kappa_N\rangle_\phi = \sum_{\eta_1 < \cdots < \eta_N} |\eta_1, \eta_2, \cdots, \eta_N\rangle_\chi \det[X_{(\eta_1, \eta_2, \cdots, \eta_N), (\kappa_1, \kappa_2, \cdots, \kappa_N)}]. \quad \text{(D.9)}$$

As a check, we note that the number of possible $N \times N$ sub-matrices of a $K \times K$ matrix is $\binom{K}{N}$, which is exactly the size of the Fermi-Fock space.

D.2 Bose systems

A Fock configuration of N bosons distributed on K single-particle modes is labeled by the set of K integers $m = (m_0, m_2, \ldots, m_{K-1})$ that specify the population of each mode – for definiteness the indexation of modes is the same as that adopted when studying bosonic

coherent states. These occupation number eigenstates are written in terms of creation operators $b^\dagger$, associated with a particular set of single-particle modes:

$$|m^i\rangle = \frac{(b_0^\dagger)^{m_0^i}(b_1^\dagger)^{m_1^i}\cdots(b_{K-1}^\dagger)^{m_{K-1}^i}}{\sqrt{m_0^i!\ m_1^i!\ \cdots\ m_{K-1}^i!}}|0\rangle, \quad \text{with} \quad \sum_{p=0}^{K-1} m_p^i = N, \quad \text{for} \quad 1 \le i \le \dim \mathcal{B}(K,N), \tag{D.10}$$

where the dimension of the bosonic Fock space at issue is[21]

$$\dim \mathcal{B}(K,N) = \frac{(K+N-1)!}{(K-1)!N!}. \tag{D.11}$$

These configurations are orthonormal, i.e. $\langle m^i|m^j\rangle = \delta_{ij}$, and we recall the well-known relations:

$$\begin{cases} b_p|m^i\rangle & = \sqrt{m_p^i}\,|m_0^i, m_1^i, \ldots, (m_p^i-1), \ldots, m_{K-1}^i\rangle \\ b_p^\dagger|m^i\rangle & = \sqrt{m_p^i+1}\,|m_0^i, m_1^i, \ldots, (m_p^i+1), \ldots, m_{K-1}^i\rangle \\ \hat{n}_p|m^i\rangle & = m_p^i\,|m^i\rangle \end{cases}. \tag{D.12}$$

D.2.1 Matrix elements

Again we consider the family of Hamiltonians with the general form:

$$\hat{H} = \hat{H}_1 + \hat{H}_2, \quad \text{with:} \quad \hat{H}_1 = \sum_{pq} \varepsilon_{pq}\, b_p^\dagger b_q, \quad \hat{H}_2 = \tfrac{1}{2}\sum_{pq} u_{pq}\, b_p^\dagger b_q^\dagger b_q b_p = \tfrac{1}{2}\sum_{pq} u_{pq}\,(\hat{n}_p\hat{n}_q - \hat{n}_p\delta_{pq}). \tag{D.13}$$

Let us first look at the one-body term $\hat{H}_1$. Diagonal matrix elements are elementary since $\langle m^i|b_p^\dagger b_q|m^i\rangle$ vanishes if $p \neq q$; hence:

$$\langle m^i|\hat{H}_1|m^i\rangle = \sum_p \varepsilon_{pp}\, m_p^i. \qquad \text{(one-body, diagonal)} \tag{D.14}$$

As in the fermionic case, in order to get the non-diagonal elements one must realize that the only way $\langle m^i|b_p^\dagger b_q|m^j\rangle$ is non-zero is if the pair of configurations $|m^i\rangle$ and $|m^j\rangle$ differs by the placement of a single boson, in such a way that they are generated by the action of creation operators on a common $(N-1)$-particle Fock state $|\tilde{m}\rangle$. Mathematically, if these 'first-neighbor' configurations differ by the occupation of their r and s modes one may write: $|m^i\rangle = (m_r^i)^{-1/2}\, b_r^\dagger\,|\tilde{m}\rangle$ and $|m^j\rangle = (m_s^j)^{-1/2}\, b_s^\dagger\,|\tilde{m}\rangle$, and one may convince oneself that the 'linking state' $|\tilde{m}\rangle$ is uniquely defined for each such a pair. Thus from the above considerations we have:

$$\langle m^i|\hat{H}_1|m^j\rangle = (m_r^i\, m_s^j)^{-1/2}\sum_{pq}\varepsilon_{pq}\langle\tilde{m}|\, b_r b_p^\dagger b_q b_s^\dagger\,|\tilde{m}\rangle. \tag{D.15}$$

For $r \neq s$ (so that m^i differs from m^j) there is only one possible contraction of operators,

and the sum evaluates to:

$$\sum_{pq} \varepsilon_{pq} \langle \tilde{m}| \, \overbrace{b_r \, b_p^\dagger} \overbrace{b_q \, b_s^\dagger} \, |\tilde{m}\rangle = \varepsilon_{rs} \langle \tilde{m}| (\hat{n}_r + 1)(\hat{n}_s + 1) |\tilde{m}\rangle = \varepsilon_{rs} (\tilde{m}_r + 1)(\tilde{m}_s + 1) = \varepsilon_{rs} m_r^i \, m_s^j.$$

Hence the desired non-diagonal matrix element is given by the recipe:

$$\text{if } \begin{cases} |m^i\rangle = (m_r^i)^{-1/2} \, b_r^\dagger \, |\tilde{m}\rangle \\ |m^j\rangle = (m_s^j)^{-1/2} \, b_s^\dagger \, |\tilde{m}\rangle \end{cases} \quad \Rightarrow \quad \langle m^i | \hat{H}_1 | m^j \rangle = \varepsilon_{rs} (m_r^i m_s^j)^{1/2}. \quad \text{(one-body, off-diagonal)} \tag{D.16}$$

Finally, the two-body term, which involves only occupation number operators, is diagonal in the chosen representation, giving the trivial result:

$$\langle m^i | \hat{H}_2 | m^i \rangle = \tfrac{1}{2} \sum_{pq} u_{pq} \, m_p^i m_q^i - \tfrac{1}{2} \sum_p u_{pp} \, m_p^i. \quad \text{(two-body, diagonal)} \tag{D.17}$$

D.2.2 Transformation of bosonic Fock states

Once more we investigate the effect that unitary transformations on the single-particle space have on many-body states, this time with bosons. The analysis, however, is much more complicated than in the fermionic case, since the occupation of each of the K available modes may exceed unity.

Let us begin by establishing some notation:

$$\text{if } \; |\phi_j\rangle = a_j^\dagger |0\rangle \; \text{ and } \; |\chi_j\rangle = b_j^\dagger |0\rangle, \; \text{ then: } \; |\phi_j\rangle = \textstyle\sum_{i=1}^K |\chi_i\rangle X_{ij} \; \Rightarrow \; a_j^\dagger = \sum_{i=1}^K b_i^\dagger X_{ij}. \tag{D.18}$$

Thus, the transformation $\chi \to \phi$ is given in terms of a $K \times K$ unitary matrix X, with $a^\dagger$ and $b^\dagger$ being the creation operators associated with modes of type ϕ and χ, respectively. In this subsection, for clarity of exposition, we shall depart from the convention (motivated by the coherent-state formalism) of labeling the single-particle modes from 0 to $d = K - 1$; in what follows, the more usual labeling, with indexes from 1 to K, is employed, as anticipated in (D.18).

Furthermore, we write bosonic states defined in terms of different single-particle modes as:

$$|m\rangle_\phi = |m_1, m_2, \ldots, m_K\rangle_\phi = (m!)^{-1/2} (a_1^\dagger)^{m_1} (a_2^\dagger)^{m_2} \cdots (a_K^\dagger)^{m_K} |0\rangle, \tag{D.19a}$$

$$|n\rangle_\chi = |n_1, n_2, \ldots, n_K\rangle_\chi = (n!)^{-1/2} (b_1^\dagger)^{n_1} (b_2^\dagger)^{n_2} \cdots (b_K^\dagger)^{n_K} |0\rangle. \tag{D.19b}$$

where we have abbreviated: $m! = (m_1! m_2! \cdots m_K!)$, and similarly, $n! = (n_1! n_2! \cdots n_K!)$.

Now, with the help of the multinomial theorem, each of the factors in (D.19a) can be

expressed in terms of the $b^\dagger$ operators:

$$(a_j^\dagger)^{m_j} = \Big(\sum_i b_i^\dagger X_{ij}\Big)^{m_j}$$
$$= \sum_{\sigma_{1j}}\sum_{\sigma_{2j}}\cdots\sum_{\sigma_{Kj}}\binom{m_j}{\sigma_{1j}\cdots\sigma_{Kj}}(b_1^\dagger X_{1j})^{\sigma_{1j}}(b_2^\dagger X_{2j})^{\sigma_{2j}}\ldots(b_K^\dagger X_{Kj})^{\sigma_{Kj}}\ \cdot\ \delta\Big(\textstyle\sum_{i=1}^K\sigma_{ij}, m_j\Big),$$

where all sums range from 0 to N – we have purposely introduced a Kronecker delta in order to assure that the σ's add to the correct value (they cannot exceed N since $0 \leq m_j \leq N$, with $1 \leq j \leq K$). The choice of notation for the sums' indexes is no accident, as will become evident in a moment.

When all factors of (D.19a) are put in the form shown above, we get, after some adjustments,

$$\begin{aligned}|m\rangle_\phi = \sqrt{m!}\sum_\sigma \delta(\textstyle\sum_i\sigma_{i1}, m_1)\delta(\sum_i\sigma_{i2}, m_2)\cdots\delta(\sum_i\sigma_{iK}, m_K)\\ \times\Big(\frac{X_{11}^{\sigma_{11}}}{\sigma_{11}!}\frac{X_{21}^{\sigma_{21}}}{\sigma_{21}!}\cdots\frac{X_{K1}^{\sigma_{K1}}}{\sigma_{1K}!}\Big)\Big(\frac{X_{12}^{\sigma_{12}}}{\sigma_{12}!}\frac{X_{22}^{\sigma_{22}}}{\sigma_{22}!}\cdots\frac{X_{K2}^{\sigma_{K2}}}{\sigma_{K2}!}\Big)\cdots\Big(\frac{X_{1K}^{\sigma_{1K}}}{\sigma_{1K}!}\frac{X_{2K}^{\sigma_{2K}}}{\sigma_{2K}!}\cdots\frac{X_{KK}^{\sigma_{KK}}}{\sigma_{KK}!}\Big)\\ \times(b_1^\dagger)^{(\sum_j\sigma_{1j})}(b_2^\dagger)^{(\sum_j\sigma_{2j})}\cdots(b_K^\dagger)^{(\sum_j\sigma_{Kj})}|0\rangle.\end{aligned} \tag{D.20}$$

Notice that the multinomial factors have been dismantled; the product appearing in the numerator, $(m_1!m_2!\ldots m_K!)$, has been factored out of the sum – hence the $\sqrt{m!}$ in front of the expression – while the $\sigma!$ terms appearing in the denominator have been distributed among the X matrix elements. Also, the commuting operators $b^\dagger$ have been grouped together.

The sum in (D.20) is over all $K\times K$ matrices σ whose entries are non-negative integers less than or equal to N.[i] The delta functions, however, filter out a special set of matrices, namely, those whose column sums are equal to the occupations $(m_1, m_2, \ldots, m_K)$ of the ϕ-mode state. Thus we deduce that the σ matrices that give a non-vanishing contribution in (D.20) have the property that the sum of all of their elements adds up to N, since:

$$\textstyle\sum_i\sigma_{ij} = m_j \ \Rightarrow\ \sum_{ij}\sigma_{ij} = N, \tag{D.21}$$

for the set of occupation numbers satisfies: $\sum_j m_j = N$. Meanwhile, the exponent of each $b_i^\dagger$ in Eq. (D.20) is just the sum of the entries of the i-th row of matrix σ. Denoting these row sums by $n_1, n_2, \ldots, n_K$, we see that (D.21) immediately implies:

$$n_i = \textstyle\sum_j\sigma_{ij} \ \Rightarrow\ \sum_i n_i = N. \tag{D.22}$$

We therefore conclude that, in Eq. (D.20), each product of $b^\dagger$'s that acts on the vacuum

[i] Notice that, if a given entry of the transformation matrix is null then the set of σ matrices that contribute in (D.20) is restricted to those with a zero in the corresponding entry.

originates a specific χ-mode Fock state with a total of N bosons. Our task now is to further disentangle the summation, in such a way that all matrices σ with *fixed* row sums are collected together, allowing us to factor out the χ-mode configurations.

With that purpose in mind, let us denote by $\mathcal{A}(m;N,K)$ the set of all $K\times K$ matrices whose entries are integers ranging from 0 to N and whose column sums are $m_1,m_2,\ldots,m_K$, respectively; for compactness, we write simply $\mathcal{A}(m)$, omitting the parameters N,K.

The key point is that matrices belonging to $\mathcal{A}(m)$ can be unambiguously classified according to their row sums; in other words, the set is made out of non-overlaping subsets $\mathcal{B}(n,m)$, each of which is composed of matrices with specific column *and* row sums, $(m_1,m_2,\ldots,m_K)$ and $(n_1,n_2,\ldots,n_K)$, respectively; thus any sum over all $\sigma\in\mathcal{A}(m)$ can be safely partitioned as below:

$$\sum_{\sigma\in\mathcal{A}(m)}(\cdots)=\sum_{|n|=N}\left\{\sum_{\sigma\in\mathcal{B}(m,n)}(\cdots)\right\}.$$

In what concerns Eq. (D.20) this observation leads to:

$$|m\rangle_\phi=\sqrt{m!}\sum_{|n|=N}\left\{\sum_{\sigma\in\mathcal{B}(m,n)}\left[\textstyle\prod_{ij}(X_{ij}^{\sigma_{ij}}/\sigma_{ij}!)\right](b_1^\dagger)^{n_1}(b_2^\dagger)^{n_2}\cdots(b_K^\dagger)^{n_K}|0\rangle\right\}$$

We have thus accomplished our goal: all terms giving rise to the same row sums are grouped together. Finally, using definition (D.19b) and factoring out the χ-mode bosonic Fock states, we arrive at the desired formula:

$$|m_1,m_2,\ldots,m_K\rangle_\phi=\sqrt{m!}\sum_{|n|=N}\sqrt{n!}\left\{\sum_{\sigma\in\mathcal{B}(m,n;N,K)}\left[\textstyle\prod_{ij}(X_{ij}^{\sigma_{ij}}/\sigma_{ij}!)\right]\right\}|n_1,n_2,\ldots,n_K\rangle_\chi. \tag{D.23}$$

Since N is often very large (if not macroscopic) with K typically in the range $\sim 10-100$, the dimension of the bosonic Fock space is usually extremely large; therefore so is the number of σ matrices that have to be constructed for a generic term in (D.23), rendering numerical implementation of this result intractable for most problems[ii] (except, perhaps, those with K small). There was no need, though, for carrying out such Fock-space transformations in this work.

[ii] Matrices with definite row and column sums are mathematical objects known as 'contingency tables' and play a central role in statistical analysis. The problem of finding the total number of tables for definite row and column marginals, when the latter are large, is by itself a formidable one; let alone the problem of listing all such tables.

Appendix E

Spectral analysis

E.1 Auto-correlation function and spectral density

Let us consider a closed quantum system described by a Hamiltonian $\hat{H}$, living in a Hilbert space of dimension n. Let $|\psi_0\rangle$ be the state of the system at $t = 0$. The probability amplitude for recurrence of the initial state at time $t > 0$ is

$$a(\psi; t) = \langle\psi_0|\psi_t\rangle = \langle\psi_0|e^{-\frac{i}{\hbar}\hat{H}t}|\psi_0\rangle. \tag{E.1}$$

This quantity is known as the *auto-correlation function* (ACF).[i]

The ACF contains information about stationary energies of the system. In order to appreciate this we introduce the function $I(\psi; E)$, the *spectral density* (also known as 'power spectrum') given in units of inverse energy:

$$I(\psi; E) \equiv \langle\psi_0|\delta(E - \hat{H})|\psi_0\rangle. \tag{E.2}$$

If we denote an eigenstate of $\hat{H}$ with energy E_m by $|E_m\rangle$, and make use of the closure relation: $\sum_{m=1}^{n} |E_m\rangle\langle E_m| = \hat{1}$, we are able to express (E.2) as:

$$I(\psi; E) = \sum_{m=1}^{n} |\langle E_m|\psi_0\rangle|^2 \, \delta(E - E_m). \tag{E.3}$$

In this way, we see that the eigenstates that participate in the dynamics give rise to energy peaks in the graph of $I(\psi; E)$. The greater the intensity of the peak the greater the overlap between $|\psi_0\rangle$ and the corresponding eigenstate (or collection of degenerate eigenstates). Notice that for a closed system the time label of $|\psi\rangle$ in Eq. (E.3) is arbitrary – we prefer, for the sake of definiteness, to write everything in terms of the initial state.

[i] This Appendix is essentially a transcript of Section 1.3 of H.-D. Meyer's lecture notes on the MCTDH method, cf. Ref. [80]; this topic is covered here for the sake of completeness.

The spectral density is related to the ACF by a simple energy-time Fourier transform:

$$\begin{aligned} I(\psi;E) &= \langle\psi_0|\delta(E-\hat{H})|\psi_0\rangle \\ &= (2\pi\hbar)^{-1}\int_{-\infty}^{+\infty} dt\ \langle\psi_0|e^{\frac{i}{\hbar}(E-\hat{H})t}|\psi_0\rangle = (2\pi\hbar)^{-1}\int_{-\infty}^{+\infty} dt\ a(\psi;t)e^{\frac{i}{\hbar}Et}, \end{aligned}$$

where we adopt the following convention for Fourier integrals:

$$f(t) = \int_{-\infty}^{+\infty}\frac{d\omega}{2\pi}\, f(\omega)e^{-i\omega t}, \quad \tilde{f}(\omega) = \int_{-\infty}^{+\infty} dt\, f(t)e^{i\omega t}, \tag{E.4}$$

and thus: $\delta(\omega-\omega') = (2\pi)^{-1}\int_{-\infty}^{+\infty} dt\, e^{i(\omega-\omega')t}$.

The propagation of $|\psi_0\rangle$ is most often conducted forward in time. It is therefore more appropriate to get rid of the integral over negative t. Since $\hat{H}$ is hermitian, the equality $a(\psi;-t) = a(\psi;t)^*$ holds; straightforward manipulations in the time integral then enable $I(\psi;E)$ to be rewritten as[80]

$$I(\psi;E) = (\pi\hbar)^{-1}\int_0^{+\infty} dt\ \mathrm{Re}[\, a(\psi;t)e^{\frac{i}{\hbar}Et}\,]. \tag{E.5}$$

However, in order for this expression to be useful we must account for the fact that the final propagation time, hereby denoted τ, is finite. The recommended procedure is to employ a 'window function' $g_\tau(t)$ according to the prescription:

$$I_g(\psi;E) = (\pi\hbar)^{-1}\int_0^{\infty} dt\ g_\tau(t)\ \mathrm{Re}\,[\, a(t)e^{\frac{i}{\hbar}Et}\,]. \tag{E.6}$$

The (real and dimensionless) function $g_\tau(t)$ must satisfy:[80]

$$g_\tau(t) = 0,\ \text{for}\ |t|>\tau; \quad g_\tau(0) = 1,\ g_\tau(t) = g_\tau(-t); \quad 0 \le g_\tau(t) \le 1. \tag{E.7}$$

The purpose of the window function is to ensure that the time signal terminates in a smooth fashion, thus avoiding spurious oscillations that would otherwise be caused by a sharp cutoff.

Now, (E.6) implies $I_g(\psi;E) = (2\pi\hbar)^{-1}\int_{-\infty}^{+\infty} dt\ g_\tau(t)\ a(\psi;t)e^{\frac{i}{\hbar}Et}$, and, denoting the Fourier transform of $g_\tau(t)$ by $\tilde{g}_\tau(\omega)$, we observe that $I_g(\psi;E)$ can be written in terms of a convolution product:

$$I_g(\psi;E) = \int_{-\infty}^{+\infty}\frac{d\omega}{2\pi}\,\tilde{g}_\tau(\omega)I(E-\hbar\omega). \tag{E.8}$$

Substitution of (E.3) in the above expression reveals that the net result is that the delta

peaks of the 'bare' spectral density $I(\psi; E)$ are replaced by smoother peaks shaped as $\tilde{g}_\tau$:

$$I_g(\psi; E) = \int_{-\infty}^{+\infty} \frac{d\omega}{2\pi}\, \tilde{g}_\tau(\omega) I(E - \hbar\omega) = \sum_{m=1}^{n} |\langle E_m|\psi_0\rangle|^2 \int_{-\infty}^{+\infty} \frac{d\omega}{2\pi}\, \tilde{g}_\tau(\omega)\, \delta(E - \hbar\omega - E_m)$$
$$= (2\pi\hbar)^{-1} \sum_{m=1}^{n} |\langle E_m|\psi_0\rangle|^2\, \tilde{g}_\tau((E - E_m)/\hbar). \tag{E.9}$$

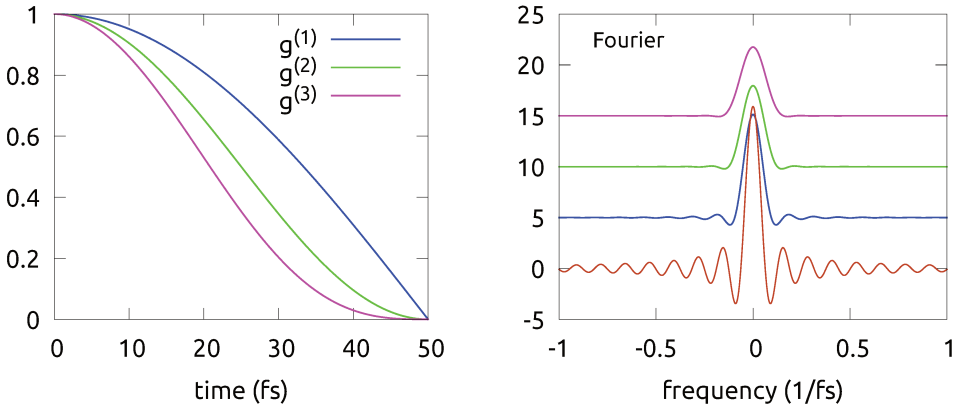

Figure E.1: Left: Window functions of Eq. (E.10) for $n = 1, 2, 3$. The final propagation time is $\tau = 50$ fs. Right: Fourier transforms (same color code). For clarity curves have been stacked at intervals of 5.0 units of intensity. The sharp cutoff case is the bottommost, dark-orange curve.

In the problems studied in Chapter 5, the spectral density is computed using window functions of the following kind:

$$g_\tau^{(k)}(t) = \theta(\tau - |t|)\, [\cos(\pi t/2\tau)]^k, \quad k = 0, 1, 2, 3. \tag{E.10}$$

For reference, we list their Fourier transforms:[80]

$$\tilde{g}_\tau^{(0)}(\omega) = 2\tau \cdot \frac{\sin(\omega\tau)}{\omega\tau}, \tag{E.11a}$$
$$\tilde{g}_\tau^{(1)}(\omega) = \frac{4\tau}{\pi} \cdot \frac{\cos(\omega\tau)}{(1 - 2\omega\tau/\pi)(1 + 2\omega\tau/\pi)}, \tag{E.11b}$$
$$\tilde{g}_\tau^{(2)}(\omega) = \tau \cdot \frac{\sin(\omega\tau)}{\omega\tau(1 - \omega\tau/\pi)(1 + \omega\tau/\pi)}, \tag{E.11c}$$
$$\tilde{g}_\tau^{(3)}(\omega) = \frac{8\tau}{3\pi} \cdot \frac{\cos(\omega\tau)}{(1 - 2\omega\tau/\pi)(1 + 2\omega\tau/\pi)(1 - 2\omega\tau/3\pi)(1 + 2\omega\tau/3\pi)}. \tag{E.11d}$$

The functions in Eq. (E.10) are displayed on the left panel of Fig. E.1 for a final propagation time $\tau = 50$ fs. The shape of the peaks for each case is shown in the right panel, with the same color code. Notice how the spurious oscillations are obliterated as the order k of $g_\tau^{(k)}$ increases; at the same time, peaks get shorter and wider and resolution is lost – in applications one seeks to balance both effects.

Typeset with LaTeX and BibTeX using the Kile editor (http://kile.sourceforge.net/index.php).
All code written in C language using the GNU Scientific Library (https://www.gnu.org/software/gsl/).
All figures created with gnuplot (http://www.gnuplot.info/), except Fig. 5.19, created with GChemPaint (http://www.nongnu.org/gchempaint/), and the 'Thesis map' at page 18, created with LibreOffice Draw (https://www.libreoffice.org/).